

Functional characterization of *Bartonella*  
effector protein C (BepC)  
in the context of infection

**Inauguraldissertation**

zur  
Erlangung der Würde eines Doktors der Philosophie  
vorgelegt der  
Philosophisch-Naturwissenschaftlichen Fakultät  
der Universität Basel

von  
Simon Marlaire  
von Belgien

Basel, 2019

Genehmigt von der Philosophisch-Naturwissenschaftlichen Fakultät auf Antrag von

Prof. Dr. Christoph Dehio

Prof. Dr. Urs Jenal

Basel, den 24.04.2018

Prof. Dr. Martin Spiess

Dekan



## **Statement of my Thesis**

This work was carried out in the group of Prof. Christoph Dehio in the focal area of Infection Biology at the Biozentrum of the University of Basel, Switzerland.

My PhD committee consisted of:

Prof. Dr. Christoph Dehio

Prof. Dr. Urs Jenal

Prof. Dr. Martin Spiess

My thesis is written in a cumulative format. It consists of an introduction covering the major aspects related to my work followed by results and discussion chapters presenting my research that contains a manuscript in preparation and additional data related to my project. Finally, I resume the major findings of my thesis and provide suggestions for the future progression of the project.



## Abstract

A wide variety of bacterial pathogens evolved a panel of virulence factors in order to subvert cellular processes and achieve a successful infection. Bacteria of the genus *Bartonella* translocate a cocktail of effector proteins (Beps) via a type IV secretion system (T4SS) into mammalian cells. BepC, one of the most conserved effectors in the *Bartonella* species of the lineage 4, has been previously shown to be involved in the internalization of bacterial aggregates and migration defect *in vitro*.

In this work, we show that the effector BepC localizes at cell-to-cell contact and triggers strong actin rearrangements as well as the formation of bacterial aggregates during infection of human cells. The actin phenotype is induced by BepC from different *Bartonella* species, indicating an important role of this effector during pathogenesis.

BepC pull-down from infected cells led to the identification of two interacting partners, GEF-H1 and MRCK $\alpha$ , which are two host proteins involved in the RhoA and Cdc42 pathways, respectively. We demonstrate that the ability of BepC to bind GEF-H1 and MRCK $\alpha$  highly correlates with its ability to trigger actin rearrangements. Accordingly, infected cells show an increase of GTP-bound RhoA and phosphorylated myosin light chain while both RhoA and its downstream effector ROCK are required for actin rearrangements mediated by BepC. Thus, our results indicate that BepC activates the RhoA pathway by interacting with GEF-H1 and thereby inducing actin rearrangements although MRCK $\alpha$  might also be involved.

The majority of Beps, including BepC, carries an enzymatic FIC domain that is usually involved in posttranslational modifications. Most Fic proteins carry a canonical FIC motif that is essential for ATP binding and the transfer of AMP onto the target protein (AMPylation). By contrast, BepC is characterized by a non-canonical FIC motif and only displays a weak AMPylation and phosphorylation activity, independently from its conserved motif. Nevertheless, structural analysis and binding assays demonstrate that ATP binds to the FIC domain of BepC and is critical for its thermal stability.

In absence of FIC domain, BepC loses its ability to localize at cell junctions, to interact with GEF-H1 and MRCK $\alpha$ , and to trigger actin rearrangement, suggesting a central role for this domain in the effector function. However, a conserved FIC motif is not necessary to trigger actin rearrangements, which indicates that BepC acts by protein-protein interaction rather than by posttranslational modification. Thus, we propose that BepC is recruited to cell contacts where it triggers the activation of the RhoA pathway by interacting with GEF-H1 and eventually leads to actin rearrangements, possibly with the help of MRCK $\alpha$ .

Ultimately, the subversion of RhoA signaling by BepC could help *Bartonella* to interfere with the immune response by preventing phagocytosis or impair cell migration. Furthermore, it could play an important role in the disruption of the endothelial barrier in order to reach the blood and establish a long-lasting bacteremia inside the host.

## Table of Content

1	Introduction	1
1.1	Rho GTPases	2
1.1.1	Rho GTPase regulation	3
1.1.2	Cellular processes regulated by Rho GTPases	4
1.2	Bacterial effectors and toxins acting on Rho GTPase signaling	9
1.2.1	Activation of Rho GTPases	9
1.2.2	Inactivation of Rho GTPases	11
1.3	Bacteria of the genus <i>Bartonella</i>	13
1.3.1	Infection cycle of <i>Bartonella</i>	13
1.3.2	Phylogeny of the genus <i>Bartonella</i>	14
1.3.3	VirB/VirD4 type IV secretion system	15
1.3.4	<i>Bartonella</i> effector proteins (Beps)	16
1.4	<i>Bartonella</i> effector protein C (BepC)	19
1.4.1	Structural studies of the BepC FIC domain	22
1.4.2	BepC in the context of pathogenesis	25
1.5	References	28
2	Aim of my thesis	37
3	Research article	39
3.1	Results	40
3.1.1	BepC is responsible for actin cytoskeleton rearrangements during infection of human cells	40
3.1.2	BepC from different <i>Bartonella</i> species induces actin stress fiber formation in HeLa cells	41
3.1.3	The FIC domain of BepC is required for actin rearrangements	42
3.1.4	A conserved BID domain is required for actin stress fiber formation mediated by BepC	44
3.1.5	GEF-H1 and MRCK $\alpha$ interact with BepC during cell infection	44
3.1.6	BepC <sub>Bhe</sub> increases GTP-bound RhoA during infection of HeLa cells	46
3.1.7	The inhibition of the RhoA pathway decreases BepC <sub>Bhe</sub> -mediated actin stress fiber formation	46
3.1.8	BepC <sub>Bhe</sub> increases myosin light chain phosphorylation in HeLa cells and HUVECs during infection	47
3.1.9	BepC <sub>Bhe</sub> localizes to cell-to-cell contacts during infection	47
3.1.10	BepC <sub>Bhe</sub> does not trigger RhoA pathway activation by microtubules depolymerization	48
3.1.11	BepC <sub>Bhe</sub> induces the aggregation of vimentin intermediate filaments	49
3.1.12	Focal adhesions and adherens junctions are maintained in presence of BepC	49

3.2	Discussion.....	50
3.3	Figures.....	58
3.4	References.....	77
4	Additional results .....	81
4.1	Results.....	82
4.1.1	Recombinant BepC <sub>Bhe</sub> (FIC-OB) is modified after overexpression in <i>E. coli</i> .....	82
4.1.2	BepC <sub>Bhe</sub> (FIC-OB) has residual auto-AMPylation and auto-phosphorylation activities <i>in vitro</i> .....	83
4.1.3	A conserved FIC motif is not required for the auto-AMPylation of BepC <sub>Bhe</sub> (FIC-OB).....	84
4.1.4	BepC <sub>Bhe</sub> (FIC-OB) does not AMPylate or ADP-ribosylate a host protein <i>in vitro</i> .....	84
4.1.5	BepC <sub>Bhe</sub> (FIC-OB) is stabilized by nucleoside tri- and di-phosphates as well as pyrophosphate. ....	85
4.1.6	A conserved FIC motif is required for the thermal stability of BepC. ....	86
4.1.7	BepC does not require magnesium to have auto-AMPylation activity and to bind nucleotides derivatives.....	86
4.1.8	BepC belongs to the class I Fic proteins. ....	87
4.2	Discussion.....	90
4.3	Figures.....	94
4.4	References.....	112
5	General conclusion and outlook .....	113
5.1	General conclusion .....	114
5.2	Outlook.....	115
5.2.1	Enzymatic activity of the FIC domain of BepC.....	115
5.2.2	Antagonism between BepC and BepE. ....	116
5.2.3	Cooperation between BepC and BepF. ....	117
5.2.4	Participation of MRCK $\alpha$ in the actin phenotype mediated by BepC.....	117
5.2.5	Characterization of the interaction between BepC, GEF-H1, and MRCK $\alpha$ .....	118
5.2.6	Host specificity.....	119
5.2.7	Investigation of the role of BepC in pathogenesis. ....	119
5.3	References.....	121
6	Materials and methods .....	122
7	Acknowledgement .....	137
8	Curriculum vitae.....	139

# Introduction

Infectious diseases imply the establishment of a competition between the host and the pathogen in which bacteria typically choose between two different tactics. In one hand, a frontal attack involving fast bacterial replication, acute symptoms, and a short period of incubation in order to overwhelm rapidly the host immune response. On the other hand, a stealth attack that is frequently characterized by a slow infection process in which the pathogens manipulate the immune system, establish a long-lasting infection, and adopt an intracellular lifestyle. To face the challenge to meet defensive attacks as well as to exploit the host functions to the pathogen's benefit for survival, growth, and spreading, many stealth bacteria evolved a panel of virulence factors to interfere with cell functions. Among those are toxins, which are secreted in their surrounding environment, and effectors, which are directly translocated inside the host cell via a type III or a type IV secretion system (T3SS/T4SS). Signaling pathways regulated by small GTPases are often subverted by these virulence factors as they are involved in a multitude of cellular processes that can be modulated to the advantage of the pathogen.

## **1.1 Rho GTPases**

The 20 GTPases of the Rho family are involved in many cellular processes, including cell migration, cell division, cell adhesion, lymphocyte development, and endothelial and epithelial permeability [1-8]. Thus, their activity is tightly controlled by different mechanisms. Rho GTPases are distributed in eight subgroups in which Rho, Rac, and Cdc42 are the most conserved among eukaryotes [9] (Fig. 1.1).



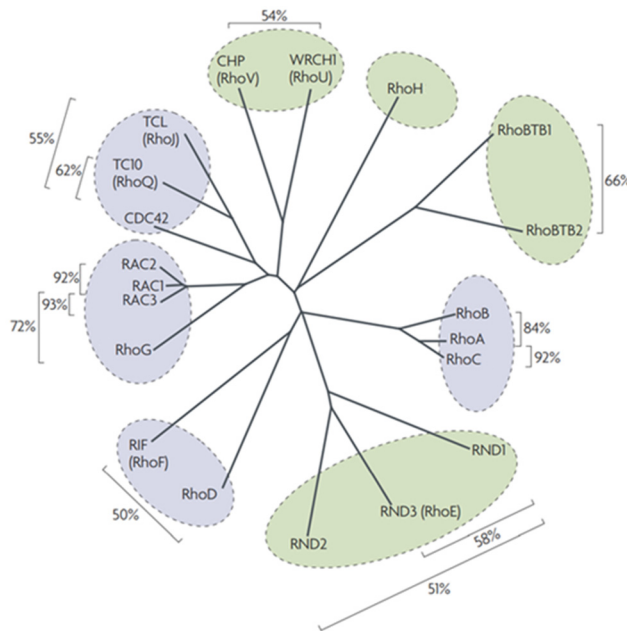


**Figure 1.1. Rho GTPase family.**

Rho GTPases are divided into eight subfamilies according to their repartition in the phylogenetic tree. By contrast with classical Rho GTPases (in gray), which hydrolyze GTP, atypical Rho GTPases (in green) are predominantly GTP-bound due to the absence of a GTPase activity or an increased nucleotide exchange. They are regulated by protein stability, gene expression or phosphorylation rather than by GEFs (Guanine nucleotide exchange factors) and GAPs (GTPase activating proteins) [10, 11]. Amino acid sequence identity is indicated in %. Adapted from [12].

### 1.1.1 Rho GTPase regulation.

Most GTPases alternate between an inactive GDP-bound conformation and an active GTP-bound conformation. This switch is regulated by guanine nucleotide exchange factors (GEFs), GTPase-activating proteins (GAPs), and guanine nucleotide dissociation inhibitors (GDIs) (Fig. 1.2). There are 79 identified mammalian GEFs of the Rho GTPase family, while between 59 and 70 proteins containing a RhoGAP domain have been predicted in the human genome, indicating a complex degree of regulation [1, 13].

In order to get activated and to interact with downstream effectors, GDP-bound Rho GTPases need to localize to the plasma membrane. Most Rho GTPases are posttranslationally modified by prenylation on a C-terminal CAAX motif (where C represents cysteine, A an aliphatic amino acid, and X a terminal amino acid) and occasionally by palmitoylation, mediating the association with membranes [14, 15]. GDIs extract Rho GTPases from membranes by masking the hydrophobic tail linked to the prenyl group, thereby sequestering them in the cytosol and preventing their activation [16]. Additionally, GDIs act as chaperones and suppress

the degradation of inactive Rho GTPases to maintain a stable pool readily available for activation [17].

In response to a stimulus, GEFs promote the exchange of GDP by GTP and activate Rho GTPases. The mechanism of activation by GEF is a multi-step process leading to the decrease of the affinity for the nucleotide, resulting in the release of GDP. Although GTPases have generally similar affinity for GDP and GTP, the binding of GTP is favored due to a ten times higher cytosolic concentration in comparison with GDP [18, 19]. Due to conformational changes, Rho GTPases are able to interact with downstream effectors, leading to their activation. More than 70 Rho GTPase effectors have been described, many of them are kinases or scaffolding proteins playing a role in a multitude of cellular processes [20].

Despite their name, GTPases have a very slow intrinsic GTP hydrolysis activity, which by itself would not be suitable for a short-term activation of signaling pathways. GAPs interact with GTPases and insert a so-called arginine finger in the active site, thereby stabilizing the transition state and stimulating their hydrolysis activity [18, 21, 22]. Once inactivated, the Rho GTPases are available for a new cycle.

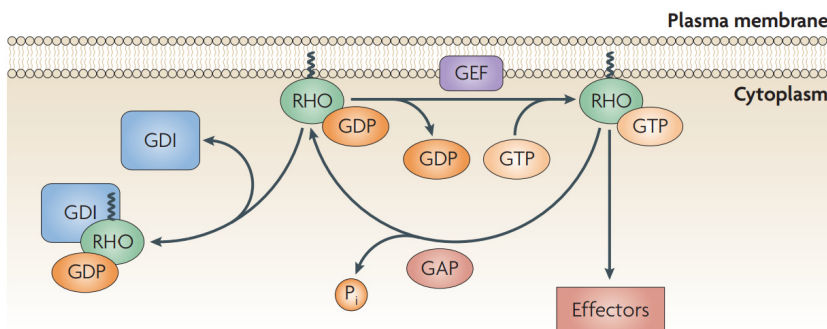


**Figure 1.2. Regulation of Rho GTPases.**

Rho GTPases (RHO, in green) are anchored in the plasma membrane via a lipid group (zigzag line) or sequestered in the cytosol by guanine nucleotide dissociation inhibitors (GDI, in blue). After an external stimulus, guanine nucleotide exchange factors (GEF, in purple) activate the GTPase by promoting the exchange of GDP for GTP. Once activated, they interact with their effectors and modulate downstream signaling pathways. GTPase-activating proteins (GAP, in red) stimulate the hydrolysis of GTP in GDP and inorganic phosphate (Pi), thereby inactivating the GTPase. Taken from [1].

### 1.1.2 Cellular processes regulated by Rho GTPases.

Rho GTPases are regulating a multitude of cellular processes that require the mobilization of the actin cytoskeleton such as cell migration, endothelial and epithelial barrier integrity, and phagocytosis. Additionally, they also participate in the immune defense by regulating inflammatory response and bacterial killing mechanisms.

Rho (Ras homolog gene family member), Rac (Ras-related C3 botulinum toxin substrate), and Cdc42 (cell division control protein 42 homolog) are the best characterized Rho GTPase subfamilies and the most ubiquitously expressed in mouse tissues [9]. Once activated, they interact with a large set of downstream effectors that principally participate in the reorganization of the actin cytoskeleton (Fig. 1.3). In cell culture, the activation of RhoA and its isoforms RhoB and RhoC lead to actomyosin contraction and actin stabilization, thereby promoting the formation of actin stress fibers [23]. By contrast, Rac1, Rac2, Rac3, and RhoG trigger lamellipodia formation while Cdc42 stimulates the formation of filopodia [24, 25].

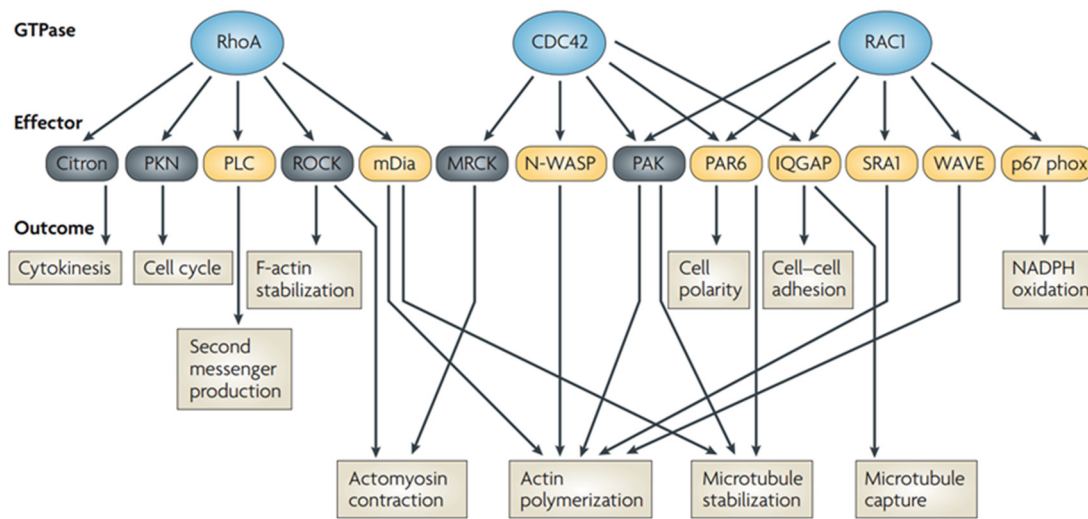


**Figure 1.3. Downstream effectors activated by RhoA, Cdc42, and Rac1.**

The activation of Rho GTPases results in the stimulation of a wide variety of cellular processes via their downstream effectors, including cytoskeletal dynamics and NADPH oxidation [26]. Effectors with a kinase activity are indicated in grey. Taken from [20].

### 1.1.2.1 Cell migration

Cell motility is a complex process involved in many physiological and pathological events including embryogenesis, angiogenesis, cancer invasion, and immune response. Efficient migration requires a dynamic remodeling of the actin cytoskeleton and the formation of multiple cellular structures such as lamellipodia, filopodia, actin stress fibers, and cell adhesions. The migration starts with the initiation of cell protrusions at the leading edge, followed by the formation of new adhesions to the extracellular matrix (ECM). After anchorage, the next step consists of the contraction of the cell body, which is mediated by actomyosin. Finally, the retraction coupled to the detachment of the rear tail concludes the migration process.

The spatiotemporal regulation of these events is tightly controlled by GTPases of the Rho family. The formation of filopodia is initiated by Cdc42 via the activation of N-WASP (neuronal

Wiskott–Aldrich syndrome protein) and WASP, which induces the ARP (actin-related protein) 2/3 complex. Rac1 also activates the ARP2/3 complex but via the WAVE (WASP family verprolin homologous protein) complex to form the branched lamellipodial actin network. The ARP2/3 complex binds to pre-existing actin filaments and serves as a seed for the polymerization and the branching of a new actin filament, which contribute to the formation of protrusions [27].

Cell motion requires the coupling of the actin cytoskeleton to the ECM via focal adhesions (FAs), which provides an anchorage for traction. The binding of integrins to ECM proteins initiates the formation of nascent adhesions at the leading edge of migrating cells. Clustered integrins recruit a multitude of proteins via their cytoplasmic domain, such as the adaptor and integrin-activator protein talin, vinculin and paxillin, and the focal adhesion kinase (FAK) [28, 29]. As the lamellipodium moves forward, the assembly of adhesions in focal complexes is driven by Rac, FAK, and paxillin. In the lamellum, Rac signaling decreases while Rho mediates the maturation of focal complexes into stable focal adhesions [5, 30].

After stabilization of focal adhesions, the tension needed for forward movement is generated by actomyosin contraction, which is linked to actin stress fiber formation. Rho and Cdc42 cooperate to regulate cell body contraction via their respective downstream effectors, ROCK (Rho-associated protein kinase) and MRCK (myotonic dystrophy kinase-related Cdc42-binding kinase) [31].

The two human homologs ROCK1 and ROCK2 (hereafter referred to as ROCK) share 64% of amino acid sequence identity and are ubiquitously expressed. ROCK directly phosphorylates the myosin regulatory light chain 2 (MLC2), which increases the ATPase activity of non-muscle myosin II (MYO2) and promotes actomyosin contraction. In addition, ROCK also phosphorylates a regulatory subunit of the myosin light chain phosphatase (MLCP) complex, thereby inactivating it and leading to increased MLC2 phosphorylation. Finally, ROCK activates LIMK1/2 (LIM kinase) which, in turn, phosphorylates and inactivates the actin-severing protein Cofilin1 [32, 33]. As cofilin is depolymerizing F-actin, its inactivation results in the stabilization of actin filaments within the cells.

There are three homologous MRCK proteins in humans (henceforth referred to as MRCK), which are annotated with a Greek letter ( $\alpha$ ,  $\beta$ ,  $\gamma$ ). MRCK $\alpha$  and MRCK $\beta$  share 61% of amino acid identity and are ubiquitously expressed, while MRCK $\gamma$  is less related (44% identity with MRCK $\beta$ ) and its expression is restricted to fewer tissues [34]. MRCK and ROCK belong to the DMPK (Dystrophia myotonica protein kinase) family of kinases that phosphorylate MLC2 [35]. As their kinase domains have a high amino acid and structural homology [36], it is not surprising that MRCK targets the same substrates as ROCK, including MLC2, MLCP, and LIMK1 [37-39].

However, MRCK and ROCK differ in the spatial regulation of actomyosin contraction. Depending on the heavy chain isoform, MYO2 preferentially localizes to the cell periphery at the leading front (MYO2A) or to the cell body and the rear end (MYO2B) [40]. Interestingly, MRCK $\alpha/\beta$  are recruited to the lamella and the lamellipodia via adaptor proteins and regulate the activity of MYO2A, which contribute to the actomyosin retrograde flow in the lamella and contractile force generation [37, 41, 42]. By contrast, ROCK regulates the distribution of MYO2B and participates in tail retraction during migration [43, 44].

The release of cell rear adhesions is the last step of cell migration. Although the exact process remains elusive, it is mainly controlled by the combination of actomyosin contraction and an activation of the protease calpain, which is able to degrade focal adhesions proteins, including FAK, integrins, vinculin, and talin [45, 46].

#### **1.1.2.2 Epithelial and endothelial permeability**

Epithelial and endothelial tissues serve as semipermeable barriers between different compartments in the body. Their permeability is strictly regulated by Rho GTPases and depends on the integrity of tight junctions (TJs) and adherens junctions (AJs) [4, 47]. Both junctions are composed of adhesive proteins, which form intercellular zipper-like structures and interact intracellularly with the actin cytoskeleton.

TJs consist of claudins and occludins, which are connected to the actomyosin cytoskeleton via ZO proteins (Zonula occludens) [48]. In endothelial and epithelial cells, RhoA is involved in the regulation of TJs by being locally activated by p114GEF, while the activity of Rac1 and Cdc42 is downregulated [49, 50].

Endothelial AJs are composed of VE-cadherin (vascular endothelial-cadherin) that is associated with  $\alpha/\beta$  catenins, which mediate the interaction with the actin cytoskeleton. Rac1 and Cdc42 participate in the stabilization of AJs by sequestering IQGAP1, a protein preventing the interaction between catenin and actin [51, 52]. By contrast, RhoA contributes to AJs destabilization by actomyosin contraction through the activation of ROCK [53].

Such barrier structures do not only participate in compartmentalization, resilience against mechanical stress, and control of substance diffusion within an organism, but also serve as the first line of defense against intruding pathogens.

#### **1.1.2.3 Inflammatory response**

Pattern recognition receptors (PRRs) recognize pathogen-associated molecular patterns (PAMPs), such as lipopolysaccharides (LPS), which are conserved molecules specific to pathogens. Toll-like receptors (TLRs) are PRRs located at the plasma membrane of innate immune cells and, once activated, lead to an inflammatory response via downstream signaling.

Rac1 is required for the activation of NF- $\kappa$ B, a key regulator of cytokine production, triggered by TLR2. While RhoA is needed for the synthesis of proinflammatory cytokines by human monocytes downstream of TLR2 and TLR4 [54-56]. Nucleotide binding oligomerization domain-like receptors (NOD-like receptors, NLRs) are cytosolic PRRs. Two of these receptors, NOD1 and NOD2, participate in the recognition of bacterial products [57]. NOD1 is ubiquitously expressed, while NOD2 is mainly restricted to monocytes and epithelial cells of the intestine [58, 59]. Upon stimulation, NOD1 or NOD2 form a complex, the nodosome, with receptor-interacting protein (RIP) and other binding partners. The assembly of the nodosome induces the activation of NF- $\kappa$ B and mitogen-activated protein (MAP) kinases, leading to proinflammatory and antimicrobial responses [60]. Rac1 activity is required for the activation of the NOD1 signaling pathway by peptidoglycan, and activated Rac1 is associated with NOD2 in membrane ruffles [61, 62]. Other Rho GTPases also seem to be involved in nodosome activation as constitutively active RhoA and Cdc42 activate the NOD1 signaling pathway [61].

#### 1.1.2.4 Phagocytosis

Complementary to the immune response mediated by PRRs, phagocytosis of pathogens by immune cells constitutes an effective defense mechanism by physically eliminating the threat and promoting an inflammatory response. Macrophages can take up bacteria via the Fc receptor (FcR) or via the complement receptor  $\alpha$ M $\beta$ 2, which is composed of the integrin subunit  $\alpha$ M (CD11b) and  $\beta$ 2 (CD18) [63, 64]. After opsonization of the bacteria by immunoglobulins, phagocytic cells bind the antibody via the Fc receptor present at the cell surface. The subsequent engulfment of bacteria always requires a re-organization of filamentous actin (F-actin), which is regulated by Rho GTPases. Cdc42, Rac1, Rac2, and RhoG participate in FcR-dependent phagocytosis, while RhoA does not seem to be required [65]. By contrast, the activity of RhoA and RhoG, but not of Rac1 or Cdc42, is required for phagocytosis mediated by  $\alpha$ M $\beta$ 2 integrins [66, 67].

#### 1.1.2.5 Bacterial killing

After bacterial uptake by phagocytes, the enzyme complex NADPH oxidase (NOX) 2 is assembled at the membrane of the phagosome and reduces oxygen to superoxide in the phagosomal lumen, thereby contributing to bacterial killing [68]. NOX2 is necessary for host defense mediated by neutrophils but is also playing a role in macrophages [69, 70]. Rac2, which is the Rac isoform predominantly expressed in human neutrophils, participates in the activation of NOX2 and thereby enhances the production of reactive oxygen species (ROS) [71, 72]. Additionally, Rac2 is involved in the release of primary granules by neutrophils, which contain enzymes capable of damaging the bacteria [73]. Murine neutrophils and macrophages deficient in Rac2 show a reduction in superoxide production [74, 75]. In human patients with

recurrent bacterial infection, immunodeficiency due to the expression of dominant negative Rac2 was reported [76, 77].

## 1.2 Bacterial effectors and toxins acting on Rho GTPase signaling.

In order to hijack the Rho GTPase signaling cascade for their own benefit, bacteria have developed a wide variety of strategies. Many of the virulence factors manipulate Rho GTPases by mimicking or directly activating the eukaryotic regulatory proteins GEF, GDI, and GAP. By contrast, some virulence factors directly target Rho GTPases by posttranslational modifications in order to prevent their interaction with downstream effectors or to inhibit their GTPase activity (Fig. 1.4). As most cellular processes need a fine balance between activation and inactivation, a strong stimulation or inhibition of the same pathway will often have similar consequences such as an alteration of the epithelial and endothelial barriers, phagocytosis inhibition, cell entry facilitation, or host immune defense manipulation [78].

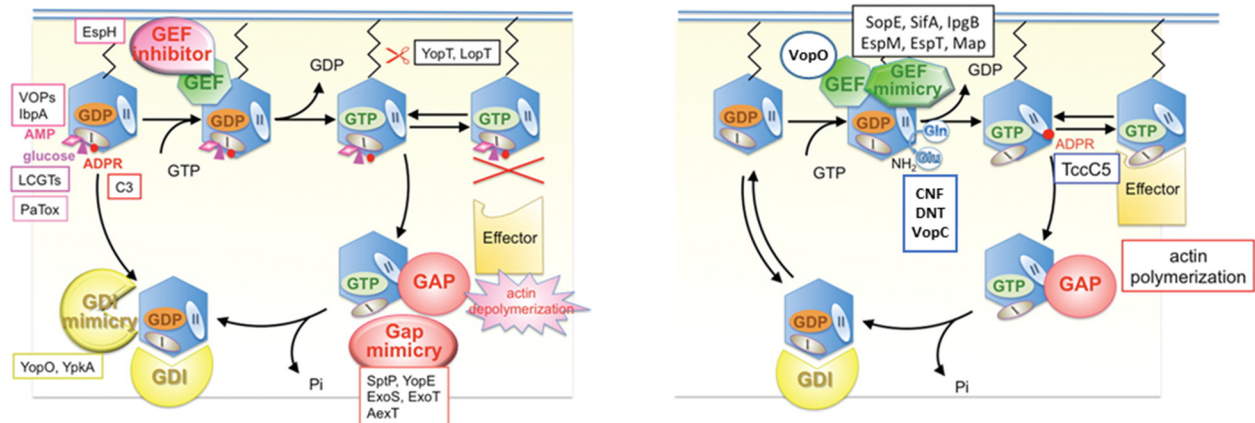


**Figure 1.4. Inactivation and activation of Rho GTPase signaling by bacterial toxins and effectors.**

Left panel: inactivation of small GTPases by posttranslational modifications, cleavage, GAP mimicry, GDI mimicry, or GEF inhibition. Right panel: activation of small GTPases by GEF activation, GEF mimicry, and inhibition of intrinsic GTPase activity. Adapted from [78].

### 1.2.1 Activation of Rho GTPases.

#### 1.2.1.1 GEF mimicry.

Effectors harboring a WxxxE motif activate small GTPases by mimicking GEF and promoting the exchange of GDP for GTP. Although they do not have an overall structural similarity with eukaryotic GEFs, they share a conserved structure element characterized by helices arranged in a V-shape and a catalytic loop [79, 80].

During infection, *Salmonella* Typhimurium translocates four different effectors harboring a WxxxE motif via its T3SS into the host cell. SopE and SopE2 are playing key roles in pathogenesis, as they are involved in cell invasion, the alteration of tight junctions, and the activation of NF- $\kappa$ B [81-83]. The two other effectors, SifA and SifB, localize to the *Salmonella*-containing vacuole but do not induce any actin rearrangements [84]. In cultured cells, SopE induces the formation of lamellipodia by activating Rac1/2, Cdc42, and RhoG, while SopE2 promotes filopodia formation by activating Cdc42 [85, 86]. While the function of SifB is still unknown, SifA plays an important role in intracellular survival and is required *in vitro* for the replication of *Salmonella* in macrophages [87, 88]. Surprisingly, SifA does not trigger nucleotide exchange although it interacts with GDP-bound RhoA, possibly due to the presence of an additional N-terminal domain [89].

IpgB1 from *Shigella flexneri* activates Rac1 via the Elmo-Dock180 complex and directly activates Cdc42 to induce the formation of membrane ruffles and promote cell invasion [90-92]. By contrast, IpgB2 activates RhoA as well as ROCK, leading to stress fiber formation and NF- $\kappa$ B activation [80, 90, 93, 94].

Another example of a GEF mimicry for Cdc42 is the Map effector of enteropathogenic *E. coli* (EPEC) and enterohemorrhagic *E. coli* (EHEC). Other effectors of EHEC, EspM1 and EspM2, are only activating RhoA and induce actin stress fiber formation [90, 95, 96]. Map and EspM are promoting pathogenesis by altering tight junctions [97, 98].

EspT, from EPEC and the closely related mouse pathogen *Citrobacter rodentium*, induces lamellipodia formation and membrane ruffles by activating Rac1 and Cdc42, thereby promoting pathogen invasion of non-phagocytic cells [99, 100].

#### 1.2.1.2 Interaction with GEF.

Instead of incorporating a GEF activity, bacterial effectors may directly activate host GEFs to provoke a similar outcome. VopO, from *Vibrio parahaemolyticus*, is interacting with GEF-H1, thereby activating the RhoA pathway and leading to actin stress fiber formation. This effector is involved in disruption of the epithelial barrier, which could facilitate bacterial dissemination in the host. Interestingly, VopO does not share any sequence homology or motif with any other effectors and the mechanism of activation is still unknown [101].

#### 1.2.1.3 Posttranslational modifications.

To date, all virulence factors that have been shown to activate Rho GTPases by posttranslational modifications target the same glutamine residue that is critical for the intrinsic GTPase activity. Thereby unable to hydrolyze GTP, the modified Rho GTPases stay permanently activated.



The TccC5 toxin produced by the insect pathogen *Photobacterium luminescens* is ADP-ribosylating RhoA, Rac, and Cdc42 by using NAD (nicotinamide adenine dinucleotide) as a substrate. The activation of the Rho GTPases affects the actin cytoskeleton and participates in phagocytosis inhibition [102, 103].

Another strategy to impair the GTPase activity is the deamination of the glutamine into glutamic acid. The toxin CNF1 (cytotoxic necrotizing factor) from pathogenic *E. coli* and *Yersinia pseudotuberculosis* catalyzes the deamination of Rho, Rac, and Cdc42 [104]. The coordinated activation of Rho, Rac, and Cdc42 promotes cell invasion, while the activation of RhoA by CNF1 of *E. coli* seems to play a role in the transgression of the blood-brain barrier [105].

The T3SS effector VopC, from *Vibrio parahaemolyticus*, is a homolog of the catalytic domain of CNF1. Although it only deaminates Rac1 and Cdc42, it is able to induce actin stress fiber formation and facilitates the internalization of the bacteria by non-phagocytic cells [106, 107].

DNT (dermonecrotic toxin) from *Bordetella bronchiseptica*, is also able to activate the same GTPases as does CNF1 by deamination. However, it preferentially modifies the glutamine by *trans*-glutamination using polyamines such as spermine and spermidine, leading to the assembly of actin stress fibers and the formation of focal adhesions [108-110].

## **1.2.2 Inactivation of Rho GTPases.**

### **1.2.2.1 GEF inhibition.**

In order to prevent FcR-mediated phagocytosis by mouse macrophages, EPEC and EHEC modulate GTPase signaling to their advantage by translocating the T3SS effector EspH into eukaryotic cells [111]. This effector directly binds to several Rho GEFs, which prevents their interaction with Rho GTPases. The absence of Rho GTPase activation ultimately induces focal adhesion disassembly, caspase-3 activation, and cytotoxicity in HeLa cells [112].

### **1.2.2.2 GDI mimicry.**

GEF activation can also be prevented by effectors that mimic GDIs and sequester Rho GTPases in their inactive form in the cytosol. The two *Yersinia* T3SS effectors YopO and YpkA do so based on an interaction of their C-terminal domain with RhoA and Rac. YpkA participates in the virulence in *Yersinia* by blocking the Rac-dependent phagocytosis mediated by the FcR [113-115].

### **1.2.2.3 GAP mimicry.**

In the translocated cocktail of T3SS effectors of *Yersinia* and several other pathogens are proteins that regulate the Rho GTPase pathways by mimicking GAPs, leading to enhanced GTP turnover and eventually to the inhibition of phagocytosis. One of the best-characterized

effectors with this function is YopE from *Yersinia*, which targets Rac1, RhoG, RhoA, and Cdc42. Excepting the arginine finger necessary to its GAP function, YopE has no structural similarity with eukaryotic GAPs. However, the structure of YopE is similar to ExoS and SptP from *Pseudomonas aeruginosa* and *Salmonella enterica*, respectively [116, 117]. Interestingly, ExoS, and likewise ExoT and AexT from *Aeromonas*, have a dual activity with an ADP-ribosylating domain in addition of their GAP domain, which adds another level of complexity to the regulation of host signaling pathways [118-121].

#### 1.2.2.4 GTPase release from the plasma membrane.

A further strategy to reduce levels of active small GTPases is to manipulate their membrane binding. YopT and LopT, two effectors from *Yersinia* and *Photobacterium luminescens*, respectively, are related to papain-like cysteine proteases and have an antiphagocytic effect [122, 123]. They inhibit Rho GTPase signaling by cleaving Rho, Rac, and Cdc42 at their C-termini, which releases them from the membrane and leads to their inactivation by host GDIs [123-126].

#### 1.2.2.5 Posttranslational modifications.

To enhance the association of Rho GTPases with GDIs, C3 exoenzyme is a toxin secreted by *Clostridium botulinum* while other pathogens, such as *Staphylococcus aureus*, produce related exoenzymes [127-130]. C3 toxin uses NAD as a substrate to ADP-ribosylate GDP-bound RhoA, RhoB, and RhoC on an asparagine residue [131-133]. In addition to preventing the activation of Rho by GEFs, this modification also promotes the association of the GTPases with GDIs, thereby leading to the accumulation of the inactive GTPase in the cytosol where they get degraded by the proteasome [134, 135]. The C3 toxin is involved in many aspects of pathogenesis, such as migration and invasion of lymphocytes as well as phagocytosis [136, 137]

The large clostridial glucosylating toxins (LCGTs) are expressed by various bacteria of the genus *Clostridium*. These toxins disorganize the actin cytoskeleton and intercellular junctions, thus participating in the alteration of the intestinal barrier [138]. LCGTs are characterized by a DxD motif that is necessary to catalyze the glucosylation of Rho GTPases by using UDP-glucose or UDP-N-acetylglucosamine as a substrate [139, 140]. The modification of a specific threonine residue prevents the interaction with downstream effectors, the activation by GEFs and at last the GTP hydrolysis [141-143]. Ultimately, GTP-bound GTPases accumulate at the membrane without being able to activate their downstream signaling partners [144].

VopS from *Vibrio parahaemolyticus* and IbpA from *Histophilus somni* belong to another set of effectors modifying small GTPases during infection. They catalyze the transfer of an AMP moiety (AMPylation) from ATP to a threonine or tyrosine residue of Rac, Cdc42, and RhoA.

Also in this case, the modification prevents the interaction between the Rho GTPases and their respective downstream effectors, leading to the collapse of the actin cytoskeleton and the disruption of actin-dependent immune functions such as phagocytosis [145, 146]. In addition, VopS prevents the generation of superoxide by NOX2 and the activation of an NF- $\kappa$ B-mediated immune response [147]. The enzymatic activity of VopS and IbpA is linked to the presence of a FIC domain.

Bacteria of the genus *Bartonella* also encode a multitude of Fic proteins that are translocated via a T4SS in the host cell during infection. Unpublished results indicate that several *Bartonella* effector proteins (Beps) modify Rho GTPases by transferring an AMP moiety catalyzed by their FIC domain. As they target the same tyrosine residue as IbpA, this modification is presumably preventing the activation of downstream effectors.

### **1.3 Bacteria of the genus *Bartonella***

The genus *Bartonella* is composed of gram-negative, facultative intracellular pathogens belonging to the class of  $\alpha$ -proteobacteria. *B. bacilliformis* (*Bba*) is a human pathogen responsible for Carrion's disease, which is characterized by an acute phase with hemolytic anemia (Oroya fever) and a subsequent chronic phase associated with multiple vasoproliferative lesions on the skin (Verruga Peruana) [148]. Recently, *Bartonella ancashensis* (*Ban*) has been discovered as a new human pathogen causing Verruga Peruana [149, 150]. *Bartonella quintana* (*Bqu*) also has human as its reservoir host in which it establishes a persistent infection. *Bqu* is the causative agent of trench fever, leading to a five days cyclic fever, bone pain, headache and lasting bacteremia. *B. henselae* (*Bhe*) is the most common species infecting humans although its natural host is the cat, which displays an asymptomatic intraerythrocytic bacteremia. After incidental transmission to humans via a bite or scratches, immunocompetent individuals develop the so-called cat scratch disease that leads to lymphadenopathy and fever. In immunocompromised humans, the infection by *Bqu* and *Bhe* leads to bacillary angiomatosis with multiple vasoproliferative tumors [151].

#### **1.3.1 Infection cycle of *Bartonella*.**

The transmission of *Bartonella* between natural hosts can occur by direct contact or via blood-sucking arthropods, in which the bacteria are present in the gut (Fig. 1.5). The infection cycle starts with the dermal inoculation via contaminated feces. It is speculated that the bacteria reach a dermal niche rich in intrinsically migratory dendritic cells. Subsequently, the infected dendritic cells are used by *Bartonella* as carriers in order to disseminate inside the host. There, bacteria supposedly invade endothelial cells to form the blood-seeding niche, from where they are synchronously released into the bloodstream. For *Bartonella* species of the lineage 4 (lineages: see below, chapter 1.3.2), the adhesion to red blood cells is mediated via the Trw

T4SS and results in their colonization. Finally, bacteria replicate two or three times inside a vacuole and reside for the remaining lifespan of the erythrocytes in their lumen. The cycle is completed once *Bartonella* colonizes the gut of another arthropod after being taken during a blood meal from the infected host [152-154].

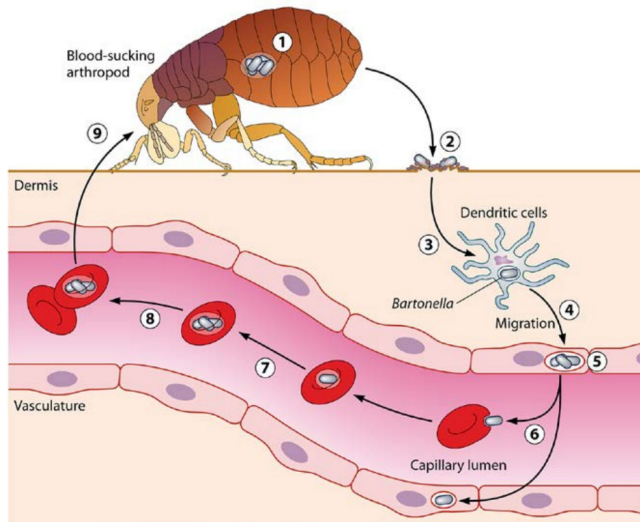


**Figure 1.5. Model of *Bartonella* infection cycle in the reservoir host.**

*Bartonella* replicates in the arthropod vector and is excreted in their feces (1). The dermis of the reservoir host is inoculated via a small lesion or abrasion (2). Bacteria colonize a “dermal niche”, which is proposed to be populated by dendritic cells (3) and which facilitates bacterial dissemination in the host (4). Endothelial cells are believed to be colonized and to form a “blood seeding niche” (5), from which the bacteria would be periodically released into the bloodstream to invade erythrocytes and re-infect the blood-seeding niche (6). After intra-erythrocytic replication (7), *Bartonella* persists in the red blood cells (8) before being taken up by another bloodsucking arthropod, which completes their infectious cycle (9). Adapted from [155].

### 1.3.2 Phylogeny of the genus *Bartonella*.

The *Bartonella* genus contains over 30 species that are separated into four different lineages (L1-L4) (Fig. 1.6) [156]. The members of L1 are exclusively human pathogens, while the reservoir hosts of L2 are limited to ruminants, which suggests a low capacity to adapt to novel hosts. Additionally, the high virulence of *B. bacilliformis* associated with significant morbidity indicates a low adaptation to their human host. However, most *Bartonella* species of L3 and L4 adopt a stealth infection strategy that results in long-lasting infections that do not cause obvious disease symptoms in the reservoir host [151]. The variety of mammalian hosts is associated with the high diversity of species, which is presumably due to adaptive radiation in the evolution of *Bartonella*. This process and the host adaptability are thought to be significantly shaped by the VirB/D4 T4SS, which was several times independently acquired through horizontal gene transfer [151, 157].

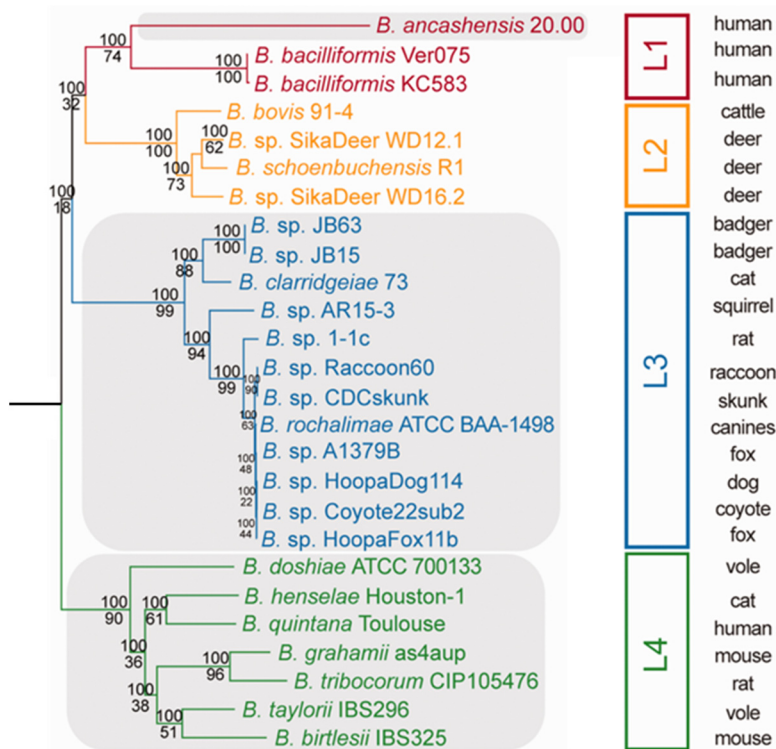


**Figure 1.6. Phylogenetic tree of the genus *Bartonella*.**

Phylogeny of *Bartonella* based on the nucleotide sequence alignment of 509 concatenated core genes. Lineages encoding a VirB/D4 T4SS are highlighted in grey. Corresponding reservoir hosts are indicated on the right-hand side of the tree. Adapted from [156].

### 1.3.3 VirB/VirD4 type IV secretion system.

The T4SS are ancestrally related to conjugation systems and play an important role in the infection cycle of several bacterial pathogens such as *Agrobacterium tumefaciens*, *Bordetella pertussis*, *Legionella pneumophila*, *Helicobacter pylori*, *Brucella*, and *Bartonella* [158, 159].

*Bartonella* species of the lineages 3 and 4, as well as *B. ancashensis* (L1), harbor a VirB/VirD4 T4SS involved in the translocation of bacterial effectors into the host cell during infection. This secretion system is composed of 12 proteins encoded by the *virB* operon and the *virD4* gene. The coupling protein VirD4 is an ATPase mediating the interaction between the T4SS and its substrates, such as bacterial effectors [160]. It also participates in providing energy for the assembly of the machinery and effector translocation with two other ATPases, VirB4 and VirB11 [161, 162]. VirB3 together with VirB6-10 form the translocation channel of the T4SS, spanning both bacterial membranes. VirB7, VirB9, and VirB10 compose its core complex, while VirB2 and VirB5 assemble to form the pilus structure [163, 164].

*Bartonella* species of the lineage 4 encode a second T4SS in the *trw* locus, which is lacking a coupling protein. Although the Trw T4SS is probably not able to translocate bacterial effectors, it is required for red blood cell invasion and the establishment of an intraerythrocytic bacteremia [165].

### 1.3.4 *Bartonella* effector proteins (Beps).

Beps share a common domain architecture in which the C-terminus consists of at least one BID (Bep intracellular delivery) domain and a positively charged tail, while the N-terminus is more divergent and can harbor additional domains (Fig. 1.7).

The majority of all Beps carries an N-terminal FIC (filamentation induced by cAMP) domain, indicating its central role in pathogenesis. The FIC-BID domain organization represents the ancestral effector gene from which other effectors derived via gene duplication, domain shuffling, and sequence variation [166].

A subset of effectors contains tandem-repeat tyrosine-phosphorylation motifs that serve as phosphorylation sites for host kinases. Once modified, some of these effectors recruit host proteins carrying a SH2 domain, which can dock to the phosphorylated tyrosines. This presumably leads to the modulation of cellular processes to the advantage of *Bartonella* [167].

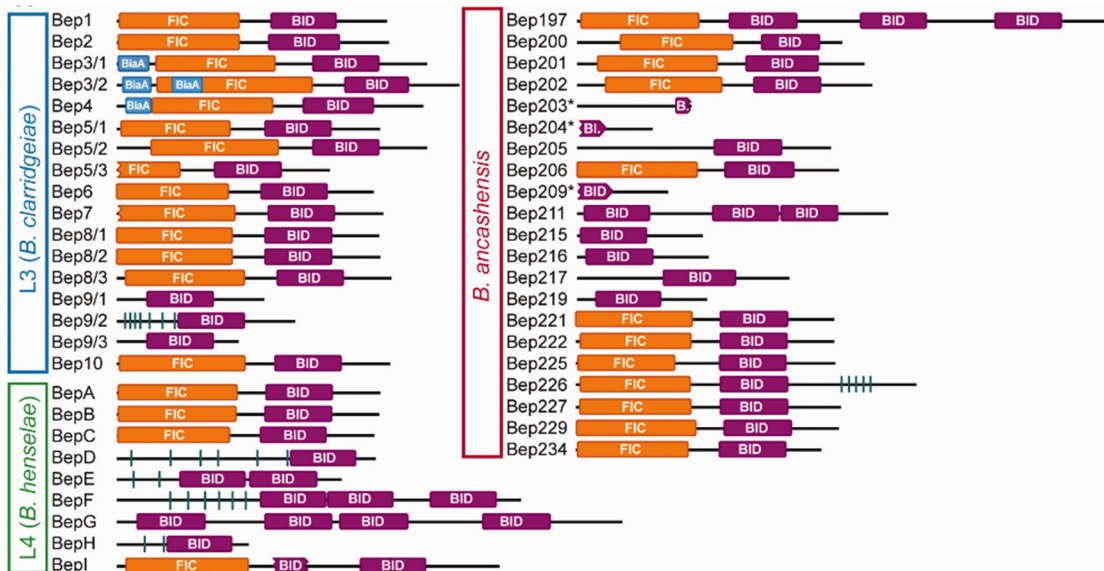


Figure 1.7. Domain architecture of *Bartonella* effector proteins.

Domain architecture of Beps found in *B. ancashensis*, *B. clarridgeiae* (lineage 3 - L3) and *B. henselae* (lineage 4 - L4). The effectors absent in these species are shown from *B. rochalimae* (Bep4) or *B. tribocorum* (BepH and BepI). FIC domains are colored in orange, BID domains in purple and BiaA (Bep-interacting antitoxin) in blue. Predicted tyrosine phosphorylation motifs are depicted as vertical green lines. Taken from [156].

#### 1.3.4.1 BID domain

The BID domain, together with the positively charged tail, is an evolutionary conserved bipartite translocation signal that is also present in conjugative relaxases [168]. 3D structures indicate that the domain is folded into an antiparallel four-helix bundle, which is characterized by the presence of a positively charged hook at the top [169]. Despite some conserved residues exposed on the surface, the BID domain displays significant variability and could mediate specific protein-protein interactions with host proteins.

The presence of additional BID domains in Beps of the lineage 4 and *Ban* indicates that during evolution they might have acquired functions beyond serving the effector translocation process. The BID domains of BepA, BepE, BepF, and BepG, have been shown to play a significant role during *Bartonella* infection [170-172]. However, the molecular mechanisms have been identified only for the BID domain of BepA, which binds the host adenylyl cyclase. The interaction increases the enzymatic activity of the cyclase by GαS and thereby leads to the elevation of the intracellular cyclic AMP (cAMP) concentration [173]. Ultimately, the translocation of BepA by *Bartonella* protects infected cells against apoptosis [174].

#### 1.3.4.2 FIC domain

Fic proteins form a family of proteins harboring a conserved FIC domain catalyzing posttranslational modifications of a target protein. The acronym FIC originates from “filamentation induced by cAMP”, which corresponds to the phenotype caused by a mutation in the gene encoding the first identified Fic protein [175].

FIC domains are characterized by a core composed of six α-helices and containing a signature FIC motif (HxFx(D/E)GNGRxxR, hereafter referred to as the canonical FIC motif) [176]. This motif plays a key role in the transfer of a phosphate-containing group on residues containing a hydroxyl group (Thr, Ser, Tyr). Most of the modifications that have been described are using ATP as a substrate to add an AMP moiety (AMPylation) on a target protein.

However, the activity of Fic proteins is not restricted to AMPylation and some Fic proteins are able to use various substrates to catalyze other posttranslational modifications. AnkX from *Legionella pneumophila* transfers a phosphocholine moiety onto small GTPases of the RAB family, which leads to the modification of vesicular trafficking and promotes bacterial survival [177]. The GTPase-related domain of the bacterial elongation factor Tu (EF-Tu) is phosphorylated by the Fic protein Doc of *E. coli* [178]. It is suggested that the modification of EF-Tu plays a role in the formation of persisters and the organization of the bacterial cytoskeleton [179-181].

Fic proteins are not only targeting proteins with a domain related to small GTPases. AvrAC from the plant pathogen *Xanthomonas campestris* transfers a UMP moiety to two different

plant kinases that are involved in immune defense. Interestingly, AvrB from *Pseudomonas syringae* lacks all conserved residues of the FIC motif, although it shares the same topology with other Fic proteins [182]. Despite the absence of the catalytic residues, this effector induces the phosphorylation of the plant immune regulator RIN4 by RIPK [183]. Although the vast majority of proteins with a FIC domain is found in bacteria, they are present in all domains of life. HYPE (huntingtin-interacting protein E) is the only human Fic protein and has the particularity to form homodimers via its FIC domain [184]. HypE orthologs AMPylate the ATPase domain of BiP (also known as GRP78), a chaperone in the endoplasmic reticulum playing an important role in the unfolded protein response [185, 186].

In *Bartonella* species of the lineages 3 and 4, preliminary results indicate that the FIC domains of Bep1, BepA, and Bep197 share a conserved function by AMPylating Rho GTPases [187] (and unpublished results by Isabel Sorg and Jenifer Sen). Bep2 also targets the cytoskeleton by directly AMPylating vimentin and tubulin *in vitro* [188, 189]. However, the consequences of these modifications during infection remain elusive. For the majority of Beps harboring a FIC domain, the enzymatic activity and the host target remain largely unknown.

#### 1.3.4.3 Class I Fic proteins are reminiscent of toxin-antitoxin modules

Most proteins of the Fic family can be attributed to one of three different classes according to the configuration of their regulatory module. This module is characterized by an inhibitory  $\alpha$ -helix ( $\alpha_{inh}$ ) with a conserved (S/T)xxxE(G/N) motif. The invariant glutamate modifies the conformation of the substrate in the active site, thereby inhibiting the posttranslational modification of the target protein [190]. While in class II and class III Fic proteins the inhibitory helix is directly linked to the N- or the C-terminus of the proteins, respectively,  $\alpha_{inh}$  of class I Fic proteins is present as a distinct protein. Class I Fic proteins are exclusively present in bacteria and represent 5 % of the bona fide AMPylation-competent Fic proteins. This arrangement of Fic protein and  $\alpha_{inh}$  is reminiscent of toxin-antitoxin modules [176]. Hence, the regulatory module of class I Fic proteins is often referred to as the antitoxin. The spatial separation of the inhibitory helix and the Fic protein allows to remove the regulatory module and thereby to tune the activity of the Fic protein. In absence of  $\alpha_{inh}$  the expression of class I Fic proteins is highly toxic to bacteria.

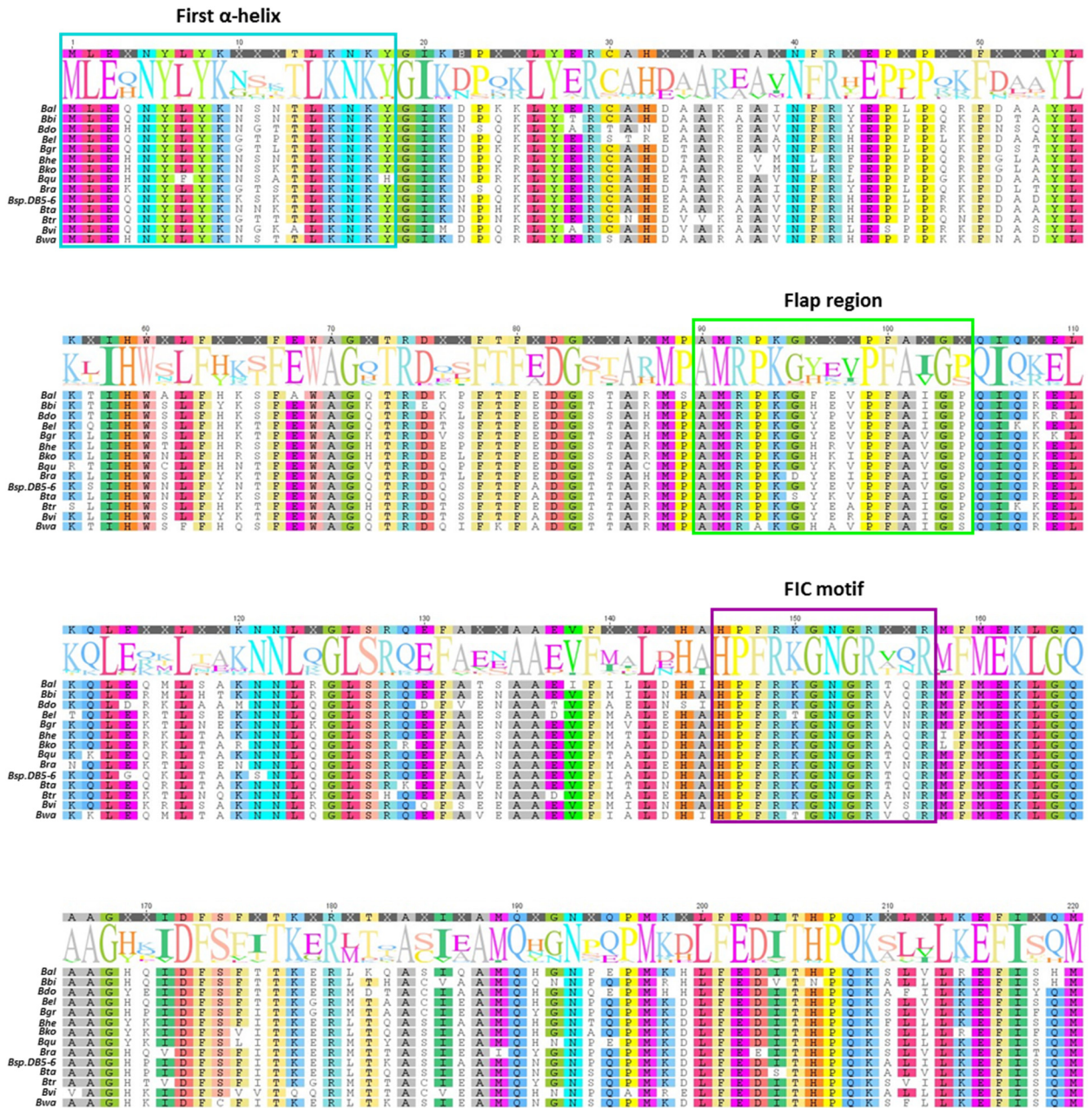
VbhT of *B. schoenbuchensis* is the best-characterized class I Fic protein of *Bartonella*. When expressed in *E. coli*, VbhT inhibits bacterial growth by AMPylating DNA gyrase and topoisomerase IV [191]. The activity of VbhT is repressed by its interaction with VbhA antitoxin, which competes with ATP binding [190]. Bep1, Bep2, and BepA also belong to class I Fic proteins, while Bep3 and Bep4 from the lineage 3 belong to the class II [188, 189, 192]. For many other Beps, the attribution to the different classes of Fic proteins is not yet elucidated.



## 1.4 *Bartonella* effector protein C (BepC)

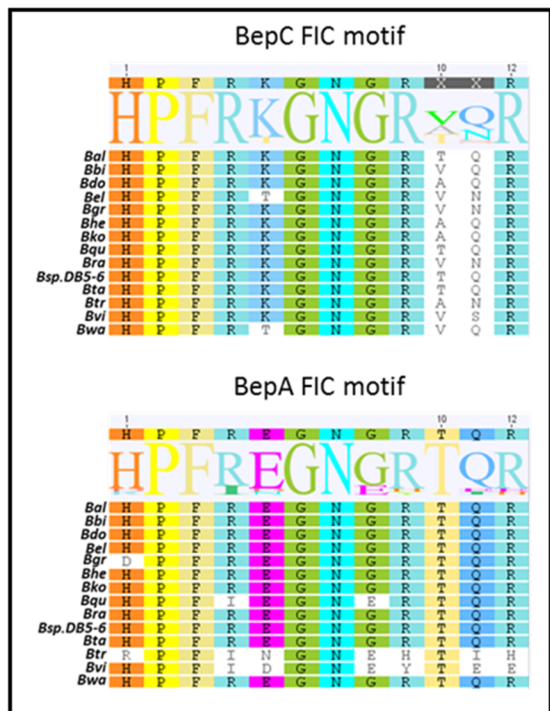
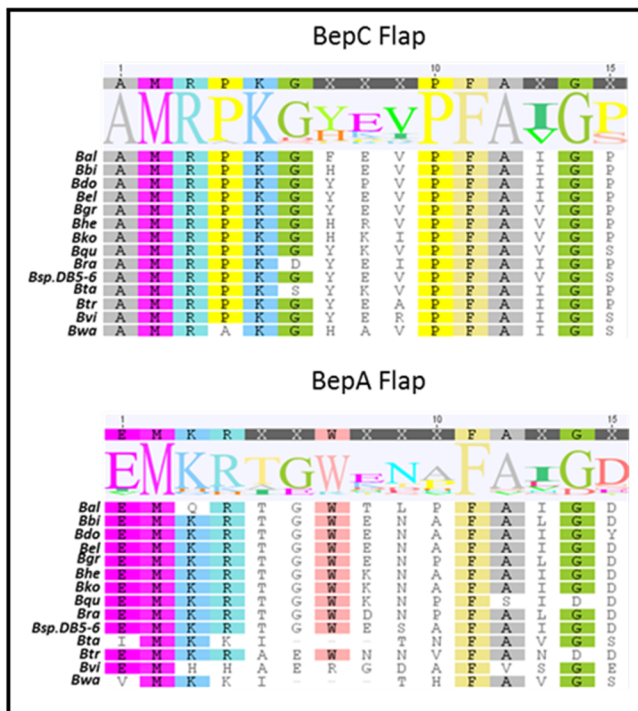
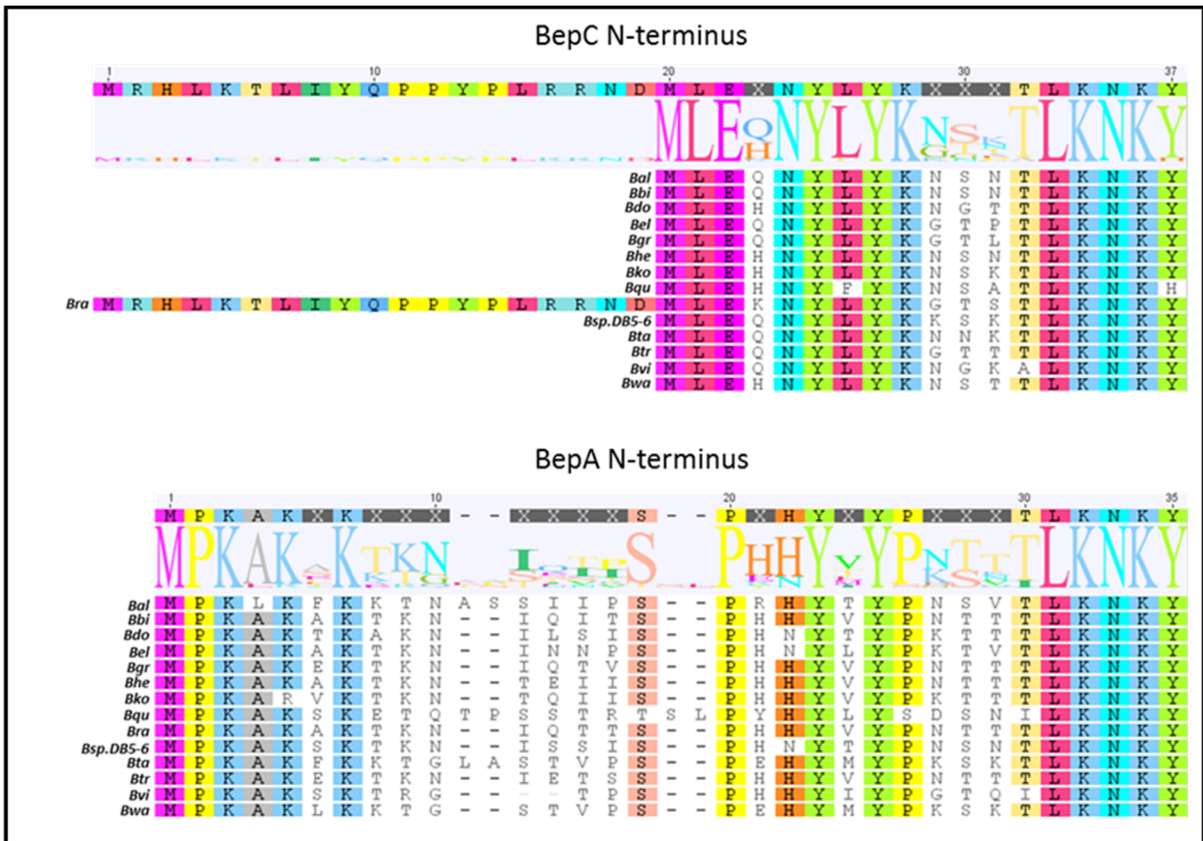
One Bep for which the Fic protein class affiliation had not been studied is BepC. BepC is present in all *Bartonella* species of the lineage 4, suggesting an important role in pathogenesis and making it a prime candidate for further investigations. BepC displays the ancestral effector architecture consisting of a highly conserved N-terminal FIC domain (Alignment 1.1) and a more divergent C-terminal BID domain. A central OB (oligosaccharide binding) fold is also present between the FIC and BID domains of BepC. Its five-stranded  $\beta$ -barrel structure is found in many Beps and conjugative relaxases, suggesting that it has been acquired together with the BID domain during evolution [187]. Although its role remains elusive, the OB fold could simply serve as a linker as well as it may have acquired a new function.

- Introduction -



**Alignment 1.1. FIC domain of BepC (amino acids 1-220) from *Bartonella* species of the lineage 4.**

The first 19 amino acids of BepC<sub>Bra</sub> are not displayed in this alignment. The first  $\alpha$ -helix (positions 1-18) is framed in cyan, the Flap region in green and the FIC motif in magenta. Highlighted residues have a sequence identity of at least 75%.



Alignment 1.2. N-terminus, Flap region, and FIC motif of BepC and BepA from *Bartonella* species of the lineage 4.

Comparison of the sequences of the N-terminus, the Flap and the FIC motif of BepC (framed in alignment 1) with the corresponding sequences of BepA. Highlighted residues have a sequence identity of at least 75%.

### 1.4.1 Structural studies of the BepC FIC domain.

The FIC domain of BepC from *Bartonella tribocorum* (BepC<sub>Btr</sub>) was co-crystallized with AMP-PNP, a non-hydrolysable analog of ATP, in the active site (Fig. 1.8). The FIC domain is organized in two lobes separated by a channel that is surrounded by highly conserved residues. The nucleotide occupies the central part of the channel and is framed by a  $\beta$ -hairpin (Flap) on one side and by the FIC motif on the other side.

In Fic proteins with a canonical FIC motif (HxFx(D/E)GNGRxxR), the conserved histidine activates the hydroxyl group of a target protein residue for a nucleophilic attack on the substrate phosphodiester bond. The invariant arginine residues directly stabilize the negative charges of the nucleotide phosphate, while an ion of magnesium is mediating the interaction with the negatively charged residue in the FIC motif (D/E) (Fig. 1.9A).

BepC is characterized by a non-canonical FIC motif (HxFxKGNRxxR), which differs from the canonical motif in a lysine instead of the acidic residue (D/E). Alternatively, the lysine is replaced by a threonine residue in two *Bartonella* species (Alignment 1.2). The 3D structure indicates that the lysine is directly interacting with the  $\alpha$ - and  $\beta$ -phosphates of the ATP analog (Fig. 1.9B). The superimposition of the ATP crystallized in VbhT and the AMP-PNP that is present in the active site of BepC<sub>Btr</sub> suggests that the  $\alpha$ -phosphate is in the right position to be targeted by a nucleophilic attack (Fig. 1.9C). All the other residues composing the FIC motif are strictly conserved, suggesting their importance for the function of BepC.

A  $\beta$ -hairpin located next to the active site and referred to as the Flap is present in all Fic proteins, Doc of *E. coli* excluded. This region participates in the docking of the target protein by forming an intermolecular antiparallel  $\beta$ -sheet, which leads to the positioning of the target hydroxyl into the active site [182, 193, 194]. In BepC, the residues composing the Flap region are highly conserved except for three residues forming the extremity of the loop. The sequence strongly differs from the Flap of BepA, the only other Fic Bep present in all *Bartonella* species of the lineage 4, potentially indicating a specific role in host protein binding (Alignment 1.2).

Some Fic proteins, such as lbpA and VopS, contain an additional N-terminal domain involved in target recognition [193, 195]. Although BepC does not harbor this distinct domain, its first  $\alpha$ -helix (residues 1-18) contains 14 residues highly conserved throughout different *Bartonella* species (Alignment 1.2). Eight of these residues are also highly conserved between BepC and BepA, which could indicate an important function in structural organization. However, this conserved patch exposed at the protein surface and localized next to the active site might also participate in target binding (Fig. 1.8). It is interesting to note that only BepC from *B. rattimassiliensis* has an extended N-terminus while this is a common feature among BepA proteins of different species.



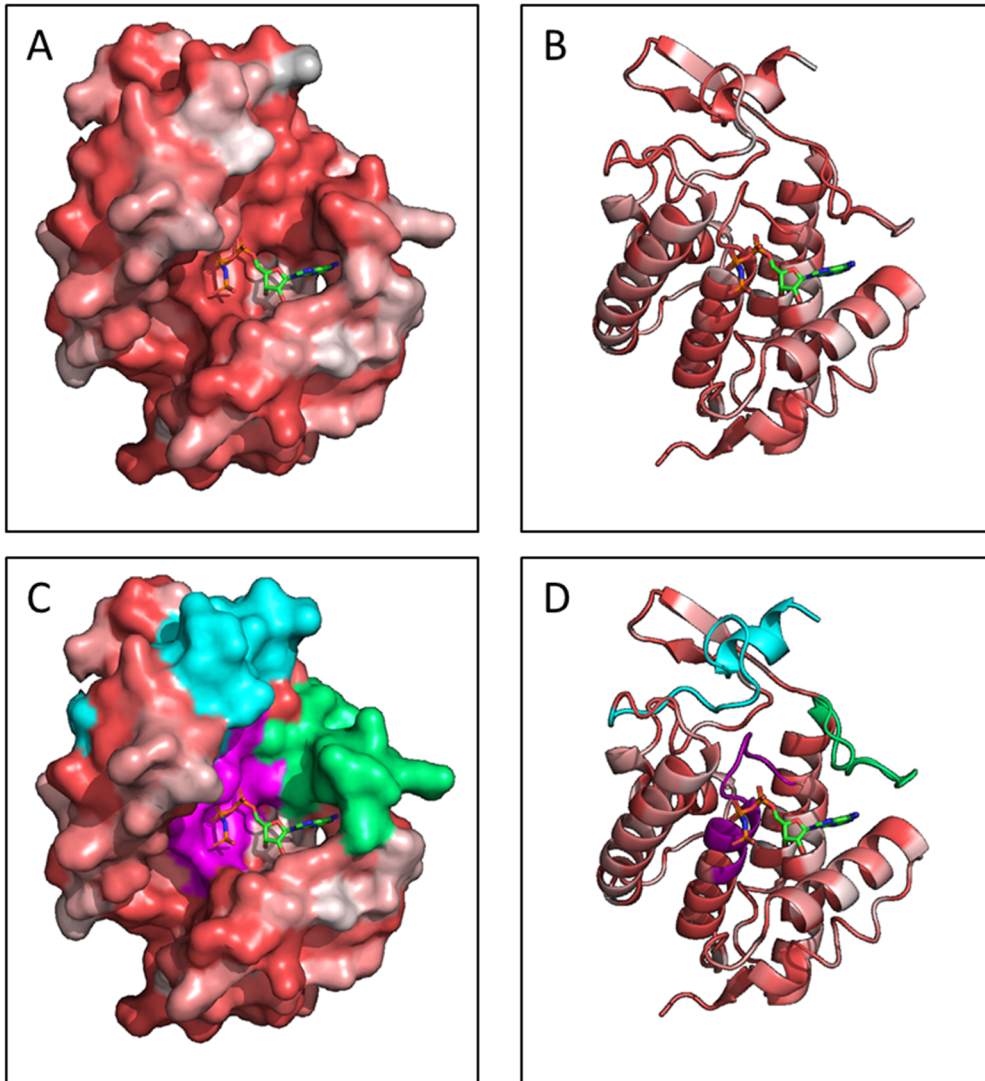


**Figure 1.8. Crystal structure of the FIC domain of BepC<sub>Btr</sub> (3-209) coordinating a nucleotide analog.**

**A.** Surface representation of the crystal structure of BepC<sub>Btr</sub> with AMP-PNP, a non-hydrolysable derivative of ATP, in the active site. The red color gradient represents pairwise identity based on 14 alignments of BepC from different *Bartonella* species. The most conserved residues are represented in red and less conserved residues in white. **B.** Cartoon representation of (A) **C.** Reproduction of (A) with the first  $\alpha$ -helix (amino acids 3-18) in cyan, the Flap region in green and the FIC motif in magenta. **D.** Cartoon representation of (C). Structure solved by the Seattle Structural Genomics Center for Infectious Disease (SSGCID) consortium. Models done in Pymol in collaboration with Markus Huber.

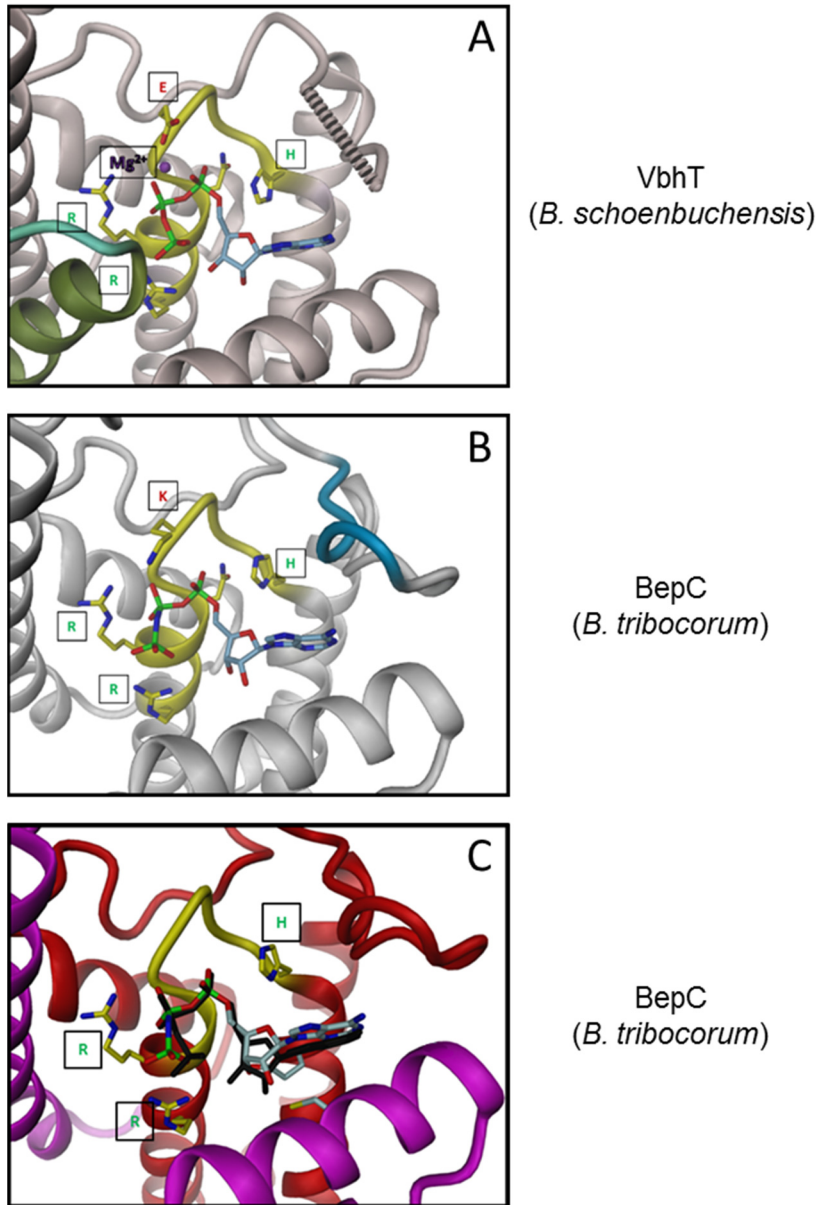


**Figure 1.9. BepC<sub>Btr</sub> binds an ATP derivative in an AMPylation-compatible configuration.**

Cartoon representation of the FIC domain of BepC<sub>Btr</sub>. The core residues of the FIC motif are represented as yellow sticks. **A.** Crystal structure of the FIC domain of VbhT with ATP in the active site. Mg<sup>2+</sup> mediates the interaction between the glutamate of the FIC domain (highlighted in red) and the phosphates of the ATP. **B.** Crystal structure of the FIC domain of BepC<sub>Btr</sub> with AMP-PNP in the active site. The conserved lysine (in red) directly interacts with the phosphate of the ATP derivative. The Flap is partially highlighted in blue. **C.** Superimposition of the ATP of VbhT (in black) and the crystal structure of the FIC domain of BepC<sub>Btr</sub> with AMP-PNP. Structure solved by the Seattle Structural Genomics Center for Infectious Disease (SSGCID) consortium. Models done by Frederic Stanger.

### 1.4.2 BepC in the context of pathogenesis.

The role of BepC during infection has so far been investigated in the context of other effectors, primarily BepE and BepF.

#### 1.4.2.1 Cell fragmentation induced by BepC.

BepC induces cell fragmentation of infected endothelial cells due to a rear-end detachment defect during migration [170]. However, the presence of BepE is able to suppress this deleterious effect mediated by BepC. BepE is composed of a N-terminus containing tandem-repeat tyrosine-phosphorylation motifs and two C-terminal BID domains. Interestingly, the phosphotyrosine-containing motifs, which recruit host signaling proteins with a SH2 domain [167], do not contribute to the phenotype reduction. By contrast, the two BID domains or the C-terminal BID domain alone are able to overcome cell fragmentation mediated by BepC. The molecular mechanism underlying this process and the putative host target of BepE remain elusive. As BepE interferes with the inhibitory effect of a C3-toxin derivative that inactivates RhoA, RhoB, and RhoC, it is conceivable that BepE interferes with the RhoA pathway acting on the cytoskeleton. The recruitment of BepE to cell-cell contacts and to the rear-end of migrating cells is supportive of an effect on the cytoskeleton. *In vivo*, rats infected intradermally (i.d.) with *B. tribocurum* lacking *bepD* and *bepE* (*Btr ΔbepDE*) do not develop bacteremia, while intravenous inoculation produces a long-lasting infection. Complementation with full-length BepE or the BID domains only restored the ability of *Btr ΔbepDE* to establish bacteremia after i.d. infection [170]. Based on these results, BepE plays an important role during the dermal stage of infection and is required to reach the blood. For this transition from the dermis to the blood, the ancestrally related *Brucella abortus* and also *Bordetella bronchiseptica* are known to use dendritic cells as a shuttle for the bacterial dissemination in the host [196, 197]. Thus, it is thinkable that *Bartonella* is able to take the same route. In such a scenario, it is proposed that the presence of BepE is necessary to ensure the migration, as BepC impairs cell motility *in vitro*.

#### 1.4.2.2 BepC induces, together with BepF, invasome formation

As it is the case on the organismic level, the detailed understanding of the *Bartonella* infection process is also limited on the cellular level. *In vitro* investigations with *Bartonella henselae* suggest a multi-step invasion process, the so-called invasome formation, during which large clusters of bacteria are engulfed via actin-rich protrusions [198] (Fig. 1.10). The term invasome corresponds to the host cellular structure characterized by a compact actin ring composed of stress fibers that participate in the internalization of a bacterial aggregate.

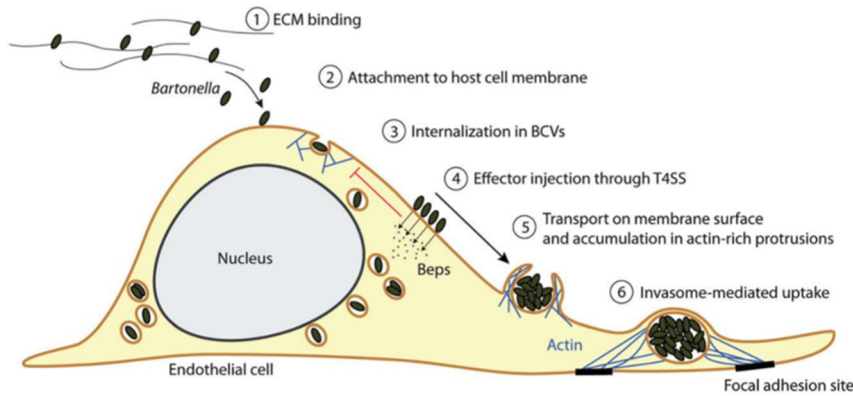


**Figure 1.10. *Bhe* induces invasome formation.**

*B. henselae* binds to the extracellular matrix (ECM) via outer membrane proteins (1) and to the plasma membrane of the host cell (2). Individual bacteria are internalized in *Bartonella* containing vacuoles (BCVs), which localize to the periphery of the nucleus (3). After translocation of Beps into the cytoplasm of the host cell, the uptake of single bacteria is inhibited (4) and leads to the formation of large bacterial aggregates at the surface of the plasma membrane (5). Such bacterial clusters are engulfed via actin-rich protrusions to form an invasome (6). Taken from [199].

Invasome formation can be triggered by different effectors, either by BepG alone or by BepC in collaboration with BepF [172, 200]. It has been established that out of the three BID domains in BepF the two first ones are sufficient to give rise to invasome formation together with BepC. Interestingly, the invasome formation ability of the first BID domain depends on a WxxxE motif, which is found in GEF-mimicking bacterial effectors (see chapter 1.2.1.1). The function of BepF can be substituted by the expression of constitutively active Rac1 or Cdc42, suggesting that the effector is tuning their activity during the infection process. Speaking for such a stimulation are the formation of filopodia-like structures and membrane protrusions in cultured cells in presence of BepF [171] and that invasome formation requires WAVE, WASP, and Arp2/3, which are downstream effectors of Rac1 and Cdc42 signaling. Additionally, cofilin 1, a protein controlling the actin turnover and that is regulated by Rho and Cdc42, is also required for BepC and BepF-triggered invasome formation [200]. However, the exact molecular mechanism to initiate invasome formation is not fully resolved. The current model is based on the finding that BepC together with BepF (as well as BepG alone) lead to the inhibition of BCV formation following the endocytic uptake of single bacteria [172, 200]. The accumulation of *B. henselae* at the cell membrane induces a subsequent clustering of *Bhe*-bound integrin  $\beta 1$  and concomitant actin rearrangements, which ultimately leads to invasome formation. This hypothesis is supported by the requirement of integrin  $\beta 1$ , talin1, paxillin, vinculin, FAK, and Src, which are all major contributors to integrin  $\beta 1$ -mediated outside-in signaling and thus to invasome formation [201]. The actual correspondence to this model needs corroboration and the physiological role of invasome formation remains to be investigated. It may be speculated



that bacteria transcytose in invasomes to cross the endothelial barrier in order to be released into the bloodstream [159]. The clustering of *Bhe* observed *in vitro* resembles *in vivo* aggregates of *Bartonella* found in the proximity of proliferating endothelial cells of bacillary angiomatosis lesions [202].

## 1.5 References

1. Tybulewicz, V.L. and R.B. Henderson, *Rho family GTPases and their regulators in lymphocytes*. Nat Rev Immunol, 2009. **9**(9): p. 630-44.
2. Lawson, C.D. and A.J. Ridley, *Rho GTPase signaling complexes in cell migration and invasion*. J Cell Biol, 2018. **217**(2): p. 447-457.
3. Sadok, A. and C.J. Marshall, *Rho GTPases: masters of cell migration*. Small GTPases, 2014. **5**: p. e29710.
4. Komarova, Y.A., et al., *Protein Interactions at Endothelial Junctions and Signaling Mechanisms Regulating Endothelial Permeability*. Circ Res, 2017. **120**(1): p. 179-206.
5. Parsons, J.T., A.R. Horwitz, and M.A. Schwartz, *Cell adhesion: integrating cytoskeletal dynamics and cellular tension*. Nat Rev Mol Cell Biol, 2010. **11**(9): p. 633-43.
6. Zihni, C., M.S. Balda, and K. Matter, *Signalling at tight junctions during epithelial differentiation and microbial pathogenesis*. J Cell Sci, 2014. **127**(Pt 16): p. 3401-13.
7. Jaffe, A.B. and A. Hall, *Rho GTPases: biochemistry and biology*. Annu Rev Cell Dev Biol, 2005. **21**: p. 247-69.
8. Narumiya, S. and S. Yasuda, *Rho GTPases in animal cell mitosis*. Curr Opin Cell Biol, 2006. **18**(2): p. 199-205.
9. Boureux, A., et al., *Evolution of the Rho family of ras-like GTPases in eukaryotes*. Mol Biol Evol, 2007. **24**(1): p. 203-16.
10. Aspenstrom, P., A. Ruusala, and D. Pacholsky, *Taking Rho GTPases to the next level: the cellular functions of atypical Rho GTPases*. Exp Cell Res, 2007. **313**(17): p. 3673-9.
11. Chardin, P., *Function and regulation of Rnd proteins*. Nat Rev Mol Cell Biol, 2006. **7**(1): p. 54-62.
12. Heasman, S.J. and A.J. Ridley, *Mammalian Rho GTPases: new insights into their functions from in vivo studies*. Nat Rev Mol Cell Biol, 2008. **9**(9): p. 690-701.
13. Rossman, K.L., C.J. Der, and J. Sondek, *GEF means go: turning on RHO GTPases with guanine nucleotide-exchange factors*. Nat Rev Mol Cell Biol, 2005. **6**(2): p. 167-80.
14. Roberts, P.J., et al., *Rho Family GTPase modification and dependence on CAAX motif-signaled posttranslational modification*. J Biol Chem, 2008. **283**(37): p. 25150-63.
15. Navarro-Lerida, I., et al., *A palmitoylation switch mechanism regulates Rac1 function and membrane organization*. EMBO J, 2012. **31**(3): p. 534-51.
16. Scheffzek, K., et al., *The Rac-RhoGDI complex and the structural basis for the regulation of Rho proteins by RhoGDI*. Nat Struct Biol, 2000. **7**(2): p. 122-6.
17. Garcia-Mata, R., E. Boulter, and K. Burridge, *The 'invisible hand': regulation of RHO GTPases by RHOGDIs*. Nat Rev Mol Cell Biol, 2011. **12**(8): p. 493-504.
18. Vetter, I.R. and A. Wittinghofer, *The guanine nucleotide-binding switch in three dimensions*. Science, 2001. **294**(5545): p. 1299-304.
19. Bos, J.L., H. Rehmann, and A. Wittinghofer, *GEFs and GAPs: critical elements in the control of small G proteins*. Cell, 2007. **129**(5): p. 865-77.
20. Iden, S. and J.G. Collard, *Crosstalk between small GTPases and polarity proteins in cell polarization*. Nat Rev Mol Cell Biol, 2008. **9**(11): p. 846-59.
21. Rittinger, K., et al., *Structure at 1.65 Å of RhoA and its GTPase-activating protein in complex with a transition-state analogue*. Nature, 1997. **389**(6652): p. 758-62.
22. Bourne, H.R., *G proteins. The arginine finger strikes again*. Nature, 1997. **389**(6652): p. 673-4.
23. Pellegrin, S. and H. Mellor, *Actin stress fibres*. J Cell Sci, 2007. **120**(Pt 20): p. 3491-9.
24. Steffen, A., et al., *Rac function is crucial for cell migration but is not required for spreading and focal adhesion formation*. J Cell Sci, 2013. **126**(Pt 20): p. 4572-88.

25. Nobes, C.D. and A. Hall, *Rho, rac, and cdc42 GTPases regulate the assembly of multimolecular focal complexes associated with actin stress fibers, lamellipodia, and filopodia*. *Cell*, 1995. **81**(1): p. 53-62.
26. Hall, A., *Rho GTPases and the actin cytoskeleton*. *Science*, 1998. **279**(5350): p. 509-14.
27. Mattila, P.K. and P. Lappalainen, *Filopodia: molecular architecture and cellular functions*. *Nat Rev Mol Cell Biol*, 2008. **9**(6): p. 446-54.
28. Mitra, S.K., D.A. Hanson, and D.D. Schlaepfer, *Focal adhesion kinase: in command and control of cell motility*. *Nat Rev Mol Cell Biol*, 2005. **6**(1): p. 56-68.
29. Friedl, P. and K. Wolf, *Tumour-cell invasion and migration: diversity and escape mechanisms*. *Nat Rev Cancer*, 2003. **3**(5): p. 362-74.
30. Vicente-Manzanares, M., et al., *Non-muscle myosin II takes centre stage in cell adhesion and migration*. *Nat Rev Mol Cell Biol*, 2009. **10**(11): p. 778-90.
31. Wilkinson, S., H.F. Paterson, and C.J. Marshall, *Cdc42-MRCK and Rho-ROCK signalling cooperate in myosin phosphorylation and cell invasion*. *Nat Cell Biol*, 2005. **7**(3): p. 255-61.
32. Maekawa, M., et al., *Signaling from Rho to the actin cytoskeleton through protein kinases ROCK and LIM-kinase*. *Science*, 1999. **285**(5429): p. 895-8.
33. Riento, K. and A.J. Ridley, *Rocks: multifunctional kinases in cell behaviour*. *Nat Rev Mol Cell Biol*, 2003. **4**(6): p. 446-56.
34. Unbekandt, M. and M.F. Olson, *The actin-myosin regulatory MRCK kinases: regulation, biological functions and associations with human cancer*. *J Mol Med (Berl)*, 2014. **92**(3): p. 217-25.
35. Kale, V.P., et al., *The regulatory roles of ROCK and MRCK kinases in the plasticity of cancer cell migration*. *Cancer Lett*, 2015. **361**(2): p. 185-96.
36. Zhao, Z. and E. Manser, *Myotonic dystrophy kinase-related Cdc42-binding kinases (MRCK), the ROCK-like effectors of Cdc42 and Rac1*. *Small GTPases*, 2015. **6**(2): p. 81-8.
37. Lee, I.C., T. Leung, and I. Tan, *Adaptor protein LRAP25 mediates myotonic dystrophy kinase-related Cdc42-binding kinase (MRCK) regulation of LIMK1 protein in lamellipodial F-actin dynamics*. *J Biol Chem*, 2014. **289**(39): p. 26989-7003.
38. Leung, T., et al., *Myotonic dystrophy kinase-related Cdc42-binding kinase acts as a Cdc42 effector in promoting cytoskeletal reorganization*. *Mol Cell Biol*, 1998. **18**(1): p. 130-40.
39. Tan, I., et al., *Phosphorylation of a novel myosin binding subunit of protein phosphatase 1 reveals a conserved mechanism in the regulation of actin cytoskeleton*. *J Biol Chem*, 2001. **276**(24): p. 21209-16.
40. Sandquist, J.C. and A.R. Means, *The C-terminal tail region of nonmuscle myosin II directs isoform-specific distribution in migrating cells*. *Mol Biol Cell*, 2008. **19**(12): p. 5156-67.
41. Tan, I., et al., *A tripartite complex containing MRCK modulates lamellar actomyosin retrograde flow*. *Cell*, 2008. **135**(1): p. 123-36.
42. Cai, Y., et al., *Nonmuscle myosin IIA-dependent force inhibits cell spreading and drives F-actin flow*. *Biophys J*, 2006. **91**(10): p. 3907-20.
43. Kolega, J., *Asymmetric distribution of myosin IIB in migrating endothelial cells is regulated by a rho-dependent kinase and contributes to tail retraction*. *Mol Biol Cell*, 2003. **14**(12): p. 4745-57.
44. Worthylake, R.A., et al., *RhoA is required for monocyte tail retraction during transendothelial migration*. *J Cell Biol*, 2001. **154**(1): p. 147-60.
45. Palecek, S.P., et al., *Physical and biochemical regulation of integrin release during rear detachment of migrating cells*. *J Cell Sci*, 1998. **111 ( Pt 7)**: p. 929-40.
46. Glading, A., D.A. Lauffenburger, and A. Wells, *Cutting to the chase: calpain proteases in cell motility*. *Trends Cell Biol*, 2002. **12**(1): p. 46-54.
47. Arnold, T.R., R.E. Stephenson, and A.L. Miller, *Rho GTPases and actomyosin: Partners in regulating epithelial cell-cell junction structure and function*. *Exp Cell Res*, 2017. **358**(1): p. 20-30.

48. Schneeberger, E.E. and R.D. Lynch, *The tight junction: a multifunctional complex*. Am J Physiol Cell Physiol, 2004. **286**(6): p. C1213-28.
49. Tornavaca, O., et al., *ZO-1 controls endothelial adherens junctions, cell-cell tension, angiogenesis, and barrier formation*. J Cell Biol, 2015. **208**(6): p. 821-38.
50. Terry, S.J., et al., *Spatially restricted activation of RhoA signalling at epithelial junctions by p114RhoGEF drives junction formation and morphogenesis*. Nat Cell Biol, 2011. **13**(2): p. 159-66.
51. Noritake, J., et al., *IQGAP1: a key regulator of adhesion and migration*. J Cell Sci, 2005. **118**(Pt 10): p. 2085-92.
52. Kuroda, S., et al., *Role of IQGAP1, a target of the small GTPases Cdc42 and Rac1, in regulation of E-cadherin-mediated cell-cell adhesion*. Science, 1998. **281**(5378): p. 832-5.
53. Wojciak-Stothard, B. and A.J. Ridley, *Rho GTPases and the regulation of endothelial permeability*. Vascul Pharmacol, 2002. **39**(4-5): p. 187-99.
54. Arbibe, L., et al., *Toll-like receptor 2-mediated NF-kappa B activation requires a Rac1-dependent pathway*. Nat Immunol, 2000. **1**(6): p. 533-40.
55. Chen, L.Y., et al., *IL-1 receptor-associated kinase and low molecular weight GTPase RhoA signal molecules are required for bacterial lipopolysaccharide-induced cytokine gene transcription*. J Immunol, 2002. **169**(7): p. 3934-9.
56. Teusch, N., et al., *The low molecular weight GTPase RhoA and atypical protein kinase Czeta are required for TLR2-mediated gene transcription*. J Immunol, 2004. **173**(1): p. 507-14.
57. Girardin, S.E., et al., *Nod1 detects a unique muropeptide from gram-negative bacterial peptidoglycan*. Science, 2003. **300**(5625): p. 1584-7.
58. Inohara, et al., *NOD-LRR proteins: role in host-microbial interactions and inflammatory disease*. Annu Rev Biochem, 2005. **74**: p. 355-83.
59. Ogura, Y., et al., *Nod2, a Nod1/Apaf-1 family member that is restricted to monocytes and activates NF-kappaB*. J Biol Chem, 2001. **276**(7): p. 4812-8.
60. Kestera, A.M. and A.J. Baumler, *Detection of enteric pathogens by the nodosome*. Trends Immunol, 2014. **35**(3): p. 123-30.
61. Kestera, A.M., et al., *Manipulation of small Rho GTPases is a pathogen-induced process detected by NOD1*. Nature, 2013. **496**(7444): p. 233-7.
62. Legrand-Poels, S., et al., *Modulation of Nod2-dependent NF-kappaB signaling by the actin cytoskeleton*. J Cell Sci, 2007. **120**(Pt 7): p. 1299-310.
63. Springer, T.A., *Adhesion receptors of the immune system*. Nature, 1990. **346**(6283): p. 425-34.
64. Nimmerjahn, F. and J.V. Ravetch, *Fcgamma receptors as regulators of immune responses*. Nat Rev Immunol, 2008. **8**(1): p. 34-47.
65. Mao, Y. and S.C. Finnemann, *Regulation of phagocytosis by Rho GTPases*. Small GTPases, 2015. **6**(2): p. 89-99.
66. Caron, E. and A. Hall, *Identification of two distinct mechanisms of phagocytosis controlled by different Rho GTPases*. Science, 1998. **282**(5394): p. 1717-21.
67. Tzircotis, G., V.M. Braga, and E. Caron, *RhoG is required for both FcgammaR- and CR3-mediated phagocytosis*. J Cell Sci, 2011. **124**(Pt 17): p. 2897-902.
68. Nauseef, W.M., *How human neutrophils kill and degrade microbes: an integrated view*. Immunol Rev, 2007. **219**: p. 88-102.
69. Singel, K.L. and B.H. Segal, *NOX2-dependent regulation of inflammation*. Clin Sci (Lond), 2016. **130**(7): p. 479-90.
70. Pizzolla, A., et al., *Reactive oxygen species produced by the NADPH oxidase 2 complex in monocytes protect mice from bacterial infections*. J Immunol, 2012. **188**(10): p. 5003-11.
71. Diebold, B.A. and G.M. Bokoch, *Molecular basis for Rac2 regulation of phagocyte NADPH oxidase*. Nat Immunol, 2001. **2**(3): p. 211-5.
72. Bedard, K. and K.H. Krause, *The NOX family of ROS-generating NADPH oxidases: physiology and pathophysiology*. Physiol Rev, 2007. **87**(1): p. 245-313.

73. Abdel-Latif, D., et al., *Rac2 is critical for neutrophil primary granule exocytosis*. Blood, 2004. **104**(3): p. 832-9.
74. Yamauchi, A., et al., *Rac2-deficient murine macrophages have selective defects in superoxide production and phagocytosis of opsonized particles*. J Immunol, 2004. **173**(10): p. 5971-9.
75. Roberts, A.W., et al., *Deficiency of the hematopoietic cell-specific Rho family GTPase Rac2 is characterized by abnormalities in neutrophil function and host defense*. Immunity, 1999. **10**(2): p. 183-96.
76. Ambruso, D.R., et al., *Human neutrophil immunodeficiency syndrome is associated with an inhibitory Rac2 mutation*. Proc Natl Acad Sci U S A, 2000. **97**(9): p. 4654-9.
77. Williams, D.A., et al., *Dominant negative mutation of the hematopoietic-specific Rho GTPase, Rac2, is associated with a human phagocyte immunodeficiency*. Blood, 2000. **96**(5): p. 1646-54.
78. Popoff, M.R., *Bacterial factors exploit eukaryotic Rho GTPase signaling cascades to promote invasion and proliferation within their host*. Small GTPases, 2014. **5**.
79. Bulgin, R., et al., *Bacterial guanine nucleotide exchange factors SopE-like and WxxxE effectors*. Infect Immun, 2010. **78**(4): p. 1417-25.
80. Klink, B.U., et al., *Structure of Shigella IpgB2 in complex with human RhoA: implications for the mechanism of bacterial guanine nucleotide exchange factor mimicry*. J Biol Chem, 2010. **285**(22): p. 17197-208.
81. Boyle, E.C., N.F. Brown, and B.B. Finlay, *Salmonella enterica serovar Typhimurium effectors SopB, SopE, SopE2 and SipA disrupt tight junction structure and function*. Cell Microbiol, 2006. **8**(12): p. 1946-57.
82. Bruno, V.M., et al., *Salmonella Typhimurium type III secretion effectors stimulate innate immune responses in cultured epithelial cells*. PLoS Pathog, 2009. **5**(8): p. e1000538.
83. Bakshi, C.S., et al., *Identification of SopE2, a Salmonella secreted protein which is highly homologous to SopE and involved in bacterial invasion of epithelial cells*. J Bacteriol, 2000. **182**(8): p. 2341-4.
84. Figueira, R. and D.W. Holden, *Functions of the Salmonella pathogenicity island 2 (SPI-2) type III secretion system effectors*. Microbiology, 2012. **158**(Pt 5): p. 1147-61.
85. Hardt, W.D., et al., *S. typhimurium encodes an activator of Rho GTPases that induces membrane ruffling and nuclear responses in host cells*. Cell, 1998. **93**(5): p. 815-26.
86. Friebel, A., et al., *SopE and SopE2 from Salmonella typhimurium activate different sets of RhoGTPases of the host cell*. J Biol Chem, 2001. **276**(36): p. 34035-40.
87. Beuzon, C.R., et al., *Salmonella maintains the integrity of its intracellular vacuole through the action of SifA*. EMBO J, 2000. **19**(13): p. 3235-49.
88. Brumell, J.H., et al., *SifA permits survival and replication of Salmonella typhimurium in murine macrophages*. Cell Microbiol, 2001. **3**(2): p. 75-84.
89. Ohlson, M.B., et al., *Structure and function of Salmonella SifA indicate that its interactions with SKIP, SseJ, and RhoA family GTPases induce endosomal tubulation*. Cell Host Microbe, 2008. **4**(5): p. 434-46.
90. Huang, Z., et al., *Structural insights into host GTPase isoform selection by a family of bacterial GEF mimics*. Nat Struct Mol Biol, 2009. **16**(8): p. 853-60.
91. Ohya, K., et al., *IpgB1 is a novel Shigella effector protein involved in bacterial invasion of host cells. Its activity to promote membrane ruffling via Rac1 and Cdc42 activation*. J Biol Chem, 2005. **280**(25): p. 24022-34.
92. Handa, Y., et al., *Shigella IpgB1 promotes bacterial entry through the ELMO-Dock180 machinery*. Nat Cell Biol, 2007. **9**(1): p. 121-8.
93. Alto, N.M., et al., *Identification of a bacterial type III effector family with G protein mimicry functions*. Cell, 2006. **124**(1): p. 133-45.
94. Fukazawa, A., et al., *GEF-H1 mediated control of NOD1 dependent NF-kappaB activation by Shigella effectors*. PLoS Pathog, 2008. **4**(11): p. e1000228.
95. Arbeloa, A., et al., *EspM2 is a RhoA guanine nucleotide exchange factor*. Cell Microbiol, 2010. **12**(5): p. 654-64.

96. Arbeloa, A., et al., *Subversion of actin dynamics by EspM effectors of attaching and effacing bacterial pathogens*. Cell Microbiol, 2008. **10**(7): p. 1429-41.
97. Dean, P. and B. Kenny, *Intestinal barrier dysfunction by enteropathogenic Escherichia coli is mediated by two effector molecules and a bacterial surface protein*. Mol Microbiol, 2004. **54**(3): p. 665-75.
98. Simovitch, M., et al., *EspM inhibits pedestal formation by enterohaemorrhagic Escherichia coli and enteropathogenic E. coli and disrupts the architecture of a polarized epithelial monolayer*. Cell Microbiol, 2010. **12**(4): p. 489-505.
99. Bulgin, R., et al., *The T3SS effector EspT defines a new category of invasive enteropathogenic E. coli (EPEC) which form intracellular actin pedestals*. PLoS Pathog, 2009. **5**(12): p. e1000683.
100. Bulgin, R.R., et al., *EspT triggers formation of lamellipodia and membrane ruffles through activation of Rac-1 and Cdc42*. Cell Microbiol, 2009. **11**(2): p. 217-29.
101. Hiyoshi, H., et al., *Interaction between the type III effector VopO and GEF-H1 activates the RhoA-ROCK pathway*. PLoS Pathog, 2015. **11**(3): p. e1004694.
102. Lang, A.E., et al., *Photorhabdus luminescens toxins ADP-ribosylate actin and RhoA to force actin clustering*. Science, 2010. **327**(5969): p. 1139-42.
103. Lang, A.E., S. Kuhn, and H.G. Mannherz, *Photorhabdus luminescens Toxins TccC3 and TccC5 Affect the Interaction of Actin with Actin-Binding Proteins Essential for Treadmilling*. Curr Top Microbiol Immunol, 2017. **399**: p. 53-67.
104. Hoffmann, C. and G. Schmidt, *CNF and DNT*. Rev Physiol Biochem Pharmacol, 2004. **152**: p. 49-63.
105. Wang, M.H. and K.S. Kim, *Cytotoxic necrotizing factor 1 contributes to Escherichia coli meningitis*. Toxins (Basel), 2013. **5**(11): p. 2270-80.
106. Okada, R., et al., *The Vibrio parahaemolyticus effector VopC mediates Cdc42-dependent invasion of cultured cells but is not required for pathogenicity in an animal model of infection*. Cell Microbiol, 2014. **16**(6): p. 938-47.
107. Zhang, L., et al., *Type III effector VopC mediates invasion for Vibrio species*. Cell Rep, 2012. **1**(5): p. 453-60.
108. Schmidt, G., et al., *Lysine and polyamines are substrates for transglutamination of Rho by the Bordetella dermonecrotic toxin*. Infect Immun, 2001. **69**(12): p. 7663-70.
109. Horiguchi, Y., et al., *Bordetella bronchiseptica dermonecrotizing toxin induces reorganization of actin stress fibers through deamidation of Gln-63 of the GTP-binding protein Rho*. Proc Natl Acad Sci U S A, 1997. **94**(21): p. 11623-6.
110. Horiguchi, Y., et al., *Bordetella bronchiseptica dermonecrotizing toxin stimulates assembly of actin stress fibers and focal adhesions by modifying the small GTP-binding protein rho*. J Cell Sci, 1995. **108 ( Pt 10)**: p. 3243-51.
111. Dong, N., L. Liu, and F. Shao, *A bacterial effector targets host DH-PH domain RhoGEFs and antagonizes macrophage phagocytosis*. EMBO J, 2010. **29**(8): p. 1363-76.
112. Wong, A.R., et al., *The interplay between the Escherichia coli Rho guanine nucleotide exchange factor effectors and the mammalian RhoGEF inhibitor EspH*. MBio, 2012. **3**(1).
113. Groves, E., et al., *Sequestering of Rac by the Yersinia effector YopO blocks Fcgamma receptor-mediated phagocytosis*. J Biol Chem, 2010. **285**(6): p. 4087-98.
114. Prehna, G., et al., *Yersinia virulence depends on mimicry of host Rho-family nucleotide dissociation inhibitors*. Cell, 2006. **126**(5): p. 869-80.
115. Navarro, L., et al., *Identification of a molecular target for the Yersinia protein kinase A*. Mol Cell, 2007. **26**(4): p. 465-77.
116. Evdokimov, A.G., et al., *Crystal structure of the Yersinia pestis GTPase activator YopE*. Protein Sci, 2002. **11**(2): p. 401-8.
117. Aepfelbacher, M., et al., *Activity modulation of the bacterial Rho GAP YopE: an inspiration for the investigation of mammalian Rho GAPs*. Eur J Cell Biol, 2011. **90**(11): p. 951-4.
118. Krall, R., et al., *Pseudomonas aeruginosa ExoT is a Rho GTPase-activating protein*. Infect Immun, 2000. **68**(10): p. 6066-8.

119. Garrity-Ryan, L., et al., *The ADP ribosyltransferase domain of Pseudomonas aeruginosa ExoT contributes to its biological activities*. Infect Immun, 2004. **72**(1): p. 546-58.
120. Fehr, D., et al., *Aeromonas exoenzyme T of Aeromonas salmonicida is a bifunctional protein that targets the host cytoskeleton*. J Biol Chem, 2007. **282**(39): p. 28843-52.
121. Kulich, S.M., D.W. Frank, and J.T. Barbieri, *Purification and characterization of exoenzyme S from Pseudomonas aeruginosa 388*. Infect Immun, 1993. **61**(1): p. 307-13.
122. Viboud, G.I., E. Mejia, and J.B. Bliska, *Comparison of YopE and YopT activities in counteracting host signalling responses to Yersinia pseudotuberculosis infection*. Cell Microbiol, 2006. **8**(9): p. 1504-15.
123. Brugirard-Ricaud, K., et al., *Site-specific antiphagocytic function of the Photorhabdus luminescens type III secretion system during insect colonization*. Cell Microbiol, 2005. **7**(3): p. 363-71.
124. Schmidt, G., *Yersinia enterocolitica outer protein T (YopT)*. Eur J Cell Biol, 2011. **90**(11): p. 955-8.
125. Sorg, I., et al., *The C terminus of YopT is crucial for activity and the N terminus is crucial for substrate binding*. Infect Immun, 2003. **71**(8): p. 4623-32.
126. Sorg, I., et al., *Recombinant Yersinia YopT leads to uncoupling of RhoA-effector interaction*. Infect Immun, 2001. **69**(12): p. 7535-43.
127. Aktories, K., *Bacterial protein toxins that modify host regulatory GTPases*. Nat Rev Microbiol, 2011. **9**(7): p. 487-98.
128. Popoff, M.R. and P. Bouvet, *Clostridial toxins*. Future Microbiol, 2009. **4**(8): p. 1021-64.
129. Wilde, C., et al., *A novel C3-like ADP-ribosyltransferase from Staphylococcus aureus modifying RhoE and Rnd3*. J Biol Chem, 2001. **276**(12): p. 9537-42.
130. Just, I., G. Schallehn, and K. Aktories, *ADP-ribosylation of small GTP-binding proteins by Bacillus cereus*. Biochem Biophys Res Commun, 1992. **183**(3): p. 931-6.
131. Sehr, P., et al., *Glucosylation and ADP ribosylation of rho proteins: effects on nucleotide binding, GTPase activity, and effector coupling*. Biochemistry, 1998. **37**(15): p. 5296-304.
132. Bourmeyster, N., et al., *Copurification of rho protein and the rho-GDP dissociation inhibitor from bovine neutrophil cytosol. Effect of phosphoinositides on rho ADP-ribosylation by the C3 exoenzyme of Clostridium botulinum*. Biochemistry, 1992. **31**(51): p. 12863-9.
133. Barth, H., et al., *Neosynthesis and activation of Rho by Escherichia coli cytotoxic necrotizing factor (CNF1) reverse cytopathic effects of ADP-ribosylated Rho*. J Biol Chem, 1999. **274**(39): p. 27407-14.
134. Genth, H., et al., *Entrapment of Rho ADP-ribosylated by Clostridium botulinum C3 exoenzyme in the Rho-guanine nucleotide dissociation inhibitor-1 complex*. J Biol Chem, 2003. **278**(31): p. 28523-7.
135. Fujihara, H., et al., *Inhibition of RhoA translocation and calcium sensitization by in vivo ADP-ribosylation with the chimeric toxin DC3B*. Mol Biol Cell, 1997. **8**(12): p. 2437-47.
136. Aktories, K., C. Wilde, and M. Vogelsgesang, *Rho-modifying C3-like ADP-ribosyltransferases*. Rev Physiol Biochem Pharmacol, 2004. **152**: p. 1-22.
137. Barth, H., et al., *Clostridial C3 Toxins Target Monocytes/Macrophages and Modulate Their Functions*. Front Immunol, 2015. **6**: p. 339.
138. Popoff, M.R. and B. Geny, *Rho/Ras-GTPase-dependent and -independent activity of clostridial glucosylating toxins*. J Med Microbiol, 2011. **60**(Pt 8): p. 1057-69.
139. Jank, T. and K. Aktories, *Structure and mode of action of clostridial glucosylating toxins: the ABCD model*. Trends Microbiol, 2008. **16**(5): p. 222-9.
140. Aktories, K. and I. Just, *Clostridial Rho-inhibiting protein toxins*. Curr Top Microbiol Immunol, 2005. **291**: p. 113-45.
141. Herrmann, C., et al., *Functional consequences of monoglucosylation of Ha-Ras at effector domain amino acid threonine 35*. J Biol Chem, 1998. **273**(26): p. 16134-9.

142. Just, I., et al., *Glucosylation of Rho proteins by Clostridium difficile toxin B*. Nature, 1995. **375**(6531): p. 500-3.
143. Just, I., et al., *The enterotoxin from Clostridium difficile (ToxA) monoglucosylates the Rho proteins*. J Biol Chem, 1995. **270**(23): p. 13932-6.
144. Genth, H., K. Aktories, and I. Just, *Monoglucosylation of RhoA at threonine 37 blocks cytosol-membrane cycling*. J Biol Chem, 1999. **274**(41): p. 29050-6.
145. Worby, C.A., et al., *The fic domain: regulation of cell signaling by adenylylation*. Mol Cell, 2009. **34**(1): p. 93-103.
146. Yarbrough, M.L., et al., *AMPylation of Rho GTPases by Vibrio VopS disrupts effector binding and downstream signaling*. Science, 2009. **323**(5911): p. 269-72.
147. Woolery, A.R., et al., *AMPylation of Rho GTPases subverts multiple host signaling processes*. J Biol Chem, 2014. **289**(47): p. 32977-88.
148. Maguina, C., H. Guerra, and P. Ventosilla, *Bartonellosis*. Clin Dermatol, 2009. **27**(3): p. 271-80.
149. Hang, J., et al., *Complete Genome Sequence of Bartonella ancashensis Strain 20.00, Isolated from the Blood of a Patient with Verruga Peruana*. Genome Announc, 2015. **3**(6).
150. Blazes, D.L., et al., *Novel Bartonella agent as cause of verruga peruana*. Emerg Infect Dis, 2013. **19**(7): p. 1111-4.
151. Harms, A. and C. Dehio, *Intruders below the radar: molecular pathogenesis of Bartonella spp*. Clin Microbiol Rev, 2012. **25**(1): p. 42-78.
152. Fournier, P.E., et al., *Experimental model of human body louse infection using green fluorescent protein-expressing Bartonella quintana*. Infect Immun, 2001. **69**(3): p. 1876-9.
153. Higgins, J.A., et al., *Acquisition of the cat scratch disease agent Bartonella henselae by cat fleas (Siphonaptera: Pulicidae)*. J Med Entomol, 1996. **33**(3): p. 490-5.
154. Dehio, C., U. Sauder, and R. Hiestand, *Isolation of Bartonella schoenbuchensis from Lipoptena cervi, a blood-sucking arthropod causing deer ked dermatitis*. J Clin Microbiol, 2004. **42**(11): p. 5320-3.
155. Siamer, S. and C. Dehio, *New insights into the role of Bartonella effector proteins in pathogenesis*. Curr Opin Microbiol, 2015. **23**: p. 80-5.
156. Harms, A., et al., *Evolutionary Dynamics of Pathoadaptation Revealed by Three Independent Acquisitions of the VirB/D4 Type IV Secretion System in Bartonella*. Genome Biol Evol, 2017. **9**(3): p. 761-776.
157. Guy, L., et al., *A gene transfer agent and a dynamic repertoire of secretion systems hold the keys to the explosive radiation of the emerging pathogen Bartonella*. PLoS Genet, 2013. **9**(3): p. e1003393.
158. Cascales, E. and P.J. Christie, *The versatile bacterial type IV secretion systems*. Nat Rev Microbiol, 2003. **1**(2): p. 137-49.
159. Dehio, C. and R.M. Tsolis, *Type IV Effector Secretion and Subversion of Host Functions by Bartonella and Brucella Species*. Curr Top Microbiol Immunol, 2017. **413**: p. 269-295.
160. Cascales, E. and P.J. Christie, *Definition of a bacterial type IV secretion pathway for a DNA substrate*. Science, 2004. **304**(5674): p. 1170-3.
161. Wallden, K., A. Rivera-Calzada, and G. Waksman, *Type IV secretion systems: versatility and diversity in function*. Cell Microbiol, 2010. **12**(9): p. 1203-12.
162. Atmakuri, K., E. Cascales, and P.J. Christie, *Energetic components VirD4, VirB11 and VirB4 mediate early DNA transfer reactions required for bacterial type IV secretion*. Mol Microbiol, 2004. **54**(5): p. 1199-211.
163. Chandran, V., et al., *Structure of the outer membrane complex of a type IV secretion system*. Nature, 2009. **462**(7276): p. 1011-5.
164. Low, H.H., et al., *Structure of a type IV secretion system*. Nature, 2014. **508**(7497): p. 550-553.
165. Dehio, C., *Infection-associated type IV secretion systems of Bartonella and their diverse roles in host cell interaction*. Cell Microbiol, 2008. **10**(8): p. 1591-8.



166. Engel, P., et al., *Parallel evolution of a type IV secretion system in radiating lineages of the host-restricted bacterial pathogen Bartonella*. PLoS Genet, 2011. **7**(2): p. e1001296.
167. Selbach, M., et al., *Host cell interactome of tyrosine-phosphorylated bacterial proteins*. Cell Host Microbe, 2009. **5**(4): p. 397-403.
168. Schulein, R., et al., *A bipartite signal mediates the transfer of type IV secretion substrates of Bartonella henselae into human cells*. Proceedings of the National Academy of Sciences of the United States of America, 2005. **102**(3): p. 856-61.
169. Stanger, F.V., et al., *The BID Domain of Type IV Secretion Substrates Forms a Conserved Four-Helix Bundle Topped with a Hook*. Structure, 2017. **25**(1): p. 203-211.
170. Okujava, R., et al., *A translocated effector required for Bartonella dissemination from derma to blood safeguards migratory host cells from damage by co-translocated effectors*. PLoS Pathog, 2014. **10**(6): p. e1004187.
171. Truttmann, M.C., P. Guye, and C. Dehio, *BID-F1 and BID-F2 domains of Bartonella henselae effector protein BepF trigger together with BepC the formation of invasome structures*. PLoS one, 2011. **6**(10): p. e25106.
172. Rhomberg, T.A., et al., *A translocated protein of Bartonella henselae interferes with endocytic uptake of individual bacteria and triggers uptake of large bacterial aggregates via the invasome*. Cell Microbiol, 2009. **11**(6): p. 927-45.
173. Pulliainen, A.T., et al., *Bacterial effector binds host cell adenylyl cyclase to potentiate Galphas-dependent cAMP production*. Proc Natl Acad Sci U S A, 2012. **109**(24): p. 9581-6.
174. Schmid, M.C., et al., *A translocated bacterial protein protects vascular endothelial cells from apoptosis*. PLoS Pathog, 2006. **2**(11): p. e115.
175. Kawamukai, M., et al., *Nucleotide sequences of fic and fic-1 genes involved in cell filamentation induced by cyclic AMP in Escherichia coli*. J Bacteriol, 1989. **171**(8): p. 4525-9.
176. Harms, A., F.V. Stanger, and C. Dehio, *Biological Diversity and Molecular Plasticity of FIC Domain Proteins*. Annu Rev Microbiol, 2016. **70**: p. 341-60.
177. Mukherjee, S., et al., *Modulation of Rab GTPase function by a protein phosphocholine transferase*. Nature, 2011. **477**(7362): p. 103-6.
178. Ridley, A.J. and A. Hall, *The small GTP-binding protein rho regulates the assembly of focal adhesions and actin stress fibers in response to growth factors*. Cell, 1992. **70**(3): p. 389-99.
179. Helaine, S., et al., *Internalization of Salmonella by macrophages induces formation of nonreplicating persisters*. Science, 2014. **343**(6167): p. 204-8.
180. Roy, C.R. and J. Cherfils, *Structure and function of Fic proteins*. Nat Rev Microbiol, 2015. **13**(10): p. 631-40.
181. Defeu Soufo, H.J., et al., *Translation elongation factor EF-Tu modulates filament formation of actin-like MreB protein in vitro*. J Mol Biol, 2015. **427**(8): p. 1715-27.
182. Kinch, L.N., et al., *Fido, a novel AMPylation domain common to fic, doc, and AvrB*. PLoS One, 2009. **4**(6): p. e5818.
183. Liu, J., et al., *A receptor-like cytoplasmic kinase phosphorylates the host target RIN4, leading to the activation of a plant innate immune receptor*. Cell Host Microbe, 2011. **9**(2): p. 137-46.
184. Bunney, T.D., et al., *Crystal structure of the human, FIC-domain containing protein HYPE and implications for its functions*. Structure, 2014. **22**(12): p. 1831-43.
185. Sanyal, A., et al., *A novel link between Fic (filamentation induced by cAMP)-mediated adenylylation/AMPylation and the unfolded protein response*. J Biol Chem, 2015. **290**(13): p. 8482-99.
186. Preissler, S., et al., *AMPylation matches BiP activity to client protein load in the endoplasmic reticulum*. Elife, 2015. **4**: p. e12621.
187. Harms, A., *FIC domain toxins are the origin of intra- and inter-kingdom effectors of Bartonella*. PhD thesis, 2014.

188. Pielek, K., et al., *An experimental strategy for the identification of AMPylation targets from complex protein samples*. Proteomics, 2014. **14**(9): p. 1048-52.
189. Pielek, K., *From FIC to BID: Target Identification and Functional Characterization of Bartonella Effector Proteins*. PhD thesis, 2013.
190. Engel, P., et al., *Adenylylation control by intra- or intermolecular active-site obstruction in Fic proteins*. Nature, 2012. **482**(7383): p. 107-10.
191. Harms, A., et al., *Adenylylation of Gyrase and Topo IV by FicT Toxins Disrupts Bacterial DNA Topology*. Cell Rep, 2015. **12**(9): p. 1497-507.
192. Harms, A., *FIC domains of Bartonella effector proteins - AMPylation and beyond*. Master thesis, 2010.
193. Xiao, J., et al., *Structural basis of Fic-mediated adenylylation*. Nat Struct Mol Biol, 2010. **17**(8): p. 1004-10.
194. Palanivelu, D.V., et al., *Fic domain-catalyzed adenylylation: insight provided by the structural analysis of the type IV secretion system effector BepA*. Protein Sci, 2011. **20**(3): p. 492-9.
195. Luong, P., et al., *Kinetic and structural insights into the mechanism of AMPylation by VopS Fic domain*. J Biol Chem, 2010. **285**(26): p. 20155-63.
196. Salcedo, S.P., et al., *Brucella control of dendritic cell maturation is dependent on the TIR-containing protein Btp1*. PLoS Pathog, 2008. **4**(2): p. e21.
197. Skinner, J.A., et al., *Bordetella type III secretion modulates dendritic cell migration resulting in immunosuppression and bacterial persistence*. J Immunol, 2005. **175**(7): p. 4647-52.
198. Dehio, C., et al., *Interaction of Bartonella henselae with endothelial cells results in bacterial aggregation on the cell surface and the subsequent engulfment and internalisation of the bacterial aggregate by a unique structure, the invasome*. J Cell Sci, 1997. **110 ( Pt 18)**: p. 2141-54.
199. Eicher, S.C. and C. Dehio, *Bartonella entry mechanisms into mammalian host cells*. Cell Microbiol, 2012. **14**(8): p. 1166-73.
200. Truttmann, M.C., T.A. Rhomberg, and C. Dehio, *Combined action of the type IV secretion effector proteins BepC and BepF promotes invasome formation of Bartonella henselae on endothelial and epithelial cells*. Cellular microbiology, 2011. **13**(2): p. 284-99.
201. Truttmann, M.C., et al., *Bartonella henselae engages inside-out and outside-in signaling by integrin beta1 and talin1 during invasome-mediated bacterial uptake*. J Cell Sci, 2011. **124**(Pt 21): p. 3591-602.
202. Dehio, C., *Recent progress in understanding Bartonella-induced vascular proliferation*. Curr Opin Microbiol, 2003. **6**(1): p. 61-5.

**Aim of my thesis**

- Aim of my thesis -

Started in December 2013, the aim of my thesis was to address the function of one of the most conserved effectors within *Bartonella* species of the lineage 4, named BepC. Although it was established that BepC participates in the internalization of bacterial aggregates and impairs host-cell migration, the underlying cellular mechanisms, as well as its host target(s), have not yet been identified.

To understand BepC involvement in *Bartonella* pathogenesis, I first investigated the role of this effector in the context of bacterial infection by using fluorescence microscopy. From these experiments, I could establish that BepC induces rearrangements of the host-cell actin cytoskeleton. Following this result, I aimed to demonstrate by which mechanism BepC triggers the actin phenotype by using molecular biology techniques, which revealed the activation of a Rho GTPase signaling pathway by host protein interaction.

Additionally, I attempted to determine a possible enzymatic activity for the FIC domain of BepC by applying various biochemical techniques.

# Research article

## 3.1 Results

### 3.1.1 BepC is responsible for actin cytoskeleton rearrangements during infection of human cells.

Previous studies have revealed that BepC of *Bartonella henselae* (BepC<sub>Bhe</sub>) affects the actin cytoskeleton during infection. The ectopic expression of mCherry-BepC<sub>Bhe</sub> in Human Umbilical Vein Endothelial Cells (HUVECs) induces cell fragmentation due to a deficiency in rear-end detachment during migration, which is abolished by another effector, BepE [1]. BepC<sub>Bhe</sub>, together with BepF<sub>Bhe</sub>, has been also shown to trigger the internalization of large bacterial aggregates in HeLa cells and HUVECs [2, 3]. The uptake is associated with the formation of a cellular structure characterized by an actin ring, known as invasome [4].

To study the effect of BepC in the context of infection and without having interferences from other effectors, a plasmid encoding BepC (*pbepC*) has been conjugated in a strain of *Bhe* in which all genes encoding Beps have been deleted (*Bhe ΔbepA-G*). The ectopic expression of BepC is under control of an IPTG-inducible promoter. As an *in vitro* infection model, human cells were infected with either *Bhe ΔbepA-G* expressing BepC or, as a negative control, with *Bhe ΔbepA-G* carrying the empty plasmid (*pEmpty*). After incubation and fixation, cells were stained for DNA, F-actin, and *Bartonella* before being analyzed by fluorescence microscopy.

As *Bartonella* is associated with vascular tumor formation and endothelial cells are proposed to form the blood seeding niche [5, 6], we infected HUVECs as an *in vitro* model to mimic host cell infection (Fig. 3.1). In comparison with uninfected cells, HUVECs infected with *Bhe ΔbepA-G pEmpty* did not show any morphological change. As previously reported [7], *Bartonella* were distributed around the nucleus, indicating that Beps are not required for the internalization of the bacteria in HUVECs. The infection with *Bhe ΔbepA-G* expressing Flag-tagged BepC<sub>Bhe</sub> led to a reduction of cell density, suggesting cytotoxic effect, detachment, cell growth inhibition, or a combination of these factors. The remaining cells showed actin rearrangements, in accordance with previous results [1].

As BepC also contributes to invasome formation in HeLa cells [2, 3], we were wondering whether it would also induce actin rearrangements in this cell line. To verify it, we infected HeLa cells with *Bartonella* expressing BepC<sub>Bhe</sub> using the same infection conditions as for HUVECs (Fig. 3.1). HeLa cells did not show a reduced cell density but displayed strong actin rearrangements such as stress fibers, which make them a suitable model to study the actin phenotype mediated by BepC. Interestingly, the bacteria were not equally distributed around the nucleus but formed aggregates. However, these bacterial clusters were different from invasomes as they were not surrounded by an actin ring. Although it is not clear whether the bacteria are extracellular or intracellular, this result suggests that, during invasome formation,

BepC may induce the clustering of bacteria at the surface of the host cell while BepF could be required to complete the internalization.

In EA.hy926, a hybrid cell line with endothelial characteristics, BepC<sub>Bhe</sub> also induced actin rearrangements and bacterial clustering (Fig. 3.1) but not as strong as the phenotype observed in HeLa cells. There was also no visible reduction of cell density in contrast to HUVEC infection. The reason why these cells are less sensitive to the effect of BepC<sub>Bhe</sub> remains unclear.

For each cell type, the intensity of the actin phenotype was proportional to the multiplicity of infection (MOI), the time of incubation, and the concentration of IPTG used to induce *bepC* expression (Fig. 3.S1). The influence of these parameters suggests that the effect on actin rearrangement directly correlates with the amount of BepC translocated inside the host cell.

### **3.1.2 BepC from different *Bartonella* species induces actin stress fiber formation in HeLa cells.**

BepC is highly conserved among the *Bartonella* species of the lineage 4, which suggest a critical role in pathogenesis. To determine if the effect of BepC on the actin cytoskeleton is conserved among *Bartonella*, we infected HeLa cells with *Bhe ΔbepA-G* ectopically expressing BepC of *Bqu*, *Btr*, *Bta*, and *Bgr*. After 48 hours of infection, cells infected with *Bhe ΔbepA-G* expressing BepC of *Bhe*, *Bqu*, *Btr*, and *Bta* displayed actin stress fiber formation with different levels of intensity (Fig. 3.2). BepC<sub>Bqu</sub> induced the strongest phenotype and generated some cell fragmentation while BepC<sub>Bgr</sub> did not trigger any actin rearrangement during infection. Interestingly, only BepC<sub>Bhe</sub> and BepC<sub>Bqu</sub> expression resulted in the formation of bacterial aggregates on top of the cells.

Although BepC<sub>Bgr</sub> did not have an effect on the actin cytoskeleton, our data suggest that triggering actin rearrangements is a shared function among BepC of several *Bartonella* species of the lineage 4. Considering that the level of ectopic expression in *Bhe ΔbepA-G* was comparable (data not shown), the variations in phenotype intensity are probably related to a difference in function, translocation efficiency, host specificity, or a combination of these factors.

As BepC<sub>Bhe</sub> induces invasome formation together with BepF<sub>Bhe</sub> in HUVECs and HeLa cells [2, 3], we were interested to test whether BepC of other *Bartonella* species could also participate in this phenotype. To answer this question, we co-infected HeLa cells with *Bhe ΔbepA-G* expressing BepC from different species and *Bhe ΔbepC,G*, a strain that is expressing BepF but depleted of BepG, as this effector is inducing invasome formation by itself [7].

Surprisingly, only HeLa cells co-infected with *Bhe ΔbepC,G* and *Bhe ΔbepA-G* expressing BepC<sub>Bhe</sub> triggered invasome formation (Fig. 3.3). Even BepC<sub>Bqu</sub>, which also induced bacterial

aggregation on top of the cells (Fig. 3.2), was not able to participate to invasome formation. However, the co-infection with *Bhe ΔbepC,G* led to a reduction of actin stress fibers in all conditions. This observation suggests that other Beps translocated by *Bhe ΔbepC,G*, probably Bep<sub>E<sub>Bhe</sub></sub> but also possibly other effectors, interfere with actin rearrangements mediated by BepC of *Bhe*, *Bqu*, *Btr*, and *Bta*.

Overall, these results suggest that inducing actin rearrangements is not sufficient to participate, together with Bep<sub>F<sub>Bhe</sub></sub>, in the uptake of bacterial clusters via invasome formation.

### 3.1.3 The FIC domain of BepC is required for actin rearrangements.

As BepC is composed of a N-terminal FIC domain, a central OB fold and a C-terminal BID domain, we wanted to determine which regions of the protein are required for the actin phenotype. Knowing that Fic proteins catalyze posttranslational modifications [8], we assumed that BepC might enzymatically modify a host protein via its FIC domain and thereby induces actin rearrangements.

First, we infected HeLa cells and HUVECs with *Bhe ΔbepA-G* expressing Bep<sub>C<sub>Bhe</sub></sub> without its FIC domain (Bep<sub>C<sub>Bhe</sub></sub> OB-BID). The absence of actin stress fibers in HeLa cells (Fig. 3.4) and the absence of cell density reduction in HUVECs (Fig. 3.5) indicated that the FIC domain of BepC plays a critical role in these phenotypes.

The next step was to analyze whether a potential enzymatic activity would be required to mediate the actin phenotype. Therefore, HeLa cells and HUVECs were infected with *Bhe ΔbepA-G* expressing Bep<sub>C<sub>Bhe</sub></sub> harboring mutations in the conserved FIC motif.

Since the exchange of the conserved histidine for an alanine is sufficient for some Fic proteins to lose their enzymatic activity [9], a similar mutation (H146A) was introduced into Bep<sub>C<sub>Bhe</sub></sub>. Infection of HeLa cells (Fig. 3.4) with *Bhe ΔbepA-G* expressing Bep<sub>C<sub>Bhe</sub></sub> H146A resulted in actin stress fiber formation with a similar intensity to Bep<sub>C<sub>Bhe</sub></sub> wild-type. This suggested that the conserved histidine is not required for actin rearrangement.

However, some Fic proteins keep a reduced enzymatic activity *in vitro* despite the mutation of the conserved histidine [10]. Thus, we also mutated the lysine and the two arginines that were shown to interact with the ATP derivative (Fig. 1.9) in addition to the mutated histidine (Bep<sub>C<sub>Bhe</sub></sub><sup>\*\*\*\*</sup> = Bep<sub>C<sub>Bhe</sub></sub> H146A, K150A, R154A, R157A). Surprisingly, HeLa cells (Fig. 3.4) and HUVECs (Fig. 3.5) infected with *Bhe ΔbepA-G* expressing Bep<sub>C<sub>Bhe</sub></sub><sup>\*\*\*\*</sup> still showed strong actin rearrangements. The persistence of the phenotype suggests that a conserved FIC motif, and therefore a functional catalytic site, was not essential for the disruption of the actin cytoskeleton. Thus, it is unlikely that actin rearrangements result from an enzymatic activity catalyzed by BepC.



As BepC harbors a non-canonical FIC motif and has a lysine in place of an acidic residue (Alignment 1.2), it might have lost its enzymatic activity. Therefore, we analyzed whether BepC with a canonical FIC motif, and thus a putative AMPylation activity, would have an effect on actin stress fiber formation. To do so, a canonical FIC motif was restored by exchanging the lysine for a glutamate (BepC<sub>Bhe</sub> K150E). As observed for the other FIC motif mutants, the actin phenotype was still visible in HeLa cell infected with *Bhe*  $\Delta$ bepA-G expressing BepC<sub>Bhe</sub> K150E (Fig. 3.4). Assuming that an enzymatic activity would have been restored with a canonical FIC motif, this result suggests that it would not interfere with the effect of BepC on the actin cytoskeleton.

Since the conserved FIC motif does not seem to be required for actin rearrangements but the deletion of the FIC domain abolished the phenotype, we wanted to investigate which regions of the FIC domain would be functionally relevant. Considering the Flap as one of the most conserved regions of BepC (Alignment 1.2) and that this region participates in the interaction between Fic proteins and their host target [11-13], we proposed that it could induce actin rearrangements by interacting with a putative host protein.

To test this hypothesis, we exchanged 10 amino acids of the Flap of BepC<sub>Bhe</sub> (AMRPKGMRVP) for the corresponding residues of the Flap of BepA<sub>Bhe</sub> (EMKRTGWKNA), which differs by eight amino acids (Alignment 1.2). HeLa cells (Fig. 3.4) and HUVECs (Fig. 3.5) infected with *Bhe*  $\Delta$ bepA-G expressing BepC<sub>Bhe</sub> (Flap BepA<sub>Bhe</sub>) were still displaying actin rearrangements, indicating that a conserved Flap is not required for actin rearrangements.

Another highly conserved region of the FIC domain of BepC is the first  $\alpha$  helix, which contains tyrosine residues that could be targeted by auto-modification (Alignment 1.2). To check whether this region plays a role in actin rearrangements, we infected HeLa cells with *Bhe*  $\Delta$ bepA-G expressing BepC<sub>Bhe</sub> without the helix (BepC<sub>Bhe</sub> 19-532). In comparison with BepC<sub>Bhe</sub> wild-type, the deletion of this region did not show an influence on actin stress fiber formation (Fig. 3.4).

In summary, the FIC domain of BepC is required for both actin stress fiber formation and cell fragmentation. However, the FIC motif does not seem to participate in actin rearrangements, suggesting that the actin phenotype is not linked to an enzymatic activity. Additionally, the first helix and a conserved Flap are not necessary to trigger the actin phenotype. As these regions are highly conserved, it is plausible that they have another function that is not associated with the actin phenotype. The region of the FIC domain that is essential to the effect on the actin cytoskeleton remains unidentified.

### 3.1.4 A conserved BID domain is required for actin stress fiber formation mediated by BepC.

As already demonstrated for several Beps [1, 2, 7, 14], individual BID domains have acquired supplementary functions in host cells in addition to their role as a translocation signal. Although the BID domain of BepC is not sufficient to induce the actin phenotype by itself, we wanted to determine if it participates in actin rearrangements.

To answer this question, we exchanged the BID domain of BepC<sub>Bhe</sub> with the one of BepA<sub>Bhe</sub> and ectopically expressed the hybrid protein in *Bhe ΔbepA-G*. Infected HeLa cells did not show any actin rearrangements or bacterial aggregates (Fig. 3.4). Assuming a correct folding and the translocation of the hybrid protein, the absence of the phenotype suggests that the BID domain of BepC has also an important role in actin rearrangements and is not only required for protein translocation.

### 3.1.5 GEF-H1 and MRCK $\alpha$ interact with BepC during cell infection.

In order to identify which host protein could interact with BepC<sub>Bhe</sub> during cell infection and participate in the actin phenotype, we infected HeLa cells with *Bhe ΔbepA-G* expressing BepC<sub>Bhe</sub> with a triple Flag-tag on the N-terminus. After cell lysis, BepC<sub>Bhe</sub> was pulled down with antibodies targeting the Flag-tag and bound proteins were analyzed by mass spectrometry. In comparison with HeLa cells infected with *Bhe ΔbepA-G* carrying an empty plasmid, six proteins showed an increase of more than 8 fold with a q-value lower than 0.01 (Fig. 3.6A). As only one peptide was identified for three of these six proteins, their relevance is uncertain. As expected, one of the three other proteins was identified as BepC<sub>Bhe</sub>. The two other proteins, GEF-H1 and MRCK $\alpha$ , were particularly interesting as they play a role in actin rearrangements. GEF-H1 promotes the activation of RhoA pathway by exchanging GDP for GTP, thereby leading to actin stress fiber formation via ROCK. However, MRCK $\alpha$  directly phosphorylates myosin light chain (MLC2) and inhibits the myosin light chain phosphatase (MLCP), which also result in actin stress fiber formation (Fig. 3.6B).

To validate the results of the mass spectrometry, an additional pull-down experiment was performed and subsequently analyzed by western blot against Flag-tag, GEF-H1 or MRCK $\alpha$ . The detection of GEF-H1 and MRCK $\alpha$  among the bound proteins confirmed the interaction between BepC<sub>Bhe</sub> wild-type and these two proteins (Fig. 3.7A). Moreover, the absence of GEF-H1 and MRCK $\alpha$  in the pull-down fractions of cells infected with *Bhe ΔbepA-G* carrying the empty plasmid and uninfected cells excluded any unspecific binding.

To determine which domain is necessary for the interaction between BepC<sub>Bhe</sub> and GEF-H1 or MRCK $\alpha$ , we infected HeLa cells with *Bhe ΔbepA-G* expressing truncated forms of 3XFlag-BepC<sub>Bhe</sub> (Fig. 3.7A). Interestingly, the deletion of the FIC domain (BepC<sub>Bhe</sub> OB-BID) completely

prevented both GEF-H1 and MRCK $\alpha$  to co-immunoprecipitate with BepC<sub>Bhe</sub>. This result indicates that the FIC domain of BepC<sub>Bhe</sub> is required to interact with the two host proteins.

In order to identify which region of the FIC domain could be involved in the interaction, we performed a pull-down on HeLa cells infected with *Bhe*  $\Delta$ bepA-G expressing BepC<sub>Bhe</sub> with a mutated FIC motif (Fig. 3.7A). The mutation of the catalytic histidine (BepC<sub>Bhe</sub> H146A) and the restoration of a canonical FIC motif (BepC<sub>Bhe</sub> K150E) did not have any influence on the interaction, suggesting that a functional active site is not required for binding. Nevertheless, the mutation of the residues (BepC<sub>Bhe</sub> \*\*\*\*\*) that were shown to interact with the ATP derivative in BepC<sub>Btr</sub> (Fig. 1.9) reduced the interaction with GEF-H1 and MRCK $\alpha$ . This finding suggests that the ability of the FIC domain to bind a nucleotide might help for the interaction.

However, the replacement of the Flap (BepC<sub>Bhe</sub> (Flap BepA<sub>Bhe</sub>)) or the deletion of the first  $\alpha$ -helix (BepC<sub>Bhe</sub> 19-532), two highly conserved regions of the FIC domain, did not reduce binding of GEF-H1 and MRCK $\alpha$  (Fig. 3.7A). Therefore, the two host proteins probably interact with another region of the FIC domain.

Finally, the exchange of the BID domain of BepC<sub>Bhe</sub> with the domain of BepA<sub>Bhe</sub> also showed a reduction of interaction but this rather seems to be linked to a lower amount of effector in the pull-down fraction (Fig. 3.7A). Although it would require more investigation, this result tends to show that a conserved BID domain is not necessary for the interaction and that the FIC-OB domains of BepC might be sufficient to bind GEF-H1 and MRCK $\alpha$ .

The pull-down of BepC from infected HUVECs showed similar results and confirmed that GEF-H1 co-precipitated together with BepC<sub>Bhe</sub> full-length (Fig. 3.7B). The mutations of the FIC motif (BepC<sub>Bhe</sub> \*\*\*\*\*) also decreased the interaction between GEF-H1 and BepC<sub>Bhe</sub> while the deletion of the whole FIC domain totally prevented it. The interaction with MRCK $\alpha$  during infection of HUVECs has not been investigated yet.

To further confirm BepC interaction with GEF-H1 and MRCK $\alpha$ , we decided to check whether we could co-immunoprecipitate BepC by reciprocal pull-down (Fig. 3.8). As before, HeLa cells were infected with *Bhe*  $\Delta$ bepA-G expressing BepC<sub>Bhe</sub> with or without its FIC domain or carrying the empty plasmid.

After MRCK $\alpha$  pull-down, only BepC<sub>Bhe</sub> full-length was detected in the pull-down fraction, which confirms that the FIC domain is necessary for the interaction (Fig. 3.8). Surprisingly, GEF-H1 also co-immunoprecipitated with MRCK $\alpha$ , even in absence of BepC<sub>Bhe</sub>. This either suggests that MRCK $\alpha$  and GEF-H1 are directly or indirectly interacting together, which has never been demonstrated before, or that GEF-H1 unspecifically binds to agarose beads. Nevertheless, the presence of GEF-H1 was not detected in the negative controls of the previous experiment (Fig. 3.7) and mass spectrometry showed an enrichment of 32 fold in comparison with the negative

control (Fig. 3.6A). Thus, our previous results exclude an unspecific binding of GEF-H1 to the beads, which support the hypothesis of a complex between BepC<sub>Bhe</sub>, GEF-H1, and MRCK $\alpha$ . However, the pull-down of GEF-H1 indicated that neither BepC nor MRCK $\alpha$  co-immunoprecipitated with GEF-H1. A possible explanation is that the antibody used to pull-down GEF-H1 is binding to the site of interaction for BepC<sub>Bhe</sub> and MRCK $\alpha$ , thereby preventing the co-immunoprecipitation of the two proteins.

In summary, our results indicate that the FIC domain of BepC<sub>Bhe</sub> is required for the interaction with GEF-H1 and MRCK $\alpha$ . Although the ability to bind a nucleotide might help for target binding, the presence of the first helix or the conservation of the FIC motif, the Flap, or the BID domain is not critical for the interaction. So far, it remains elusive whether BepC<sub>Bhe</sub> interacts directly or indirectly with MRCK $\alpha$  and GEF-H1 or if they form a complex during cell infection.

### **3.1.6 BepC<sub>Bhe</sub> increases GTP-bound RhoA during infection of HeLa cells.**

Once GEF-H1 is activated in physiological conditions, it interacts with RhoA and promotes the exchange of GDP for GTP to activate the small GTPase [15]. Thus, if BepC modulates the activity of GEF-H1, it should have an effect on the amount of GTP-bound RhoA.

To test this hypothesis, we infected serum-starved HeLa cells, which should have a reduced basal activation of the RhoA pathway [16], with *Bhe*  $\Delta$ *bepA-G* expressing BepC<sub>Bhe</sub> or carrying the empty plasmid. After 24 hours, the active form of RhoA was quantified by G-LISA in two independent experiments (Fig. 3.9). Preliminary data showed more than 20% increase in GTP-bound RhoA in comparison with the uninfected cells and the negative control. Therefore, this result suggests that BepC is activating the RhoA pathway, presumably by interacting with GEF-H1.

### **3.1.7 The inhibition of the RhoA pathway decreases BepC<sub>Bhe</sub>-mediated actin stress fiber formation.**

As BepC seems to activate GEF-H1, the inhibition of RhoA pathway components should decrease actin stress fiber formation mediated by BepC (Fig. 3.6B). For this purpose, we used two different inhibitors targeting either RhoA or ROCK. Rho inhibitor I is composed of the exoenzyme C3 transferase from *Clostridium botulinum* that inhibits RhoA, RhoB, and RhoC by ADP-ribosylation. This modification prevents the activation of the small GTPases by GEF and increases their sequestration in the cytoplasm by GDI [17]. The other inhibitor (Y27632) is a small molecule binding to the active site of the kinase ROCK, which thereby prevents the phosphorylation of myosin light chain. It is important to note that this inhibitor was also described to inhibit MRCK $\alpha$ , which is a close relative of ROCK, but with a ten-fold lower efficiency [18].

After infection of HeLa cells with *Bhe ΔbepA-G* expressing BepC<sub>Bhe</sub> and the apparition of the actin phenotype, we treated the cells with the two inhibitors (Fig. 3.10). The inhibition of Rho or ROCK led to the loss of actin stress fibers, indicating that the RhoA pathway plays a major role in maintaining the actin phenotype. This result also demonstrates that actin stress fiber formation mediated by BepC<sub>Bhe</sub> can be reverted or modulated by regulating the RhoA pathway at the level of RhoA or ROCK.

### **3.1.8 BepC<sub>Bhe</sub> increases myosin light chain phosphorylation in HeLa cells and HUVECs during infection.**

According to our findings, the translocation of BepC into the host cell should lead to an increase of myosin light chain (MLC2) phosphorylation via an indirect activation of ROCK and, possibly, MRCKα. MRCKα mono-phosphorylates MLC on the serine 19 while ROCK is able to di-phosphorylate MLC on both threonine 18 and serine 19 [19]. Furthermore, the two kinases also inhibit the myosin light chain phosphatase (MLCP) via phosphorylation (Fig. 3.6B).

To confirm that BepC increases MLC phosphorylation, we infected HeLa cells and HUVECs with *Bhe ΔbepA-G* expressing BepC<sub>Bhe</sub> (Fig. 3.11) and determined MLC phosphorylation on Ser19 by immunostaining. Fluorescence microscopy showed an increase of myosin light chain phosphorylation in both HeLa cells and HUVECs. This increase was also independent of the conserved FIC motif, suggesting that it is not linked to a potential enzymatic activity of BepC. The increase of phosphorylation is in accordance with a BepC dependent activation of the RhoA pathway via GEF-H1 and, possibly, an activation of MRCKα.

### **3.1.9 BepC<sub>Bhe</sub> localizes to cell-to-cell contacts during infection.**

During Ea.hy926 infection with *Bhe* wild-type, BepC<sub>Bhe</sub> localizes to the invasomes via its BID domain [20]. In absence of other effectors, the ectopic expression of mCherry fused to BepC<sub>Bhe</sub> in HUVECs suggests a localization of the effector to the membrane [1].

To further study BepC localization during cell infection, we expressed BepC<sub>Bhe</sub> in *Bhe ΔbepA-G* with a triple Flag-tag on the N-terminus. After translocation in HUVECs, BepC<sub>Bhe</sub> was enriched at cell-to-cell contacts in several cells (Fig. 3.12). The fluorescent dots could correspond to BepC<sub>Bhe</sub> localized in bacteria although this requires further confirmation. Interestingly, BepE<sub>Bhe</sub> was also shown to localize to cell junctions during infection of HUVECs [1].

To determine which domain of BepC<sub>Bhe</sub> was important for the localization to cell contacts, HeLa cells were infected with *Bhe ΔbepA-G* expressing truncated versions of BepC<sub>Bhe</sub> (Fig. 3.13A and Fig. 3.13B). Although BepC<sub>Bhe</sub> localization to cell junctions was less consistent in HeLa

cells, preliminary results showed that the deletion of the whole FIC domain resulted in the relocalization of BepC<sub>Bhe</sub> (OB-BID) to the cellular membrane and/or to the cytoplasm.

Knowing that the FIC domain is necessary for the recruitment to cell contacts, we wanted to determine if the FIC motif, the Flap, or the first helix play a role in BepC localization. BepC<sub>Bhe</sub> with the mutated conserved histidine (H146A) or a canonical FIC motif (K150E) showed both a localization pattern similar to BepC<sub>Bhe</sub> wild-type. However, the localization of BepC<sub>Bhe</sub> with mutated residues that are important to bind a nucleotide derivative (BepC<sub>Bhe</sub><sup>\*\*\*\*</sup>) appeared more diffused. Additionally, the exchange of the Flap or the deletion of the first helix did not have any influence on localization, despite their high degree of conservation.

To test whether a conserved BID domain is also necessary for localization to cell contacts, we infected HeLa cells with *Bhe*  $\Delta$ bepA-G expressing BepC<sub>Bhe</sub> with the BID domain of BepA<sub>Bhe</sub> (Fig. 3.13A and Fig. 3.13B). However, only some spots were visible, indicating either that the effector is not translocated inside the cells, which could explain the absence of actin phenotype, or that it is not detected by the antibody targeting the Flag-tag. An improper folding of the chimeric protein could also be an explanation.

Overall, our data indicate that the FIC domain is required for localization to cell-to-cell contacts while the OB-BID domains localize to the plasma membrane or distribute in the cytosol. However, the absence of the first helix, the exchange of the Flap, and mutations of the conserved histidine and lysine in the FIC motif does not have an influence on localization. Interestingly, the ability of the FIC domain to bind a nucleotide might have a slight influence on localization although this needs further investigation.

### **3.1.10 BepC<sub>Bhe</sub> does not trigger RhoA pathway activation by microtubules depolymerization.**

The T3SS effectors EspG, EspG2, and Orf3 of enteropathogenic *Escherichia coli* (EPEC) were shown to induce the collapse of the microtubule network in mouse fibroblasts, leading to the release of GEF-H1 and to actin stress fiber formation via the activation of the RhoA pathway [21, 22].

To test whether BepC could also use the same strategy to induce actin rearrangements, HeLa cells and HUVECs infected with *Bhe*  $\Delta$ bepA-G expressing BepC<sub>Bhe</sub> were stained for tubulin. At a late stage of infection, infected HeLa cells showed a reorganization of the microtubules around actin stress fibers (Fig. 3.S2A). The regions with high actin density had a low abundance of microtubules, presumably due to space constraints inside the cell. Although the microtubule network appeared denser, BepC<sub>Bhe</sub> did not have a strong influence on microtubules organization in HUVECs at an intermediate state of actin phenotype (Fig. 3.S2B).

This result confirms that BepC does not induce actin rearrangements during infection via the disruption of the microtubule network in order to release GEF-H1.

### **3.1.11 BepC<sub>Bhe</sub> induces the aggregation of vimentin intermediate filaments.**

Vimentin is a type III intermediate filament playing a role in maintaining cell integrity and anchoring organelles [23]. Interestingly, HeLa cells and HUVECs infected with *Bhe ΔbepA-G* expressing BepC<sub>Bhe</sub> showed vimentin clustering (Fig. 3.S3). Mutations in the FIC motif did not have an influence on this phenotype in HUVECs, suggesting that a functional active site is not required to induce this phenotype.

### **3.1.12 Focal adhesions and adherens junctions are maintained in presence of BepC.**

As the RhoA pathway is known to regulate cellular adhesions [24], we wanted to know if BepC has an influence on focal adhesion assembly.

To do so, we infected HeLa cells with *Bhe ΔbepA-G* expressing BepC<sub>Bhe</sub> and stained them for phosphorylated paxillin (pPaxillin) and talin, two components of focal adhesions [25]. The staining of pPaxillin did not show any obvious influence of BepC<sub>Bhe</sub> on the abundance or on the localization of focal adhesions in HeLa cells (Fig. 3.S4A). This would suggest that BepC does not alter the ability of the cells to bind to the extracellular matrix. Interestingly, the cytosolic fraction of talin seems to relocalize to the extremity of elongated cells in presence of BepC<sub>Bhe</sub>. However, it did not seem to correspond to focal adhesions as pPaxillin staining did not show such relocalization (Fig. 3.S4B). It is still unclear whether the relocalization of talin is directly linked to an effect of BepC or related to cytoskeleton rearrangements.

Pathogenic bacteria often target cell junctions via their effectors in order to cross the endothelial or the epithelial barrier and colonize new compartments [26]. As the RhoA pathway is known to regulate adherens junctions [27], which are essential to maintain the integrity of the endothelial barrier, we wanted to determine if BepC could disrupt this type of cellular junctions during infection.

To answer this question, we infected HUVECs with *Bhe ΔbepA-G* expressing BepC<sub>Bhe</sub> and stained cells for VE-cadherin, a component of adherens junctions (Fig. 3.S5). In presence of BepC<sub>Bhe</sub>, the remaining infected cells that were still in contact with each other were able to maintain adherens junctions. According to this result, the translocation of BepC does not seem to have a drastic effect on adherens junctions during cell infection although the reduction of cell density would certainly impair endothelial permeability.

## 3.2 Discussion

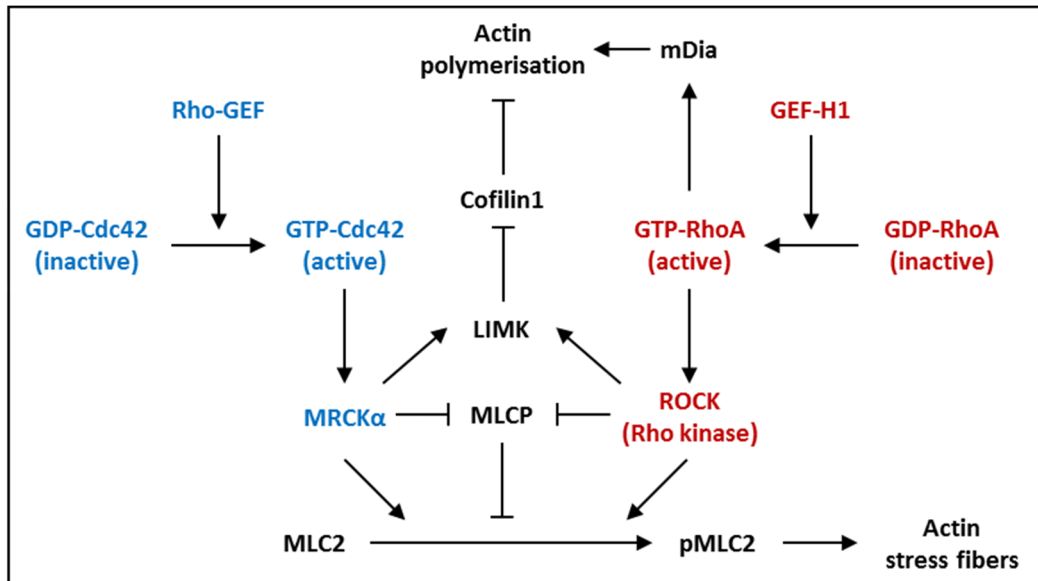
Pathogenic bacteria subvert cellular processes by activating Rho GTPases via bacterial effectors and toxins in order to facilitate the infection [21, 28-34]. As the cytoskeleton plays a major role in bacterial uptake, endothelial and epithelial barrier integrity as well as immune cell migration, it is a common target for bacterial effectors. During infection, bacteria of the genus *Bartonella* translocate effector proteins (Beps) into mammalian cells via a type IV secretion system. BepC, one of the most conserved effectors in the *Bartonella* species of the lineage 4, participates in the engulfment of bacterial aggregates and affects dendritic cell (DCs) migration *in vitro* [1-3]. In this study, we demonstrate that BepC interacts with GEF-H1 and MRCK $\alpha$  to induce actin rearrangements in human cells via the activation of the RhoA pathway.

### **The cytoskeleton rearrangements mediated by BepC correlate with the function of GEF-H1 and MRCK $\alpha$ .**

GEF-H1 and MRCK $\alpha$  are involved in the RhoA and the Cdc42 pathways, respectively, which participate in actin stress fiber formation and actin polymerization (see representation below). In physiological conditions, the stimulation of GEF-H1 activates RhoA by promoting the exchange of GDP for GTP [35]. Subsequently, GTP-bound RhoA interacts with ROCK, which increases phosphorylated myosin light chain (pMLC2) by direct modification via its kinase domain and indirectly by inhibiting MLCP (myosin light chain phosphatase). The increase of pMLC2 promotes actomyosin contraction and ultimately leads to actin stress fiber formation [36-38]. Additionally, the activation of the RhoA pathway promotes actin polymerization via the activation of LIMK1 by ROCK, which in turn phosphorylates and inactivates the actin-severing protein cofilin1 [36, 39]. Furthermore, RhoA activates the formin mDia (mammalian diaphanous), which induces unbranched actin polymerization [40]. MRCK $\alpha$  phosphorylates exactly the same targets as ROCK via its kinase domain, leading to actin stress fiber formation and actin polymerization [39, 41, 42]. Therefore, the stimulation of GEF-H1 or MRCK $\alpha$  by BepC<sub>Bhe</sub> could both results in the increase of phosphorylated myosin light chain and the actin rearrangements observed during cell infection. However, our data indicate that the RhoA pathway plays a major role in the actin phenotype as inhibitors of RhoA and ROCK drastically reduce the actin stress fibers in HeLa cells infected with *Bhe*  $\Delta$ bepA-G expressing BepC<sub>Bhe</sub>. Therefore, the interaction of BepC<sub>Bhe</sub> with MRCK $\alpha$  is probably not sufficient to maintain actin rearrangements during infection. Nevertheless, ROCK and MRCK $\alpha$  have distinct roles in the spatial regulation of MLC2 phosphorylation and cooperate during cell migration [43]. ROCK is involved in actin stress fiber formation in the center of the cell and in rear-end retraction during migration [44, 45]. By contrast, MRCK $\alpha$  is recruited via adaptor proteins to the cell periphery where it participates in cell migration via the regulation of lamellar actomyosin retrograde flow and lamellipodial F-actin dynamic [39, 46]. In conclusion, a potential activation of both GEF-



H1 and MRCK $\alpha$  would have a synergic effect on actin rearrangements rather than being redundant.



**Involvement of the Cdc42 (in blue) and the RhoA (in red) pathways in actin stress fiber formation and actin polymerization.**

Interestingly, the translocation of BepC<sub>Bhe</sub> in HUVECs and HeLa cells leads to the aggregation of vimentin, which also participates in the cytoskeleton [47]. Vimentin is one of the most frequent components of intermediate filaments and is involved in many processes such as angiogenesis, cell migration, and cell adhesion [48, 49]. Considering that ROCK phosphorylates vimentin on Ser71 and inhibits its ability to form filaments *in vitro* [50, 51], the activation of the RhoA pathway by BepC<sub>Bhe</sub> probably leads to vimentin rearrangements. Furthermore, the inactivation of vimentin increases actin stress fiber assembly via the stimulation of GEF-H1 by phosphorylation [52]. Thus, the aggregation of vimentin might boost the effect of BepC on actin rearrangements. Interestingly, the Fic effector Bep2 from *Bartonella rochalimae* has been described to AMPylate vimentin *in vitro* [53], although the biological function of this modification remains elusive. Additionally, SpyA from *Streptococcus pyogenes* ADP-ribosylates vimentin on Arg 44/49 and induce the collapse of vimentin in HeLa cells [54], suggesting that targeting intermediate filaments could have a positive impact on pathogenesis.

**The actin phenotype, the localization to cell contacts, and the interaction with GEF-H1 and MRCK $\alpha$  are correlated.**

Strikingly, there is a high correlation between the ability of BepC<sub>Bhe</sub> to localize to cell contacts, to trigger the actin phenotype and to interact with GEF-H1 and MRCK $\alpha$  (Table 1). Therefore, it is tempting to speculate that BepC is recruited to cell contacts by interacting with GEF-H1 and/or MRCK $\alpha$ , which results in the activation of the RhoA pathway and actin rearrangements. This model is further supported by the fact that GEF-H1 localizes to tight junctions [55].

Condition	<i>Bhe ΔbepA-G</i>	Actin rearrangements	Interaction with GEF-H1	Interaction with MRCKα	Cell-to-cell contact localization
Negative control	<i>pEmpty</i>	No	X	X	X
Wild-type	<i>pbepC<sub>Bhe</sub></i>	Yes	Yes	Yes	Yes
FIC domain modification	<i>pbepC<sub>Bhe</sub> H146A</i>	Yes	Yes	Yes	Yes
	<i>pbepC<sub>Bhe</sub> K150E</i>	Yes	Yes	Yes	Yes
	<i>pbepC<sub>Bhe</sub> ****</i>	Yes	Yes	Yes	Yes
	<i>bepC<sub>Bhe</sub> (Flap BepA)</i>	Yes	Yes	Yes	Yes
BID domain modification	<i>pbepC<sub>Bhe</sub> (BID BepA)</i>	No	Yes	Yes	No
Truncated protein	<i>pbepC<sub>Bhe</sub> (19-532)</i>	Yes	Yes	Yes	Yes
	<i>pbepC<sub>Bhe</sub> (OB-BID)</i>	No	No	No	No

**Table 1. Summary of actin rearrangements, interaction with GEF-H1 and MRCKα, and localization for all the tested conditions.**

The color code corresponds to the comparison with the wild-type condition. Green: comparable, orange: reduced, red: negative.

According to this model, as the FIC domain of BepC<sub>Bhe</sub> is required to interact with GEF-H1 and MRCKα during infection of HeLa cells and HUVECs, its absence should result in the redistribution of the truncated effector to the plasma membrane or to the cytoplasm, which is observed in HeLa cells infected with *Bhe ΔbepA-G* expressing BepC<sub>Bhe</sub> (OB-BID). Furthermore, the absence of actin rearrangements in these cells is also in accordance this model.

By contrast, the deletion of the first helix and the exchange of the Flap do not impair the ability of BepC<sub>Bhe</sub> to bind GEF-H1 and MRCKα, indicating that they do not participate in the binding interface. Thus, BepC<sub>Bhe</sub> (19-532) and BepC<sub>Bhe</sub> (Flap BepA<sub>Bhe</sub>) could be recruited to cell contacts where they induce actin rearrangements.

Interestingly, mutations of the conserved histidine (H146A) and the conserved lysine (K150E) do not influence actin rearrangements. Thus, it is likely that BepC<sub>Bhe</sub> does not induce actin rearrangements via a posttranslational modification of GEF-H1 or MRCKα but rather via protein-protein interaction.

However, multiple mutations in the FIC motif of BepC (BepC<sub>Bhe</sub> \*\*\*\*) reduce the binding with GEF-H1 and MRCKα, which could explain the more diffuse localization in HeLa cells. As the mutated residues (H146A, K150A, R154A, R157A) participate in the binding of the nucleotide in the active site of the FIC domain (Fig. 1.9), the presence of a nucleotide might help for the stabilization of the FIC domain and thereby facilitate the interaction. Nevertheless, the reduced interaction and the scattered localization were sufficient to promote actin rearrangements.

The only inconsistency with the proposed model is that BepC<sub>Bhe</sub> with the BID domain of BepA<sub>Bhe</sub> is still able to interact with GEF-H1 and MRCK $\alpha$  although it does not localize to cell contacts or induce actin stress fibers in HeLa cells. However, it is possible that the chimeric protein is not translocated during infection and is sequestered in the bacteria, as suggested by the localization pattern. Thus, BepC (BID BepA<sub>Bhe</sub>) would only interact with the two host proteins during the co-immunoprecipitation assay after cell lysis of bacteria and HeLa cells. Nevertheless, we can conclude that a conserved BID domain is not required to bind GEF-H1 and MRCK $\alpha$ . Whether the FIC domain alone is sufficient for cell-to-cell contact localization, actin phenotype, or protein interaction remains to be tested.

In order to validate this model, co-localization studies involving the detection of GEF-H1, MRCK $\alpha$ , and BepC in host cells by confocal microscopy will be required.

### **How GEF-H1 and MRCK $\alpha$ might be regulated by BepC.**

The virulence factors produced by bacterial pathogens are using a wide variety of strategies to activate the Rho GTPase pathways, including GEF mimicry, GEF interaction and posttranslational modifications [56] (See chapter 1.2.1). However, the molecular mechanism by which BepC is activating the RhoA pathway via its interaction with GEF-H1 is still unknown. As BepC does not contain a WxxxE motif that is shared by GEF mimicking bacterial effectors and as a conserved FIC motif is not required for actin rearrangements, it is unlikely that BepC activates the RhoA pathway by exchanging GDP for GTP or by posttranslational modification.

In a physiological state, the activity of GEF-H1 is negatively regulated by the phosphorylation of serine residues located on its C-terminus. This modification leads to the recruitment of the 14-3-3 protein and to the localization of the GEF-H1 to the microtubules, which inhibits its ability to activate Rho GTPases [57-60]. Thus, some bacterial effectors induce microtubule depolymerization to release GEF-H1 and activate the RhoA pathway, thereby manipulating the actin cytoskeleton [21]. However, our data indicate that BepC does not induce the activation of the RhoA pathway via the collapse of the microtubule network, although it seems to be reorganized around actin stress fibers.

Interestingly, the T3SS effector VopO from *Vibrio parahaemolyticus* also activates the RhoA pathway by interacting with GEF-H1, thereby leading to actin stress fiber formation [32]. Although they do not share any sequence homology and the mechanism of activation by VopO is elusive, it is conceivable that BepC may act in a similar manner by protein-protein interaction.

Concerning MRCK $\alpha$ , it is not clear whether the interaction with BepC would lead to its activation. As the stimulation of the RhoA pathway via GEF-H1 is likely to be sufficient to induce actin rearrangements, it is possible that BepC posttranslationally modifies MRCK $\alpha$  and that the modification would not have a drastic impact on the actin phenotype. Reciprocally, it cannot

be excluded that MRCK $\alpha$  could act on BepC as some effectors have been shown to be modified and regulated by host enzymes [61]. To date, no molecular mechanism involving the manipulation of a downstream binding partner of Rho GTPases and a virulence factor has been described. Interestingly, GEF mimicking effectors with a WxxxE motif were initially proposed to induce actin rearrangements via a GTPase mimicry function as they interact with downstream ligands of the Rho GTPases *in vitro* [62]. Whether this function is biologically relevant during pathogenesis remains unclear.

#### **Conservation of BepC function among *Bartonella* species of the lineage 4.**

BepC from various *Bartonella* species of the lineage 4 induces actin stress fiber formation in HeLa cells, suggesting that rearrangements of the cytoskeleton mediated by BepC play a critical role in the establishment of infection by *Bartonella*. Whether the difference in actin rearrangements intensity is due to a translocation defect, a loss of function, or host specificity remains to be tested. As heterologous GEF-H1 and MRCK $\alpha$  have high sequence identities between the different mammalian hosts targeted by *Bartonella* of the lineage 4 (Table 2), it is conceivable that BepC from a specific species would be able to interact indifferently with GEF-H1 and MRCK $\alpha$  from rodents, cats, dogs, and humans. Thus, if *Bartonella* infects a mammal that is not its reservoir host, such as *Bhe* infecting humans, BepC will probably be able to participate in pathogenesis by mediating actin rearrangements.

<b>GEF-H1</b>	<i>Homo sapiens</i>	<i>Felis catus</i>	<i>Rattus norvegicus</i>	<i>Mus musculus</i>
<i>Homo sapiens</i>		93.4%	89.1%	88.6%
<i>Felis catus</i>	93.4%		88.0%	87.7%
<i>Rattus norvegicus</i>	89.1%	88.0%		98.3%
<i>Mus musculus</i>	88.6%	87.7%	98.3%	

<b>MRCK<math>\alpha</math></b>	<i>Homo sapiens</i>	<i>Felis catus</i>	<i>Rattus norvegicus</i>	<i>Mus musculus</i>
<i>Homo sapiens</i>		97.2%	96.0%	96.1%
<i>Felis catus</i>	97.2%		95.4%	95.5%
<i>Rattus norvegicus</i>	96.0%	95.4%		98.3%
<i>Mus musculus</i>	96.1%	95.5%	98.3%	

**Table 2. Sequence identities between GEF-H1 and MRCK $\alpha$  of different mammalian hosts of *Bartonella*.**

### **Biological consequences of the activation of the RhoA pathway by BepC.**

The translocation of BepC by *Bartonella* stimulates the RhoA pathway by interacting with GEF-H1 and possibly modulates the activity of MRCK $\alpha$ . As the RhoA pathway and MRCK $\alpha$  are involved in a wide variety of cellular processes, the function of BepC might vary according to the cell types infected by *Bartonella* through the different stages of the infection cycle.

As *Bartonella* successfully invade dendritic cells *in vitro* and requires to be transported from the dermis to the blood-seeding niche, it has been proposed that dendritic cells are colonized during the dermal stage of host infection [1]. In absence of BepE, the translocation of BepC impairs the migration of DCs through an endothelial cell layer *in vitro* [1]. According to experimental data on migrating endothelial cells, the migration defect is due to a defect in rear-end detachment [1], which is controlled by the actomyosin contraction and the degradation of focal adhesion [63, 64]. As RhoA promotes actomyosin contraction via ROCK and MLC2 phosphorylation [65-67], the activation of the RhoA pathway via the interaction of BepC with GEF-H1 is likely responsible for the migration defect. Additionally, MRCK $\alpha$  is involved in cell migration by contributing to the actomyosin lamellar retrograde flow [68]. Thus, a potential modulation of its activity by BepC would possibly have an increased defect on cell migration. Furthermore, RhoA also plays a role in the maturation of focal adhesions during migration [24, 45, 69]. As BepC activates the RhoA pathway, it might stabilize focal adhesions and interfere with their dissociation from the extracellular matrix, which could then results in the cell fragmentation observed in migrating endothelial cells due to a deficiency in rear-end detachment [1]. This hypothesis is further supported by our data suggesting that HeLa cells are able to maintain focal adhesions in presence of BepC despite actin rearrangements. Eventually, BepC could interfere with immune cells motility by disturbing the regulation of the RhoA pathway, as reported for the C3 toxin that impairs macrophage migration [44, 70]. By contrast, a spatiotemporal regulation of BepC function by BepE could allow the dissemination of *Bartonella* in the host by using DCs as a shuttle in a similar manner as the ancestrally related

*Brucella abortus* as well as *Bordetella bronchiseptica*, *Burkholderia pseudomallei*, and *Francisella tularensis* [71-74].

To colonize new compartments, pathogens specifically target cellular junctions of the endothelium and the epithelial barriers in order to increase their permeability, which is controlled by Rho GTPases (See chapter 1.1.2.2). As *Bartonella* establishes a bacteremia into the reservoir host, it has probably developed a strategy to cross the endothelial barrier. Interestingly, GEF-H1 is involved in endothelial barrier regulation and is recruited to tight junctions in epithelial cells, thereby regulating the paracellular permeability [55, 75]. Accordingly, RhoA is involved in the regulation of tight junctions and adherens junctions in endothelial and epithelial cells [76-78]. More specifically, the activation of the RhoA pathway increases vascular permeability [78-81] by targeting adherens junctions [27, 82]. Surprisingly, BepC does not seem to have a strong effect on adherens junctions of infected HUVECs. Nevertheless, the remaining cells that are still in contact are probably less affected by BepC and the reduction of cell density completely disorganizes the confluent cell layer. Thus, the interaction of GEF-H1 and the subsequent activation of the RhoA pathway by BepC might help *Bartonella* to disrupt the endothelial barrier and establish bacteremia.

A wide variety of pathogens blocks phagocytosis via virulence factors that modulates Rho GTPases pathways (See chapter 1.2). In *Bartonella*, BepG<sub>Bhe</sub> and BepC<sub>Bhe</sub> together with BepF<sub>Bhe</sub> prevent the endocytosis of single bacteria, which is a prerequisite to bacterial aggregation on the cell surface and to invasome formation [3, 7]. However, the presence of bacterial clusters in HeLa cells and EA.hy926 displaying a strong actin phenotype suggests that BepC alone is sufficient to block bacterial uptake and to initiate the first step of invasome formation. Furthermore, bacterial aggregates seem to correlate with the intensity of actin stress fiber formation as only BepC of *Bhe* and *Bqu* are able to induce it, in contrast to BepC from other *Bartonella* species that displays a weaker phenotype. Therefore, the activation of the RhoA pathway by BepC and the resulting formation of actin stress fibers might prevent the phagocytosis of *Bartonella* by immune cells.

Although the exact function of invasome formation remains elusive and its biological relevance needs to be confirmed *in vivo*, it might reflect a unique strategy of *Bartonella henselae* to invade host cells. As knocking down GEF-H1 significantly reduces invasome formation mediated by BepC<sub>Bhe</sub> and BepF<sub>Bhe</sub> (unpublished data from Dr. Simone Eicher), it is likely that BepC participates in the engulfment process by activating the RhoA pathway via its interaction with GEF-H1. Surprisingly, only BepC of *Bhe* is able to participate in invasome formation together with BepF<sub>Bhe</sub> although BepC of *Bqu*, *Btr* and *Bta* induce actin rearrangements. Furthermore, BepC<sub>Bqu</sub> is not able to trigger invasome formation while it triggers bacterial aggregates in HeLa cells. These observations indicate that neither actin stress fiber formation nor bacterial

clustering mediated by BepC is sufficient to promote invasome formation in collaboration with BepF<sub>Bhe</sub>. As BepF<sub>Bhe</sub> is proposed to modulate the Rac1 and Cdc42 pathways [2] and BepC activates the RhoA pathway, a fine tuning of the different pathways might be necessary for invasome formation. Therefore, BepC from other *Bartonella* species might not be able to cooperate efficiently with BepF<sub>Bhe</sub> to promote the internalization of bacterial clustering. Another possibility would be that BepC<sub>Bhe</sub> has acquired an additional function that is necessary for invasome formation. Reciprocally, BepF of other *Bartonella* species might also not be able to participate in invasome formation as only BepF<sub>Bhe</sub> and BepF<sub>Bgr</sub> harbor in their first BID domain a conserved WxxxE motif, which participates in invasome formation and is found in GEF mimicking bacterial effectors (See chapter 1.2.1.1) [2]. Thus, more investigations are required to determine whether invasome formation could be specific to *Bhe*.

*Bartonella* triggers NF-κB-dependent proinflammatory response related to the VirB/D4 T4SS in HUVECs, which could contribute to angiogenesis but also initiate innate and adaptive immune responses [83-85]. Interestingly, the activation of NF-κB upon epithelial cell invasion by *Shigella* is mediated by GEF-H1, which interacts with the pattern recognition receptor NOD1 [86]. Additionally, GEF-H1 is also regulating the NOD2-dependent NF-κB activation that controls proinflammatory cytokines expression in mouse macrophages [87]. Furthermore, constitutively active RhoA stimulates the NOD1 signaling pathway in HEK293 cells [88]. Thus, it is tempting to speculate that the interaction of GEF-H1 with BepC, and the following stimulation of the RhoA pathway, could be sensed via the NOD1 and NOD2 signaling pathways that would activate NF-κB and thereby an immune response. If this hypothesis can be confirmed, BepE could play an important role in maintaining *Bartonella* below the radar of the immune system by reducing the activation of the RhoA pathway.

### **Summary.**

In conclusion, we identified a new strategy by which *Bartonella* can exploit the host cell functions by targeting signaling pathways regulated by Rho GTPases. The translocation of BepC into the host cell leads to its recruitment at cell-to-cell contact and to actin rearrangements due to the activation of the RhoA pathway via the interaction with GEF-H1 and possibly to the modulation of MRCKα. As a result, the subversion of cellular processes by BepC could help *Bartonella* to escape the immune system by preventing phagocytosis and immune cell migration and/or play a role in disrupting the endothelial barrier and eventually allow the bacteria to reach the blood and establish a bacteremia into the reservoir host.



### 3.3 Figures

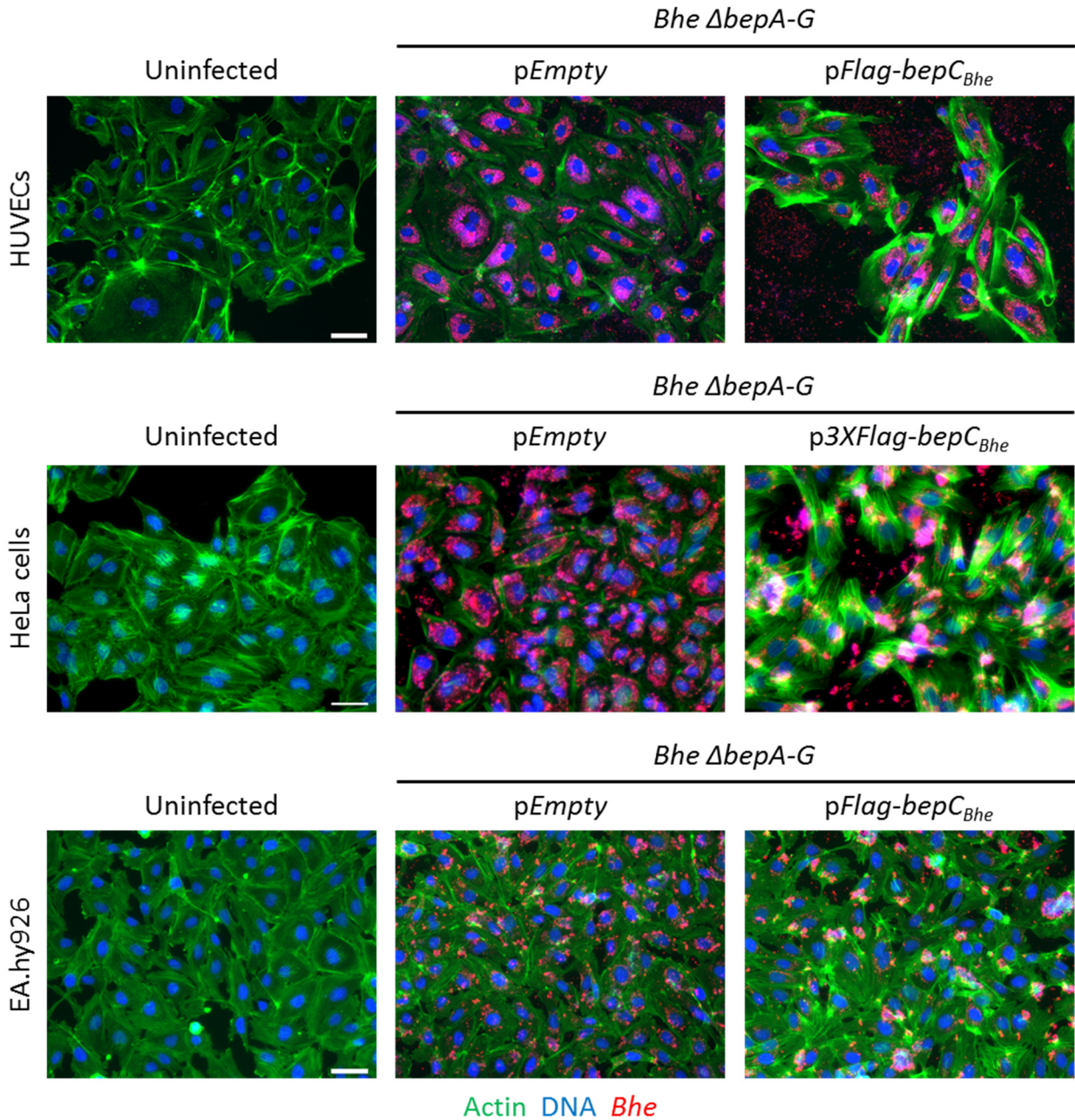


**Figure 3.1. BepC<sub>Bhe</sub> induces actin rearrangements in various human cells.**

HeLa cells and HUVECs were infected at a MOI = 400 and EA.hy926 at a MOI = 800 with the indicated bacterial strain. After 48 hours of infection, the cells were fixed and stained by immunocytochemistry before being analyzed by fluorescence microscopy. F-actin is represented in green, DNA in blue, and *Bartonella* in red (scale bar = 50  $\mu$ m).



*Bhe*  $\Delta$ *bepA-G*

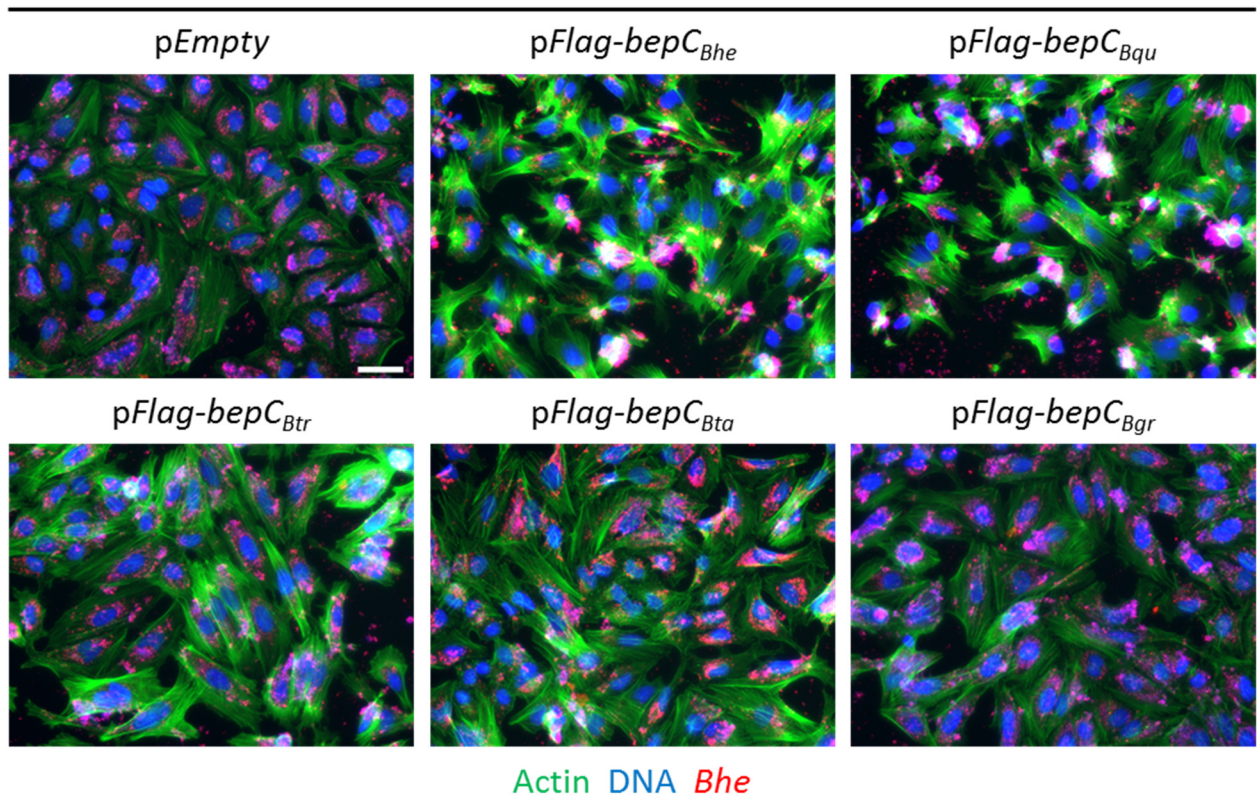


**Figure 3.2. BepC of different *Bartonella* species induces actin stress fibers in HeLa cells.**

HeLa cells were infected with the indicated bacterial strain at a MOI = 400. After 48 hours of infection, the cells were fixed and stained by immunocytochemistry before being analyzed by fluorescence microscopy. F-actin is represented in green, DNA in blue, and *Bartonella* in red (scale bar = 50  $\mu$ m).

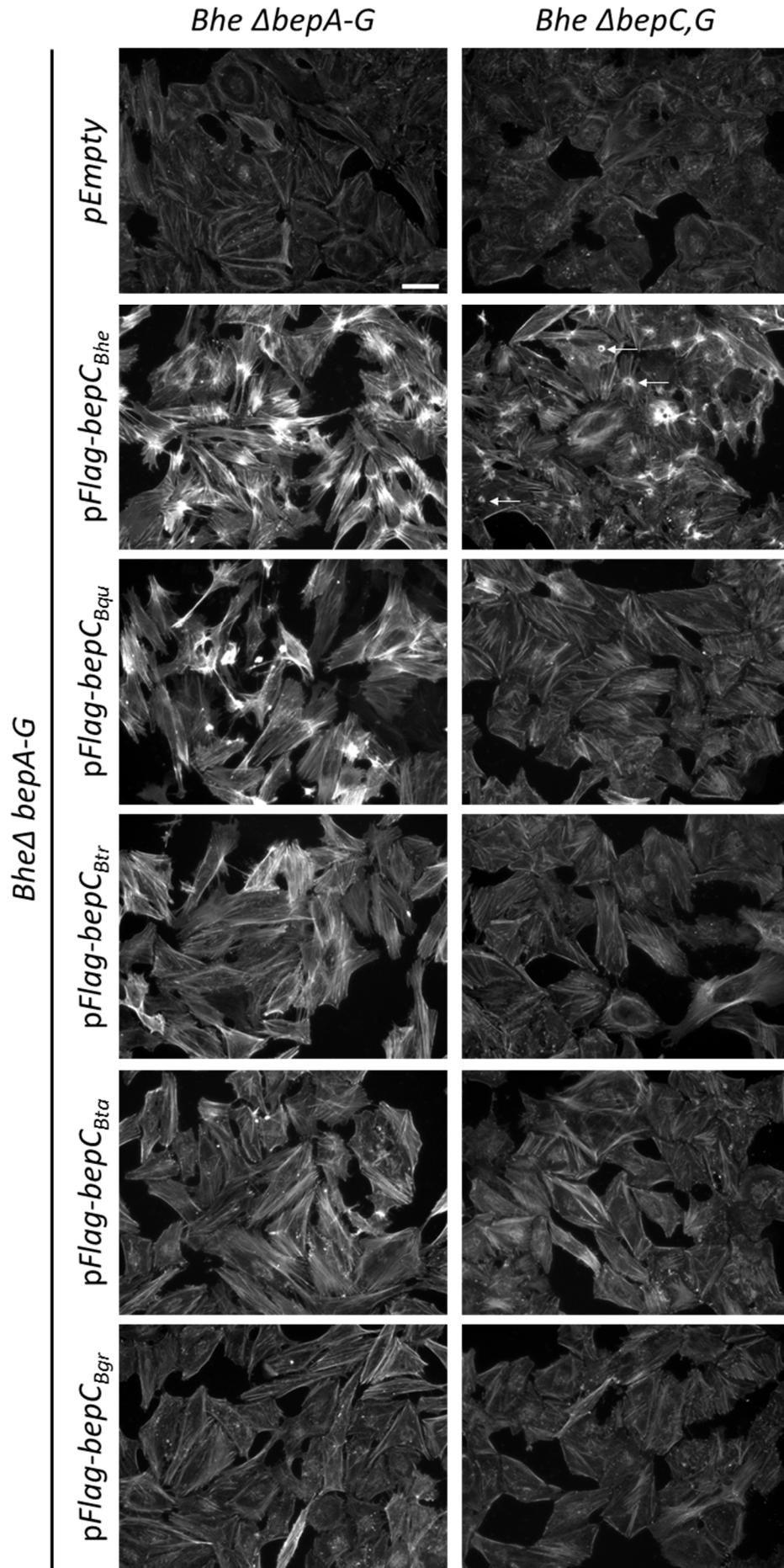


**Figure 3.3. Only BepC<sub>Bhe</sub> is able to participate to invasome formation together with BepF<sub>Bhe</sub> during infection of HeLa cells.** HeLa cells were co-infected at MOI = 400 (2 x MOI = 200) with two different strains, *Bhe ΔbepA-G* or *Bhe ΔbepC,G* in combination with *Bhe ΔbepA-G* with the empty plasmid or expressing BepC of different *Bartonella* species. After 48 hours of infection, the cells have been fixed and stained by immunocytochemistry before being analyzed by fluorescence microscopy. F-actin is represented in white (scale bar = 50 μm). Some invasomes are indicated with white arrows.



*Bhe*  $\Delta$ *bepA-G*

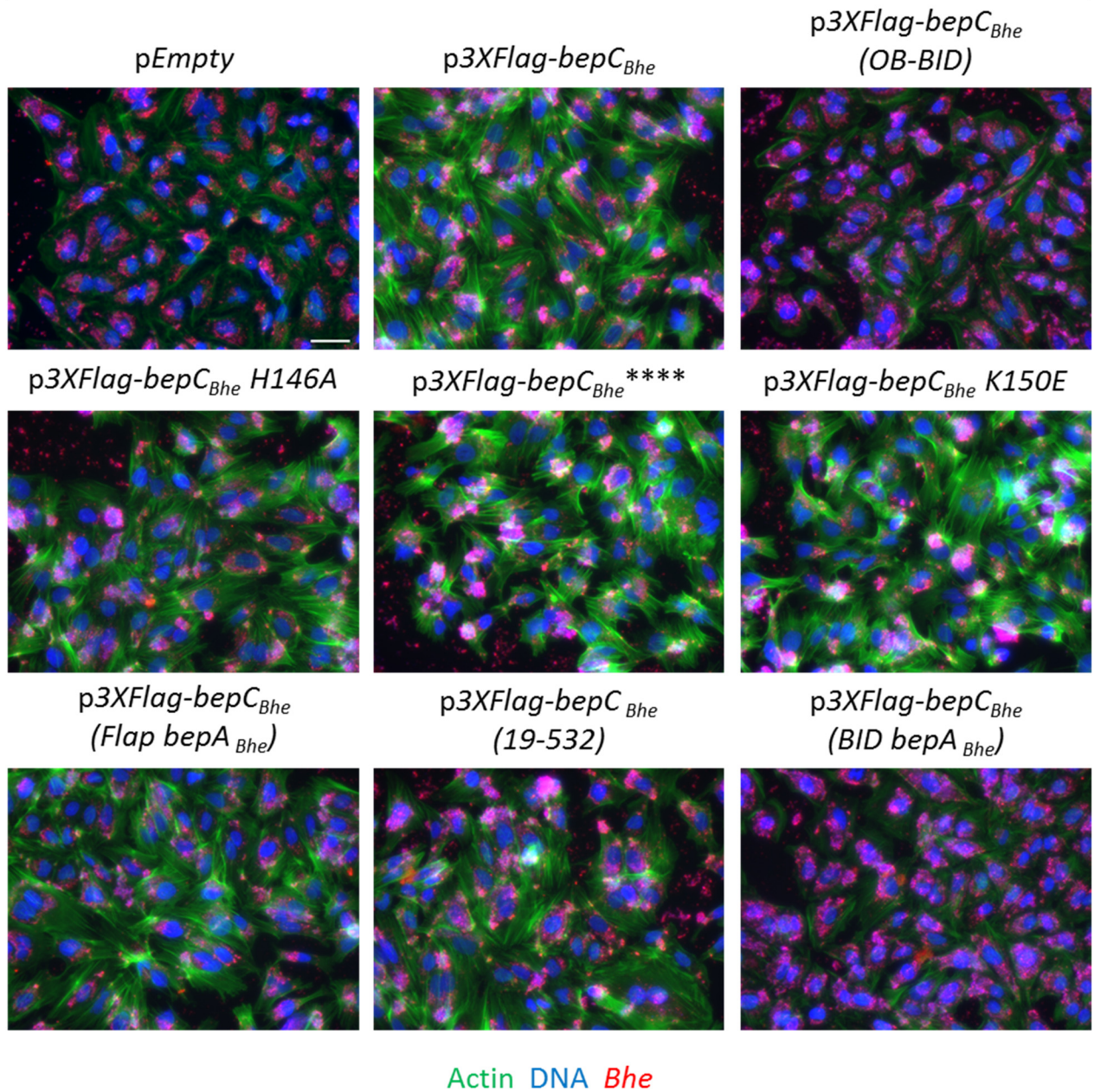


**Figure 3.4. The FIC and the BID domains of *BepC*<sub>Bhe</sub> are required for actin stress fiber formation in HeLa cells but not a conserved Flap or FIC motif.**

HeLa cells were infected with the indicated bacterial strain at a MOI = 400. After 48 hours of infection, the cells were fixed and stained by immunocytochemistry before being analyzed by fluorescence microscopy. F-actin is represented in green, DNA in blue, and *Bartonella* in red (scale bar = 50  $\mu$ m). *BepC*<sub>Bhe</sub> \*\*\*\* = *BepC*<sub>Bhe</sub> H146A, K150A, R154A, R157A.

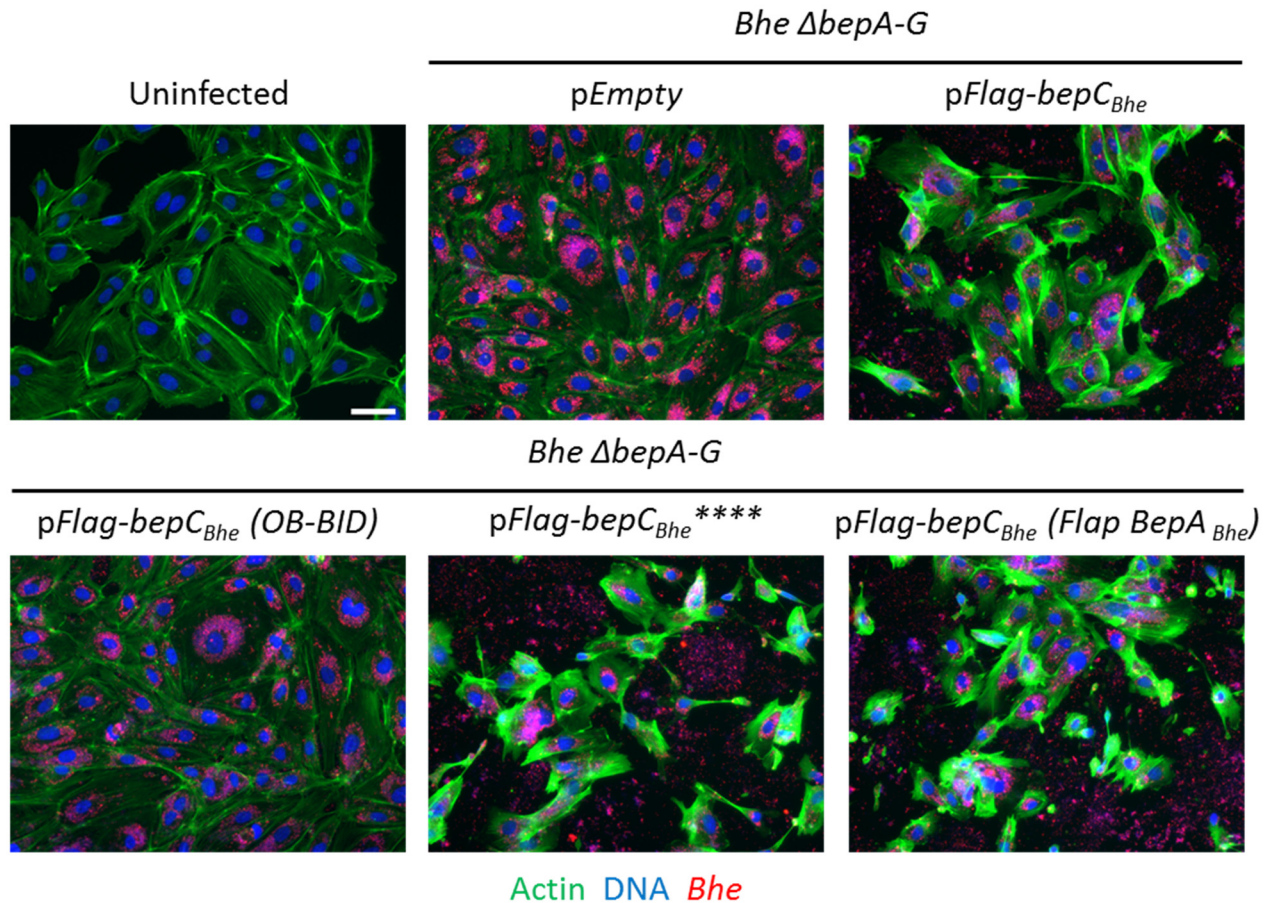


**Figure 3.5. The FIC domain of BepC<sub>Bhe</sub> is required for cell fragmentation in HUVECs but not a conserved Flap or FIC motif.**

HUVECs were infected with the indicated bacterial strain at a MOI = 400. After 48 hours of infection, the cells were fixed and stained by immunocytochemistry before being analyzed by fluorescence microscopy. F-actin is represented in green, DNA in blue, and *Bartonella* in red (scale bar = 50  $\mu$ m). BepC<sub>Bhe</sub> \*\*\*\* = BepC<sub>Bhe</sub> H146A, K150A, R154A, R157A.

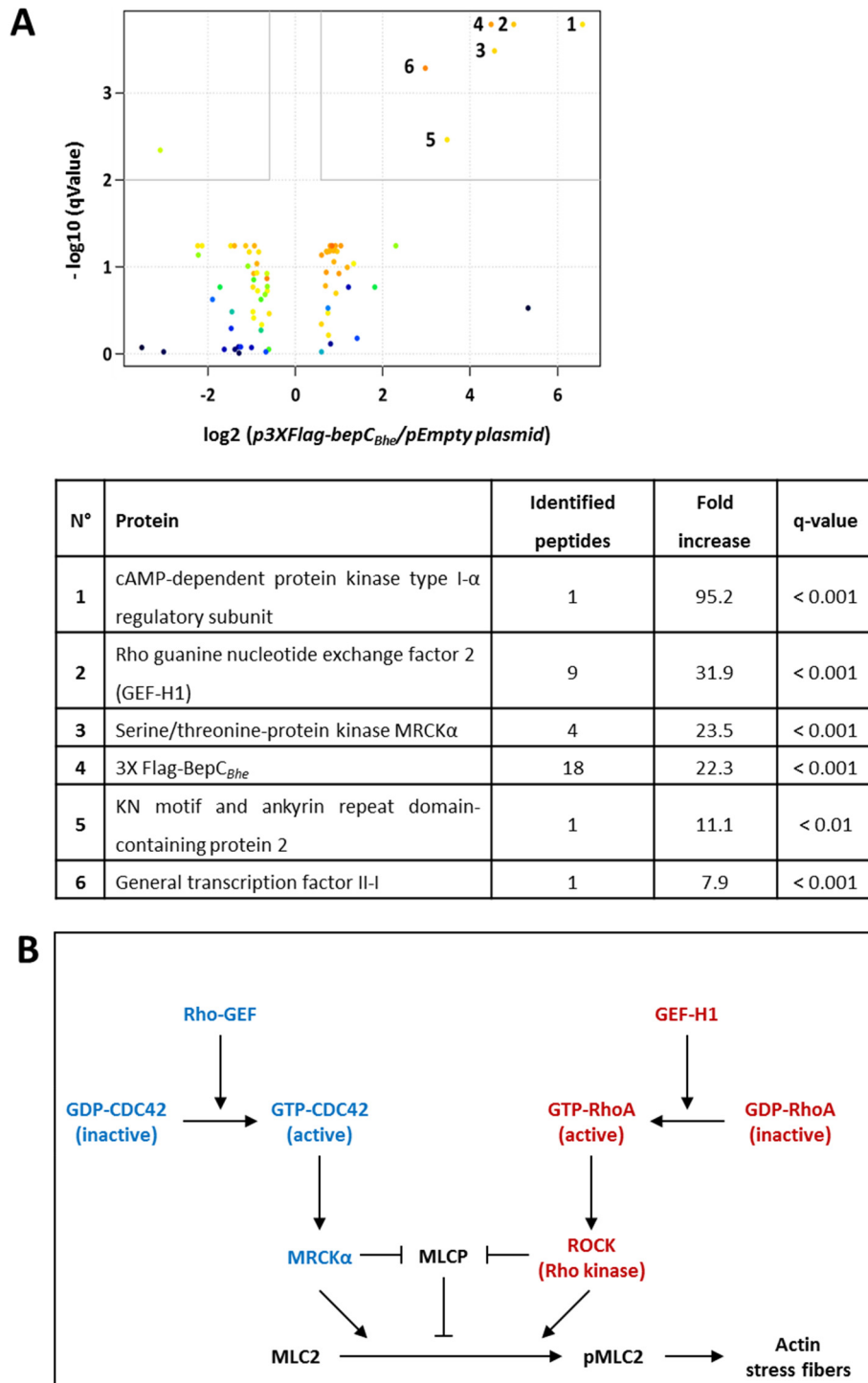
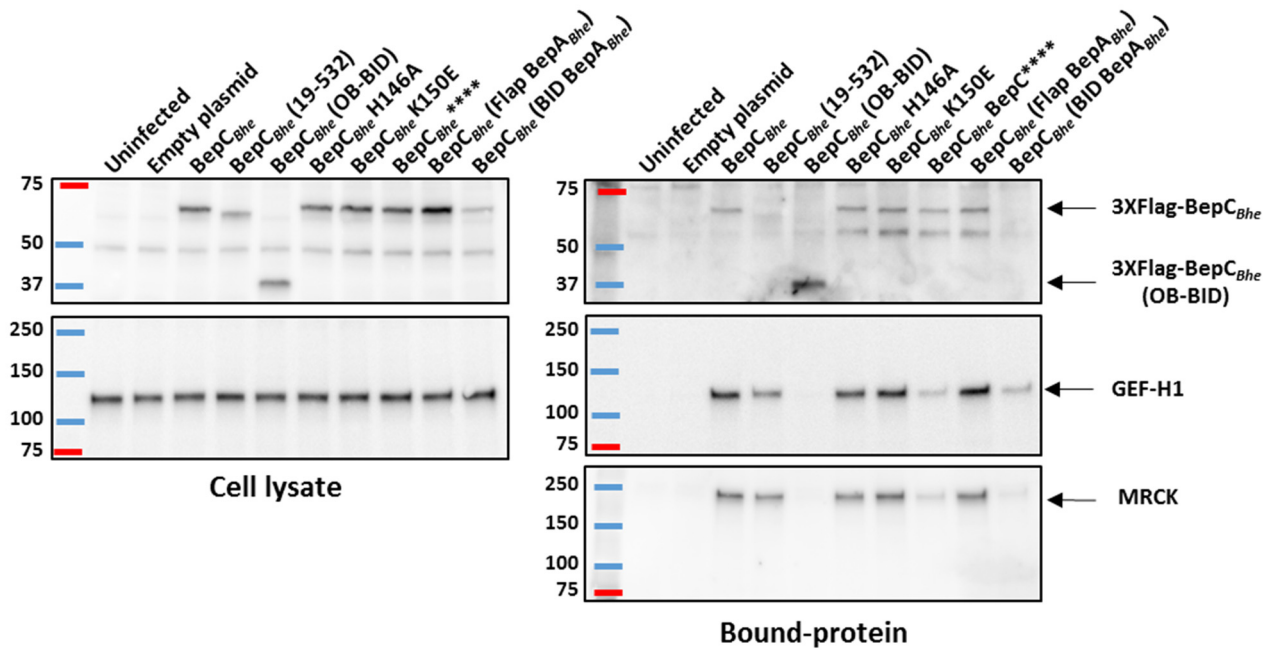


**Figure 3.6. GEF-H1 and MRCK $\alpha$  co-immunoprecipitate with BepC<sub>Bhe</sub> after HeLa cell infection**

**A)** HeLa cells were infected with *Bhe*  $\Delta$ *bepA-G* expressing 3XFlag-BepC<sub>Bhe</sub>, or carrying the empty plasmid as a negative control, at a MOI = 200. After 24 hours of infection, the cells were lysed and incubated in presence of anti-Flag antibody. 3XFlag-BepC<sub>Bhe</sub> and its interacting partners were pulled-down with protein G agarose beads before being eluted with SDS. Samples were analyzed by mass spectrometry and compared to the negative control (technical triplicates). Proteins enriched after pull-down of 3XFlag-BepC from infected HeLa cell lysates are indicated on the volcano plot and summarized in the table. **B)** GEF-H1 and MRCK $\alpha$  participate in actin stress fiber formation by activating the RhoA pathway or directly phosphorylating myosin light chain, respectively. MLCP = Myosin light chain phosphatase.



**A**



**B**

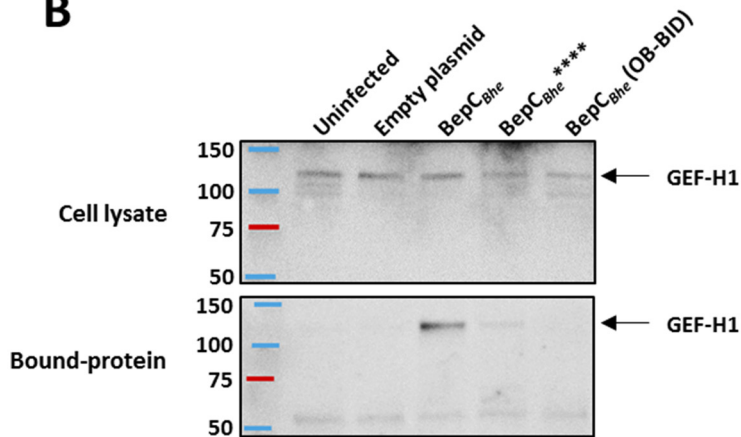


**Figure 3.7. The FIC domain is necessary for the interaction between BepC<sub>Bhe</sub> and GEF-H1 or MRCK $\alpha$  but not a conserved FIC motif or Flap.**

Human cells were infected with *Bhe*  $\Delta$ *bepA-G* carrying the empty plasmid or expressing Flag-tagged BepC<sub>Bhe</sub> wild-type, mutants, or truncated versions at a MOI = 200. After 24 hours of infection, the cells were lysed and incubated in presence of anti-Flag antibody. BepC<sub>Bhe</sub> was pulled-down with protein G agarose beads before being eluted with SDS. Cell lysates before pull-down and samples after pull-down were analyzed by western blot. **A)** Samples from HeLa cells infected with *Bhe*  $\Delta$ *bepA-G* expressing 3XFlag-tagged BepC<sub>Bhe</sub> were analyzed by western blot against Flag-tag, GEF-H1, and MRCK $\alpha$ . **B)** Samples from HUVECs infected with *Bhe*  $\Delta$ *bepA-G* expressing 1XFlag-tagged BepC<sub>Bhe</sub> were analyzed by western blot against GEF-H1. BepC<sub>Bhe</sub> \*\*\*\* = BepC<sub>Bhe</sub> H146A, K150A, R154A, R157A.

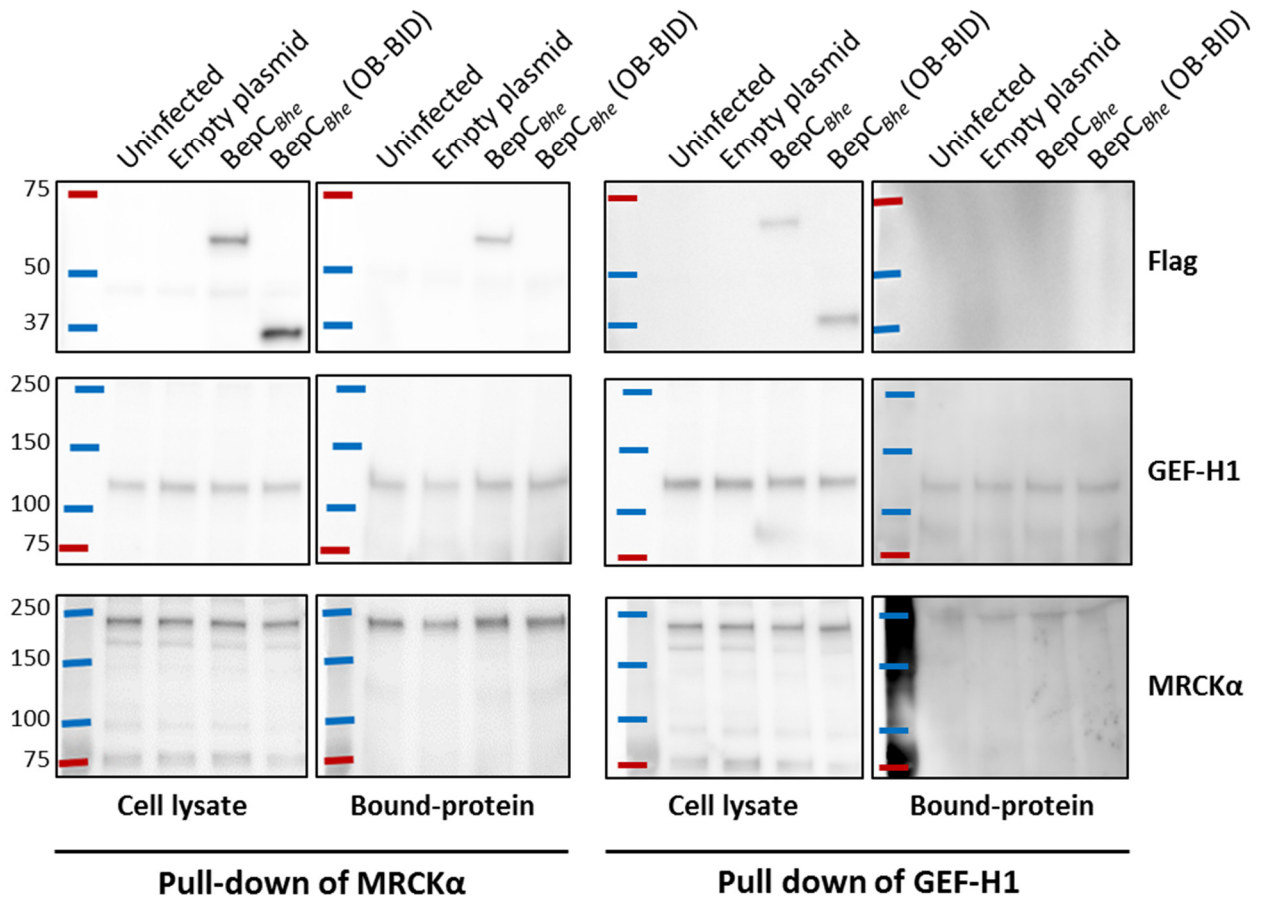
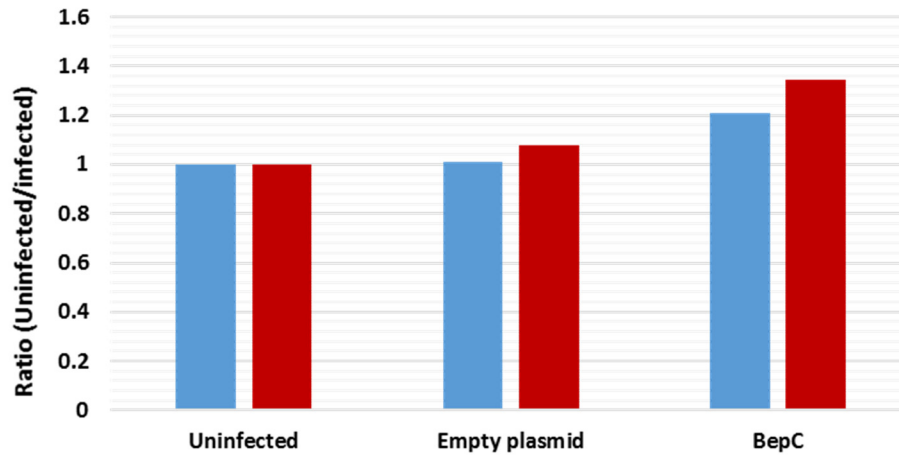


**Figure 3.8. BepC<sub>Bhe</sub> co-immunoprecipitates with MRCKα but not with GEF-H1 after HeLa cells infection.**

HeLa cells were infected with *Bhe ΔbepA-G* expressing 3XFlag-tagged BepC<sub>Bhe</sub>, or carrying the empty plasmid, at a MOI = 200. After 24 hours of infection, the cells were lysed and incubated in presence of anti-MRCKα or anti-GEF-H1 antibody. MRCKα or GEF-H1 were pulled-down with protein G agarose beads before being eluted with SDS. Cell lysates before pull-down and samples after pull-down were analyzed by western blot against Flag-tag, GEF-H1, or MRCKα.



Condition	Experiment 1	Experiment 2
Uninfected	1	1
Empty plasmid	1.01	1.08
BepC	1.21	1.35

**Figure 3.9. BepC<sub>Bhe</sub> increases GTP-bound RhoA during infection of HeLa cells.**

Serum-starved HeLa cells were infected with *Bhe*  $\Delta bepA-G$  carrying the empty plasmid or expressing BepC<sub>Bhe</sub> at a MOI = 400. After 24 hours of infection, G-LISA was used to evaluate the relative RhoA activation level. The experiment was performed in independent duplicates (red and blue).



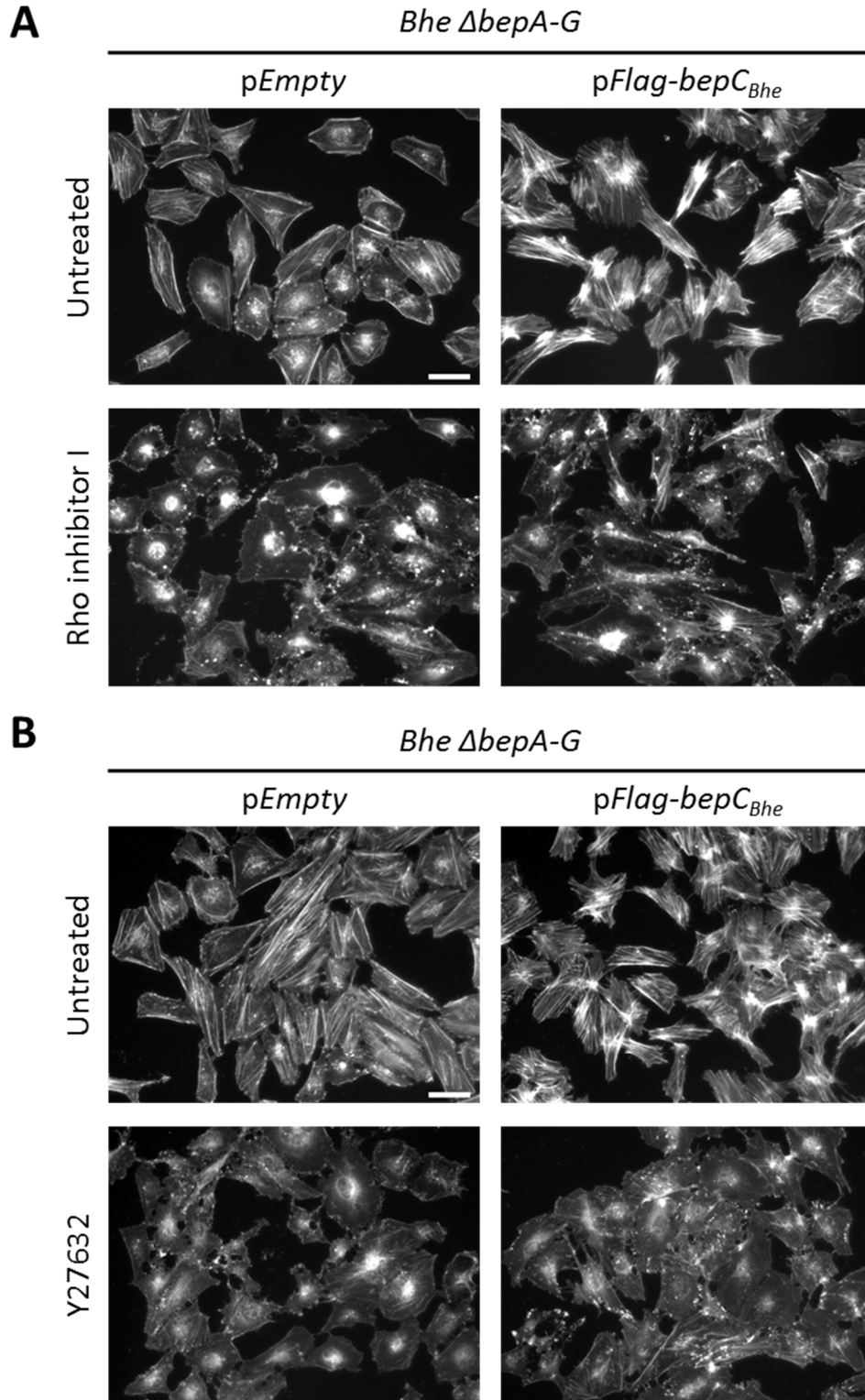


**Figure 3.10. Inhibition of RhoA or ROCK reduces actin stress fiber formation mediated by BepC<sub>Bhe</sub>.**

HeLa cells were infected with the indicated bacterial strain at a MOI = 200. After 24 hours of infection, the cells were treated with inhibitors before being fixed, stained by immunocytochemistry and analyzed by fluorescence microscopy. F-actin is represented in white (scale bar = 50  $\mu$ m). **A**) HeLa cells have been incubated 2 hours in absence or in presence of 2  $\mu$ g/ml of Rho inhibitor I. **B**) HeLa cells have been incubated 1 hour in absence or in presence of 20  $\mu$ M of Y27632.

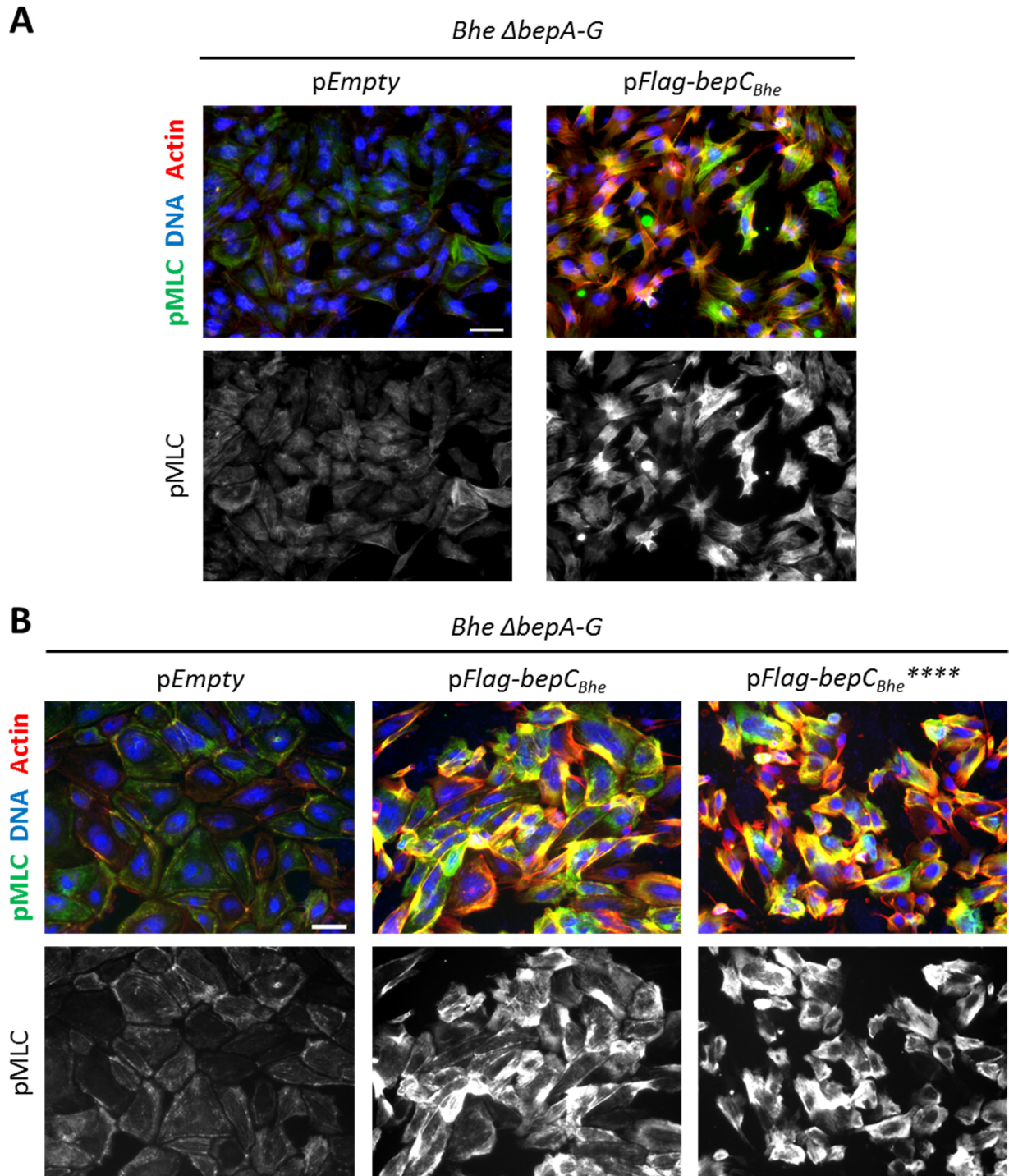


**Figure 3.11. BepC<sub>Bhe</sub> increases myosin light chain phosphorylation in HeLa cells and HUVECs during infection.**

Human cells were infected with the indicated bacterial strain. After infection, the cells were fixed and stained by immunocytochemistry before being analyzed by fluorescence microscopy. Phosphorylated myosin light chain is represented in green or white, DNA in blue, and F-actin in red (scale bar = 50  $\mu$ m). **A)** HeLa cells were infected at a MOI = 800 for 48 hours. **B)** HUVECs were infected at a MOI = 200 for 24 hours. BepC<sub>Bhe</sub><sup>\*\*\*\*</sup> = BepC<sub>Bhe</sub> H146A, K150A, R154A, R157A.

*Bhe*  $\Delta$ *bepA-G*

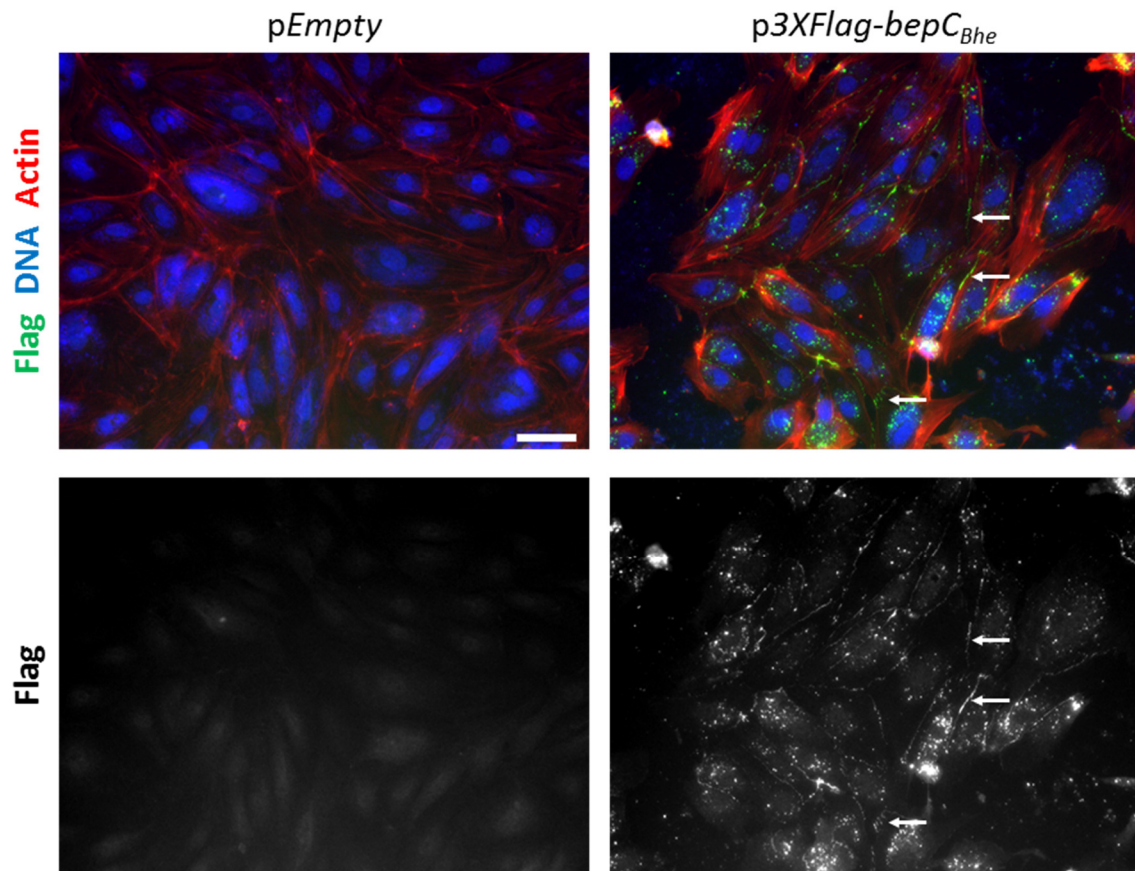


**Figure 3.12. BepC<sub>Bhe</sub> localizes to cell-to-cell contacts during infection of HUVECs.**

HUVECs were infected with the indicated bacterial strain at MOI = 100. After 48 hours of infection, the cells were fixed and stained by immunocytochemistry before being analyzed by fluorescence microscopy. 3XFlag-BepC<sub>Bhe</sub> is represented in green or white, DNA in blue, and F-actin in red (scale bar = 50  $\mu$ m). White arrows indicate BepC<sub>Bhe</sub> localized to cell junctions.



*Bhe*  $\Delta$ *bepA-G*

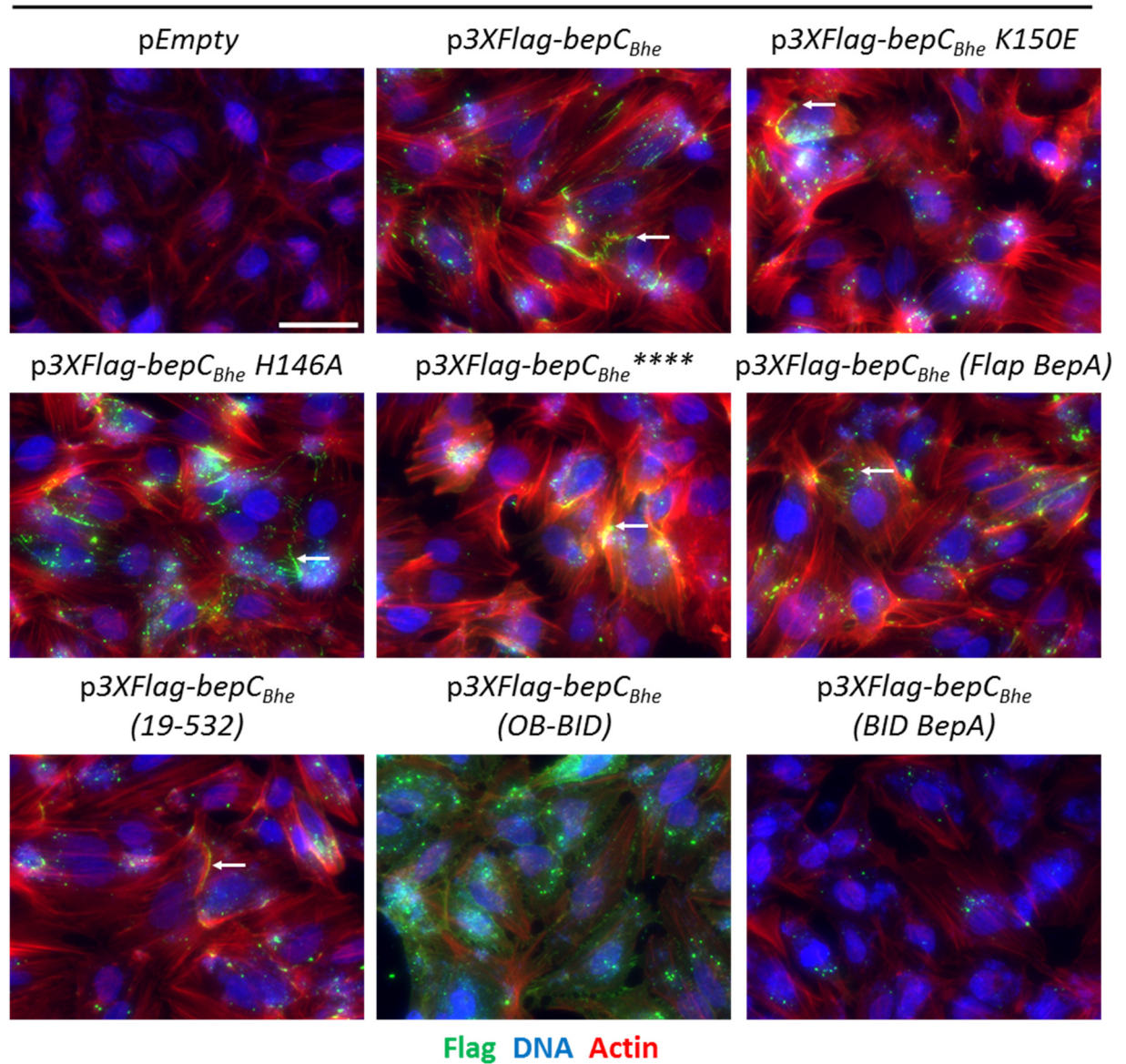


**Figure 3.13A. The FIC and the BID domains of BepC<sub>Bhe</sub> but not the conserved Flap or FIC motif are required for localization to cell-to-cell contacts in HeLa cells.**

HeLa cells were infected with the indicated bacterial strain at a MOI = 400. After 48 hours of infection, the cells were fixed and stained by immunocytochemistry before being analyzed by fluorescence microscopy. F-actin is represented in red, DNA in blue, and 3XFlag-BepC<sub>Bhe</sub> in green (scale bar = 50  $\mu$ m). White arrows indicate BepC<sub>Bhe</sub> localized to cell junctions. BepC<sub>Bhe</sub> \*\*\*\* = BepC<sub>Bhe</sub> H146A, K150A, R154A, R157A.

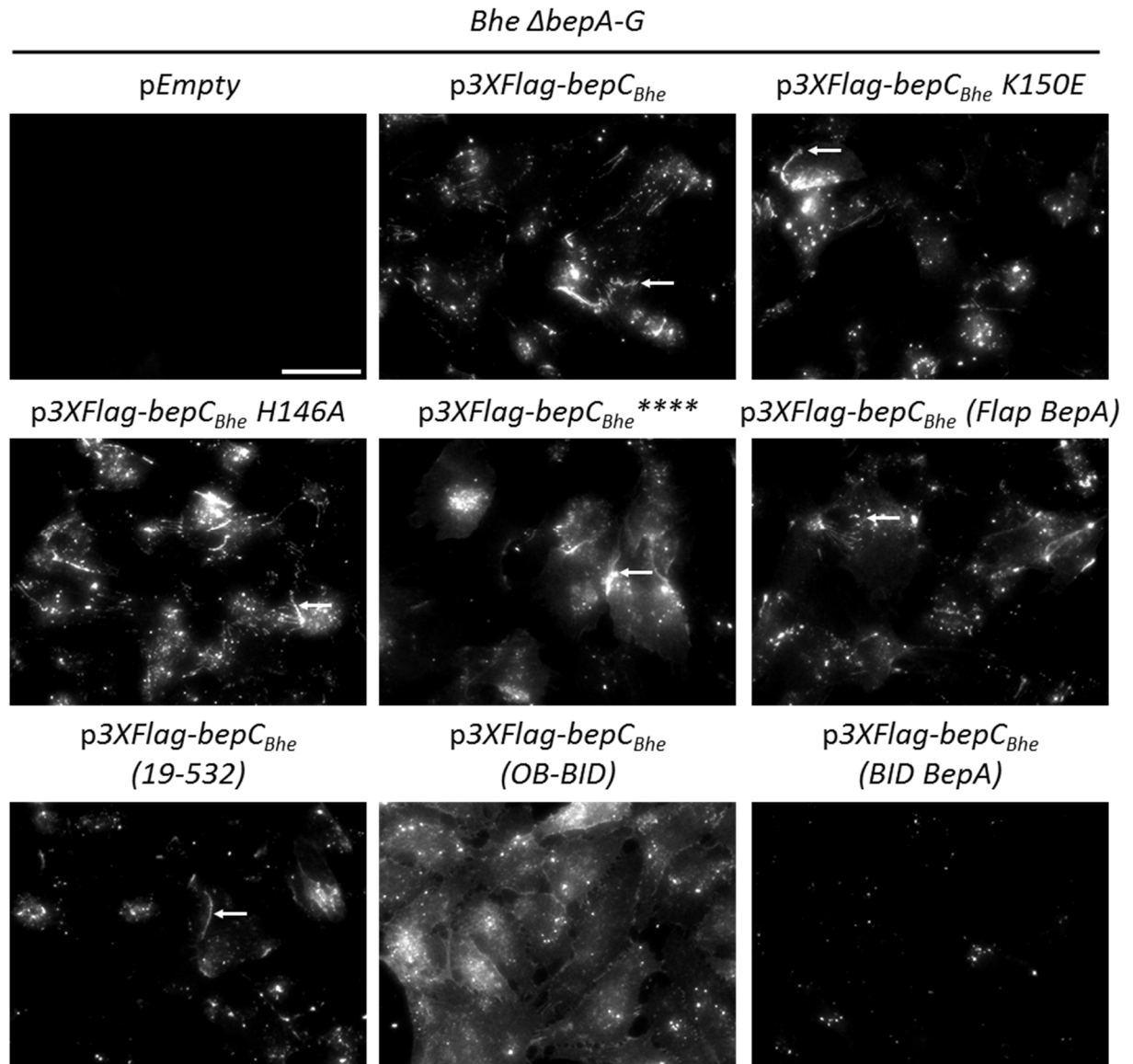


**Figure 3.13B. The FIC and the BID domains of BepC<sub>Bhe</sub> but not the conserved Flap region or FIC motif are required for localization to cell-to-cell contacts in HeLa cells.**

HeLa cells were infected with the indicated bacterial strain at a MOI = 400. After 48 hours of infection, the cells were fixed and stained by immunocytochemistry before being analyzed by fluorescence microscopy. 3XFlag-BepC<sub>Bhe</sub> is represented in white (scale bar = 50  $\mu$ m). White arrows indicate BepC<sub>Bhe</sub> localized to cell junctions. BepC<sub>Bhe</sub>\*\*\*\* = BepC<sub>Bhe</sub> H146A, K150A, R154A, R157A.



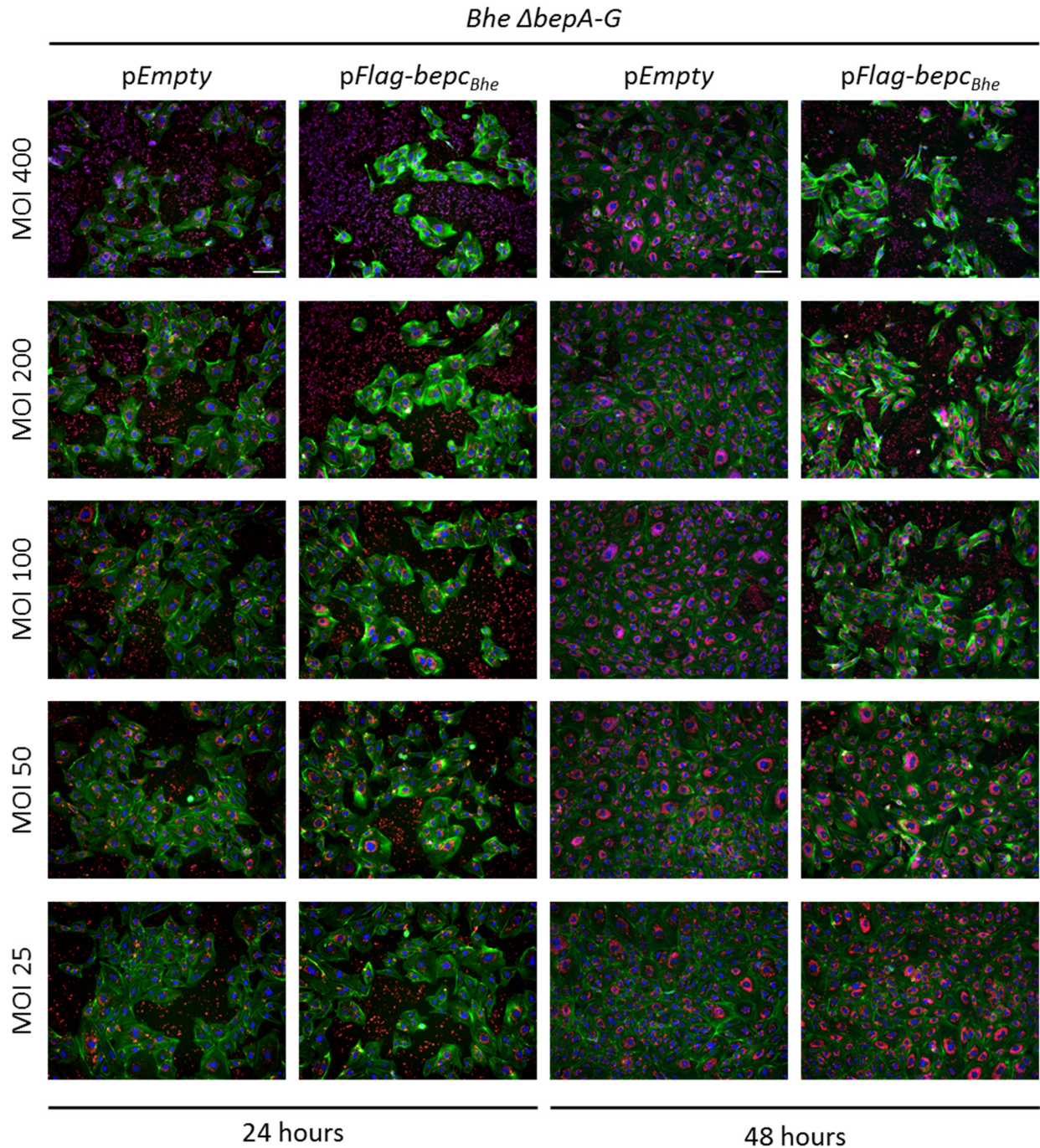


**Figure 3.S1. The intensity of the actin phenotype mediated by BepC is related to the MOI and the duration of infection.**

HeLa cells were infected with the indicated bacterial strain at a different MOI for 24 or 48 hours. After infection, the cells were fixed and stained by immunocytochemistry before being analyzed by fluorescence microscopy. F-actin is represented in green, DNA in blue, and *Bartonella* in red (scale bar = 100  $\mu$ m).

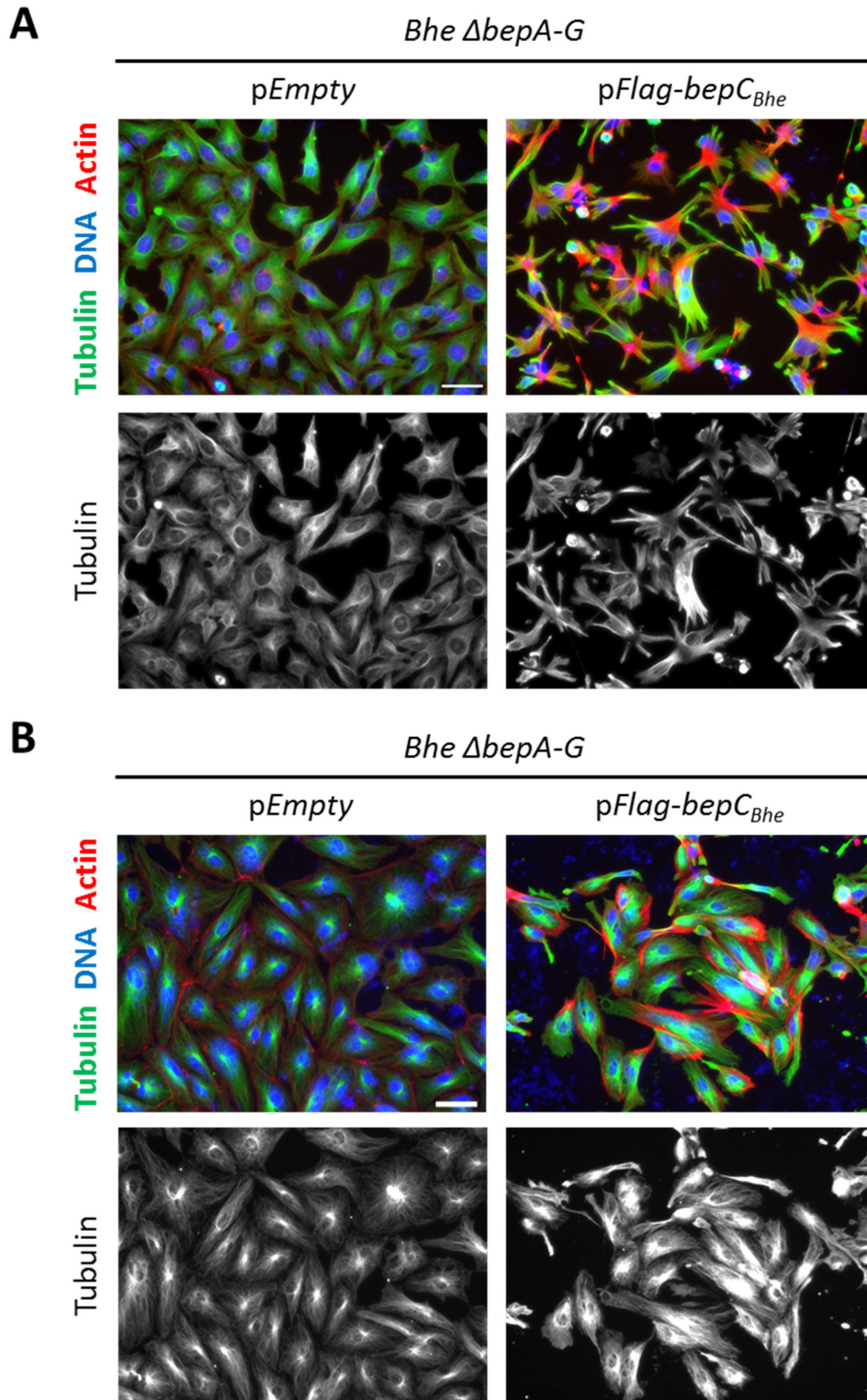


**Figure 3.S2. BepC<sub>Bhe</sub> induces tubulin network reorganization in HeLa cells and HUVECs during infection.**

Human cells were infected with the indicated bacterial strain. After infection, the cells were fixed and stained by immunocytochemistry before being analyzed by fluorescence microscopy. Tubulin is represented in green or white, DNA in blue, and F-actin in red (scale bar = 50  $\mu$ m). **A)** HeLa cells were infected at a MOI = 800 for 48 hours. **B)** HUVECs were infected at a MOI = 200 for 24 hours.



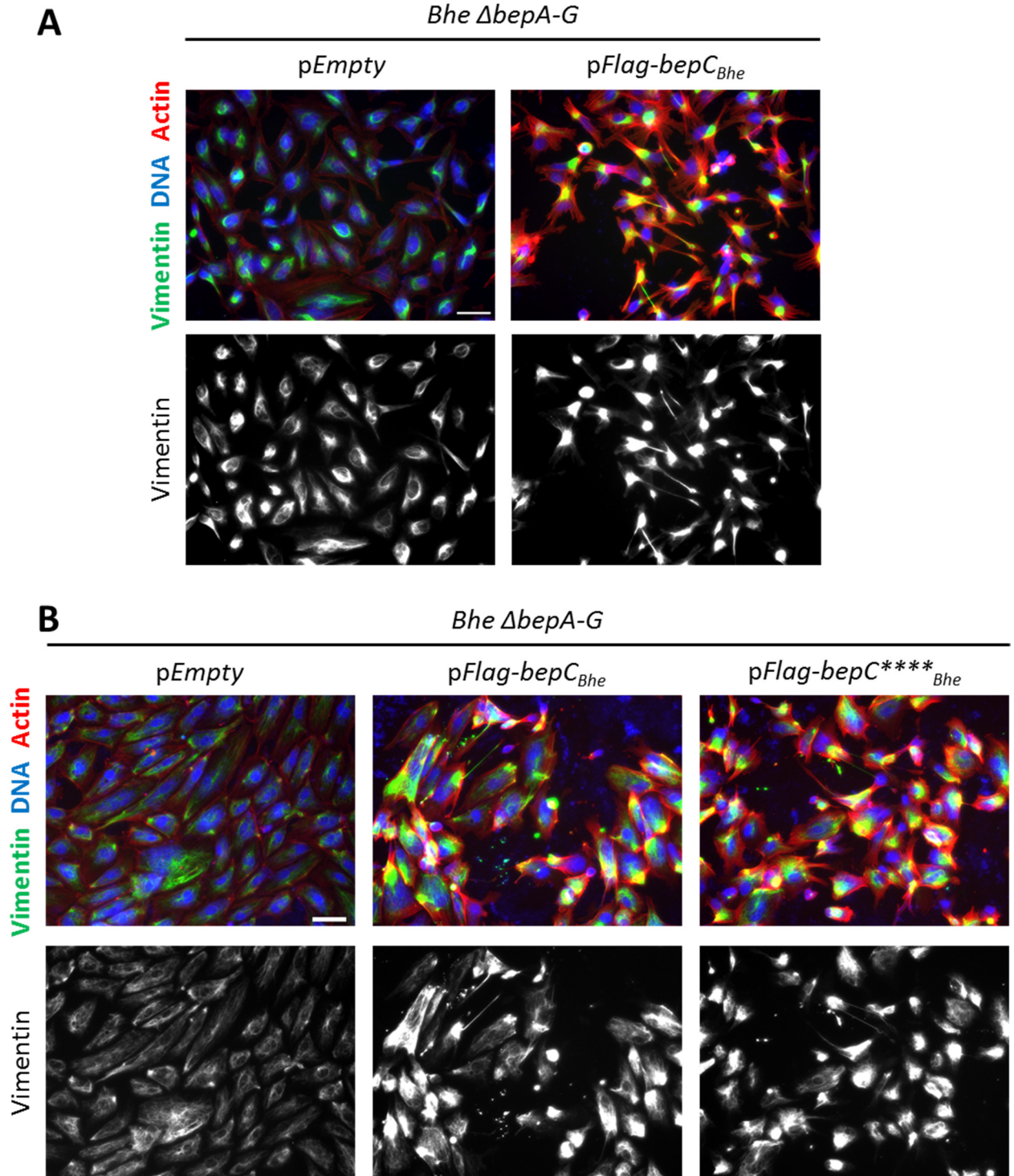


**Figure 3.S3. BepC<sub>Bhe</sub> induces the aggregation of vimentin intermediate filaments in HeLa cells and HUVECs during infection.**

Human cells were infected with the indicated bacterial strain. After infection, the cells were fixed and stained by immunocytochemistry before being analyzed by fluorescence microscopy. Vimentin is represented in green or white, DNA in blue, and F-actin in red (scale bar = 50  $\mu$ m). **A)** HeLa cells were infected at a MOI = 800 for 48 hours. **B)** HUVECs were infected at a MOI = 200 for 24 hours. BepC<sub>Bhe</sub><sup>\*\*\*\*</sup> = BepC<sub>Bhe</sub> H146A, K150A, R154A, R157A.



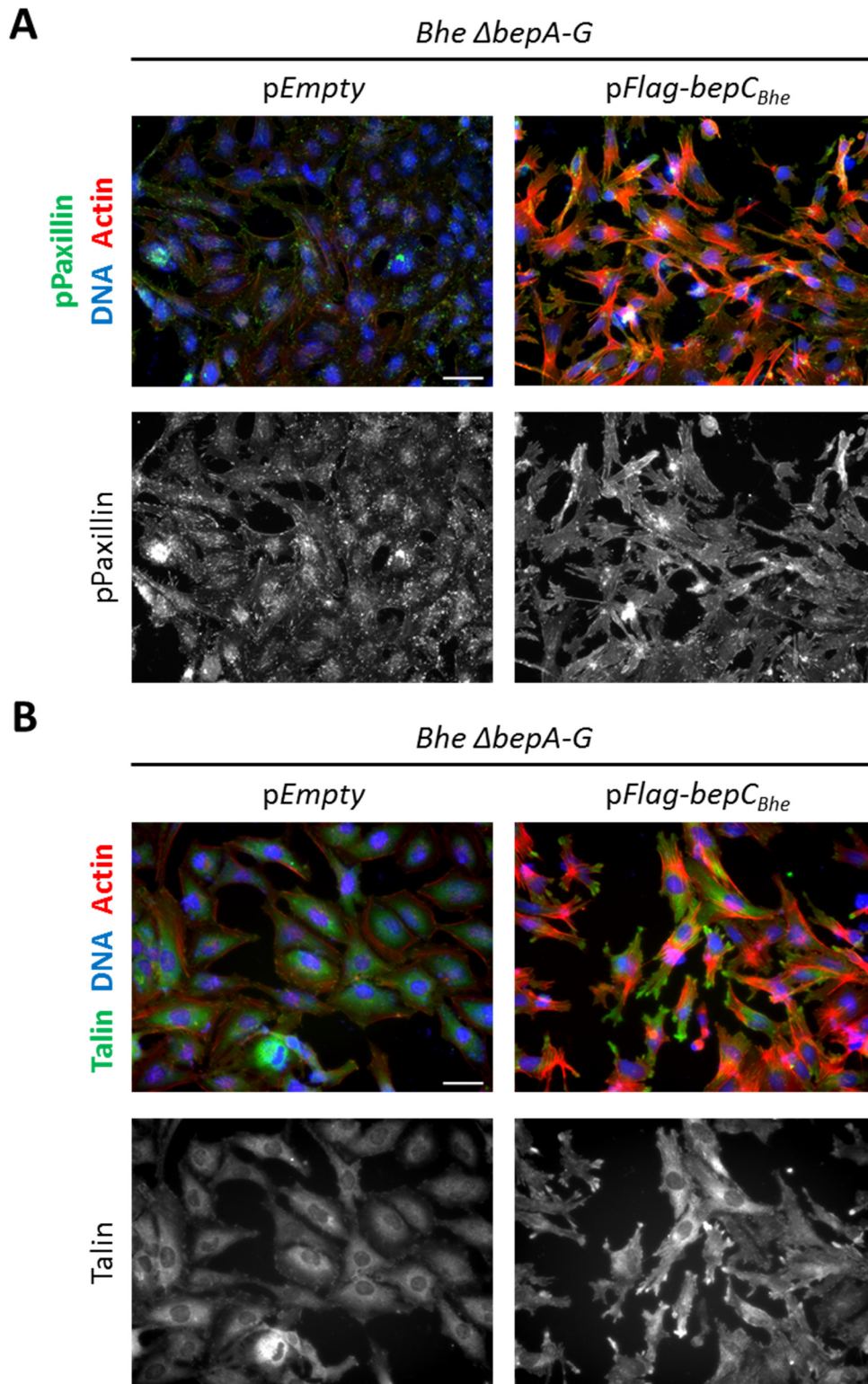


**Figure 3.S4. BepC<sub>Bhe</sub> induces the re-localization of the cytosolic fraction of talin but does not have an effect on focal adhesions.**

HeLa cells were infected with the indicated bacterial strain. After infection, the cells were and stained by immunocytochemistry before being analyzed by fluorescence microscopy. **A)** HeLa cells were infected for 48 hours at a MOI = 800. Phosphorylated paxillin is represented in green or white, DNA in blue, and F-actin in red. **B)** HeLa cells were infected for 48 hours at a MOI = 400. Talin is represented in green or white, DNA in blue, and F-actin in red.

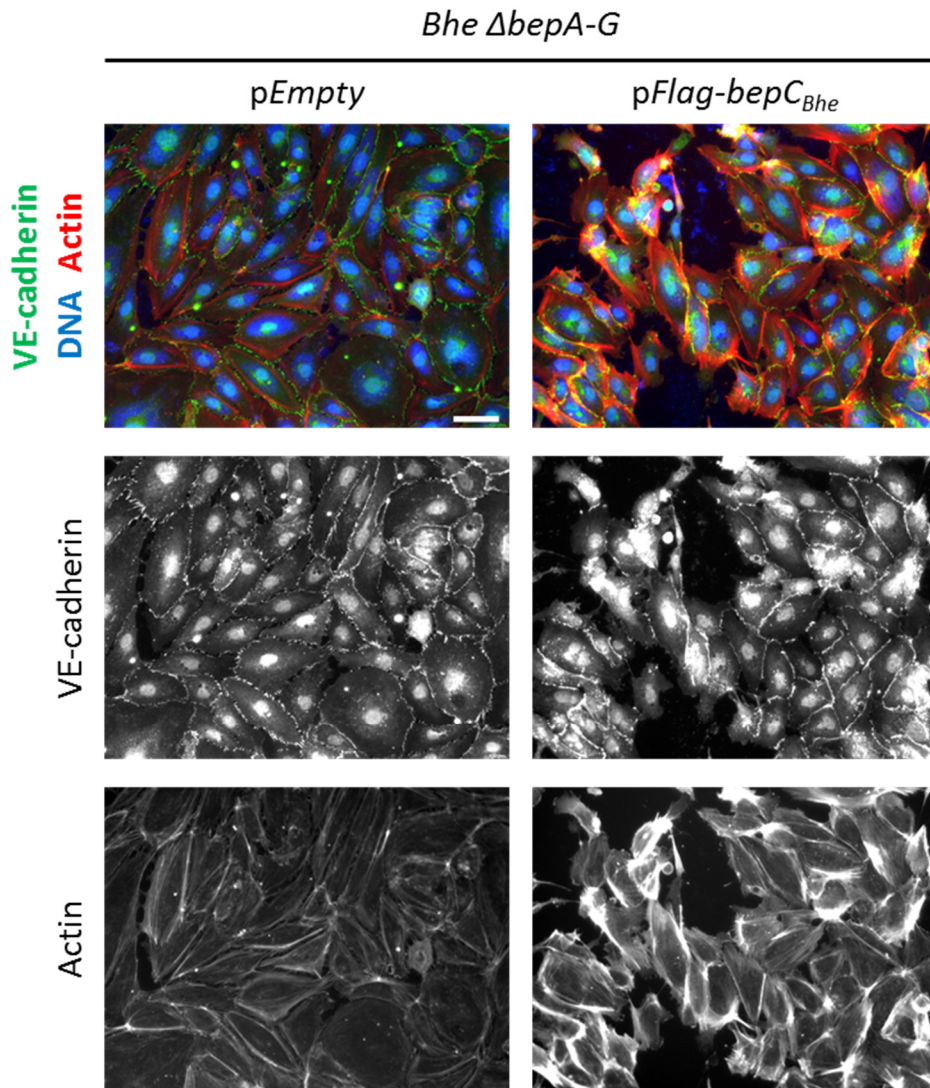


**Figure 3.S5. HUVECs are still able to form adherens junctions after infection with *Bhe*  $\Delta$ *bepA-G* expressing *BepC<sub>Bhe</sub>*.**

HUVECs were infected with the indicated bacterial strain at a MOI = 200. After 24 hours of infection, the cells were fixed and stained by immunocytochemistry before being analyzed by fluorescence microscopy. VE-cadherin is represented in green or white, DNA in blue, and F-actin in red (scale bar = 50  $\mu$ m).

### 3.4 References

1. Okujava, R., et al., *A translocated effector required for Bartonella dissemination from derma to blood safeguards migratory host cells from damage by co-translocated effectors*. PLoS Pathog, 2014. **10**(6): p. e1004187.
2. Truttmann, M.C., P. Guye, and C. Dehio, *BID-F1 and BID-F2 domains of Bartonella henselae effector protein BepF trigger together with BepC the formation of invasome structures*. PloS one, 2011. **6**(10): p. e25106.
3. Truttmann, M.C., T.A. Rhomberg, and C. Dehio, *Combined action of the type IV secretion effector proteins BepC and BepF promotes invasome formation of Bartonella henselae on endothelial and epithelial cells*. Cellular microbiology, 2011. **13**(2): p. 284-99.
4. Dehio, C., et al., *Interaction of Bartonella henselae with endothelial cells results in bacterial aggregation on the cell surface and the subsequent engulfment and internalisation of the bacterial aggregate by a unique structure, the invasome*. J Cell Sci, 1997. **110** ( Pt 18): p. 2141-54.
5. Dehio, C., *Bartonella-host-cell interactions and vascular tumour formation*. Nat Rev Microbiol, 2005. **3**(8): p. 621-31.
6. Dehio, C. and R.M. Tsois, *Type IV Effector Secretion and Subversion of Host Functions by Bartonella and Brucella Species*. Curr Top Microbiol Immunol, 2017. **413**: p. 269-295.
7. Rhomberg, T.A., et al., *A translocated protein of Bartonella henselae interferes with endocytic uptake of individual bacteria and triggers uptake of large bacterial aggregates via the invasome*. Cell Microbiol, 2009. **11**(6): p. 927-45.
8. Harms, A., F.V. Stanger, and C. Dehio, *Biological Diversity and Molecular Plasticity of FIC Domain Proteins*. Annu Rev Microbiol, 2016. **70**: p. 341-60.
9. Yarbrough, M.L., et al., *AMPylation of Rho GTPases by Vibrio VopS disrupts effector binding and downstream signaling*. Science, 2009. **323**(5911): p. 269-72.
10. Worby, C.A., et al., *The fic domain: regulation of cell signaling by adenylylation*. Mol Cell, 2009. **34**(1): p. 93-103.
11. Xiao, J., et al., *Structural basis of Fic-mediated adenylylation*. Nat Struct Mol Biol, 2010. **17**(8): p. 1004-10.
12. Kinch, L.N., et al., *Fido, a novel AMPylation domain common to fic, doc, and AvrB*. PLoS One, 2009. **4**(6): p. e5818.
13. Palanivelu, D.V., et al., *Fic domain-catalyzed adenylylation: insight provided by the structural analysis of the type IV secretion system effector BepA*. Protein Sci, 2011. **20**(3): p. 492-9.
14. Pulliainen, A.T., et al., *Bacterial effector binds host cell adenylyl cyclase to potentiate Galphas-dependent cAMP production*. Proc Natl Acad Sci U S A, 2012. **109**(24): p. 9581-6.
15. Rossman, K.L., C.J. Der, and J. Sondek, *GEF means go: turning on RHO GTPases with guanine nucleotide-exchange factors*. Nat Rev Mol Cell Biol, 2005. **6**(2): p. 167-80.
16. Ren, X.D., W.B. Kiosses, and M.A. Schwartz, *Regulation of the small GTP-binding protein Rho by cell adhesion and the cytoskeleton*. EMBO J, 1999. **18**(3): p. 578-85.
17. Aktories, K., C. Wilde, and M. Vogelsgesang, *Rho-modifying C3-like ADP-ribosyltransferases*. Rev Physiol Biochem Pharmacol, 2004. **152**: p. 1-22.
18. Heikkila, T., et al., *Co-crystal structures of inhibitors with MRCKbeta, a key regulator of tumor cell invasion*. PLoS One, 2011. **6**(9): p. e24825.
19. Tan, I., et al., *Chelerythrine perturbs lamellar actomyosin filaments by selective inhibition of myotonic dystrophy kinase-related Cdc42-binding kinase*. FEBS Lett, 2011. **585**(9): p. 1260-8.
20. Hauert, B., *Identification of cellular protein targets for Bartonella effector proteins*. Master thesis, 2009.

21. Matsuzawa, T., et al., *Enteropathogenic Escherichia coli activates the RhoA signaling pathway via the stimulation of GEF-H1*. EMBO J, 2004. **23**(17): p. 3570-82.
22. Shaw, R.K., et al., *Enteropathogenic Escherichia coli type III effectors EspG and EspG2 disrupt the microtubule network of intestinal epithelial cells*. Infect Immun, 2005. **73**(7): p. 4385-90.
23. Chang, L. and R.D. Goldman, *Intermediate filaments mediate cytoskeletal crosstalk*. Nat Rev Mol Cell Biol, 2004. **5**(8): p. 601-13.
24. Ridley, A.J. and A. Hall, *The small GTP-binding protein rho regulates the assembly of focal adhesions and actin stress fibers in response to growth factors*. Cell, 1992. **70**(3): p. 389-99.
25. Mitra, S.K., D.A. Hanson, and D.D. Schlaepfer, *Focal adhesion kinase: in command and control of cell motility*. Nat Rev Mol Cell Biol, 2005. **6**(1): p. 56-68.
26. Lemichez, E., et al., *Breaking the wall: targeting of the endothelium by pathogenic bacteria*. Nat Rev Microbiol, 2010. **8**(2): p. 93-104.
27. van Buul, J.D. and I. Timmerman, *Small Rho GTPase-mediated actin dynamics at endothelial adherens junctions*. Small GTPases, 2016. **7**(1): p. 21-31.
28. Horiguchi, Y., et al., *Bordetella bronchiseptica dermonecrotizing toxin induces reorganization of actin stress fibers through deamidation of Gln-63 of the GTP-binding protein Rho*. Proc Natl Acad Sci U S A, 1997. **94**(21): p. 11623-6.
29. Klink, B.U., et al., *Structure of Shigella IpgB2 in complex with human RhoA: implications for the mechanism of bacterial guanine nucleotide exchange factor mimicry*. J Biol Chem, 2010. **285**(22): p. 17197-208.
30. Hopkins, A.M., et al., *Constitutive activation of Rho proteins by CNF-1 influences tight junction structure and epithelial barrier function*. J Cell Sci, 2003. **116**(Pt 4): p. 725-42.
31. Ohlson, M.B., et al., *Structure and function of Salmonella SifA indicate that its interactions with SKIP, SseJ, and RhoA family GTPases induce endosomal tubulation*. Cell Host Microbe, 2008. **4**(5): p. 434-46.
32. Hiyoshi, H., et al., *Interaction between the type III effector VopO and GEF-H1 activates the RhoA-ROCK pathway*. PLoS Pathog, 2015. **11**(3): p. e1004694.
33. Lang, A.E., et al., *Photorhabdus luminescens toxins ADP-ribosylate actin and RhoA to force actin clustering*. Science, 2010. **327**(5969): p. 1139-42.
34. Arbeloa, A., et al., *Subversion of actin dynamics by EspM effectors of attaching and effacing bacterial pathogens*. Cell Microbiol, 2008. **10**(7): p. 1429-41.
35. Ren, Y., et al., *Cloning and characterization of GEF-H1, a microtubule-associated guanine nucleotide exchange factor for Rac and Rho GTPases*. J Biol Chem, 1998. **273**(52): p. 34954-60.
36. Maekawa, M., et al., *Signaling from Rho to the actin cytoskeleton through protein kinases ROCK and LIM-kinase*. Science, 1999. **285**(5429): p. 895-8.
37. Riento, K. and A.J. Ridley, *Rocks: multifunctional kinases in cell behaviour*. Nat Rev Mol Cell Biol, 2003. **4**(6): p. 446-56.
38. Leung, T., et al., *The p160 RhoA-binding kinase ROK alpha is a member of a kinase family and is involved in the reorganization of the cytoskeleton*. Mol Cell Biol, 1996. **16**(10): p. 5313-27.
39. Lee, I.C., T. Leung, and I. Tan, *Adaptor protein LRAP25 mediates myotonic dystrophy kinase-related Cdc42-binding kinase (MRCK) regulation of LIMK1 protein in lamellipodial F-actin dynamics*. J Biol Chem, 2014. **289**(39): p. 26989-7003.
40. Watanabe, N., et al., *Cooperation between mDia1 and ROCK in Rho-induced actin reorganization*. Nat Cell Biol, 1999. **1**(3): p. 136-43.
41. Tan, I., et al., *Phosphorylation of a novel myosin binding subunit of protein phosphatase 1 reveals a conserved mechanism in the regulation of actin cytoskeleton*. J Biol Chem, 2001. **276**(24): p. 21209-16.
42. Leung, T., et al., *Myotonic dystrophy kinase-related Cdc42-binding kinase acts as a Cdc42 effector in promoting cytoskeletal reorganization*. Mol Cell Biol, 1998. **18**(1): p. 130-40.

43. Wilkinson, S., H.F. Paterson, and C.J. Marshall, *Cdc42-MRCK and Rho-ROCK signalling cooperate in myosin phosphorylation and cell invasion*. *Nat Cell Biol*, 2005. **7**(3): p. 255-61.
44. Worthylake, R.A., et al., *RhoA is required for monocyte tail retraction during transendothelial migration*. *J Cell Biol*, 2001. **154**(1): p. 147-60.
45. Totsukawa, G., et al., *Distinct roles of ROCK (Rho-kinase) and MLCK in spatial regulation of MLC phosphorylation for assembly of stress fibers and focal adhesions in 3T3 fibroblasts*. *J Cell Biol*, 2000. **150**(4): p. 797-806.
46. Tan, I., et al., *A tripartite complex containing MRCK modulates lamellar actomyosin retrograde flow*. *Cell*, 2008. **135**(1): p. 123-36.
47. Huber, F., et al., *Cytoskeletal crosstalk: when three different personalities team up*. *Curr Opin Cell Biol*, 2015. **32**: p. 39-47.
48. Leduc, C. and S. Etienne-Manneville, *Intermediate filaments in cell migration and invasion: the unusual suspects*. *Curr Opin Cell Biol*, 2015. **32**: p. 102-12.
49. Dave, J.M. and K.J. Bayless, *Vimentin as an integral regulator of cell adhesion and endothelial sprouting*. *Microcirculation*, 2014. **21**(4): p. 333-44.
50. Goto, H., et al., *Phosphorylation of vimentin by Rho-associated kinase at a unique amino-terminal site that is specifically phosphorylated during cytokinesis*. *J Biol Chem*, 1998. **273**(19): p. 11728-36.
51. Sin, W.C., et al., *RhoA-binding kinase alpha translocation is facilitated by the collapse of the vimentin intermediate filament network*. *Mol Cell Biol*, 1998. **18**(11): p. 6325-39.
52. Jiu, Y., et al., *Vimentin intermediate filaments control actin stress fiber assembly through GEF-H1 and RhoA*. *J Cell Sci*, 2017. **130**(5): p. 892-902.
53. Pielkes, K., et al., *An experimental strategy for the identification of AMPylation targets from complex protein samples*. *Proteomics*, 2014. **14**(9): p. 1048-52.
54. Icenogle, L.M., et al., *Molecular and biological characterization of Streptococcal SpyA-mediated ADP-ribosylation of intermediate filament protein vimentin*. *J Biol Chem*, 2012. **287**(25): p. 21481-91.
55. Benais-Pont, G., et al., *Identification of a tight junction-associated guanine nucleotide exchange factor that activates Rho and regulates paracellular permeability*. *J Cell Biol*, 2003. **160**(5): p. 729-40.
56. Popoff, M.R., *Bacterial factors exploit eukaryotic Rho GTPase signaling cascades to promote invasion and proliferation within their host*. *Small GTPases*, 2014. **5**.
57. Patel, M. and A.V. Karginov, *Phosphorylation-mediated regulation of GEFs for RhoA*. *Cell Adh Migr*, 2014. **8**(1): p. 11-8.
58. Krendel, M., F.T. Zenke, and G.M. Bokoch, *Nucleotide exchange factor GEF-H1 mediates cross-talk between microtubules and the actin cytoskeleton*. *Nat Cell Biol*, 2002. **4**(4): p. 294-301.
59. Zenke, F.T., et al., *p21-activated kinase 1 phosphorylates and regulates 14-3-3 binding to GEF-H1, a microtubule-localized Rho exchange factor*. *J Biol Chem*, 2004. **279**(18): p. 18392-400.
60. Birkenfeld, J., et al., *Cellular functions of GEF-H1, a microtubule-regulated Rho-GEF: is altered GEF-H1 activity a crucial determinant of disease pathogenesis?* *Trends Cell Biol*, 2008. **18**(5): p. 210-9.
61. Popa, C.M., M. Tabuchi, and M. Valls, *Modification of Bacterial Effector Proteins Inside Eukaryotic Host Cells*. *Front Cell Infect Microbiol*, 2016. **6**: p. 73.
62. Alto, N.M., et al., *Identification of a bacterial type III effector family with G protein mimicry functions*. *Cell*, 2006. **124**(1): p. 133-45.
63. Palecek, S.P., et al., *Physical and biochemical regulation of integrin release during rear detachment of migrating cells*. *J Cell Sci*, 1998. **111 ( Pt 7)**: p. 929-40.
64. Glading, A., D.A. Lauffenburger, and A. Wells, *Cutting to the chase: calpain proteases in cell motility*. *Trends Cell Biol*, 2002. **12**(1): p. 46-54.
65. Heasman, S.J., et al., *Coordinated RhoA signaling at the leading edge and uropod is required for T cell transendothelial migration*. *J Cell Biol*, 2010. **190**(4): p. 553-63.



66. Nalbant, P., et al., *Guanine nucleotide exchange factor-H1 regulates cell migration via localized activation of RhoA at the leading edge*. Mol Biol Cell, 2009. **20**(18): p. 4070-82.
67. Kurokawa, K. and M. Matsuda, *Localized RhoA activation as a requirement for the induction of membrane ruffling*. Mol Biol Cell, 2005. **16**(9): p. 4294-303.
68. Gagliardi, P.A., et al., *PK1-mediated activation of MRCKalpha regulates directional cell migration and lamellipodia retraction*. J Cell Biol, 2014. **206**(3): p. 415-34.
69. Amano, M., et al., *Formation of actin stress fibers and focal adhesions enhanced by Rho-kinase*. Science, 1997. **275**(5304): p. 1308-11.
70. Barth, H., et al., *Clostridial C3 Toxins Target Monocytes/Macrophages and Modulate Their Functions*. Front Immunol, 2015. **6**: p. 339.
71. Williams, N.L., et al., *Migration of dendritic cells facilitates systemic dissemination of Burkholderia pseudomallei*. Infect Immun, 2014. **82**(10): p. 4233-40.
72. Bar-Haim, E., et al., *Interrelationship between dendritic cell trafficking and Francisella tularensis dissemination following airway infection*. PLoS Pathog, 2008. **4**(11): p. e1000211.
73. Skinner, J.A., et al., *Bordetella type III secretion modulates dendritic cell migration resulting in immunosuppression and bacterial persistence*. J Immunol, 2005. **175**(7): p. 4647-52.
74. Salcedo, S.P., et al., *Brucella control of dendritic cell maturation is dependent on the TIR-containing protein Btp1*. PLoS Pathog, 2008. **4**(2): p. e21.
75. Birukova, A.A., et al., *GEF-H1 is involved in agonist-induced human pulmonary endothelial barrier dysfunction*. Am J Physiol Lung Cell Mol Physiol, 2006. **290**(3): p. L540-8.
76. Tornavaca, O., et al., *ZO-1 controls endothelial adherens junctions, cell-cell tension, angiogenesis, and barrier formation*. J Cell Biol, 2015. **208**(6): p. 821-38.
77. Terry, S.J., et al., *Spatially restricted activation of RhoA signalling at epithelial junctions by p114RhoGEF drives junction formation and morphogenesis*. Nat Cell Biol, 2011. **13**(2): p. 159-66.
78. Wojciak-Stothard, B. and A.J. Ridley, *Rho GTPases and the regulation of endothelial permeability*. Vascul Pharmacol, 2002. **39**(4-5): p. 187-99.
79. Mikelis, C.M., et al., *RhoA and ROCK mediate histamine-induced vascular leakage and anaphylactic shock*. Nat Commun, 2015. **6**: p. 6725.
80. van Hinsbergh, V.W. and G.P. van Nieuw Amerongen, *Intracellular signalling involved in modulating human endothelial barrier function*. J Anat, 2002. **200**(6): p. 549-60.
81. van Nieuw Amerongen, G.P., et al., *Activation of RhoA by thrombin in endothelial hyperpermeability: role of Rho kinase and protein tyrosine kinases*. Circ Res, 2000. **87**(4): p. 335-40.
82. Spindler, V., N. Schlegel, and J. Waschke, *Role of GTPases in control of microvascular permeability*. Cardiovasc Res, 2010. **87**(2): p. 243-53.
83. Schmid, M.C., et al., *The VirB type IV secretion system of Bartonella henselae mediates invasion, proinflammatory activation and antiapoptotic protection of endothelial cells*. Mol Microbiol, 2004. **52**(1): p. 81-92.
84. Rahman, M.M. and G. McFadden, *Modulation of NF-kappaB signalling by microbial pathogens*. Nat Rev Microbiol, 2011. **9**(4): p. 291-306.
85. Harms, A. and C. Dehio, *Intruders below the radar: molecular pathogenesis of Bartonella spp*. Clin Microbiol Rev, 2012. **25**(1): p. 42-78.
86. Fukazawa, A., et al., *GEF-H1 mediated control of NOD1 dependent NF-kappaB activation by Shigella effectors*. PLoS Pathog, 2008. **4**(11): p. e1000228.
87. Zhao, Y., et al., *Control of NOD2 and Rip2-dependent innate immune activation by GEF-H1*. Inflamm Bowel Dis, 2012. **18**(4): p. 603-12.
88. Keestra, A.M., et al., *Manipulation of small Rho GTPases is a pathogen-induced process detected by NOD1*. Nature, 2013. **496**(7444): p. 233-7.

# Additional results

## 4.1 Results

### 4.1.1 Recombinant BepC<sub>Bhe</sub> (FIC-OB) is modified after overexpression in *E. coli*.

Since BepC is a Fic protein, we speculated that the FIC domain may catalyze posttranslational modifications on host target proteins. Furthermore, the crystal structure of the FIC domain of BepC from *Bartonella tribocorum* shows binding of AMP-PNP (a non-hydrolysable analog of ATP) in an AMPylation-competent conformation (Fig. 1.9). Nevertheless, an enzymatic activity has never been demonstrated.

To perform biochemical studies, BepC<sub>Bhe</sub> was overexpressed in *E. coli* and purified. As the full-length effector is mostly insoluble (Fig. 4.S1), only the FIC domain and the OB fold of the protein (FIC-OB) were cloned into an expression vector with C-terminal His-tag. After the first step of purification by affinity chromatography via the His-tag, the fractions were separated according to their size on a gel filtration column. The elution fractions containing BepC<sub>Bhe</sub> (FIC-OB) were analyzed by SDS-PAGE and pooled before being concentrated by filtration (Fig. 4.1A). The pooled and concentrated eluate, as well as the flow-through, were analyzed with Nanodrop (Fig. 4.1B). The absorbance spectra showed the presence of a contaminant absorbing at 260 nm in the flow-through and in the concentrated eluate, suggesting that an unknown compound was co-purifying with BepC<sub>Bhe</sub> (FIC-OB).

As some Fic proteins transfer an AMP moiety on one of their own residue (auto-modification) [1-3], it is conceivable that BepC<sub>Bhe</sub> (FIC-OB) would already be modified if its substrate is present in *E. coli*. Thus, it is likely that the presence of this moiety would prevent further auto-modification during enzymatic experiments, which could be interpreted as a low activity.

To test whether the purified BepC<sub>Bhe</sub> (FIC-OB) was already auto-modified, we analyzed the protein by mass spectrometry. As we measure the mass of the non-digested polypeptide, a difference could correspond to a single or to a combination of modifications on different residues. Four samples from independent purifications were tested, three of BepC<sub>Bhe</sub> (FIC-OB) wild-type, including one with the co-expression of the antitoxin, and one of BepC<sub>Bhe</sub> with the mutated histidine of the FIC motif (H146A) (Fig. 4.2A).

The mass spectra showed that the wild-type proteins had a mass of 34'715 Da in the three conditions. The mass of BepC<sub>Bhe</sub> H146A was 34'648 Da, the difference of 66 Da in comparison with the wild-type protein corresponded exactly to the difference of mass between a histidine and an alanine. The measured mass of the antitoxin (8'676 Da) correlates with its theoretical mass without the N-terminal methionine, suggesting that it has been removed by the *E. coli* methionine aminopeptidase [4]. If we also assume that the first methionine of BepC is cleaved, the difference between the measured mass and the theoretical mass is 284 Da for the wild-type protein and 283 Da for the mutant (Fig. 4.2B). This result suggests that the wild-type and



the mutant proteins are similarly modified. As only one peak corresponding to BepC is visible on the mass spectra, we can also assume that the vast majority of the recombinant proteins carry the same modification(s).

Overall, an unidentified compound seems to co-purify with BepC<sub>Bhe</sub> (FIC-OB) after expression in *E. coli*. However, it remains elusive whether it corresponds to a contamination or to a relevant ligand. Furthermore, our results indicate that the majority of recombinant protein is modified but independently from the presence of the antitoxin or the conserved histidine.

#### **4.1.2 BepC<sub>Bhe</sub> (FIC-OB) has residual auto-AMPylation and auto-phosphorylation activities *in vitro*.**

As indicated before, some Fic proteins are known to auto-modify themselves [1-3]. Therefore, we decided to investigate the auto-modification activity of BepC as a read-out for a potential catalytic activity that would serve for posttranslational modifications.

To test it, we incubated recombinant BepC<sub>Bhe</sub> (FIC-OB) at 30°C in presence of ATP carrying a radioactive phosphate either in  $\alpha$  or  $\gamma$  position ( $\alpha$ -<sup>32</sup>P-ATP or  $\gamma$ -<sup>32</sup>P-ATP) (Fig. 4.S2A). The autoradiography indicated that BepC<sub>Bhe</sub> (FIC-OB) is AMPylating and phosphorylating itself at the same time (Fig. 4.3). This result suggests that ATP can adopt two different orientations in the active site of BepC, one compatible with AMPylation and one with phosphorylation. Nevertheless, the auto-modification of BepC is rather slow and did not arrive at equilibrium even after 8 hours. Interestingly, a dimer of BepC is slightly visible on the polyacrylamide gel after 24 hours of incubation, although the proteins have been denatured at 95°C for 5 minutes in presence of SDS.

Based on these results, we wanted to determine which residue of the FIC domain is AMPylated. To do so, we incubated BepC<sub>Bhe</sub> (FIC-OB) in absence or in presence of ATP. After stopping the reaction, the protein was trypsinized and the peptides were analyzed by mass spectrometry to find an additional mass of 329 Da, which corresponds to an AMP moiety. Other modifications have not been investigated.

The peptide coverage was high for both samples (Fig. 4.4). Interestingly, one of the few peptides that were not detected in both conditions (MPAMRPK) is located at the beginning of the Flap region (Alignment 1.2). Some of the methionines were oxidized, probably due to technical manipulations, which resulted in a mass shift of 16 Da per residue. Surprisingly, no additional AMP moiety was found in association with any of the peptides, which suggests that BepC<sub>Bhe</sub> (FIC-OB) was not AMPylated in presence of ATP. However, it is possible that the amount of AMPylated peptides was too low to be detected or that we lost the modified peptide during the sample processing.

In summary, the radioactive assays indicate that BepC<sub>Bhe</sub> is enzymatically active and is able to slowly auto-modify itself by AMPylation and phosphorylation. Nevertheless, the AMPylated peptide could not be detected by mass spectrometry although other modifications are possible.

#### **4.1.3 A conserved FIC motif is not required for the auto-AMPylation of BepC<sub>Bhe</sub> (FIC-OB).**

To confirm that the auto-AMPylation activity depends on the FIC motif, we partially purified BepC<sub>Bhe</sub> (FIC-OB) with the mutated conserved histidine (H146A). After incubation with radioactive ATP at 25°C, the substitution of the histidine did not seem to reduce the auto-AMPylation activity of BepC in comparison with the wild-type protein (Fig. 4.5). As the mutation of the histidine is not always sufficient to prevent AMPylation [5], we also decided to mutate the residues of the FIC motif (BepC<sub>Bhe</sub><sup>\*\*\*\*</sup>) that were shown to interact with the ATP derivative in the active site of BepC<sub>Btr</sub> (Fig. 1.9). Although the activity seemed to be reduced in comparison with the wild-type effector, a signal corresponding to BepC<sub>Bhe</sub><sup>\*\*\*\*</sup> (FIC-OB) was still detected (Fig. 4.5). This result suggests that the modification is not dependent on a functional active site and might not be linked to an enzymatic activity.

The non-canonical FIC motif of BepC<sub>Bhe</sub> (HxFxKGNRxxR) only differs from the canonical motif (HxFx(D/E)GNRxxR) by a lysine residue instead of a negatively charged amino acid (D/E). Thus, we assumed that the exchange for a glutamate might restore a defective AMPylation activity. However, BepC<sub>Bhe</sub> K150E (FIC-OB) did not show an increase in radioactive signal (Fig. 4.5), suggesting that other residue(s) than the canonical FIC motif are necessary for an auto-AMPylation activity. Another hypothesis would be that BepC is not able to actively auto-modify itself but would still be able to AMPylate a target protein *in vivo*.

Therefore, the FIC motif does not seem to actively participate in the auto-modification of BepC.

#### **4.1.4 BepC<sub>Bhe</sub> (FIC-OB) does not AMPylate or ADP-ribosylate host proteins *in vitro*.**

Host-targeted Fic proteins such as Bep1 [6], VopS [7] and IbpA [5] AMPylate a subset of small GTPases by using ATP. As BepC activates the RhoA pathway and interacts with GEF-H1 and MRCK $\alpha$  during infection, we were wondering if BepC could modify one of these host proteins. To test it, we incubated BepC<sub>Bhe</sub> (FIC-OB) with a lysate of HeLa cells in presence of radioactively labeled ATP ( $\alpha$ -<sup>32</sup>P-ATP) for one hour (Fig. 4.6A). Although an auto-AMPylation activity was detected for BepC, no radioactive signal corresponding to an AMPylated host target could be observed.

As nicotinamide adenine dinucleotide (NAD<sup>+</sup>) can be used by the bacterial toxin TccC5 to modify and activate RhoA by ADP-ribosylation to induce actin stress fibers [8], we decided to

test whether BepC could also use it as a substrate (Fig. 4.S2B). Recombinant BepC<sub>Bhe</sub> (FIC-OB) was incubated in presence of HeLa cell lysate and radioactive NAD<sup>+</sup> ( $\alpha$ -<sup>32</sup>P-NAD<sup>+</sup>) for one hour (Fig. 4.6B). Only a weak signal that could reflect an auto-modification of BepC was detected while no signal corresponding to a modified target was visible in the cell lysate.

Overall, BepC (FIC-OB) does not AMPylate or ADP-ribosylate a host protein in the tested conditions. However, we can not exclude that BepC is actually able to modify a target protein, such as RhoA, GEF-H1, or MRCK $\alpha$  *in vivo* or in other experimental conditions *in vitro*.

#### **4.1.5 BepC<sub>Bhe</sub> (FIC-OB) is stabilized by nucleoside tri- and di-phosphates as well as pyrophosphate.**

Fic proteins with a non-canonical FIC motif have been shown to use other substrates than ATP to posttranslationally modify their target protein, such as CDP-choline or UTP [9, 10]. As BepC also display a non-canonical FIC motif and a slow auto-modification activity in presence of ATP, we formulated the hypothesis that this effector might use another substrate.

To test different substrates, we mixed purified BepC<sub>Bhe</sub> (FIC-OB) with increasing concentrations of nucleotide derivatives (Fig. 4.S3) and measured the thermal stability of the protein by TSA (thermal shift assay). An increase of the melting temperature (T<sub>m</sub>) of the protein in function of the concentration of the tested molecule indicates the binding of a ligand.

All tested nucleoside triphosphates (NTPs: ATP, GTP, CTP, UTP) increased the stability of BepC<sub>Bhe</sub> (FIC-OB) with a similar effect (Fig. 4.7A), suggesting that the composition of the nitrogenous base is not critical for binding. Nucleoside diphosphates (ADP, GDP) and pyrophosphate (PPi) were also able to stabilize the FIC domain but with less efficiency than NTP (Fig. 4.7B). The incubation with AMP, a nucleoside monophosphate, did not stabilize the protein which was rather surprising knowing that phosphate or sulfate buffers already increase its stability (data not shown). These data suggest that having three phosphates is optimal for the nucleosides to bind to the FIC domain of BepC. However, having only two phosphates was already reducing the ability of the nucleoside to stabilize the protein while having one phosphate completely abolished it.

To test whether a larger substrate could bind to the effector, we mixed BepC<sub>Bhe</sub> (FIC-OB) with dinucleotides (Fig. 4.7C). The result showed that NADH stabilized the FIC domain only at millimolar concentrations, implying that it is a really poor binding partner compared to NTPs. However, NADPH was as efficient as nucleoside di-phosphates, suggesting that a negative charge on the ribose helps to stabilize the FIC domain. This hypothesis is in accordance with the observation that CoASH (Fig. 4.7E), which has a phosphate on the other hydroxyl group of the ribose, was able to increase the stability of BepC.

Finally, we also tested nucleotide derivatives with diverse extensions on the  $\beta$ -phosphate, such as flavin adenine dinucleotide (FAD), ADP/UDP-glucose, CDP-choline, and UDP-GlcNAc (Fig. 4.7D and Fig. 4.8A). Although they are all composed of a nucleotide di-phosphate moiety, they were not able to increase the thermal stability of BepC. These data suggest that either these molecules were too large to fit in the active site of BepC or that their extensions were interfering with the binding in the FIC domain.

Overall, our results suggest that BepC<sub>Bhe</sub> (FIC-OB) is stabilized by a wide variety of nucleotide derivatives although it preferentially binds to nucleoside triphosphates.

#### **4.1.6 A conserved FIC motif is required for the thermal stability of BepC.**

According to our previous results, BepC<sub>Bhe</sub> H146A (FIC-OB) is still able to auto-AMPylylate itself (Fig. 4.5). Thus, we wanted to determine whether the mutation of the conserved histidine has an influence on the binding of different nucleotide derivatives.

To answer this question, we mixed BepC<sub>Bhe</sub> H146A (FIC-OB) with ATP, NADPH, and UDP-GlcNAc and compared its thermal stability to the wild-type protein (Fig. 4.8A). Even at a high concentration of nucleotide derivatives, our data did not show any stabilization of the FIC domain of BepC H146A, neither by ATP nor by NADPH. Moreover, the incubation of BepC<sub>Bhe</sub> (FIC-OB) with mutations in the FIC motif (BepC H146A, BepC<sup>\*\*\*\*</sup>, BepC K150E) at 30°C in presence of 1 mM ATP indicated that all the mutants were less stable than the wild-type protein and precipitated over time (Fig. 4.8B).

In conclusion, these observations suggested that mutations in the FIC motif prevented the ATP to bind and stabilize BepC.

#### **4.1.7 BepC does not require magnesium to have auto-AMPylation activity and to bind nucleotides derivatives.**

In Fic proteins with a canonical FIC motif, a negatively charged residue is necessary to stabilize an ion of magnesium ( $Mg^{2+}$ ) that mediates the interaction with the  $\alpha$ - and  $\beta$ -phosphates of the ATP [2]. In the non-canonical FIC motif of BepC, the lysine directly interacts with the phosphates via its positive charge (Fig. 1.9). According to this observation, BepC should not require  $Mg^{2+}$  to bind nucleotides derivatives or for its enzymatic activity.

To test this hypothesis, we mixed BepC<sub>Bhe</sub> (FIC-OB) with different concentrations of nucleotide derivatives in presence or absence of  $MgCl_2$  and measured the thermal stability of the protein. Although we could not exclude that there was no  $Mg^{2+}$  left in the condition without  $MgCl_2$ , preliminary results showed that the addition of magnesium slightly reduced the ability of nucleotides derivatives to stabilize the FIC domain (Fig. 4.9A). This effect suggests that  $Mg^{2+}$  seemed to prevent the nucleotides derivatives to bind to the active site of BepC.

In order to determine whether  $Mg^{2+}$  is necessary for the activity of BepC, we incubated BepC<sub>Bhe</sub> (FIC-OB) with radioactive ATP or NAD<sup>+</sup> in presence or in absence of MgCl<sub>2</sub> (Fig. 4.9B). The autoradiography only showed an auto-AMPylation of BepC and no auto-ADP-ribosylation. This result was in accordance with the findings of the binding experiments suggesting that NAD<sup>+</sup> does not bind to the FIC domain of BepC. The presence of  $Mg^{2+}$  greatly reduced the auto-AMPylation of BepC, possibly by interacting with the ATP in solution and preventing its binding to the active site.

In accordance with the presence of the lysine residue in its FIC motif, these results confirm that BepC does not need  $Mg^{2+}$  to bind nucleotides derivatives or have an enzymatic activity.

#### 4.1.8 BepC belongs to the class I Fic proteins.

The overexpression of Fic protein effectors can inhibit the growth of *Bartonella* in absence of antitoxin [2]. Therefore, we decided to test whether the overexpression of BepC in *Bhe* is also inducing growth inhibition, which could be problematic for infection assays.

Thus, we incubated *Bhe*  $\Delta$ bepA-G overexpressing BepC of different *Bartonella* species, or GFP as a negative control, on agar plates at different concentrations of IPTG (Fig. 4.10). In the absence or at low concentration of IPTG (10  $\mu$ M), the expression of BepC had no effect on *Bhe* growth. By contrast, all effectors inhibited the growth of the bacteria at 100  $\mu$ M of IPTG. Interestingly, the inhibition due to BepC<sub>Btr</sub> was less drastic but this difference does not seem to be linked to an expression defect (data not shown).

The role of the antitoxin is to inhibit the activity of class I Fic protein, which could be deleterious for the cell [2]. As some *Bartonella* species of the lineage 4, such as *Bqu* and *Bta*, have an antitoxin encoded directly in front of *bepC*, our hypothesis was that BepC<sub>Bhe</sub> might interact with the antitoxin of *Bartonella henselae* (AT<sub>Bhe</sub>), which could reduce its adverse effect on bacterial growth.

To test it, we co-expressed the HA-tagged AT<sub>Bhe</sub> with His-tagged BepC<sub>Bhe</sub> (FIC-OB) in *E. coli*. After cell lysis, BepC<sub>Bhe</sub> was purified by affinity chromatography and gel filtration. The analysis of the elution fractions by SDS-PAGE showed that the antitoxin was co-purified with BepC<sub>Bhe</sub> (FIC-OB), confirming an interaction with the FIC domain *in vitro* (Fig. 4.11A). The identity of the two proteins was confirmed by western blot and compared to a purified fraction of BepC<sub>Bhe</sub> (FIC-OB) that has not been co-expressed with the antitoxin (Fig. 4.11B). Interestingly, the signal detected between 37 and 50 kDa on the anti-HA western blot could correspond to a toxin-antitoxin complex although it was not visible by SDS-PAGE or by anti-Flag western blot.

Despite the presence of the endogenous antitoxin gene in *Bhe*  $\Delta$ bepA-G, the expression would probably not be sufficient to inhibit the overexpressed Fic proteins. Therefore, we co-

expressed the antitoxin and BepC<sub>Bhe</sub> from the same plasmid in order to reduce growth inhibition (Fig. 4.12). Typically, the transcription of the BepC<sub>Bhe</sub> is under the control of a single Ptaclac promoter, inducible with IPTG (A). For coupled expression, the antitoxin sequence is located downstream of a Shine-Dalgarno (SD) sequence, leading to a high expression level (strong SD) while two different combinations were tested for the effector. The first construct (B) is based on translational coupling with the stop codon of the antitoxin overlapping the start codon of the effector (TAATG). In the second construct (C), the sequence encoding BepC<sub>Bhe</sub> is located downstream a mutated SD sequence (weak SD) in order to reduce the affinity with the ribosome.

Nevertheless, the co-expression of the antitoxin could not prevent the growth defect induced by the expression of BepC<sub>Bhe</sub> at 100  $\mu$ M of IPTG, suggesting that either the growth defect was not due to a potential activity of BepC or that the antitoxin was not able to inhibit it.

To determine if a putative activity of BepC is playing a role in growth inhibition of *Bhe*  $\Delta$ bepA-G, we overexpressed BepC<sub>Bhe</sub> with mutations in the non-canonical FIC motif as well as BepF<sub>Bhe</sub> and BepE<sub>Bhe</sub> as negative controls (Fig. 4.13). Only BepC with a combination of the mutated conserved histidine and mutations of the residues interacting with the phosphates of the nucleotide (BepC\*\*\*\*) showed a slight reduction in growth inhibition at 100  $\mu$ M of IPTG. According to this result, the active site of BepC is probably not participating in growth inhibition.

To identify other regions that could be involved in the growth defect, truncated versions of BepC<sub>Bhe</sub> were overexpressed in *Bartonella* (Fig. 4.14). The deletion of the first  $\alpha$  helix, the FIC domain, and the FIC-OB domains did not restore bacterial growth, indicating that the BID domain alone has an inhibiting effect on *Bartonella* growth. This result is in accordance with the observation that mutations in the FIC motif or the co-expression of the antitoxin did not reduce the growth inhibition due to the overexpression of BepC<sub>Bhe</sub>.

As the co-expression of the antitoxin does not reduce growth inhibition, we wanted to determine whether it could have another function. As the thermal stability of the BepC<sub>Bhe</sub> (FIC-OB) is below 30°C at a low concentration of nucleotide (Fig. 4.7), we formulated the hypothesis that the antitoxin could stabilize it.

To test it, we measured the stability of BepC<sub>Bhe</sub> (FIC-OB), that has been expressed alone or co-purified with the antitoxin, in presence or in absence of ATP. Our results suggest that the presence of the antitoxin greatly increased the thermal stability of the protein, even at low ATP concentration (Fig. 4.15). This could suggest that the antitoxin acts as a chaperone by stabilizing the FIC domain of BepC inside the bacteria.

In summary, our results indicate that BepC<sub>Bhe</sub> binds to the antitoxin, which attributes the effector to the class I Fic proteins. Although it does not reduce the growth inhibition resulting

- Additional results -

from the overexpression of BepC<sub>Bhe</sub>, which is associated with the BID domain, it may act as the chaperone to stabilize the FIC domain inside *Bartonella*.

## 4.2 Discussion

*V. parahaemolyticus* and *H. somni* subvert Rho GTPase signaling cascades via the two T3SS effectors VopS and IbpA, respectively, which AMPylate Rac, Cdc42, and RhoA via their FIC domain. The modification leads to the collapse of the actin cytoskeleton and eventually to the disruption of phagocytosis [5, 7]. *Bartonella* evolved a large panel of effectors carrying a FIC domain, suggesting a central role in pathogenesis. However, the enzymatic activity and the host target remain largely unknown for most of them. BepC is characterized by a non-canonical FIC motif (HxFxKGNGRxxR), which differs from the canonical motif in a lysine instead of an acidic residue. In protein with a canonical FIC motif, the negatively charged residue interacts with an ion of magnesium that mediates the interaction with the phosphate of the nucleotide (Fig. 1.9). Nevertheless, structural studies show that the lysine present in the FIC motif of BepC directly interacts with the phosphates of the nucleotide. Although the nucleotide binds in a conformation that is compatible with AMPylation, no enzymatic activity have ever been demonstrated for BepC. Interestingly, the fact that the conserved FIC motif is not required for actin rearrangements suggests that the putative activity of BepC would have another function.

### **Recombinant BepC (FIC-OB) is modified after overexpression in *E. coli*.**

The analysis of full recombinant BepC (FIC-OB) by mass spectrometry indicates that the vast majority of purified proteins, both wild-type and histidine mutant, are modified after overexpression in *E.coli*. As many Fic proteins are able to auto-modify themselves via AMPylation [11], it is reasonable to think that BepC might modify itself if it has an enzymatic activity and is in presence of its substrate during expression. However, this would imply that the co-expression of the antitoxin or the mutation of the conserved histidine in the FIC motif do not interfere with the auto-modification activity.

If we assume that the first methionine is cleaved by the *E. coli* methionine aminopeptidase, the mass change (283-284 Da) can not correspond to auto-AMPylation as the transfer of an AMP moiety corresponds to an additional mass of 329 Da. Accordingly, the analysis of the peptides of BepC after tryptic digestion did not show any AMPylated peptide. However, other modifications have not been investigated yet.

As the mass of the full protein is measured, the mass change can correspond to several modifications. Considering that the mass spectrometry realized on peptides shows that five methionines of BepC<sub>Bhe</sub> (FIC-OB) are oxidized ( $\Delta$  mass 80 Da), the remaining difference would be 203 Da. This could correspond to a transfer of N-acetylglucosamine (GlcNac) from UDP-GlcNac. Interestingly, the proposed mechanism of the human O-GlcNac transferase is based on a catalytic histidine and a lysine to stabilize the UDP moiety (Fig. 4.S4). Furthermore, a toxin from *Clostridium novyi*, TcnA, is using UDP-GlcNac to modify and inactivate Rho



GTPases by transferring a GlcNAc moiety [12]. However, its catalytic domain has nothing in common with the FIC domain of BepC and is characterized by a DxD motif surrounded by a hydrophobic region. Although UDP-GlcNAc seems to be a poor substrate according to thermal shift assay, it might be worth to test it as a substrate for BepC by using a radioactive assay.

**BepC displays slow AMPylation and auto-phosphorylation activities, independently from the FIC motif.**

In presence of ATP, BepC has concomitant auto-AMPylation and auto-phosphorylation activities with similar kinetics. This suggests that the effector binds the ATP in two different conformations, one compatible with AMPylation and one with phosphorylation. Similarly, a dual conformation has been already observed for VbhT, a Fic protein of *Bartonella schoenbuchensis* [13], which AMPylates a bacterial gyrase [14]. However, this could also suggest that ATP is not the physiological substrate of BepC. The presence of a lysine in the FIC motif instead of a negatively charged residue might facilitate this dual activity. Thus, it would be relevant to test whether BepC with the restored canonical FIC motif still shows an auto-phosphorylation activity.

Surprisingly, no AMPylated peptide could be identified by mass spectrometry after incubation in presence of ATP. Although a loss of the AMPylated peptide during sample preparation cannot be excluded, this result suggests either that only a small fraction of protein is modified and could not be detected by mass spectrometry or that the missing peptide (MPAMRPK) carries the modification. As this peptide does not contain any tyrosine, serine or threonine residue that could be modified, it is likely that BepC is hardly AMPylated.

Furthermore, multiple mutations in the FIC motif do not result in a complete loss of activity and the restoration of a canonical motif does not increase AMPylation. This result suggests that the modification is independent of a functional active site and might not be due to an enzymatic activity. Therefore, it is possible that BepC is not able to auto-modify itself, in contrast to other Fic proteins. Additionally, the modification of the recombinant protein might interfere with a potential activity.

As BepC interacts with GEF-H1 and MRCK $\alpha$  during infection, it could be possible that BepC posttranslationally modifies them, although this activity might not be crucial for actin rearrangements. Nevertheless, no AMPylated or ADP-ribosylated host protein could be detected in HeLa cell lysate after incubation in presence of BepC with radioactive ATP or NAD<sup>+</sup>. However, BepC could still modify a protein *in vivo*, by using ATP or another substrate.

### **BepC preferentially binds to nucleoside triphosphates.**

A molecule absorbing at 260 nm is co-purified with BepC (FIC-OB) after overexpression in *E.coli*. As the OB fold has been described to bind nucleic acid [15, 16] and DNA absorbs at 260 nm, it could result from a contamination despite the use of DNase. However, this compound could correspond to a nucleotide binding to the active site of the FIC domain of BepC. Further investigation is required to identify this compound, possibly by mass spectrometry.

Due to its non-canonical FIC motif, it is conceivable that BepC uses another substrate to modify a protein target during infection. The increased thermal stability of BepC (FIC-OB) in presence of nucleotides triphosphate suggests that BepC could potentially use GTP, CTP or UTP to catalyze posttranslational modifications. Interestingly, BepA, which has a canonical FIC motif, can also use CTP and GTP for auto-modification [1]. However, it is unknown whether BepA can use these nucleotides to modify its host target during infection. The auto-modification of BepC, as well as the transfer on a protein target, could be tested by using radioactive NTPs and cell lysates.

Larger substrates such as NADPH and Co-enzyme A can also bind to the effector, possibly due to the presence of a phosphate group on the ribose. According to the structure of the FIC domain of BepC<sub>Btr</sub> (Fig. 1.9), this phosphate should be stabilized by a residue that is not part of the FIC motif. Although these two molecules are not described as a substrate for posttranslational modifications, they could be used as a co-factor to stabilize the FIC domain.

As proposed by the structure of the FIC domain of BepC<sub>Btr</sub> (Fig. 1.9), the conserved histidine of the FIC motif is necessary for the stabilization of the FIC domain in presence of ATP. Strikingly, each mutation in the FIC motif seems to affect the solubility of the protein, which could suggest that the ability to bind a nucleotide is crucial to stabilize the folding of the FIC domain. This observation could eventually explain why BepC with multiple mutations in the FIC motif (BepC\*\*\*\*) has a reduced interaction with GEF-H1 and MRCK $\alpha$  (Fig. 3.7A).

BepC does not need magnesium to bind nucleotide derivatives. The conserved lysine residue in the non-canonical FIC motif seems to be sufficient to stabilize the ATP in the active site. Interestingly, Mg<sup>2+</sup> also reduces auto-modification activity, probably by binding to the phosphate of the ATP and competing with the binding in the active site.

As the FIC motif of BepC is highly conserved, it is very likely that it plays a significant role in a function of BepC that is not linked to actin rearrangements. Whether this function would require posttranslational modification remains unknown. Even though ATP seems to be the best candidate, we cannot exclude that BepC uses another nucleotide derivative as co-factor to stabilize the FIC domain or as a substrate for posttranslational modification.

### **BepC belongs to the class I of Fic proteins**

As already observed for VbhT [2], Bep1, and Bep2, (data not shown) the overexpression of BepC from different *Bartonella* species inhibits the growth of *Bhe* in absence of antitoxin. Surprisingly, the co-expression of the antitoxin in *Bartonella* did not restore bacterial growth. In contrast with VbhT, mutations in the FIC motif hardly reduce growth inhibition. Therefore, the active site of BepC is probably not participating in the growth defect of *Bartonella*. In fact, the expression of the BID domain alone is sufficient to prevent bacterial growth, which is in accordance with the absence of positive effect of the antitoxin co-expression. The deleterious effect of the BID domain is presumably related to its tendency to localize to membranes [17] as the accumulation of effector would likely disrupts them. Although we cannot exclude that the antitoxin inhibits a potential activity that would be detrimental to the bacteria, its main role might be to serve as a chaperone to stabilize the protein. As Beps needs to be translocated inside the host cell via the T4SS, the FIC domain is probably not so stable in order to be unfolded during the process. Therefore, the antitoxin might bind to BepC to prevent unfolding and degradation before translocation.

### 4.3 Figures

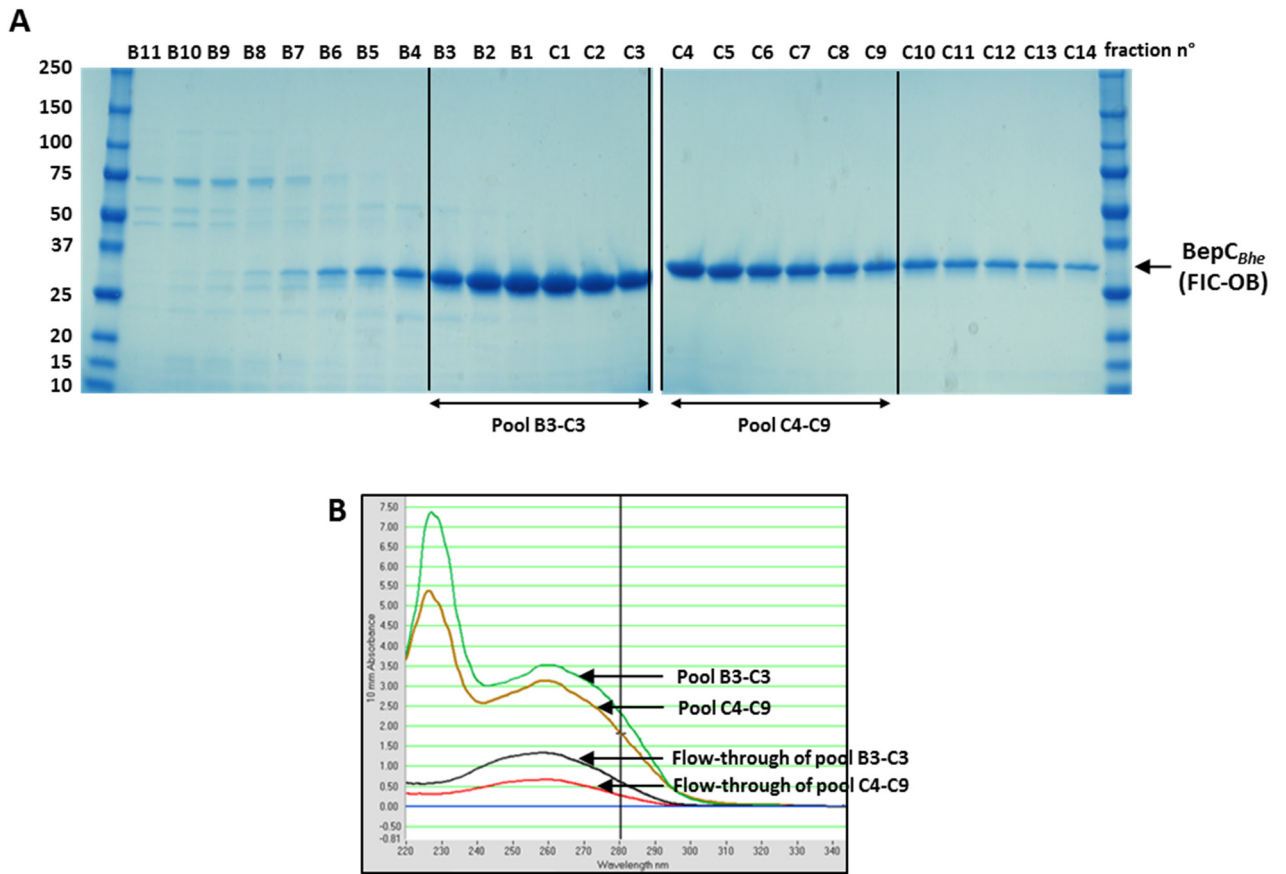


**Figure 4.1. An unknown compound absorbing at 260 nm co-purifies with BepC<sub>Bhe</sub> (FIC-OB).**

His-tagged BepC<sub>Bhe</sub> (FIC-OB) was overexpressed in *E.coli* and purified by affinity chromatography and gel filtration. Elution fractions were pooled and concentrated. **A)** SDS-PAGE of purified fractions from the gel filtration. **B)** Absorbance spectra of pooled fractions B3-C3 (green), pooled fractions C4-C9 (brown), flow-through from concentration of pooled fractions B3-C3 (black) and flow-through from concentration of pooled fractions C4-C9 (red).

- Additional results -

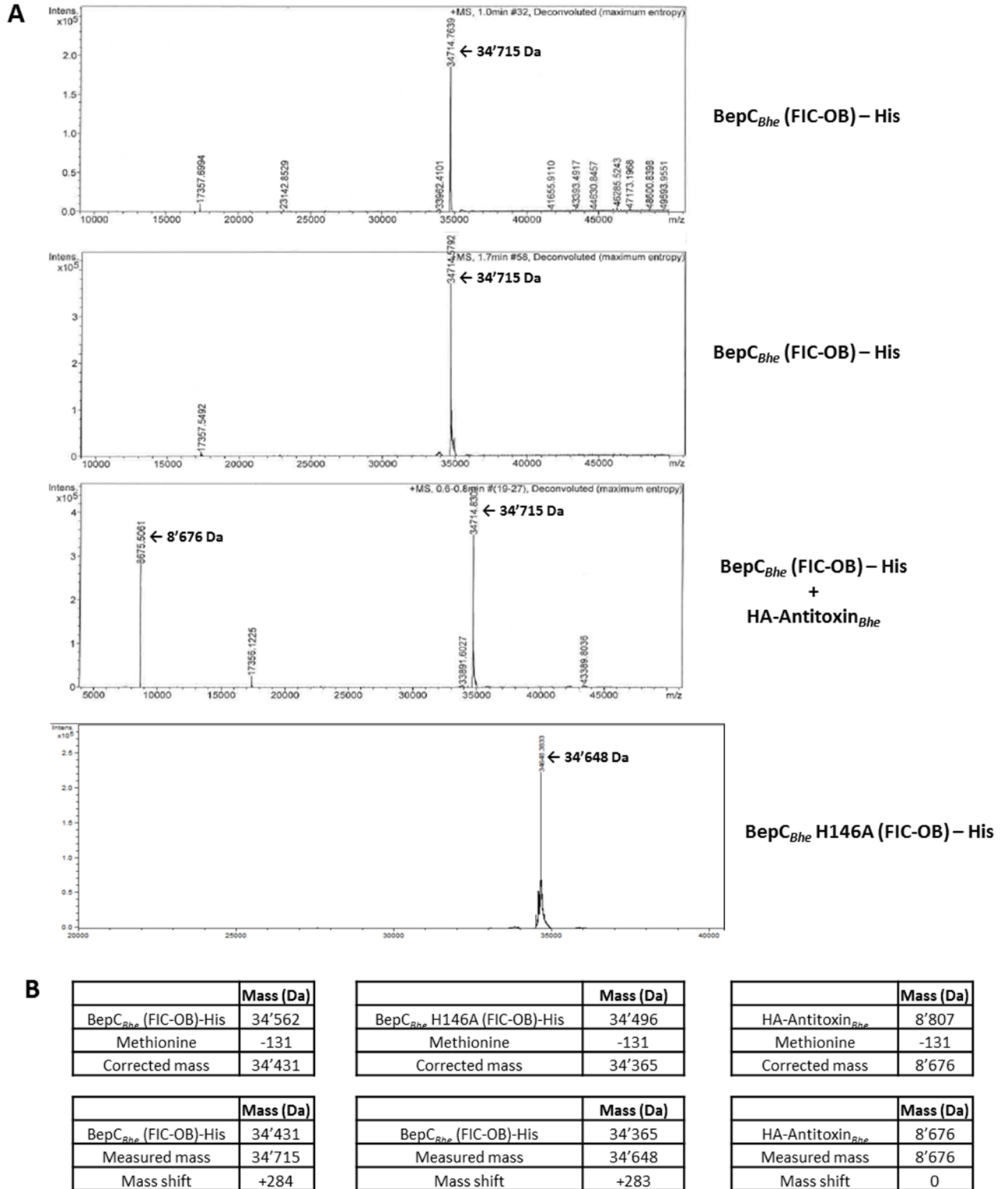


**Figure 4.2. Purified BepC<sub>Bhe</sub> (FIC-OB) have a mass shift of 283 Da.**

**A)** The masses of various recombinant BepC<sub>Bhe</sub> (FIC-OB) were analyzed by mass spectrometry after overexpression in *E. coli* followed by affinity purification and gel filtration. **B)** Calculation of the mass shift by subtracting the theoretical mass to the measured mass. Masses of posttranslational modification of interest.

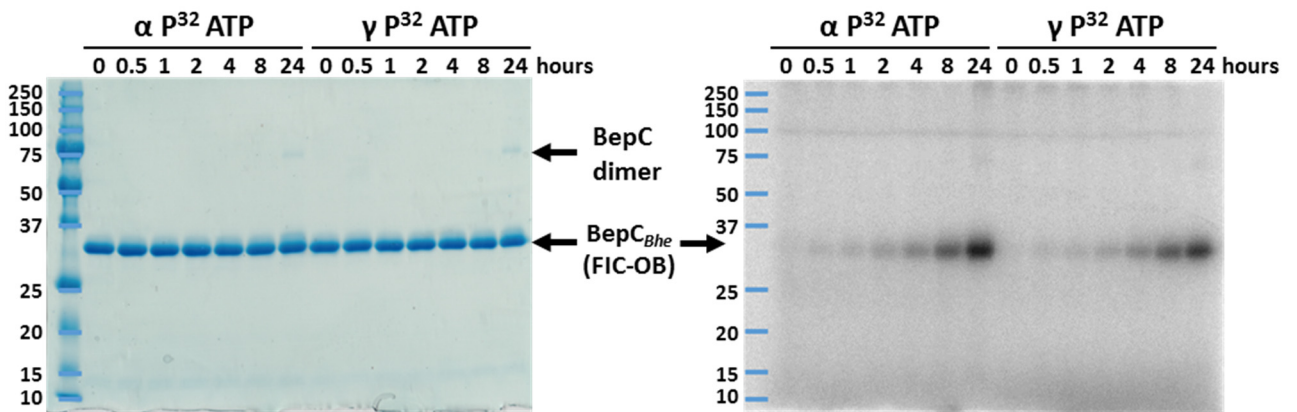


**Figure 4.3. BepC<sub>Bhe</sub> (FIC-OB) has both auto-AMPylation and auto-phosphorylation activities in presence of ATP.**

Purified BepC<sub>Bhe</sub> (FIC-OB) was incubated 0.5, 1, 2, 4, 8 or 24 hours at 30°C in presence of radioactive ATP ( $\alpha$ -<sup>32</sup>P-ATP or  $\gamma$ -<sup>32</sup>P-ATP) and 10 mM of nonradioactive ATP. The samples were loaded on a SDS-PAGE gel (left panel) and the auto-modification were detected by autoradiography (right panel).

**BepC<sub>Bhe</sub> (FIC-OB) – His**

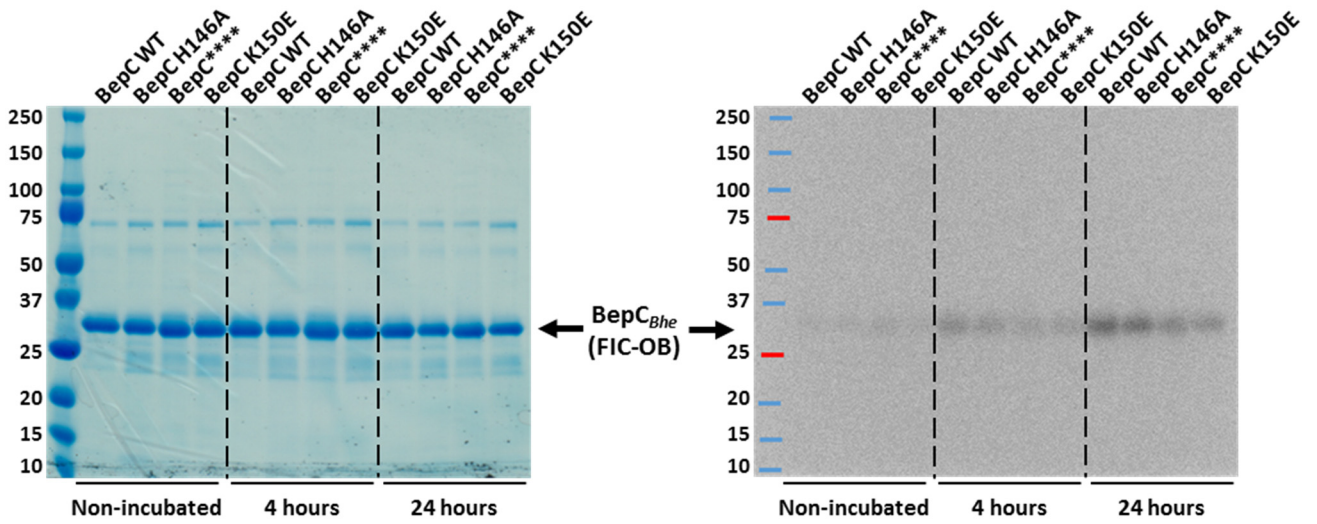
V P F A V G P Q I Q K E L K Q L E R K L M L E H N Y L Y K N S N T L K N K Y G I K D P Q R L Y E R C A H D T A R E V M N L R F E P P P Q R F G L A Y L K L I H W T L F H R S F E W A G H T R D E P F T F E D G S T A R M P A M R P K G H R  
S O M R N S G L E E I N E H I V V V A K T A K N N L O G L S R O E F A E S A A E V F M T L D H A H P L E D G E V V G H K L E D G E V V G H K D D L T P E Q V K T F R K G N G R A Q R I F M E K L G Q A A C Y K I D F S F I T K E R L T O A S I A A M O H G N T O P M K D L F E D I T H P K D L F E D I T H P K D L F E D I T H P K D L F E D I T H P M P A M R P K G H R  
O K F L L L L K E F I

**BepC<sub>Bhe</sub> (FIC-OB) – His + ATP**

V P F A V G P Q I Q K E L K Q L E R K L M L E H N Y L Y K N S N T L K N K Y G I K D P Q R L Y E R C A H D T A R E V M N L R F E P P P Q R F G L A Y L K L I H W T L F H R S F E W A G H T R D E P F T F E D G S T A R M P A M R P K G H R  
S O M R N S G L E E I N E H I V V V A K T A K N N L O G L S R O E F A E S A A E V F M T L D H A H P L E D G E V V G H K L E D G E V V G H K D D L T P E Q V K T F R K G N G R A Q R I F M E K L G Q A A C Y K I D F S F I T K E R L T O A S I A A M O H G N T O P M K D L F E D I T H P K D L F E D I T H P K D L F E D I T H P M P A M R P K G H R  
O K F L L L L K E F I

**Figure 4.4. Auto-AMPylation of BepC was not detected by mass spectrometry after incubation with ATP.**

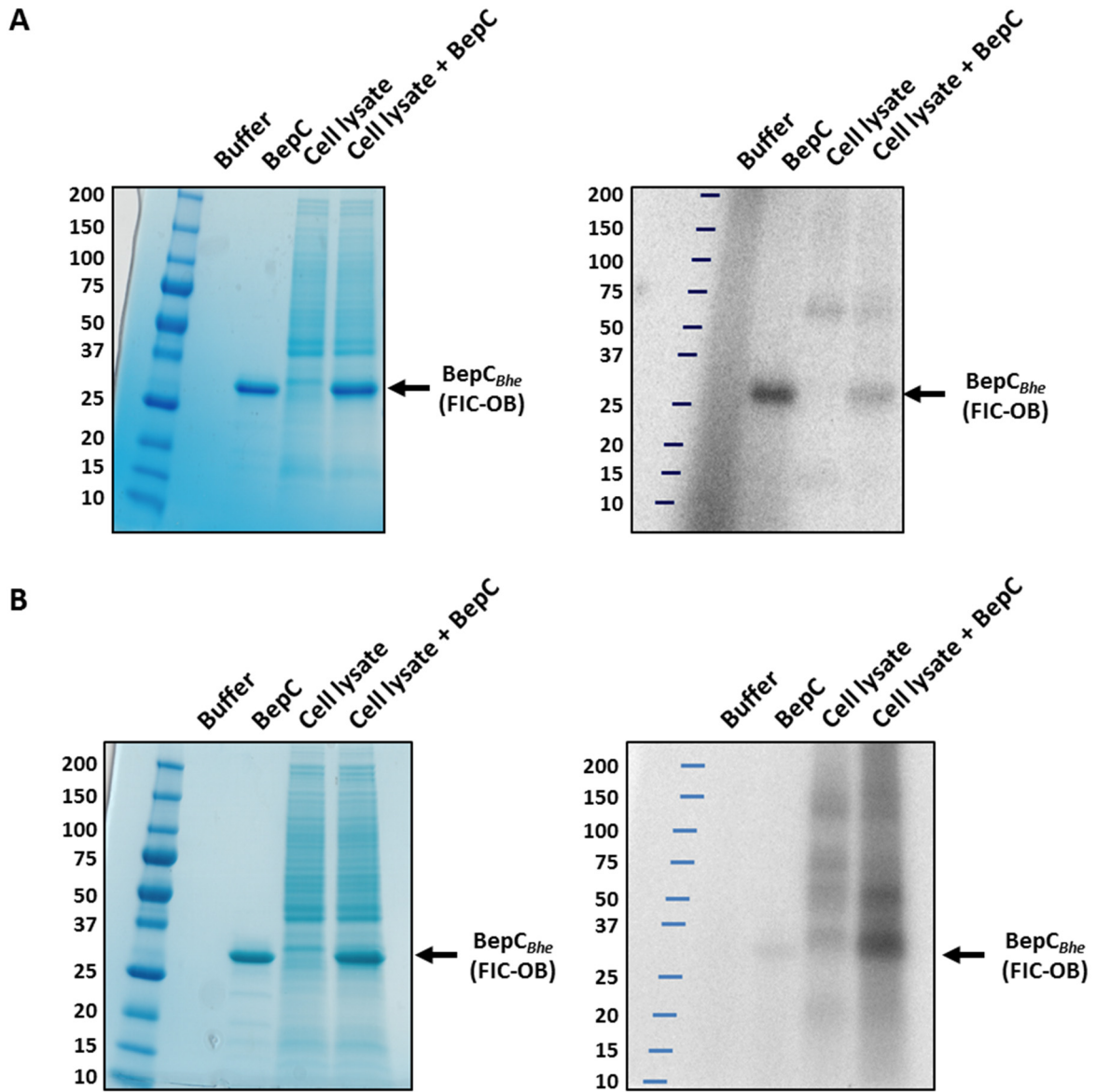
BepC<sub>Bhe</sub> (FIC-OB) was incubated in presence or in absence of 1 mM ATP for 24 hours at 30°C. The reaction was stopped by protein precipitation before being analyzed by LC-MS/MS. The peptide coverage of each sample is indicated in yellow and oxidized methionine in green.



**Figure 4.5. The auto-AMPylation activity of BepC<sub>Bhe</sub> (FIC-OB) is independent of the FIC motif.**

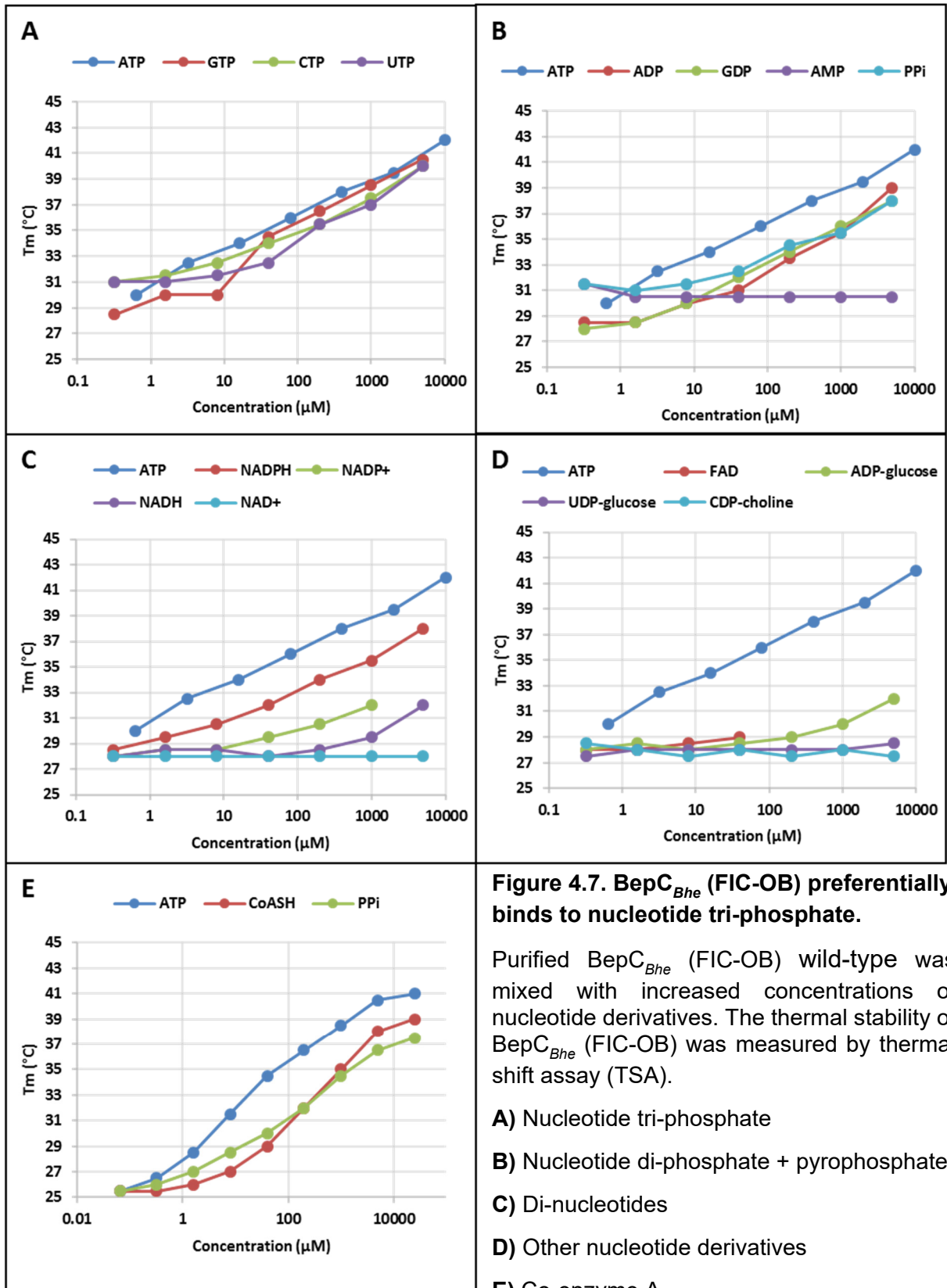
Partially purified BepC<sub>Bhe</sub> (FIC-OB) wild-type and mutants were incubated 4 and 24 hours at 25°C in presence of radioactive ATP ( $\alpha$ -<sup>32</sup>P-ATP) and 1 mM of nonradioactive ATP. Samples were loaded on a SDS-PAGE gel (right panel) and analyzed by autoradiography (left panel).





**Figure 4.6. BepC<sub>Bhe</sub> (FIC-OB) does not AMPylate or ADP-ribosylate a protein target in HeLa cell lysate in the tested conditions.**

Purified BepC<sub>Bhe</sub> (FIC-OB) wild-type was incubated 1 hour at 30°C in presence of HeLa cell lysate. Samples were loaded on a SDS-PAGE gel (left panels) and analyzed by autoradiography (right panels). **A**) Incubation with ATP ( $\alpha$ -<sup>32</sup>P-ATP) **B**) Incubation with NAD<sup>+</sup> ( $\alpha$ -<sup>32</sup>P-NAD) and 1mM of non-radioactive NAD<sup>+</sup>.



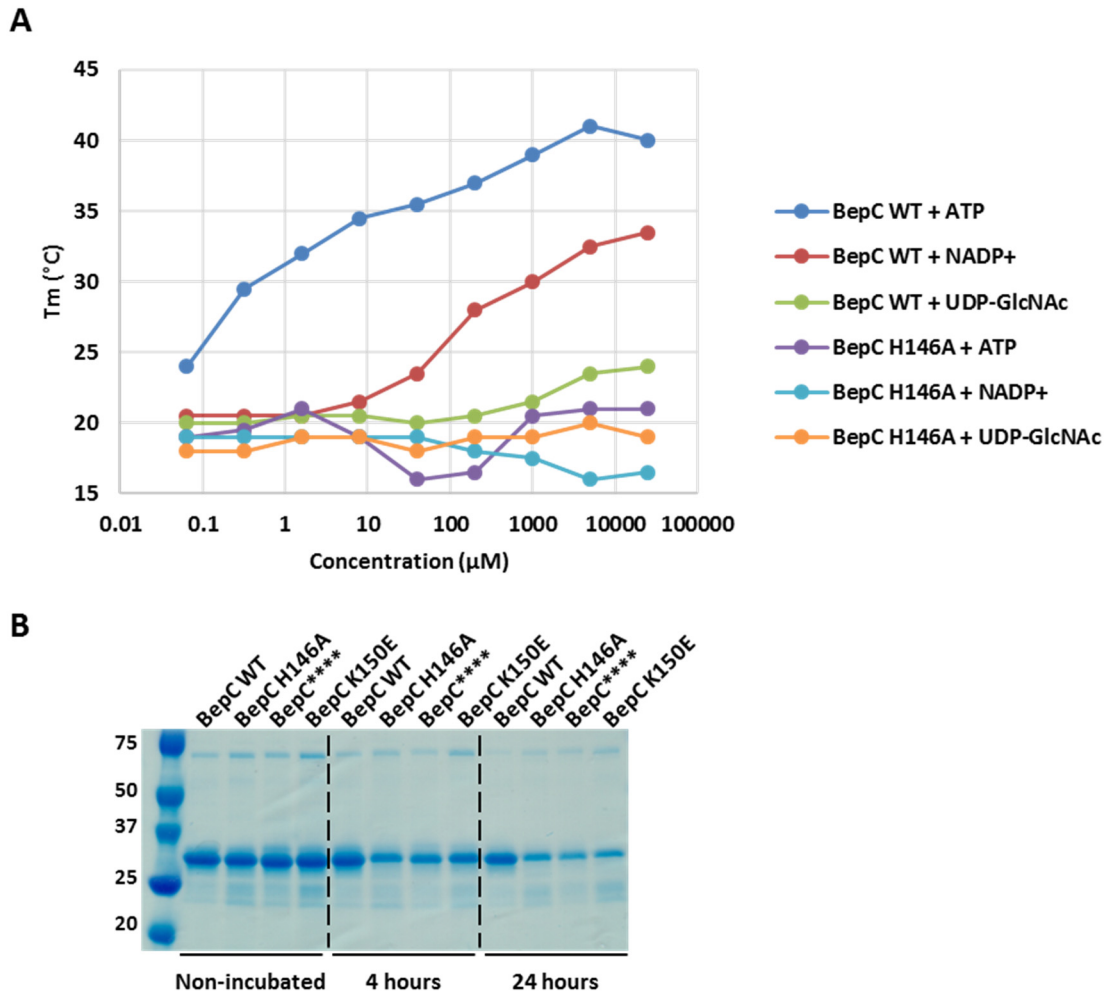
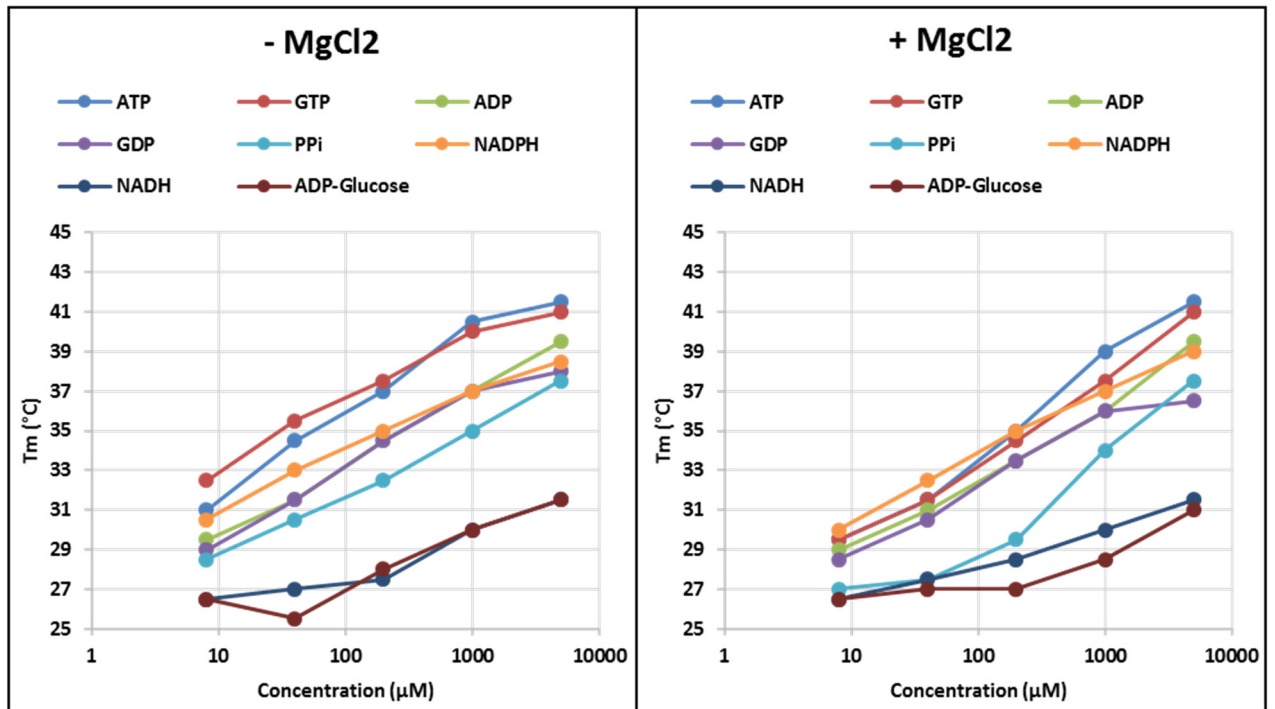


**Figure 4.8. BepC<sub>Bhe</sub> (FIC-OB) with a mutated FIC motif seems less stable than the WT protein in presence of ATP.**

Purified BepC<sub>Bhe</sub> (FIC-OB) wild-type or H146A mutant were mixed with increased concentrations of nucleotide derivatives. The thermal stability of the protein was measured by thermal shift assay (TSA). **B**) Purified BepC<sub>Bhe</sub> (FIC-OB) wild-type and mutants were incubated 4 or 24 hours at 30°C in presence of radioactive ATP ( $\alpha$ -<sup>32</sup>P-ATP) and 1 mM of nonradioactive ATP. Samples were loaded on a SDS-PAGE gel. BepC<sub>Bhe</sub><sup>\*\*\*\*</sup> = BepC<sub>Bhe</sub> H146A, K150A, R154A, R157A.

**A**



**B**

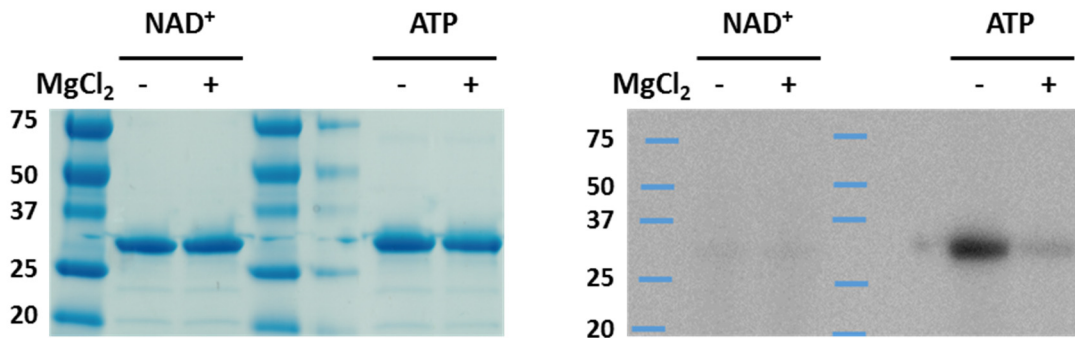


**Figure 4.9. Mg<sup>2+</sup> seems to reduce the stability of BepC<sub>Bhe</sub> (FIC-OB) and its auto-AMPylation activity.**

**A)** Purified BepC<sub>Bhe</sub> (FIC-OB) wild-type was mixed with increased concentrations of nucleotide derivatives in presence or in absence of 1 mM MgCl<sub>2</sub>. The thermal stability of BepC<sub>Bhe</sub> (FIC-OB) was measured by thermal shift assay (TSA). **B)** Purified BepC<sub>Bhe</sub> (FIC-OB) WT was incubated 1 hour at 30°C in presence of radioactive ATP (α-<sup>32</sup>P-ATP) or NAD<sup>+</sup> (α-<sup>32</sup>P-NAD) with or without 5 mM of MgCl<sub>2</sub>. Samples were loaded on a SDS-PAGE gel (left panel) and analyzed by autoradiography (right panel).

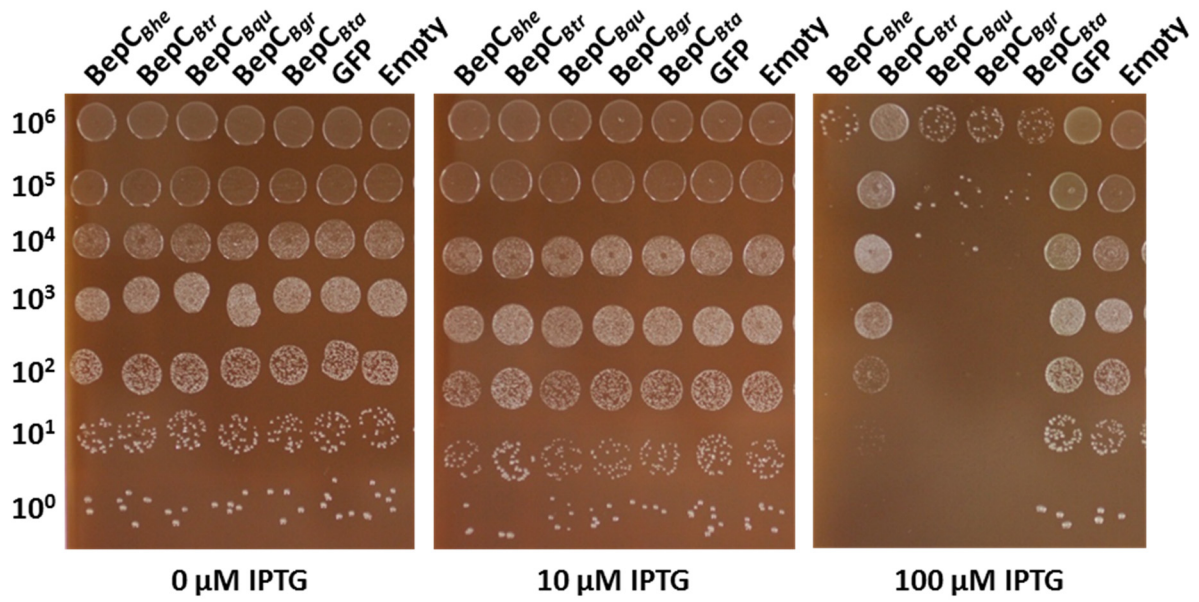


**Figure 4.10. Overexpression of BepC of different *Bartonella* species in *Bhe ΔbepA-G* induces growth inhibition.**

The expression of the indicated BepC was induced in *Bhe ΔbepA-G* in presence of different IPTG concentrations. Serial dilutions of bacteria were plated on CBA plates and incubated at 35°C for 7 days. The number of bacteria spotted on the plate is indicated on the left side.

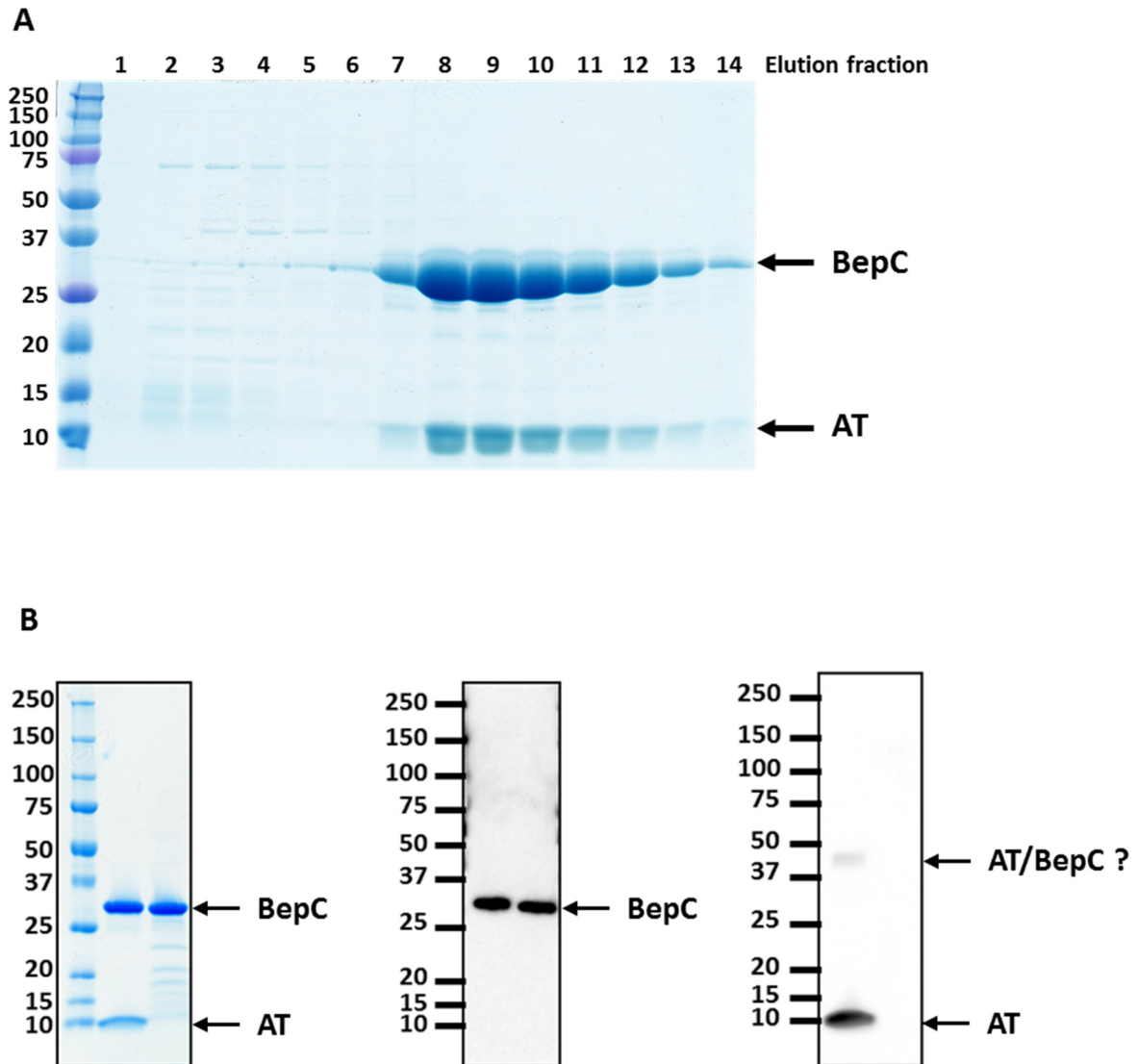


**Figure 4.11. The antitoxin of *Bhe* binds to BepC<sub>Bhe</sub> (FIC-OB).**

His-tagged BepC<sub>Bhe</sub> (FIC-OB) was co-expressed with or without HA-tagged antitoxin (AT) in *E. coli*. After bacterial lysis, BepC<sub>Bhe</sub> (FIC-OB) was purified by affinity chromatography and gel filtration. **A**) SDS-PAGE gel of the gel filtration elution fractions from the co-expression of BepC (FIC-OB) and the antitoxin. **B**) The purified proteins were resolved by SDS-PAGE (left panel) and the identity of BepC and AT was confirmed by western blot against Flag-tag (middle panel) or HA-tag (right panel).



- Additional results -

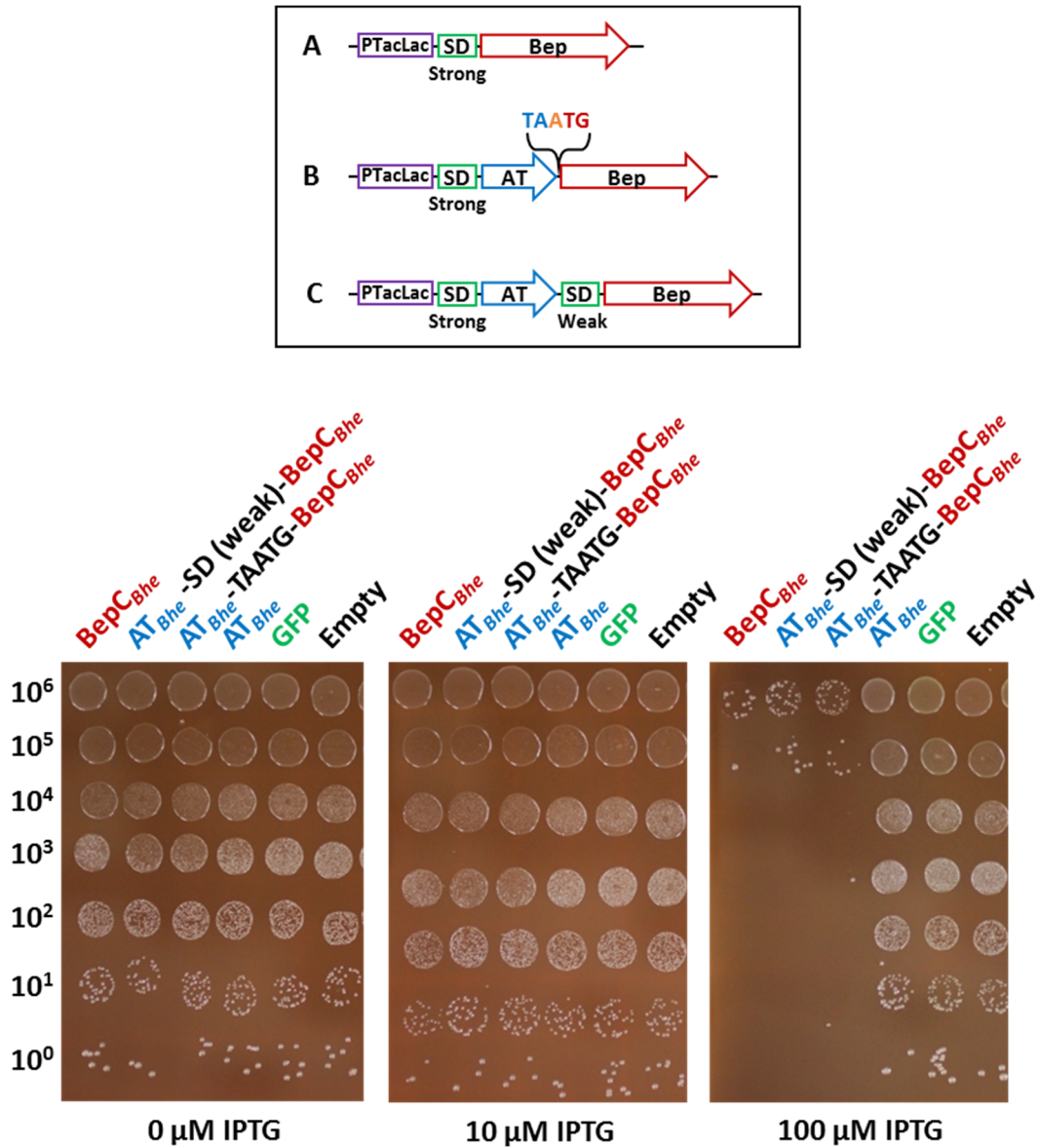


**Figure 4.12. Co-expressing the antitoxin does not reduce the growth inhibition mediated by BepC<sub>Bhe</sub> in *Bhe ΔbepA-G*.**

The expression of the indicated constructs was induced in *Bhe ΔbepA-G* in presence of different IPTG concentrations. Serial dilutions of bacteria were plated on CBA plates and incubated at 35°C for 7 days. The number of bacteria spotted on the plate is indicated on the left side.

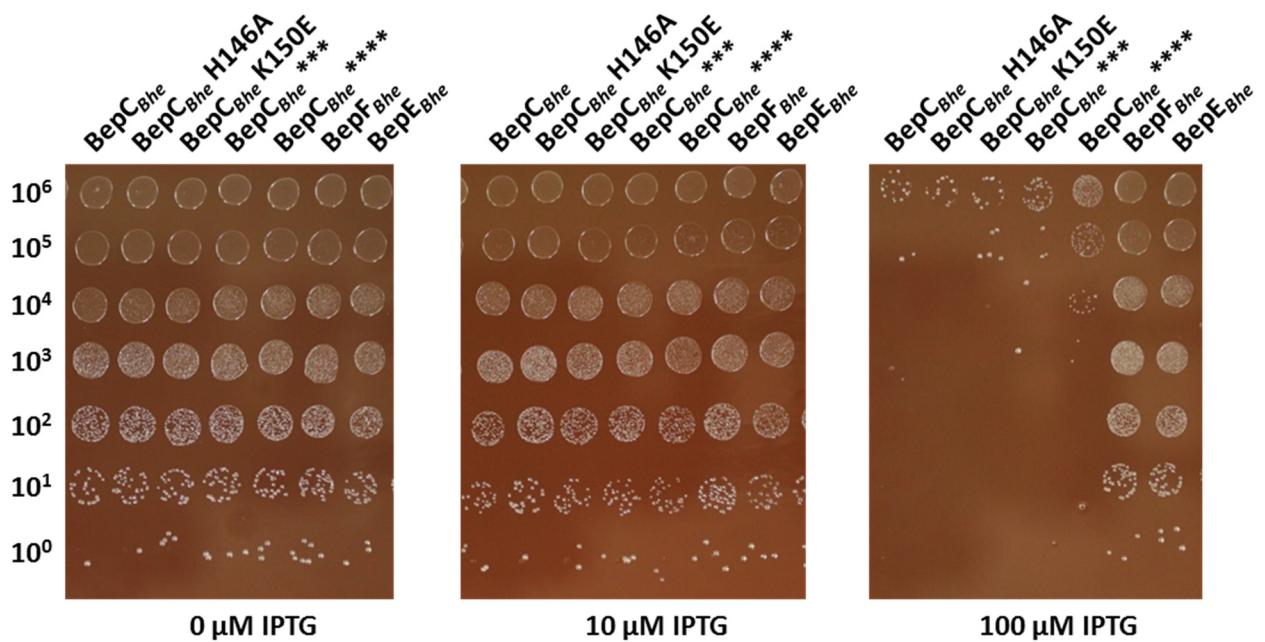


**Figure 4.13. The growth inhibition mediated by the overexpression of BepC<sub>Bhe</sub> in *Bhe*  $\Delta$ *bepA-G* is independent of the FIC motif.**

The expression of the indicated constructs was induced in *Bhe*  $\Delta$ *bepA-G* in presence of different IPTG concentrations. Serial dilutions of bacteria were plated on CBA plates and incubated at 35°C for 7 days. BepC<sub>Bhe</sub>\*\*\* = BepC<sub>Bhe</sub> K150A, R154A, R157A. BepC<sub>Bhe</sub>\*\*\*\* = BepC<sub>Bhe</sub> H146A, K150A, R154A, R157A. The number of bacteria spotted on the plate is indicated on the left side.



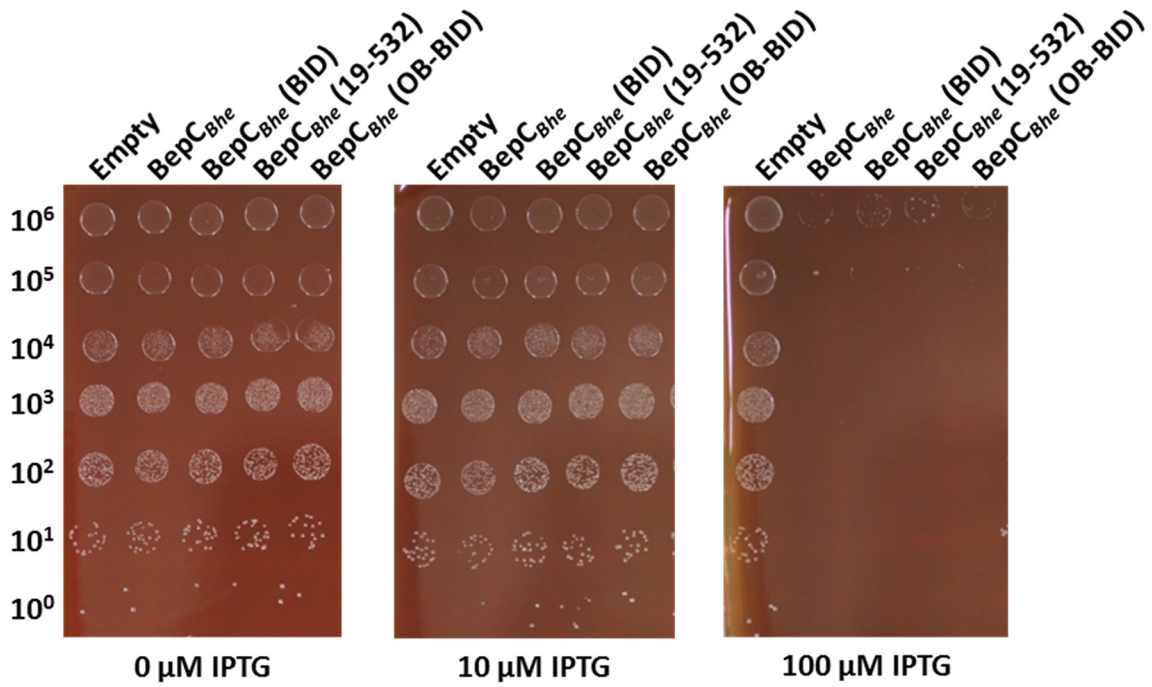


**Figure 4.14. The overexpression of the BID domain of BepC<sub>Bhe</sub> is sufficient to induce growth inhibition of *Bhe*  $\Delta$ bepA-G.**

The expression of the indicated constructs was induced in *Bhe*  $\Delta$ bepA-G in presence of different IPTG concentrations. Serial dilutions of bacteria were plated on CBA plates and incubated at 35°C for 7 days. The number of bacteria spotted on the plate is indicated on the left side.

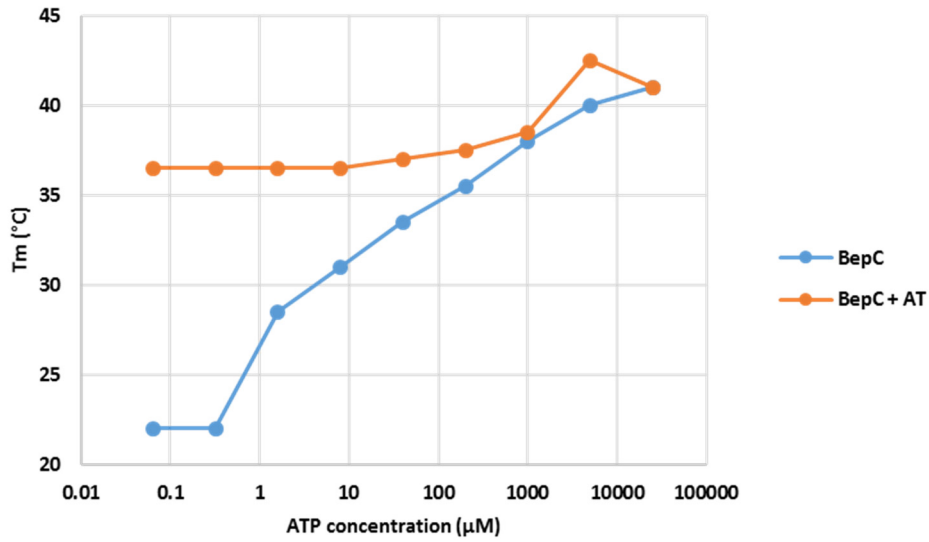


**Figure 4.15. The antitoxin- BepC<sub>Bhe</sub> (FIC-OB) complex is more stable than BepC<sub>Bhe</sub> (FIC-OB) alone.**

Purified BepC<sub>Bhe</sub> (FIC-OB) alone or BepC<sub>Bhe</sub> (FIC-OB) co-purified with the antitoxin were mixed with increased concentrations of ATP. The thermal stability of the proteins was measured by thermal shift assay (TSA).

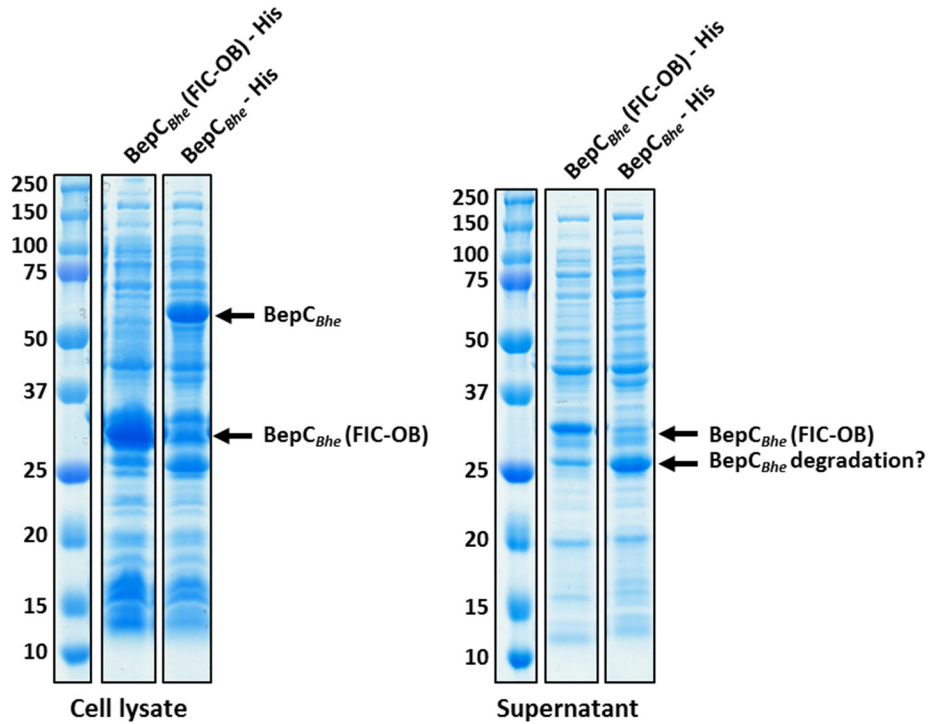


**Figure 4.S1. BepC<sub>Bhe</sub> full-length is mostly insoluble in comparison with BepC<sub>Bhe</sub> (FIC-OB).**

His-tagged BepC<sub>Bhe</sub> full length and BepC<sub>Bhe</sub> (FIC-OB) were overexpressed in *E.coli*. After cell lysis, the samples were centrifuged and only the supernatant was kept. Left panel: bacterial lysate before centrifugation. Right panel: supernatant after centrifugation.

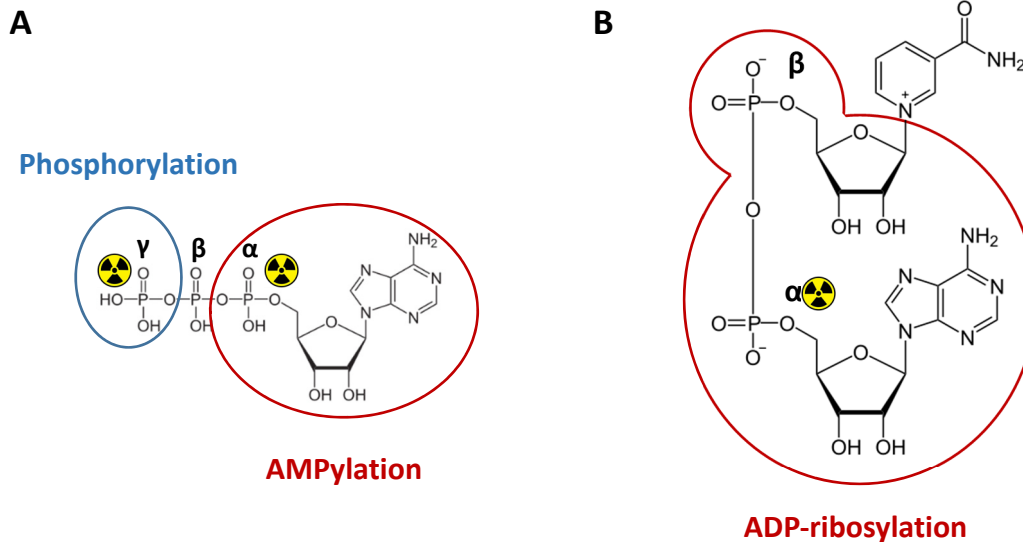


**Figure 4.S2. Schematic representation of posttranslational modifications**

**A)** Structural diagram of ATP illustrating AMPylation with the transfer of the AMP moiety carrying the radioactive  $\alpha$  phosphate (in red) or phosphorylation by transfer of the  $\gamma$  phosphate (in blue). **B)** Structural diagram of NAD<sup>+</sup> illustrating ADP-riboseylation with the transfer of the ADP-ribose carrying the radioactive  $\alpha$  phosphate.

- Additional results -

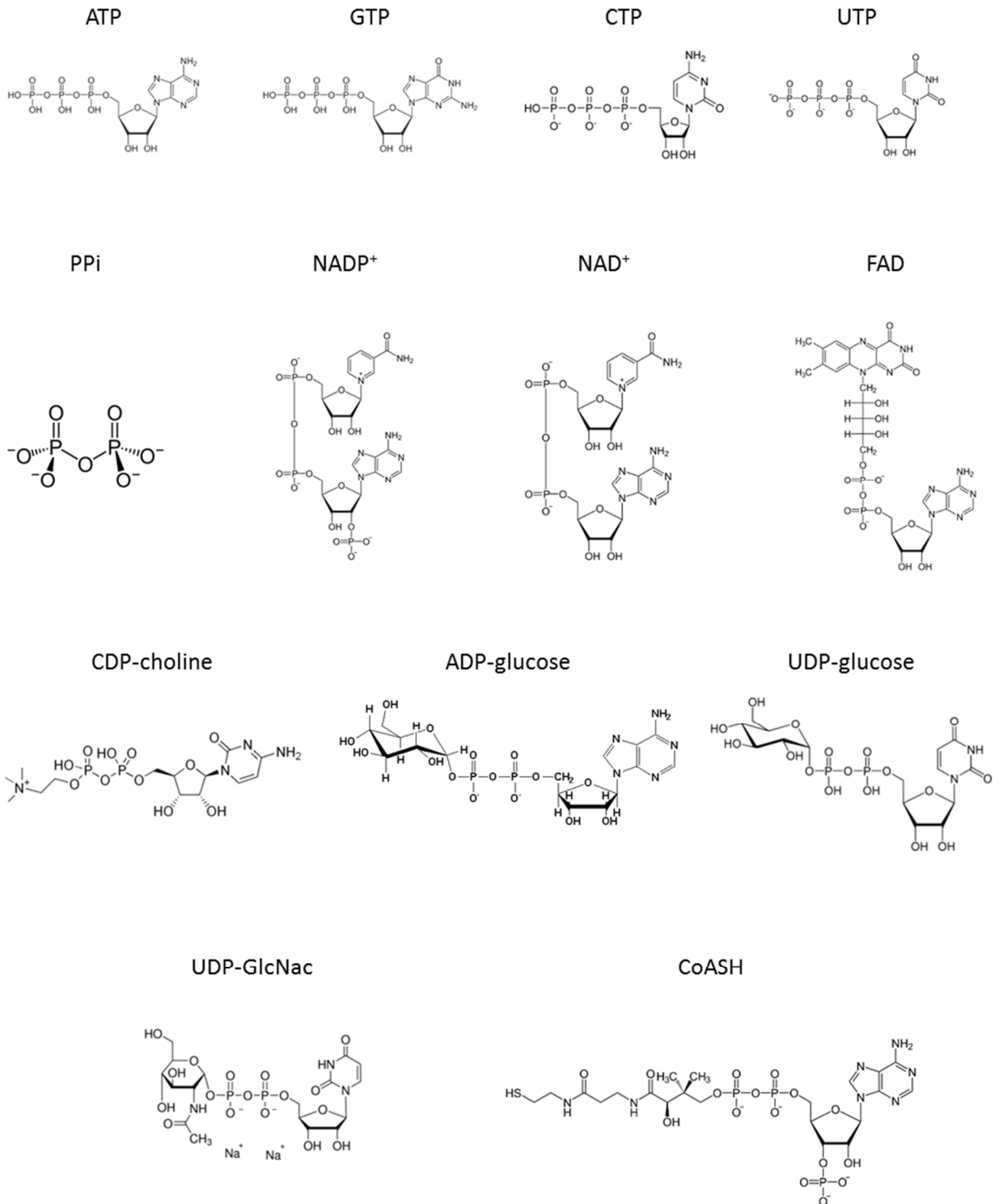
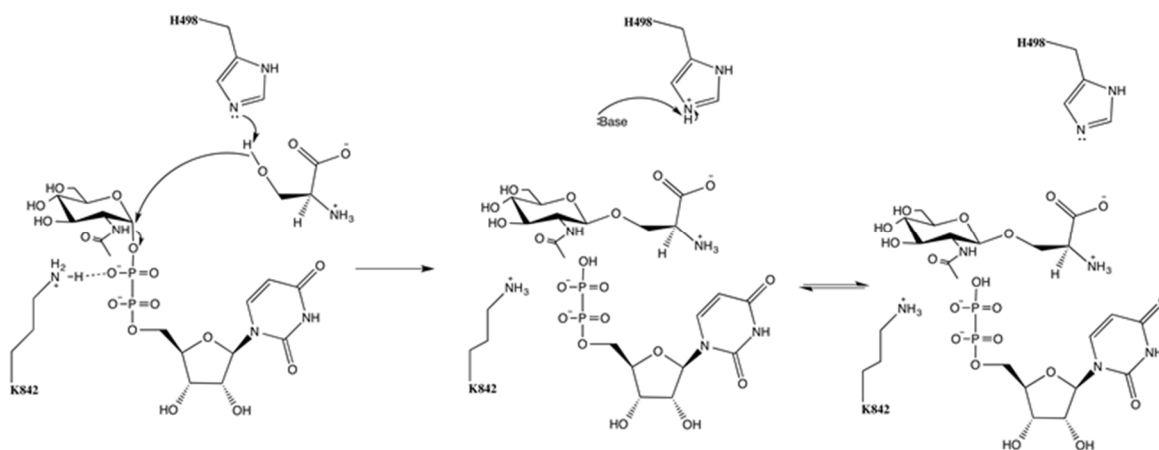


Figure 4.S3. Molecular structure of the nucleotides derivatives tested by thermal shift assay with BepC<sub>Bhe</sub> (FIC-OB).

- Additional results -



**Figure 4.S4. Proposed molecular mechanism of O-GlcNAcylation by O-GlcNAc transferase [18].**

Figure from: <https://commons.wikimedia.org/w/index.php?curid=31371846>

(Author: Messien17)

## 4.4 References

1. Palanivelu, D.V., et al., *Fic domain-catalyzed adenylylation: insight provided by the structural analysis of the type IV secretion system effector BepA*. Protein Sci, 2011. **20**(3): p. 492-9.
2. Engel, P., et al., *Adenylylation control by intra- or intermolecular active-site obstruction in Fic proteins*. Nature, 2012. **482**(7383): p. 107-10.
3. Pielas, K., et al., *An experimental strategy for the identification of AMPylation targets from complex protein samples*. Proteomics, 2014. **14**(9): p. 1048-52.
4. Ben-Bassat, A., et al., *Processing of the initiation methionine from proteins: properties of the Escherichia coli methionine aminopeptidase and its gene structure*. J Bacteriol, 1987. **169**(2): p. 751-7.
5. Worby, C.A., et al., *The fic domain: regulation of cell signaling by adenylylation*. Mol Cell, 2009. **34**(1): p. 93-103.
6. Harms, A., et al., *Evolutionary Dynamics of Pathoadaptation Revealed by Three Independent Acquisitions of the VirB/D4 Type IV Secretion System in Bartonella*. Genome Biol Evol, 2017. **9**(3): p. 761-776.
7. Yarbrough, M.L., et al., *AMPylation of Rho GTPases by Vibrio VopS disrupts effector binding and downstream signaling*. Science, 2009. **323**(5911): p. 269-72.
8. Lang, A.E., et al., *Photobacterium luminescens toxins ADP-ribosylate actin and RhoA to force actin clustering*. Science, 2010. **327**(5969): p. 1139-42.
9. Mukherjee, S., et al., *Modulation of Rab GTPase function by a protein phosphocholine transferase*. Nature, 2011. **477**(7362): p. 103-6.
10. Feng, F., et al., *A Xanthomonas uridine 5'-monophosphate transferase inhibits plant immune kinases*. Nature, 2012. **485**(7396): p. 114-8.
11. Harms, A., F.V. Stanger, and C. Dehio, *Biological Diversity and Molecular Plasticity of FIC Domain Proteins*. Annu Rev Microbiol, 2016. **70**: p. 341-60.
12. Busch, C., et al., *Characterization of the catalytic domain of Clostridium novyi alpha-toxin*. Infect Immun, 2000. **68**(11): p. 6378-83.
13. Goepfert, A., *Fic-mediated adenylylation: catalysis and regulation*. PhD thesis, 2012.
14. Birkenfeld, J., et al., *Cellular functions of GEF-H1, a microtubule-regulated Rho-GEF: is altered GEF-H1 activity a crucial determinant of disease pathogenesis?* Trends Cell Biol, 2008. **18**(5): p. 210-9.
15. Arcus, V., *OB-fold domains: a snapshot of the evolution of sequence, structure and function*. Curr Opin Struct Biol, 2002. **12**(6): p. 794-801.
16. Flynn, R.L. and L. Zou, *Oligonucleotide/oligosaccharide-binding fold proteins: a growing family of genome guardians*. Crit Rev Biochem Mol Biol, 2010. **45**(4): p. 266-75.
17. Stekhoven, D.J., et al., *Proteome-wide identification of predominant subcellular protein localizations in a bacterial model organism*. J Proteomics, 2014. **99**: p. 123-37.
18. Lazarus, M.B., et al., *Structure of human O-GlcNAc transferase and its complex with a peptide substrate*. Nature, 2011. **469**(7331): p. 564-7.

# General conclusion and outlook

## 5.1 General conclusion

Bacteria of the genus *Bartonella* disseminate in the environment via arthropods to infect a wide variety of mammals. Several species are associated with human diseases such as Oroya fever for *B. bacilliformis*, trench fever for *B. quintana*, or cat-scratch disease for *B. henselae*. Although the infection can be life-threatening for the infected host, it usually remains asymptomatic and develops in long-lasting bacteremia. The stealth infection strategy that most *Bartonella* species adopted goes hand in hand with the evolution of a panel of virulence factors in order to compete with the host immune system and to persist in an intracellular niche [1]. During infection, the bacteria translocate a cocktail of effectors into the cell via a VirB/D4 T4SS and thereby subvert cellular processes to their advantage. Among these effectors, BepC is one of the most conserved in the *Bartonella* species of the lineage 4, indicating an important role in pathogenesis. This effector was previously shown to interfere with cell migration [2] and to be involved in the engulfment of large bacterial aggregates, suggesting its contribution to cell invasion [3, 4].

In this study, we could demonstrate that BepC modulates the Rho GTPase signaling cascade, a well-known target of bacterial pathogens and their hosts (see chapter 1.2). In human cells, BepC localizes to cell contacts and induces bacterial aggregation as well as cytoskeleton rearrangements. The stimulation of actin stress fiber formation is conserved among BepC orthologs of different *Bartonella* species, such as the human pathogens *Bhe* and *Bqu*, suggesting that a significant contribution to the bacterial life cycle stands behind this phenotype.

During infection, BepC interacts with GEF-H1 and MRCK $\alpha$ , two proteins involved in actin stress fiber formation via the RhoA and Cdc42 pathways, respectively [5, 6]. We could show that the ability of BepC to induce actin rearrangement highly correlates with its ability to bind GEF-H1 and MRCK $\alpha$ . Accordingly, infected cells display an increase of GTP-bound RhoA and phosphorylated myosin light chain. Additionally, the actin phenotype mediated by BepC is visibly reduced after treatment with inhibitors of RhoA and its downstream target ROCK. Thereby our data indicate that BepC triggers actin rearrangement by activating the RhoA pathway via its interaction with GEF-H1, although MRCK $\alpha$  could act synergistically. BepC is the only known T4SS effector and the sole Fic protein that is described to modulate a Rho GTPase signaling cascade by directly interacting with GEF-H1. Apart from BepC, only the T3SS effector VopO from *Vibrio parahaemolyticus* showed an interaction with this host factor [7].

The interaction with GEF-H1 and MRCK $\alpha$ , the actin rearrangements, and the localization of BepC to cell contacts are completely abolished in a truncation mutant, in which the N-terminal FIC domain is missing. This indicates a central role for the FIC domain of BepC in these



processes. As the conserved FIC motif is not required to induce actin rearrangements, BepC is probably not activating the RhoA pathway by posttranslational modifications but rather via protein-protein interactions.

The FIC domain of BepC displays only low auto-AMPylation and auto-phosphorylation activities, which suggest that it might not be enzymatically active due to its non-canonical FIC motif. Despite such minor activity, structural analysis and binding assays demonstrate that nucleotide derivatives bind to the FIC domain of BepC and increase its thermal stability. The interesting finding that a FIC domain exerts a biological function unrelated to its catalytic activity is unique and only remotely reminiscent of the Fic protein AvrB, which lacks all residues needed for an enzymatic activity [8]. Furthermore, it opens new perspectives for the function of Beps carrying a non-canonical FIC motif and lacking an enzymatic activity.

As GEF-H1 and MRCK $\alpha$  are involved in a multitude of cellular processes, the function of BepC might vary according to the different cell types infected by *Bartonella* through the different stages of the infection cycle. Based on the activation of the Rho GTPases signaling pathway, we can speculate that BepC might participate in pathogenesis by preventing phagocytosis and immune cell migration, or help overcome the endothelial barrier in order to colonize the blood and establish bacteremia.

Finally, the identification of the host proteins and the signaling pathway targeted by BepC gives a better insight on how *Bartonella* manipulates the host cell via the injection of bacterial effectors. Concretely, the results obtained in this study provide a sound basis for future in-depth investigations on the biological function of BepC during pathogenesis in its interaction with host factors as well as with *Bartonella* effectors proteins.

## 5.2 Outlook

### 5.2.1 Enzymatic activity of the FIC domain of BepC.

As the FIC motif of BepC is highly conserved and binds nucleotide derivatives, it is reasonable to think that it displays an enzymatic activity and modifies a host protein. However, the substrate, the type of reaction, and the target remain unidentified despite our efforts. Knowing that BepC interacts with GEF-H1 and MRCK $\alpha$  during infection, it would be interesting to test whether they are posttranslationally modified. To do so, the two proteins could be pulled-down from cells infected with *Bhe*  $\Delta$ *bepA-G* expressing BepC and analyzed by mass spectrometry in order to identify a modified peptide. Additionally, we could perform AMPylation and phosphorylation assays with radioactive ATP and purified proteins.

Nevertheless, it is also possible that BepC modifies another host protein. As an enzymatic reaction generally implies a short interaction with the target, it is likely that we would not be

able to co-immunoprecipitate the host protein together with BepC. To avoid this issue, we could use BepC with multiple mutations in the FIC motif (BepC<sup>\*\*\*\*</sup>), which is probably not catalytically functional, to stabilize a complex and be able to pull-down further targets of BepC.

Additionally, the association of a phenotype with the FIC motif would provide a significant indication of a potential host target modified by BepC. Therefore, we could determine whether BepC with mutations in the FIC motif are also able to participate in invasome formation. Further, as *Bartonella* infects dendritic cells *in vitro*, we could test whether BepC is able to modulate cytokines production by those cells in a FIC-motif dependent manner.

Although our results show that BepC binds to the antitoxin of *Bhe*, this interaction does not prevent the growth inhibition associated with the overexpression of the effector in *Bartonella*. We conclude from our experiments that the growth defect is distinct from the activity of the effector on host cell as it is solely BID-dependent. Whether the antitoxin inhibits a putative activity or acts as a chaperone remains to be elucidated.

Finally, purified BepC from other *Bartonella* species could be tested by AMPylation and phosphorylation assay in order to detect a target protein in cell lysates from different cell types.

## 5.2.2 Antagonism between BepC and BepE.

Although the identity of BepE host target remains unknown, the effector was proposed to modulate the RhoA pathway during infection [2]. Additionally, BepE interferes with cell fragmentation mediated by BepC in HUVECs, suggesting an antagonist effect. Having identified BepC host targets sheds new light on the function of BepE during infection.

As BepC activates the RhoA pathway by interacting with GEF-H1, it is unlikely that BepE is also stimulating this signaling cascade. By contrast, it is conceivable that BepE counteracts the effect of BepC by disrupting the RhoA signaling. Interestingly, our data indicate that actin stress fiber formation mediated by BepC can be reversed by inhibiting the RhoA pathway with Rho and ROCK inhibitors. Thus, it would be reasonable to think that BepE could act in a similar manner to down-regulate the pathway by targeting one of its components. To determine whether BepE would prevent actin stress fiber formation, we could co-infect HeLa cells with two strains of *Bhe ΔbepA-G*, one expressing BepC and the other one BepE.

The strategies developed by pathogenic bacteria to inactivate Rho GTPases consist of GDI mimicry, GAP mimicry, GTPase release from the plasma membrane, GEF inhibition, and posttranslational modification of the GTPase (see chapter 1.2.2). As the abolition of the cell fragmentation phenotype is mediated by the BID domains of BepE, it is likely that the effector would interfere with the GTPase signaling rather by protein-protein interaction than via an

enzymatic activity. As it was performed for BepC, pulling down BepE after cell infection could lead to the identification of a potential host target, possibly associated with the RhoA pathway.

Another possibility for BepE to reduce the cell fragmentation phenotype would be to interact directly with BepC in order to inhibit its function. Interestingly, the localization of BepE and BepC to cell junctions suggests that they might be in close proximity during infection [2]. To test this hypothesis, we could determine if BepC and BepE co-localize at cell-to-cell contacts and if they interact together by co-immunoprecipitation.

### **5.2.3 Cooperation between BepC and BepF.**

In contrast to BepE, which has an antagonist effect on the cell fragmentation mediated by BepC, BepF has a synergetic effect that results in the engulfment of large bacterial aggregates (invasome). Although the host target of BepF is still unknown, the effector seems to regulate the Cdc42 and the Rac1 signaling pathway [4]. Thus, it is conceivable to think that the two effectors cooperate to tightly modulate the RhoA, Rac1 and Cdc42 pathways, which leads to invasome formation. However, our data suggest that inducing actin rearrangements or bacterial aggregation is not sufficient to trigger invasome formation. To confirm that BepC participates in invasome formation via the activation of the RhoA pathway, it would be interesting to determine whether RhoA and ROCK inhibitors would prevent the process of bacterial clustering and/or engulfment.

Furthermore, we could check if invasome formation correlates with the ability of BepC to interact GEF-H1 and MRCK $\alpha$ . To do so, the different mutants and the truncated version of BepC could be tested for invasome formation. These results would also determine if the FIC motif, the Flap region, or the BID domain of BepC are necessary for invasome formation together with BepF.

Both BepF and BepC localize to the invasome during infection with *Bhe* wild-type [4], which could indicate a potential interaction during infection. Therefore, it would be relevant to pull-down BepF after cell infection to check whether it binds to BepC. Additionally, it could reveal a potential host target that is involved in the Rac1 and/or Cdc42 pathways.

### **5.2.4 Participation of MRCK $\alpha$ in the actin phenotype mediated by BepC.**

Although BepC interacts with both GEF-H1 and MRCK $\alpha$ , our results do not allow us to conclude whether MRCK $\alpha$  participates in the actin rearrangements. However, we could exploit the fact that ROCK and MRCK $\alpha$  both phosphorylate myosin light chain (MLC2) but not on the same residue. While ROCK di-phosphorylates MLC2 (ppMLC) on Thr18 and Ser19, MRCK $\alpha$  only mono-phosphorylates MLC2 on Ser19 (pMLC) [8]. Thus, the difference of phosphorylation site could be used to determine if MRCK $\alpha$  contributes to the increase of phosphorylated myosin

light chain during cell infection with *Bhe ΔbepA-G* expressing BepC. If pMLC increases in the same proportion as ppMLC in comparison with a negative control (*Bhe ΔbepA-G pEmpty*), this would suggest that ROCK is mainly responsible for the MLC2 phosphorylation. By contrast, if pMLC increases while ppMLC stays at the same level, the phosphorylation of MLC2 can be attributed to MRCK $\alpha$ . Another method to determine the participation of MRCK $\alpha$  in actin rearrangement would be to use a selective inhibitor called chelerythrine [8]. Therefore, we could treat HeLa cells or HUVECs with this molecule to check whether BepC is still able to induce actin rearrangements or if the activity of MRCK $\alpha$  is necessary.

### **5.2.5 Characterization of the interaction between BepC, GEF-H1, and MRCK $\alpha$ .**

Until now, the interface of the FIC domain of BepC that is necessary for binding GEF-H1 and MRCK $\alpha$ , and therefore for the actin phenotype, remains unidentified. Our finding that BepC from different *Bartonella* species is able to trigger actin rearrangements indicates that the interaction is probably mediated via a highly conserved region. As neither the first helix nor a conserved Flap or FIC motif is necessary for interaction and most of the remaining residues conserved in the FIC domain of BepC are also found in BepA, it considerably reduces the possibilities. One candidate is a region composed of eleven highly conserved residues (MFMEKLGQAAG) that is located at the end of the  $\alpha$ -helix carrying the FIC motif (Fig. 5.1). Although several residues of this region are also conserved in BepA, some of them are specific to BepC and might be involved in target recognition. Therefore, it would be relevant to substitute this region with the region of BepA or introduce mutations to test whether the hybrid protein could still bind GEF-H1 and MRCK $\alpha$  and trigger actin rearrangements.

Reciprocally, it is unknown which domain(s) of GEF-H1 and MRCK $\alpha$  participate in the interaction with BepC. To answer this question, truncated versions of GEF-H1 and MRCK $\alpha$  could be ectopically expressed in eukaryotic cells that would be subsequently infected with *Bhe ΔbepA-G* expressing BepC. Then, a pull-down experiment would indicate which region of the host proteins are required for interaction. Another option would be to purify truncated GEF-H1 and MRCK $\alpha$  for pull-downs experiments with BepC.

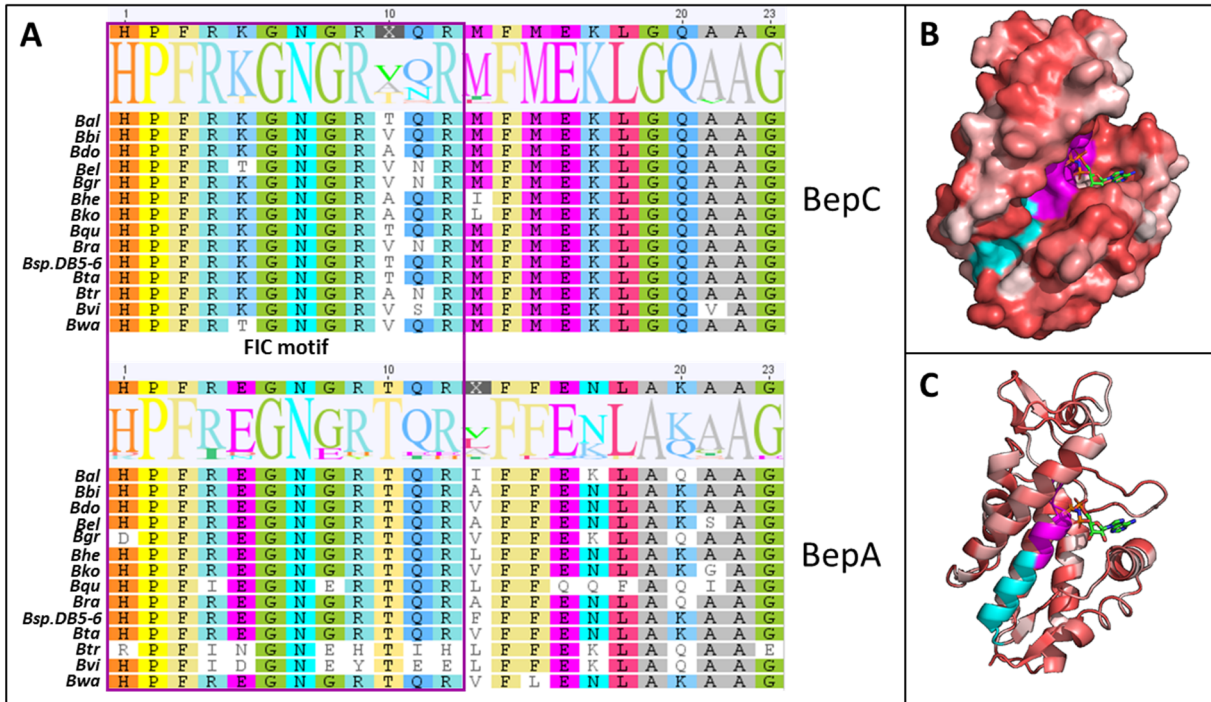


**Fig 5.1. BepC displays a highly conserved region following the FIC motif.**

**A.** Alignment of the  $\alpha$ -helices carrying the FIC motif of BepC and BepA from *Bartonella* species of the lineage 4. **B.** Surface representation of the crystal structure of BepC<sub>Btr</sub> with AMP-PNP in the active site. The red color gradient represents pairwise identity based on 14 alignments of BepC from different *Bartonella* species. The most conserved residues are represented in red and less conserved residues in white. The FIC motif is represented in magenta and the following conserved region in cyan. **C.** Cartoon representation of (B).

### 5.2.6 Host specificity

BepC of *Bhe*, *Bqu*, *Btr*, *Bta* all trigger actin stress fiber formation in HeLa cells but at a different level of intensity. Furthermore, BepC of *Bgr* did not show any actin phenotype. A translocation defect, host specificity, or a loss of function could explain these differences. To exclude a translocation defect, a plasmid encoding BepC from the different species could be transfected into eukaryotic cells in order to bypass the secretion by the T4SS. Thus, the ectopic expression would answer whether BepC from these species can trigger actin rearrangements with a similar intensity. Additionally, the host specificity of BepC could be addressed by infecting rodent cells instead of humans cells as *Bgr*, *Bta* and *Btr* have the mouse, the vole, and the rat for reservoir host, respectively.

### 5.2.7 Investigation of the role of BepC in pathogenesis.

Although we present here the host targets of BepC and describe its phenotype on endothelial and epithelial cell infection, the overall function of the effector during pathogenesis remains to be elucidated. As BepC might disrupt cellular junctions via the activation of the RhoA pathway, it could also affect the integrity of the endothelial barrier and facilitate the colonization of the

blood by *Bartonella*. In order to investigate this possibility, the permeability can be evaluated by an *in vitro* model in which HUVECs are seeded on a cell culture insert with a porous membrane. After growing to confluence and occluding the pores, the endothelial cell monolayer can be infected with *Bhe ΔbepC* and compared to *Bhe* wild-type. Then, the permeability can be tested by adding fluorescent dextran on top of the cells, which will diffuse through the porous membrane if the barrier integrity has been compromised. Additionally, this assay can be used to test whether *Bartonella* can cross the endothelial cell layer via transcytosis or by disturbing cell junctions.

During infection of HeLa cells and EA.hy926, BepC leads to the aggregation of bacteria, which seems to correspond to the first phase of invasome formation. Furthermore, BepC and BepF inhibit the endocytosis of inert microspheres [4]. If the bacterial clusters mediated by BepC remain outside the cell, this could signify that the effector alone is sufficient to block the internalization of *Bartonella* containing vacuoles. Whether the bacterial clusters are engulfed or sitting on top of the cell can be addressed by confocal microscopy. Subsequently, the inhibition of endocytosis could be investigated by measuring the uptake of fluorescent microspheres by infected cells expressing BepC.

A potential consequence of the activation of the RhoA pathway by BepC is an activation of NF-κB via NOD1 and/or NOD2 signaling, which could eventually lead to an immune response. This hypothesis can be tested by infecting HUVECs with *Bhe ΔbepA-G* expressing BepC and measure IL-8 secretion in the culture supernatant or the expression of the adhesion molecule ICAM-1 at the cell surface [9]. If BepC induces a pro-inflammatory response, it would be interesting to test whether the presence of BepE could reduce the phenotype and thereby preventing the stimulation of an immune response by the infected host.

## 5.3 References

1. Harms, A. and C. Dehio, *Intruders below the radar: molecular pathogenesis of Bartonella spp.* Clin Microbiol Rev, 2012. **25**(1): p. 42-78.
2. Okujava, R., et al., *A translocated effector required for Bartonella dissemination from derma to blood safeguards migratory host cells from damage by co-translocated effectors.* PLoS Pathog, 2014. **10**(6): p. e1004187.
3. Truttmann, M.C., P. Guye, and C. Dehio, *BID-F1 and BID-F2 domains of Bartonella henselae effector protein BepF trigger together with BepC the formation of invasome structures.* PloS one, 2011. **6**(10): p. e25106.
4. Truttmann, M.C., T.A. Rhomberg, and C. Dehio, *Combined action of the type IV secretion effector proteins BepC and BepF promotes invasome formation of Bartonella henselae on endothelial and epithelial cells.* Cellular microbiology, 2011. **13**(2): p. 284-99.
5. Leung, T., et al., *Myotonic dystrophy kinase-related Cdc42-binding kinase acts as a Cdc42 effector in promoting cytoskeletal reorganization.* Mol Cell Biol, 1998. **18**(1): p. 130-40.
6. Birkenfeld, J., et al., *Cellular functions of GEF-H1, a microtubule-regulated Rho-GEF: is altered GEF-H1 activity a crucial determinant of disease pathogenesis?* Trends Cell Biol, 2008. **18**(5): p. 210-9.
7. Hiyoshi, H., et al., *Interaction between the type III effector VopO and GEF-H1 activates the RhoA-ROCK pathway.* PLoS Pathog, 2015. **11**(3): p. e1004694.
8. Tan, I., et al., *Chelerythrine perturbs lamellar actomyosin filaments by selective inhibition of myotonic dystrophy kinase-related Cdc42-binding kinase.* FEBS Lett, 2011. **585**(9): p. 1260-8.
9. Schmid, M.C., et al., *The VirB type IV secretion system of Bartonella henselae mediates invasion, proinflammatory activation and antiapoptotic protection of endothelial cells.* Mol Microbiol, 2004. **52**(1): p. 81-92.



# Materials and methods

## DNA manipulations

Plasmids and primers used in this study are listed in at the end of the chapter.

## Bacterial strains and growth conditions

The bacterial strains used in this study are listed in at the end of the chapter.

*Bartonella* species were grown on Columbia blood agar (CBA, Oxoid, CM0331) plates containing 5% defibrinated sheep blood (CBA plates) at 35°C and 5% CO<sub>2</sub> for 3 days then expended for 2 days on new plates. When indicated, media were supplemented with 30 µg/ml kanamycin, 100 µg/ml streptomycin, and/or isopropyl-β-D-thiogalactoside (IPTG, Biochemica, A1008).

*E. coli* strains were cultivated in Luria-Bertani liquid medium (LB) or on Luria-Bertani agar on plates (LA) at 37°C overnight. Media were supplemented with 50 µg/ml kanamycin, and/or 1 mM diaminopimelic acid (DAP, Sigma, D1377).

LB - Medium (1 liter)	Amount for 1 liter
Tryptone (Difco, 211701)	10 g
Yeast extract (Oxoid, L0021)	5 g
NaCl (Merck, 106404)	10 g

LB - agar (LA plate) (1 liter)	Amount for 1 liter
Tryptone (Difco, 211701)	10 g
Yeast extract (Oxoid, L0021)	5 g
NaCl (Merck, 106404)	10 g
Agar (Difco, 214530)	13 g

## Conjugation of *Bartonella*-expression plasmids into *Bartonella*

*Bartonella henselae* Δ*bepA-G* (SIM B1-01) was grown on CBA plates in presence of 100 µg/ml streptomycin at 35°C and 5% CO<sub>2</sub> for 3 days then expanded on new plates for 2 days. The day before conjugation, 5 ml of LB containing 1 mM DAP (Sigma, D1377) and 50 µg/ml kanamycin were inoculated with the conjugation strain (JKE170) containing the plasmid of interest. After overnight incubation at 37°C, a subculture was prepared by inoculating 5 ml of LB containing 1 mM DAP (Sigma, D1377) and 50 µg/ml kanamycin with 200 µl of overnight culture before being incubated for 2 hours at 37°C.

In order to remove antibiotics, 500 µl of the subculture was centrifuged for 4 min at 4'500 rpm and the bacterial pellet was resuspended in 500 µl of M199 (Gibco, 22340-020) supplemented with 10 % of heat-inactivated fetal calf serum (ΔFCS), the washing step was repeated once. The same process was applied to *Bartonella*, bacteria were harvested in 1 ml of M199 10% ΔFCS and centrifuged for 4 min at 4'500 rpm. The bacterial pellet was resuspended in 500 µl

of M199 10% ΔFCS before being centrifuged again and resuspended in 100 μl of M199 10% ΔFCS.

20 μl of *E. coli* was mixed with 100 μl of *Bartonella* and incubated for 5 hours at 35°C, 5% CO<sub>2</sub> on a nitrocellulose filter deposited on a CBA plate supplemented with 1 mM of DAP. The filter was transferred in an Eppendorf tube containing 1 ml of M199 10% ΔFCS and the bacteria were resuspended by gently shaking. 5 μl and 50 μl were plated on a CBA plate supplemented with 30 μg/ml kanamycin and 100 μg/ml streptomycin.

### Cell culture

Human umbilical vein endothelial cells (HUVEC) were isolated as described before (Dehio *et al.*, 1997) and cultured at 37°C and 5 % CO<sub>2</sub> in Endothelial Cell Growth Medium (ECGM) (Promocell, C-22010) supplemented with Endothelial Cell Growth Medium SupplementMix (Promocell, C-39215).

HeLa cells and EA.hy926 cells were cultured at 37°C and 5 % CO<sub>2</sub> in DMEM (Sigma, D6429) supplemented with 10 % of heat-inactivated fetal calf serum (FCS).

### Cell infection for microscopy

HUVECs were plated at a density of 3'000 cells/well while on a 96-well plate (Corning, #3904) pre-coated with 0.2 % of gelatin using supplemented ECGM.

HeLa cells and EA.hy926 cells were plated at a density of 2'000 cells/well on a 96-well plate (Corning, #3904) using DMEM supplemented with 10 % of heat-inactivated FCS.

The next day, cells were infected with *Bartonella* at the indicated MOI in M199 (Gibco, 22340-020) supplemented with 10 % of heat-inactivated FCS in presence of 10 μM of IPTG. After incubation at 35°C and 5 % CO<sub>2</sub>, cells were fixed with 50 μl of 3.7 % of paraformaldehyde for 10 minutes and washed 3 times with 100 μl of PBS.

PBS pH 7.4	Amount for 1 liter
NaCl (Merk, 106404)	8 g
KCl (Merk, 104936)	0.2 g
Na <sub>2</sub> HPO <sub>4</sub> 2 H <sub>2</sub> O (Merk, 106580)	1.44 g
KH <sub>2</sub> PO <sub>4</sub> (Merk, 104873)	0.24 g

### Immunostaining

Fixed cells were permeabilized for 10 minutes with 50 μl of PBS 0.2 % BSA (Sigma, A9647) and 0.5 % Triton X-100 (Sigma, T9284). After being washed 3 times with 100 μl of PBS with 0.2 % BSA, cells were incubated overnight at 4°C in presence of the primary antibody (see

table below) diluted in 50 µl of PBS with 0.2 % BSA. After 2 more washes with 100 µl of PBS with 0.2 % BSA, cells were incubated for 2 hours in the dark in presence of the secondary antibody, DAPI (Sigma, D9542, 1 µg/ml) and DY-547P1 phalloidin (Dyomics GmbH, final concentration 1/250) diluted in 50 µl of PBS with 0.2 % BSA. Cells were finally washed 3 times with 100 µl of PBS and imaged with an MD ImagXpress Micro automated microscope from Molecular devices. Fluorescence was detected at 10x or 20x magnification, and the images were processed in MetaXpress.

Antigen	Producer (ref)	Final dilution
Rabbit anti- <i>Bartonella</i> (primary)	In-house (serum n° 2035)	1/1000
Mouse anti-Flag (primary)	Sigma, F1804	1/1000
Mouse anti-β-tubulin (primary)	Sigma, T8328	1/100-250
Mouse anti-pMLC (primary)	Cell signaling, # 3675	1/100
Mouse anti-Vimentin (primary)	Abcam ab8978	1/100-250
Mouse anti-Talin (primary)	Sigma, T3287	1/250
Rabbit anti-pPaxillin (primary)	Santa Cruz, sc-14036	1/50
Rabbit anti-VE cadherin (primary)	Bender Medsystems, BMS158	1/100
Goat anti-mouse AlexaFluor 488 (secondary)	Jackson Immuno, 115-545-146	1/250
Goat anti-rabbit Cy5 (secondary)	Jackson Immuno, 111-175-045	1/250

### Pull-down assay

HeLa cells or HUVECs were plated in round plates (Falcon, REF 353003) at a density of 363'120 or 544'000 cells per plate, respectively. The cells were then incubated overnight at 37°C and 5% CO<sub>2</sub> in DMEM complemented with 10 % heat-inactivated FCS. In the morning, cells have been infected with the indicated strain of *Bartonella* at an MOI of 200 for 24 hours at 35°C and 5% CO<sub>2</sub> in M199 (Gibco, 22340-020) supplemented with 10 % of heat-inactivated FCS in presence of 10 µM of IPTG.

After infection, cells were washed 3 times with ice-cold PBS and lysed with lysis buffer containing 50 mM Hepes (pH 7.5), 150 mM NaCl, protease inhibitor (Roche, 11836170001), phosphatase inhibitor (Roche, 04906837001), 1 % Nonidet P40 substitute (Sigma, 74385). Cell lysates were collected with a cell scraper and incubated 30 minutes on ice. After centrifugation at 20'000 x g for 30 min at 4°C, the protein concentration in the supernatant was measured with Precision Red Advanced Protein Assay Reagent (Cytoskeleton, Cat. # ADV02-A). Protein concentration was adjusted between the samples with lysis buffer.

The lysates were incubated in presence of 20 µl of protein G agarose beads (Roche, 11243233001) for 3 hours at 4°C on a rotor to reduce unspecific binding. After removing the beads by centrifugation for 30 seconds at 12'000 x g, 2 µg of mouse anti-Flag antibody (Sigma F1804) was added to the supernatant. After 3 hours of incubation at 4°C on a rotor, 20 µl of

protein G agarose was added to the lysates and incubated overnight at 4°C on a rotor. The next morning, agarose beads were collected by centrifugation for 30 seconds at 12'000 x g before being washed 2 times with lysis buffer and 2 more times with lysis buffer without NP-40. Proteins were eluted from the beads by incubation 10 minutes at 95°C in SDS sample buffer. Elution fractions and cell lysates before pull-down were analyzed by western blot.

The same protocol was applied for samples analyzed by mass spectrometry although one cell culture flask of 150 cm<sup>2</sup> was used per infection.

SDS sample buffer (1X)	Concentration
SDS	20 mg/ml
Tris HCl pH 6.8	40 mM
Bromophenol blue	1 mg/ml
Glycerol	5 %

### Protein expression and purification

100 ml of LB supplemented with 50 µg/ml of kanamycin was inoculated with SIME3-58 (*E. coli* BL21 (DE3)) containing pSIM072 encoding BepC<sub>Bhe</sub> (FIC-OB). After overnight incubation at 37°C, 50 ml of overnight culture were used to inoculate 2 liters of Terrific Broth supplemented with 50 µg/ml of kanamycin (see composition below). The culture was incubated 4 hours at 25°C to reach an OD<sub>600</sub> of approximately 0.5. Protein expression was induced with 100 µM of IPTG for 16 hours at 25°C. Bacteria were pelleted at 4°C and resuspended in 40 ml of cold lysis buffer (50 mM Tris-HCl pH 7.5, 100 mM NaCl, 2,5 mM beta-mercaptoethanol, DNaseI (AppliChem, A3778), protease inhibitor (Roche, 11836170001).

Bacteria were disrupted using French press and cell debris were pelleted by ultracentrifugation. Imidazole was then added to the supernatant to a final concentration of 20 mM. After loading on a His-Trap column (GE Healthcare), proteins binding non-specifically to the column were removed with washing buffer (50 mM Tris-HCl pH 7.5, 100 mM NaCl, 2,5mM beta-mercapto-ethanol, 150 mM imidazole). Remaining proteins were eluted with the elution buffer (50 mM Tris-HCl pH 7.5, 100 mM NaCl, 2,5mM beta-mercapto-ethanol, 500 mM imidazole) and injected on gel filtration column (HiLoad 16/60 Superdex 75 prep grade, GE Healthcare) pre-equilibrated with buffer (50 mM Tris-HCl pH 7.5, 100 mM NaCl, 2,5mM beta mercapto-ethanol). Pure protein was concentrated by filtration (Amicon Ultra-15 Centrifugal Filter Units – 10,000 NMWL).

<b>Terrific Broth</b>	<b>Amount for 1 liter</b>
Bacto-Tryptone	12 g
Bacto-Yeast Extract	24 g
Glycerol 100 %	5 ml
KH <sub>2</sub> PO <sub>4</sub>	2.31 g
K <sub>2</sub> HPO <sub>4</sub>	12.54 g

### **Protein expression and partial purification**

40 ml of LB supplemented with 50 µg/ml of kanamycin and 1% of glucose was inoculated with *E. coli* BL21 (DE3) containing the plasmid of interest. After overnight incubation at 37°C, 25 ml of overnight culture was centrifuged and the pellet was resuspended in 10 ml in Terrific Broth. Then, the bacterial suspension was used to inoculate 1 liter of Terrific Broth supplemented with 50 µg/ml of kanamycin. The culture was incubated 4 hours at 25°C to reach an OD<sub>600</sub> of approximately 0.5. Protein expression was induced with 100 µM of IPTG for 18 hours at 25°C. Bacteria were pelleted at 4°C and resuspended in 10 ml of cold lysis buffer (50 mM Tris-HCl pH 7.5, 100 mM NaCl, 2,5 mM beta-mercaptoethanol, DNaseI (AppliChem, A3778), protease inhibitor (Roche, 11836170001).

Bacteria were disrupted using French press and cell debris were pelleted by ultracentrifugation. To bind the His-tagged protein, 2 ml of nickel beads (Protino Ni-NTA Agarose, Macherey-Nagel) was added to the supernatant and incubated 1 hour at 4°C on a rotor. Subsequently, the supernatant with beads was loaded on a Poly-Prep® Chromatography Columns (Biorad). The beads were washed three times with 10 ml of cold washing buffer (50 mM Tris-HCl pH 7.5, 100 mM NaCl, 2,5mM beta-mercaptoethanol, 20 mM imidazole) to remove proteins with unspecific binding. Then, His-tagged proteins were eluted with 5 x 500 µl of elution buffer (50 mM Tris-HCl pH 7.5, 100 mM NaCl, 2,5mM beta-mercaptoethanol, 500 mM imidazole). Finally, the most concentrated fractions were pooled together and desalted by dialysis two times in 2 liters of cold buffer (50 mM Tris-HCl pH 7.5, 100 mM NaCl, 2,5mM beta mercapto-ethanol).

### **Sample preparation for mass spectrometry**

Proteins were precipitated with trichloroacetic acid and incubated 10 min at 4°C. The protein pellet was washed twice with cold acetone and resuspended with 4 M urea. Then the samples were treated with 5 mM of tris(2-carboxyethyl)phosphine (TCEP) for 30 min at 37°C in order to reduce disulfide bonds. After incubation, iodoacetamide (1.8 mg/ml final) was added to the samples to irreversibly prevent the formation of disulfide bonds and incubated for 30 min at 25°C in the dark. The samples were subsequently diluted with 0.1 M ammonium bicarbonate

to have a final concentration of urea of 1.6 M. For digestion, the proteins were incubated overnight at 37°C in presence of 1 µg of trypsin. After acidification with trifluoroacetic acid (TFA, 1 % final), the peptides were loaded on a C-18 column (The Nest group, SS18V) pre-equilibrated with buffer A (0.1 % TFA). The column was washed 3 times with buffer C (5 % acetonitrile / 95 %water (v/v) and 0.1 % TFA) and peptides were eluted with buffer B (50 % acetonitrile / 50 %water (v/v) and 0.1 % TFA). The peptides were finally dried under vacuum and kept at - 80°C. Before LC-MS/MS mass analysis, samples were resuspended in 0.1 % formic acid by sonication.

### **RhoA activation**

HeLa cells were seeded at a density of 362'656 cells/plate in DMEM 1 % FCS in three round plates (Falcon, REF 353003). After overnight incubation at 37°C and 5 % CO<sub>2</sub>, the medium was removed and HeLa cells were infected at MOI 400 with M199 1% FCS containing *Bhe ΔbepA-G* carrying the empty plasmid (SIM B1-52) or expressing BepC (SIM B2-06), one plate was left uninfected. After 24 hours of infection at 35°C, 5% CO<sub>2</sub>, the activation of RhoA was estimated using a G-LISA RhoA Activation Assay Biochem Kit (Cytoskeleton, BK124-S), according to the manufacturer's instructions.

### **Growth inhibition test for *Bartonella***

*Bartonella ΔbepA-G* overexpressing the indicated protein was grown on CBA plates for 3 days at 35°C with 5 % CO<sub>2</sub>. Bacteria were collected with a cotton swab and resuspended in M199 with 10 % heat-inactivated FCS. After OD<sub>600</sub> measurement, bacteria were diluted to have an OD<sub>600</sub> of 10<sup>-1</sup>. A serial dilution of 1/10 was performed in a 96-well plate until OD<sub>600</sub> 10<sup>-7</sup> and 10 µl of each dilution was plated on a CBA square plate supplemented with the indicated concentration of ITPG. *Bartonella* was grown for one week at 35°C with 5 % CO<sub>2</sub> and picture of the colonies were taken with a camera. Indicated bacterial number was estimated considering that OD<sub>600</sub>=1 is equal to 10<sup>9</sup> bacteria.

### **Western blotting**

The samples used for western blotting were separated by SDS-PAGE on a 4-20 % gradient gel (Mini-PROTEAN TGX Gels, Biorad, Cat# 456-1093). Gel electrophoresis was performed for 1h15 at 120 V in running buffer (Tris-glycine, 0.1% SDS). Protein were transferred on a PVDF membrane (GE Healthcare, 10600021) via wet electroblotting for 1 hour at 100 V in transfer buffer (20 % methanol, Tris-glycine) at 4°C. After transfer, the membrane was incubated for 1 hour in blocking buffer (PBS, 0.1% Tween 20 (Sigma, 93773) supplemented with 5% milk or 5% BSA according to antibody recommendation). After washing with PBS 0.1% Tween 20, the membrane was incubated overnight at 4°C in blocking buffer with the primary antibody (see table below). The membrane was washed again with PBS 0.1% Tween 20 before



being incubated 1 hour at room temperature in blocking buffer with the secondary antibody (see table below). The blots were incubated 1 min in dark with a mix of solution A and B from LumiGLO Reserve Chemiluminescent Substrate System (KPL, 54-70-00, 54-69-00). Finally, the signal was detected with LAS4000 (Fujifilm).

<b>Tris-glycine</b>	<b>Amount for 1 liter</b>
Tris (Merck, 108382)	3 g
Glycin (Sigma, 50050)	14.4 g

<b>Antigen</b>	<b>Producer (ref)</b>	<b>Final dilution</b>
Rabbit anti-GEF-H1 (primary)	Cell signaling, #4076	1/500
Rabbit anti-MRCK $\alpha$ (primary)	Abcam, ab96659	1/500
Mouse anti-Flag (primary)	Sigma, F1804	1/1000-2000
Mouse anti-HA (primary)	Cell Signaling, #2367	1/2000
Donkey anti-rabbit IgG, HRP linked (secondary)	GE Healthcare, NA934	1/1000
Sheep anti-mouse IgG, HRP linked (secondary)	GE Healthcare, NA931V	1/1000

### **Thermal shift assay**

Each step was performed on ice until analysis. Purified proteins were mixed with Sypro Orange (ThermoFisher, S6650) (12.5 X final concentration). 12  $\mu$ l of mix was transferred per well in a white 96 well qPCR plate. 3  $\mu$ l of dilution buffer (Tris 50 mM pH 7.5, 100 mM NaCl, 2.5 mM  $\beta$ -mercaptoethanol) or 3  $\mu$ l of nucleotide derivatives in dilution buffer were added per well to reach the desired concentration. The plate was spun down at 100 x g to ensure mixing. In qPCR machine (Biorad, CFX96 Real-time system), the plate was heated up from 10°C to 90°C with an increase of 0.5°C/min and fluorescence was measured at each temperature. The fluorescence intensity is then plotted against the temperature, the melting temperature ( $T_m$ ) corresponds to the inflection point of the curve.

### **Radioactive enzymatic assays**

Recombinant BepC (FIC-OB) 0.25 mg/ml was incubated with radioactively labeled ATP or NAD<sup>+</sup> in buffer (100 mM NaCl, 50 mM Tris pH 7.5, 2.5 mM  $\beta$ -mercaptoethanol). When indicated, the buffer was supplemented with MgCl<sub>2</sub> and non-radioactive ATP or NAD<sup>+</sup>. Samples were then incubated at 25°C or 30°C for the indicated period. Reactions were stopped by the addition of SDS-loading buffer and incubated for 5 min at 95°C. Samples were loaded onto 4-20 % gradient gel (Mini-PROTEAN TGX Gels, Biorad, Cat# 456-1093). Electrophoresis was performed 120 V for 90 min. The gel was stained overnight in Maier blue, gels were sealed in plastic bags and exposed on PhoSphor Screen overnight. Screens were developed using a Typhoon FLA 7000 system (GE Healthcare).

Maier Blue	Amount for 1 liter
H <sub>2</sub> O	850 ml
Ethanol (Sigma, 02890)	50 ml
ortho-Phosphoric acid (Merck, 100565)	80 g
$\alpha$ -Cyclodextrin (Roth, Nr. 4122.3)	5 g
Coomassie Brilliant Blue G-250 (Bio-rad, #1610406)	80 mg

### Cell lysate preparation for AMPylation assay

HeLa cells at passage 18 were grown at 37°C with 5 % CO<sub>2</sub> in 4 flasks of 175 cm<sup>2</sup>. After four washes with 5 ml of resuspension buffer (50 mM Tris pH 7.5, 100 mM NaCl, 2.5 mM  $\beta$ -mercapto-ethanol), cells were scraped in presence of 5 ml of resuspension buffer with proteases inhibitors (Roche, 11836170001) and DNaseI (AppliChem, A3778). Then, resuspended cells were pooled together and centrifuged for 10 min at 2'000 x g at 4°C. The supernatant was discarded and the cell pellet was resuspended with 500  $\mu$ l of resuspension buffer supplemented with protease inhibitor and DNaseI before being lysed by sonication. Cell lysates were centrifuged at 20'000 x g for 30 min at 4°C and the supernatant was used for AMPylation assay.

### Inhibitor treatment of infected HeLa cells

HeLa cells (passage 13) were seeded at a density of 2'000 cells/well on a 96-well plate (Corning, #3904) using DMEM supplemented with 10 % of heat-inactivated FCS. After overnight incubation at 37°C with 5 % CO<sub>2</sub>, cells were infected with *Bhe  $\Delta$ bepA-G* carrying the empty plasmid (SIM B1-52) or expressing BepC (SIM B2-06) at MOI=200 in M199 (Gibco, 22340-020) supplemented with 10 % of heat-inactivated FCS in presence of 10  $\mu$ M of IPTG. After 24 hours of incubation at 35°C and 5 % CO<sub>2</sub>, the medium was removed and cells were incubated with 100  $\mu$ l of inhibitor diluted in DMEM at 35°C with 5 % CO<sub>2</sub>. The treatment consisted of 2  $\mu$ g/ml of Rho inhibitor I (Cytoskeleton, CT04) for 2 hours or 20  $\mu$ M of Y27632 (Sigma, Y0503) for 1 hour. The experiment was stopped by fixation with 50  $\mu$ l of 3.7 % of paraformaldehyde for 10 minutes. Finally, the cells were washed 3 times with 100  $\mu$ l of PBS before being stained for F-actin and imaged by microscopy.

### Alignments and crystal structures

List of *Bartonella* species of the lineage 4 used for the amino acid alignments of BepC and BepA as well as for the modelization of conserved residues on the structure of BepC<sub>Btr</sub> (FIC).

Abbreviation	Genus - specie
<i>Bal</i>	<i>Bartonella alsatica</i> IBS 382
<i>Bbi</i>	<i>Bartonella birtlesii</i> LL-VM9
<i>Bdo</i>	<i>Bartonella doshiae</i> NCTC 12862
<i>Bel</i>	<i>Bartonella elizabethae</i> F9251
<i>Bgr</i>	<i>Bartonella grahamii</i> as4aup
<i>Bhe</i>	<i>Bartonella henselae</i> Houston-1
<i>Bko</i>	<i>Bartonella koehlerae</i> C-29
<i>Bqu</i>	<i>Bartonella quintana</i> str. Toulouse
<i>Bra</i>	<i>Bartonella rattimassiliensis</i> 15908
<i>Bsp. DB5-6</i>	<i>Bartonella</i> sp. DB5-6
<i>Bta</i>	<i>Bartonella taylorii</i> 8TBB
<i>Btr</i>	<i>Bartonella tribocurum</i> CIP 105476
<i>Bvi</i>	<i>Bartonella vinsonii arupensis</i> OK-94-513
<i>Bwa</i>	<i>Bartonella washoensis</i> 085-0475

Crystal structures of the FIC domain

PDB ID	Genus – specie
PDB 4WGJ	<i>Bartonella tribocurum</i> CIP 105476
PDB 3ZCB	<i>Bartonella schoenbuchensis</i> DSM 13525

### *Bartonella* strains

SIM	Genome Determinant	Plasmid	Description
SIM B1-01	<i>rpsL</i> ( <i>SmR</i> ), $\Delta$ <i>bepA-G</i>	None	
SIM B1-08	<i>rpsL</i> ( <i>SmR</i> ), $\Delta$ <i>bepA-G</i>	pSIM027	pHA-AT <sub>Bro</sub>
SIM B1-09	<i>rpsL</i> ( <i>SmR</i> ), $\Delta$ <i>bepA-G</i>	pSIM028	pHA-AT <sub>Bsp.1-1C</sub>
SIM B1-10	<i>rpsL</i> ( <i>SmR</i> ), $\Delta$ <i>bepA-G</i>	pSIM011	pHA-AT <sub>Bro-SD</sub> (strong)-Flag-Bep2 <sub>Bro</sub>
SIM B1-11	<i>rpsL</i> ( <i>SmR</i> ), $\Delta$ <i>bepA-G</i>	pSIM013	pHA-AT <sub>Bro-SD</sub> (weak)-Flag-Bep2 <sub>Bro</sub>
SIM B1-17	<i>rpsL</i> ( <i>SmR</i> ), $\Delta$ <i>bepA-G</i>	pSIM015	pFlag-Bep1 <sub>Bro</sub>
SIM B1-18	<i>rpsL</i> ( <i>SmR</i> ), $\Delta$ <i>bepA-G</i>	pSIM016	pFlag-Bep1 <sub>Bsp.1-1C</sub>
SIM B1-19	<i>rpsL</i> ( <i>SmR</i> ), $\Delta$ <i>bepA-G</i>	pSIM020	pHA-AT <sub>Bro-Flag-Bep1</sub> <sub>Bro</sub>
SIM B1-20	<i>rpsL</i> ( <i>SmR</i> ), $\Delta$ <i>bepA-G</i>	pSIM021	pHA-AT <sub>Bsp.1-1C-Flag-Bep1</sub> <sub>Bsp.1-1C</sub>
SIM B1-27	<i>rpsL</i> ( <i>SmR</i> ), $\Delta$ <i>bepA-G</i>	pSIM029	pHA-AT <sub>Bro-SD</sub> (strong)-Flag-Bep1 <sub>Bro</sub>
SIM B1-28	<i>rpsL</i> ( <i>SmR</i> ), $\Delta$ <i>bepA-G</i>	pSIM030	pHA-AT <sub>Bsp.1-1C-SD</sub> (strong)-Flag-Bep1 <sub>Bsp.1-1C</sub>
SIM B1-29	<i>rpsL</i> ( <i>SmR</i> ), $\Delta$ <i>bepA-G</i>	pSIM031	pHA-AT <sub>Bro-SD</sub> (weak)-Flag-Bep1 <sub>Bro</sub>
SIM B1-30	<i>rpsL</i> ( <i>SmR</i> ), $\Delta$ <i>bepA-G</i>	pSIM032	pHA-AT <sub>Bsp.1-1C-SD</sub> (weak)-Flag-Bep1 <sub>Bsp.1-1C</sub>
SIM B1-40	<i>rpsL</i> ( <i>SmR</i> ), $\Delta$ <i>bepC</i> , G	None	

- Materials and methods -

SIM B1-45	<i>rpsL (SmR), ΔbepA-G</i>	pSIM051	pFlag-bepC <sub>Bgr</sub>
SIM B1-46	<i>rpsL (SmR), ΔbepA-G</i>	pSIM054	pFlag-bepC <sub>Bqu</sub>
SIM B1-47	<i>rpsL (SmR), ΔbepA-G</i>	pSIM056	pHA-AT <sub>Bhe</sub> -TAATG-Flag-BepC <sub>Bhe</sub>
SIM B1-48	<i>rpsL (SmR), ΔbepA-G</i>	pSIM037	Pgfp
SIM B1-49	<i>rpsL (SmR), ΔbepA-G</i>	pSIM058	pFlag-bepC <sub>Bta</sub>
SIM B1-50	<i>rpsL (SmR), ΔbepA-G</i>	pSIM059	pFlag-bepC <sub>Bhe</sub> K150A, R154A R157A
SIM B1-51	<i>rpsL (SmR), ΔbepA-G</i>	pSIM057	pHA-AT <sub>Bhe</sub> -SD(weak)-Flag-bepC <sub>Bhe</sub>
SIM B1-52	<i>rpsL (SmR), ΔbepA-G</i>	pBZ485_a_empty	pEmpty
SIM B1-63	<i>rpsL (SmR), ΔbepA-G</i>	pSIM062	pFlag-bepC <sub>Btr</sub>
SIM B1-70	<i>rpsL (SmR), ΔbepA-G</i>	pSIM060	pFlag-bepC <sub>Bhe</sub>
SIM B1-74	<i>rpsL (SmR), ΔbepA-G</i>	pSIM073	pHA-AT <sub>Bhe</sub>
SIM B2-01	<i>rpsL (SmR), ΔbepA-G</i>	pSIM064	pFlag-bepF <sub>Bhe</sub>
SIM B2-02	<i>rpsL (SmR), ΔbepA-G</i>	pSIM071	pFlag-bepE <sub>Bhe</sub>
SIM B2-03	<i>rpsL (SmR), ΔbepA-G</i>	pSIM086	pFlag-bepC <sub>Bhe</sub> K150E
SIM B2-05	<i>rpsL (SmR), ΔbepA-G</i>	pSIM090	pFlag-bepC <sub>Bhe</sub> H146A
SIM B2-06	<i>rpsL (SmR), ΔbepA-G</i>	pSIM091	pFlag-bepC <sub>Bhe</sub>
SIM B2-07	<i>rpsL (SmR), ΔbepA-G</i>	pSIM062b	pFlag-bepC <sub>Btr</sub>
SIM B2-08	<i>rpsL (SmR), ΔbepA-G</i>	pSIM081	pFlag - bepC <sub>Bhe</sub> BepC****
SIM B2-14	<i>rpsL (SmR), ΔbepA-G</i>	pSIM097	pFlag-bepC <sub>Bhe</sub> (BID)
SIM B2-15	<i>rpsL (SmR), ΔbepA-G</i>	pSIM096	pFlag-bepC <sub>Bhe</sub> 19-532
SIM B2-16	<i>rpsL (SmR), ΔbepA-G</i>	pSIM098	pFlag-bepC <sub>Bhe</sub> (OB-BID)
SIM B2-18	<i>rpsL (SmR), ΔbepA-G</i>	pSIM107	p3xFlag-bepC <sub>Bhe</sub>
SIM B2-25	<i>rpsL (SmR), ΔbepA-G</i>	pSIM117	pFlag-bepC <sub>Bhe</sub> (FLAP BepA)
SIM B2-33	<i>rpsL (SmR), ΔbepA-G</i>	pSIM121	p3XFlag-bepC <sub>Bhe</sub> (BID BepA)
SIM B2-36	<i>rpsL (SmR), ΔbepA-G</i>	pSIM125	p3xFlag bepF <sub>Bhe</sub>
SIM B2-37	<i>rpsL (SmR), ΔbepA-G</i>	pSIM126	p3xFlag-bepE <sub>Bhe</sub>
SIM B2-38	<i>rpsL (SmR), ΔbepA-G</i>	pSIM127	p3xFlag-bepC <sub>Bhe</sub> ****
SIM B2-39	<i>rpsL (SmR), ΔbepA-G</i>	pSIM128	p3xFlag-bepC <sub>Bhe</sub> K150E
SIM B2-40	<i>rpsL (SmR), ΔbepA-G</i>	pSIM129	p3xFlag-bepC <sub>Bhe</sub> H146A
SIM B2-41	<i>rpsL (SmR), ΔbepA-G</i>	pSIM130	p3xFlag-bepC <sub>Bhe</sub> 19-532
SIM B2-42	<i>rpsL (SmR), ΔbepA-G</i>	pSIM131	p3xFlag-bepC <sub>Bhe</sub> (OB-BID)
SIM B2-43	<i>rpsL (SmR), ΔbepA-G</i>	pSIM132	p3xFlag-bepC <sub>Bhe</sub> (FLAP BepA)

**E. coli strains**

SIM E3-58	BL21(DE3) : E. coli B; F <sup>-</sup> , ompT, hsdSB(rB-, mB-), dcm, gal, λ(DE3)	pSIM072	<i>pbepC<sub>Bhe</sub> (FIC-OB) - 6XHis</i>
SIM E3-71	BL21(DE3) : E. coli B; F <sup>-</sup> , ompT, hsdSB(rB-, mB-), dcm, gal, λ(DE3)	pSIM076	<i>pbepC<sub>Bhe</sub> (FIC-OB) - 6XHis + HA-AT<sub>Bhe</sub></i>
SIM E4-25	BL21(DE3) : E. coli B; F <sup>-</sup> , ompT, hsdSB(rB-, mB-), dcm, gal, λ(DE3)	pSIM094	<i>pbepC<sub>Bhe</sub> H164A (FIC-OB) - 6XHis</i>
SIM E4-26	BL21(DE3) : E. coli B; F <sup>-</sup> , ompT, hsdSB(rB-, mB-), dcm, gal, λ(DE3)	pSIM095	<i>pbepC<sub>Bhe</sub>**** (FIC-OB) - 6XHis</i>
SIM E4-37	BL21(DE3) : E. coli B; F <sup>-</sup> , ompT, hsdSB(rB-, mB-), dcm, gal, λ(DE3)	pSIM080	<i>pbepC<sub>Bhe</sub> K150E (FIC-OB) - 6XHis</i>
JKE170	MG1655 RP4-2-Tc::[ΔMu1::aac(3)IV-ΔaphA-Δnic35-ΔMu2::zeo] ΔdapA::(erm-pir) ΔrecA ΔmcrA Δ(mrr-hsdRMS-mcrBC)	None	

**E. coli plasmids**

Plasmid	Description	Template PCR	PCR	Cloned in
pSIM049	pRSF-Duet-1 with inactivated NdeI	pRSF-Duet-1	prSIM163 prSIM164	PCR mutagenesis
pSIM065	pSIM049 with NcoI->NdeI	pSIM049	prSIM165 prSIM166	PCR mutagenesis
pSIM072	<i>pbepC<sub>Bhe</sub> (FIC-OB) - 6XHis</i>	Genomic DNA	prSIM162 prSIM161	pSIM065 (NdeI/NotI)
pSIM075	<i>pHA-AT<sub>Bhe</sub></i>	Genomic DNA	prSIM172 prSIM173	pRSF-Duet-1 (NcoI/NotI)
pSIM076	<i>pHA-AT<sub>Bhe</sub> + bepC<sub>Bhe</sub> (FIC-OB) - 6XHis</i>	pSIM072	prSIM162 prSIM171	pSIM075 (NdeI/XhoI)
pSIM080	<i>pbepC<sub>Bhe</sub> K150E (FIC-OB) - 6XHis</i>	pSST033	prSIM162 prSIM161	pSIM065 (NdeI/NotI)
pSIM094	<i>pbepC<sub>Bhe</sub> H164A (FIC-OB) - 6XHis</i>	pRC019	prSIM162 prSIM161	pSIM072 (NdeI/SalI)
pSIM095	<i>pbepC<sub>Bhe</sub>**** (FIC-OB) - 6XHis</i>	pSIM084	prSIM162 prSIM161	pSIM072 (NdeI/SalI)

## Bartonella plasmids

Plasmid	Description	Template PCR1	PCR 1	Template PCR2	PCR 2	PCR 3	Cloned in
pBZ485_a	<i>pccdB</i>						
pBZ485_a_empty	<i>pEmpty</i>	pSIM037	X	X	X	X	PCR mutagenesis
pSIM033	<i>pccdB</i>	pBZ485_a	prSIM131 prSIM132	X	X	X	PCR mutagenesis
pSIM035	<i>pgfp</i>	pSIM033	prSIM133 prSIM138	X	X	X	pSIM033 (Sacl/XhoI)
pSIM037	<i>pgfp</i>	pSIM035	prSIM149 prSIM150	X	X	X	PCR mutagenesis
pSIM051	<i>pFlag-bepC<sub>Bgr</sub></i>	Genomic DNA	prSIM106 prSIM110	PCR 1	prSIM076 prSIM110	X	pSIM037 (Sacl/NotI)
pSIM054	<i>pFlag-bepC<sub>Bqu</sub></i>	Genomic DNA	prSIM107 prSIM111	PCR 1	prSIM076 prSIM111	X	pSIM037 (Sacl/NotI)
pSIM056	<i>pHA-AT<sub>Bhe</sub>-TAATG-Flag-BepC<sub>Bhe</sub></i>	Genomic DNA	prSIM117 prSIM109	Genomic DNA	prSIM113 prSIM118	SOEING: prSIM078/prSIM109	pSIM037 (Sacl/NotI)
pSIM057	<i>pHA-AT<sub>Bhe</sub>-SD(weak)-Flag-bepC<sub>Bhe</sub></i>	Genomic DNA	prSIM099 prSIM109	Genomic DNA	prSIM113 prSIM101	SOEING: prSIM078/prSIM109	pSIM037 (Sacl/NotI)
pSIM058	<i>pFlag-bepC<sub>Bta</sub></i>	Genomic DNA	prSIM155 prSIM156	PCR 1	prSIM076 prSIM156	X	pSIM037 (Sacl/NotI)
pSIM059	<i>pFlag-bepC<sub>Bhe</sub> K150A, R154A, R157A</i>	pSST036	prSIM105 prSIM109	PCR 1	prSIM076 prSIM109	X	pSIM037 (Sacl/NotI)
pSIM062	<i>pFlag-bepC<sub>Btr</sub></i>	Genomic DNA	prSIM108 prSIM112	PCR 1	prSIM076 prSIM112	X	pSIM037 (Sacl/NotI)
pSIM073	<i>pHA-AT<sub>Bhe</sub></i>	Genomic DNA	prSIM113 prSIM173	PCR 1	prSIM078 prSIM173	X	pSIM037 (Sacl/NotI)

- Materials and methods -

Plasmid	Description	Template PCR1	PCR 1	Template PCR2	PCR 2	PCR 3	Cloned in
pSIM081	<i>pFlag - bepC<sub>Bhe</sub> BepC****</i>	pSIM084	prSIM105 prSIM109	PCR 1	prSIM076 prSIM109	X	pSIM037 (Sacl/NotI)
pSIM086	<i>pFlag-bepC<sub>Bhe</sub> K150E</i>	pSST033	prSIM105 prSIM109	PCR 1	prSIM076 prSIM109	X	pSIM037 (Sacl/NotI)
pSIM090	<i>pFlag-bepC<sub>Bhe</sub> H146A</i>	pRC019	prSIM105 prSIM109	PCR 1	prSIM076 prSIM109	X	pSIM037 (Sacl/NotI)
pSIM091	<i>pFlag-bepC<sub>Bhe</sub></i>	Genomic DNA	prSIM105 prSIM109	PCR 1	prSIM076 prSIM109	X	pSIM037 (Sacl/NotI)
pSIM096	<i>pFlag-bepC<sub>Bhe</sub> 19-532</i>	pSIM091	prSIM195 prSIM109	PCR1	prSIM076 prSIM109	X	pSIM037 (Sacl/NotI)
pSIM097	<i>pFlag-bepC<sub>Bhe</sub> (BID)</i>	pSIM091	prSIM196 prSIM109	PCR1	prSIM076 prSIM109	X	pSIM037 (Sacl/NotI)
pSIM098	<i>pFlag-bepC<sub>Bhe</sub> (OB-BID)</i>	pSIM091	prSIM197 prSIM109	PCR1	prSIM076 prSIM109	X	pSIM037 (Sacl/NotI)
pSIM107	<i>p3xFlag-bepC<sub>Bhe</sub></i>	pSIM091	prSIM202 prSIM109	PCR1	prSIM203 prSIM109	X	pSIM037 (Sacl/NotI)
pSIM117	<i>pFlag-bepC<sub>Bhe</sub> (Flap BepA)</i>	pSIM113	prSIM202 prSIM109	PCR 1	prSIM203 prSIM109	X	pSIM037 (Sacl/NotI)
pSIM121	<i>p3XFlag-bepC<sub>Bhe</sub> (BID BepA)</i>	pSIM107	prSIM203 prSIM221	pPG101	prSIM222 prSIM220	SOEING: prSIM203/prSIM220	pSIM037 (Sacl/NotI)
pSIM127	<i>p3xFlag-bepC<sub>Bhe</sub>****</i>	pSIM081	prSIM202 prSIM109	PCR 1	prSIM203 prSIM109	X	pSIM037 (Sacl/NotI)
pSIM128	<i>p3xFlag-bepC<sub>Bhe</sub> K150E</i>	pSIM086	prSIM202 prSIM109	PCR 1	prSIM203 prSIM109	X	pSIM037 (Sacl/NotI)
pSIM129	<i>p3xFlag-bepC<sub>Bhe</sub> H146A</i>	pSIM090	prSIM202 prSIM109	PCR 1	prSIM203 prSIM109	X	pSIM037 (Sacl/NotI)

- Materials and methods -

Plasmid	Description	Template PCR1	PCR 1	Template PCR2	PCR 2	PCR 3	Cloned in
pSIM130	<i>p3xFlag-bepC<sub>Bhe</sub> 19-532</i>	pSIM096	prSIM202 prSIM109	PCR 1	prSIM203 prSIM109	X	pSIM037 (Sacl/NotI)
pSIM131	<i>p3xFlag-bepC<sub>Bhe</sub> (OB-BID)</i>	pSIM098	prSIM202 prSIM109	PCR 1	prSIM203 prSIM109	X	pSIM037 (Sacl/NotI)
pSIM132	<i>p3xFlag-bepC<sub>Bhe</sub> (Flap BepA)</i>	pSIM117	prSIM202 prSIM109	PCR 1	prSIM203 prSIM109	X	pSIM037 (Sacl/NotI)



# Acknowledgement

- Acknowledgement -

First, I would like to thank Prof. Christoph Dehio for his supervision and support throughout my PhD. I am particularly grateful for his constant availability for discussion and for providing me an excellent environment for conducting experimental research.

Furthermore, I wish to thank Prof. Urs Jenal and Prof. Martin Spiess who were part of my thesis committee.

I would also like to acknowledge Dr. Kathrin Pieles who mentored my first year at the Biozentrum and introduced me to the techniques required for my lab work.

Special thanks to Dr. Simone Eicher who has always been supportive and ready to help me in the lab whenever I needed. Also big thanks for providing me FCS, PFA, and great Swiss chocolate.

Thanks to Jenifer Sen for always being cheerful and motivated. I acquired a valuable experience by supervising her master thesis and it has always been a pleasure to work with her.

I wish to thank in particular Clément and Selma who became great friends and allowed me to keep speaking French. Their presence inside and outside the lab made my life in Basel very enjoyable.

I would like to thank all the members of the Dehio group for the friendly atmosphere in the lab and all the great discussions.

Thanks to Claudia Mistl, Dr. Isabel Sorg, and Dr. Maxime Quebatte for ordering all the lab material, sometimes on very short notice.

I am grateful to Dr. Simone Eicher, Dr. Maxime Quebatte, Dr. Isabelle Sorg for the critical reading of my thesis and suggestions for improvement.

Thanks to the technical staff and to the ladies of the media kitchen for making my daily lab work much easier.

I wish to thank Claudia Erbel-Sieler, Michaela Hanisch, Dr. Anne-Cécile Hiebel, and Angie Klarer for support with the administration.

I would also wish to thank all present and past members of the PhD representatives with whom I had the pleasure to organize the PhD retreat and social events.

I was funded by the Werner Siemens Foundation “Fellowships for Excellence PhD program”.

Most importantly, I would like to thank my parents, my brother, and all my family for taking care of me all along my life. I am grateful to have them and I would have never achieved this work without their constant support.

# Curriculum vitae

## SIMON MARLAIRE

Birth date: 08.12.1990  
Nationality: Belgian

### Office address

Biozentrum University of Basel  
Infection Biology  
Klingelbergstrasse, 50/70  
CH-4056 Basel, Switzerland  
Phone: +41 61 207 21 39  
Email: simon.marlaire@unibas.ch

### Private address

Davidsbodenstrasse, 17  
CH-4056 Basel, Switzerland  
Phone +41 79 126 81 84  
Email: simon.marlaire@gmail.com

### Education and research experience

PhD in Microbiology 12.2013 to 04.2018  
University of Basel Switzerland

PhD thesis 02.2013 to 04.2018  
Focal area Infection Biology, Biozentrum Switzerland

Laboratory: Infection biology  
Advisor: Pr. Christoph Dehio  
Funding: Fellowship for excellence (12.2013 to 12.2016)  
Topic: *Functional characterization of Bartonella effector protein C (BepC) in the context of infection.*

Master degree in Biomedical Sciences 09.2011 to 08.2013  
Université Catholique de Louvain Belgium

International exchange program 04.2013 to 07.2013  
Institut de recherche en immunologie et oncologie Canada

Laboratory: Intracellular signaling  
Advisor: Pr. Marc Therrien  
Funding: Mercator-FAME grant  
Topic: *Characterization of polycomb and trithorax functions in a NUP98-HOXA9 drosophila leukemia model.*

Master thesis 11.2011 to 03.2013  
De Duve Institute Belgium

Laboratory: Protein repair & inborn errors of metabolism  
Advisor: Pr. Emile Van Schaftingen & Dr. Maria Veiga-da-Cuhna  
Topic: *Identification of the enzyme which activates glutarate into glutarylCoA and characterization of the physiological role of the protein Nit1.*

Bachelor degree in Biomedical Sciences 09.2008 to 06.2011  
Université Catholique de Louvain Belgium

Internship One week  
De Duve Institute Belgium

Laboratory: Genetics of human diseases  
Advisor: Pr. Miikka Vakkula  
Topic: *Validation of molecular tools for the study of glomulin.*

## Publications

### First author publication:

S. Marlaire, E. Van Schaftingen, M. Veiga-da-Cunha  
C7orf10 encodes succinate-hydroxymethylglutarate CoA-transferase, the enzyme that converts glutarate to glutaryl-CoA.  
*J Inherit Metab Dis* (2014).

### Co-author publication:

Peracchi *et al.*  
Nit1 is a metabolite repair enzyme that hydrolyzes deaminated glutathione.  
*Proc Natl Acad Sci U S A* (2017).

## Oral and poster presentations

Presentation at the PhD club 2017  
Switzerland

Characterization of Fic proteins in the context of pathogenesis:  
*Bartonella* effector protein C (BepC).

Poster at the Biozentrum symposium 2018  
Switzerland

Characterization of Fic proteins in the context of pathogenesis:  
*Bartonella* effector protein C (BepC).

Poster at the Fellowship For Excellence symposium 2016  
Switzerland

Characterization of Fic proteins in the context of pathogenesis:  
*Bartonella* effector protein C (BepC).

Poster at the annual PhD retreat of the Biozentrum/Pharmazentrum 2014-2015-2016-2017  
Switzerland

Characterization of Fic proteins in the context of pathogenesis:  
*Bartonella* effector protein C (BepC).

## Teaching experience

Supervision of a Master student 02.2017 to 09.2018  
Focal area Infection Biology, Biozentrum, University of Basel Switzerland

Assistant and tutor for undergraduate students in practical courses 2014 to 2017  
Focal area Infection Biology, Biozentrum, University of Basel Switzerland

## Academic activities

PhD representative 07.2014 to 06.2018  
Biozentrum, University of Basel Switzerland

Treasurer (12.2015 to 06.2018)  
Organizational committee member of the annual PhD retreat (2015, 2016, 2017)

## Languages

French: native speaker  
English: four years in an English-speaking workplace (C1)